E-ISSN: 2148-6247

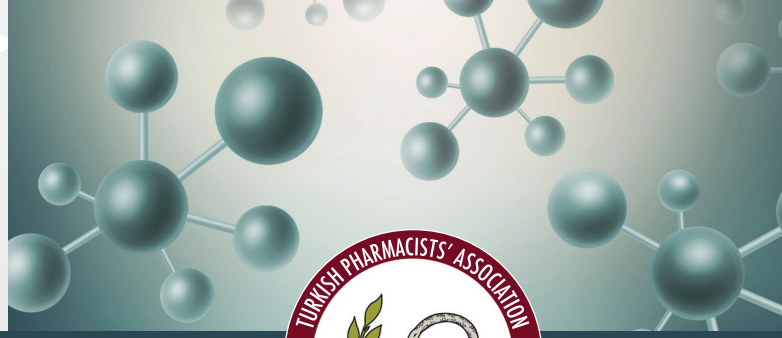

Turkish Journal of PHARMACEUTICAL SCIENCES

An Official Journal of the Turkish Pharmacists' Association, Academy of Pharmacy

Volume: 21 Issue: 5 October 2024

www.turkjps.org

Emerging Sources Citation Index

PubMed Central PubMed Scopus TRDİZİN

galenos Publishing House

Turkish Journal of
PHARMACEUTICAL SCIENCES

Turkish Journal of
PHARMACEUTICAL SCIENCES

Prof. Robert Rapoport, Ph.D.
ORCID: orcid.org/0000-0001-8554-1014
Cincinati University Faculty of Pharmacy, Department of Pharmacology and Cell Biophysics, Cincinati, USA
robertrapoport@gmail.com

Prof. Tayfun Uzbay, Ph.D.
ORCID: orcid.org/0000-0002-9784-5637
Üsküdar University Faculty of Medicine, Department of Medical Pharmacology, İstanbul, Türkiye
tayfun.uzbay@uskudar.edu.tr

Prof. Wolfgang Sadee, Ph.D.
ORCID: orcid.org/0000-0003-1894-6374
Ohio State University, Center for Pharmacogenomics, Ohio, USA
wolfgang.sadee@osumc.edu

Advisory Board

Turkish Journal of
PHARMACEUTICAL SCIENCES

Please refer to the journal's webpage (https://www.turkjps.org/) for "Editorial Policy" and "Instructions to Authors".

The editorial and publication process of the **Turkish Journal of Pharmaceutical Sciences** are shaped in accordance with the guidelines of ICMJE, WAME, CSE, COPE, EASE, and NISO. The Turkish Journal of Pharmaceutical Sciences is indexed in **PubMed, PubMed Central, Thomson Reuters / Emerging Sources Citation Index, Scopus, ULAKBİM, Türkiye Atıf Dizini, Embase, EBSCO Host, Türk Medline, Cabi, CNK**I.

The journal is published online.

Owner: Turkish Pharmacists' Association, Academy of Pharmacy

Responsible Manager: Mesut Sancar

galenos yayınevi

Publisher Contact
Address: Molla Gürani Mah. Kaçamak Sk. No: 21/1
34093 İstanbul, Türkiye
Phone: +90 (530) 177 30 97
E-mail: info@galenos.com.tr/yayin@galenos.com.tr
Web: www.galenos.com.tr | **Publisher Certificate Number:** 14521

Publication Date: October 2024
E-ISSN: 2148-6247
International scientific journal published bimonthly.

Turkish Journal of
PHARMACEUTICAL SCIENCES

CONTENTS

Original Articles

Turk J Pharm Sci 2024;21(5):376-389
DOI: 10.4274/tjps.galenos.2024.36153

ORIGINAL ARTICLE

Third-Hand Smoke Exacerbates H_2O_2-Driven Airway Responses in A549 Cells

Rengin REİS[1]*, Kübra KOLCİ[1,2], Yağmur ÖZHAN[2], Göknil Pelin COŞKUN[3], Hande SİPAHİ[2]

[1]Acıbadem Mehmet Ali Aydınlar University Faculty of Pharmacy, Department of Toxicology, İstanbul, Türkiye
[2]Yeditepe University Faculty of Pharmacy, Department of Toxicology, İstanbul, Türkiye
[3]Acıbadem Mehmet Ali Aydınlar University Faculty of Pharmacy, Department of Pharmaceutical Chemistry, İstanbul, Türkiye

ABSTRACT

Objectives: Third-hand smoke (THS) is residual smoke after extinguishing a cigarette and adhering to surfaces. Re-emission into the air also makes THS a health concern for those who suffer from respiratory diseases. The present study aimed to elucidate the mechanistic pathways involved in THS-induced respiratory toxicity and the accelerative potential of THS in an H_2O_2-induced oxidative stress model of human airway epithelia *in vitro*.

Materials and Methods: THS extracted from terrycloth exposed to 3R4F cigarettes was assessed *via* 3-(4,5-dimethylthiazol-2-yl)-2,5-diphenyltetrazolium bromide assay to identify cytotoxicity. The reactive oxygen species (ROS) level was determined *via* 2,7-dichlorofluorescein diacetate (DCFDA) fluorescence intensity in a flow cytometer, and glutathione (GSH), malondialdehyde (MDA), and catalase (CAT) activity were assessed spectrophotometrically. Interleukin-6 (IL-6) level was measured *via* enzyme-linked immunosorbent assay.

Results: THS 50% (*v/v*) with significant cytotoxicity in A549 cells upregulated intracellular ROS levels *via* a right-shifted fluorescence intensity of DCFDA compared with the control ($p < 0.05$), which was also amplified with H_2O_2 co-treatment. MDA levels remarkably increased with THS ($p < 0.05$). Both THS and THS + H_2O_2 led to notable GSH depletion, increased CAT activity, and increased IL-6 levels, which were attenuated by the negative control (N-acetylcysteine, 1 mM) ($p < 0.05$).

Conclusion: The induction of oxidative stress may be an important event in THS-induced airway toxicity that may contribute to the progression of respiratory diseases.

Keywords: Chronic airway diseases, airway inflammation, oxidative stress, third-hand smoke, cigarette

INTRODUCTION

Cigarette smoke (CS) is the main preventable cause of death worldwide, and it poses a significant health risk for both smokers and non-smokers.[1] Recently, a new toxicological concern has arisen due to the residual part of CS, third-hand smoke (THS). THS is referred to as tobacco residue and stale or aged second-hand smoke (SHS). THS is not described as rigid smoke but rather as the by products of smoking and refers to the contamination of surfaces with SHS-emitted compounds.[2] The products of chemical transformations of these constituents, and the off-gassing of volatile substances into the atmosphere, thus represent important public and environmental issues. Apart from traditional tobacco smoke, people may be exposed to THS *via* three routes: ingestion, inhalation, and dermal absorption. In particular, the most important target population is infants and toddlers residing in the homes of smokers who are vulnerable to THS because they spend more time in contact with THS-contaminated surfaces. In addition, they might indirectly be exposed to THS *via* hand-to-mouth transfer *via* contaminated objects.[3] THS has a complex chemical dynamic and consists of nicotine and tobacco-specific nitrosamines (TSNAs), which are highly carcinogenic compounds formed when tobacco burns and can react with other chemicals in the environment to create even more harmful substances, as well as volatile organic compounds (VOCs), such as benzene and formaldehyde.[4,5] Polycyclic aromatic hydrocarbons (PAHs) and heavy metals were also detected in the THS content.[6]

*Correspondence: rengin.reis@acibadem.edu.tr, Phone: +0216 500 42 59, ORCID-ID: orcid.org/0000-0002-3484-2201
Received: 13.09.2023, Accepted: 12.01.2024

Due to the inhalation of the re-released SHS-emitted compounds, the other vulnerable population might be individuals with chronic airway diseases such as chronic obstructive pulmonary disease (COPD).[7] The damage of alveolar walls characterizes COPD; in other words, its pathological basis is the injury of alveolar epithelial cells; thus, the ability of alveolar epithelial cells to proliferate is closely linked to the pathological process or prognosis of COPD.[8] COPD is considered a systemic disorder and is more common in individuals with a smoking history.[9] COPD is the most extensively studied inflammatory airway disorder induced by smoking, and its incidence rate at all stages among active smokers was > 35% over 25 years.[10] According to the latest data from the Centers for Disease Control and Prevention, COPD is usually caused by smoking, which accounts for as much as 80% of COPD-related mortality.[11] In addition, COPD remains a socioeconomic burden, especially in countries with a low sociodemographic index between 1990 and 2019.[9] Not only for COPD but also for asthma and bronchitis, THS might represent an important pre-existing factor due to the well-known effects of tobacco on these chronic airway conditions.

It is well-known that CS exposure *via* firsthand smoke or SHS exposure may harm airway epithelial cells through oxidative stress, apoptosis, necrosis, chronic inflammation, and other pathways that are not fully elucidated.[12] According to previous reports, TSNAs and other reactive chemicals can directly damage lung cells, leading to inflammation and scarring. In addition, THS exposure may induce oxidative stress, which directly disrupts lung function and may promote further inflammation in target organs. The amplified inflammatory response may also contribute to the immune response in the respiratory system and trigger chronic inflammation in the airways, leading to thickening and narrowing of the bronchial tubes, which is a hallmark of COPD. Moreover, tobacco smoke can induce epithelial and mucus dysregulation due to damage to the lining of the airways, leading to airway obstruction and difficulty breathing.[5,13-15] The precise contributions of each mechanism are still being studied; thus, THS may worsen symptoms and accelerate the progression of pre-existing respiratory conditions like COPD, asthma, and bronchitis, due to the well-known detrimental effects of tobacco on the respiratory system. Several experimental studies have revealed that THS exposure in mice made the alveolar walls in terminal respiratory bronchioles thicker with increased proinflammatory cytokine levels in lung tissues than in non-exposed animals.[13,15] In addition, THS toxins as a mixture exerted dose-dependent cytotoxicity in A549 human lung epithelial cells, mainly due to the presence of acrolein, phenol, and 2,5-dimethylfuran content.[5] In light of these limited findings, THS exposure may cause a pro-inflammatory and oxidative environment in the lungs, which increases the risk of disease progression in chronic airway diseases. It is known that when free radicals overpower antioxidants, the present oxidative imbalance may lead to stress that damages cells, proteins, and DNA, leading to various pathologies, including chronic airway diseases. This oxidative cascade also contributes to mucus hyperproduction, tissue remodeling, inflammation, airway hyperresponsiveness, and tissue damage such as fibrosis and scarring in the lining of respiratory epithelia.[16-18] The present study aimed to elucidate the mechanistic pathways involved in THS-induced respiratory toxicity and the accelerative potential of THS in an H_2O_2-induced oxidative stress model of human airway epithelia *in vitro*.

MATERIALS AND METHODS

Materials

3R4F research cigarettes were obtained from the University of Kentucky (Lexington, Kentucky, USA). The cell culture chemicals including Dulbecco's Modified Eagle Medium (DMEM), fetal bovine serum, and penicillin-streptomycin antibiotics were obtained from Gibco (USA). Other chemicals, including 3-(4,5-dimethylthiazol-2-yl)-2,5-diphenyl tetrazolium bromide (MTT), nicotine standard, DTNB-Ellman's reagent 5,5'-Dithiobis (2-nitrobenzoic acid) (#D8130), sodium bicarbonate (#S6014), cobalt (II) nitrate hexahydrate, and catalase (CAT) enzyme (#C9322), were purchased from Sigma-Aldrich (USA). The kit used for the analysis of cellular reactive oxygen species (ROS) (ab113851) was from Abcam (Germany) and the analysis of interleukin-6 (IL-6) level was assessed *via* the human IL-6 Enzyme-Linked Immunosorbent Assay (ELISA) kit (Elabscience, E-EL-H6156, USA).

Methods

Extraction of THS

THS was extracted from a terrycloth that was manually exposed to 2 of 3R4F research cigarettes (11.0 mg total particulate matter/cigarette; 9.4 mg tar/cigarette; 0.73 mg nicotine/cig, and 12 mg CO/cigarette) in a polystyrene chamber according to the International Organization for Standardization British Standards Institution (ISO BSI 10993-12),[19] with a slight modification in the number of cigarettes used in our previous study.[20] According to the previously mentioned method, once the smoke exposure in the chamber ceased, the mainstream and sidestream smoke was mixed with the minivan in the chamber for 5 minutes, and the exposed terrycloth was extracted in DMEM at 37 °C for 24 hours. The standardization of THS was achieved through the weighing of the tar of different filter papers used for THS batches according to the method of Martins-Green et al.[14]

Nicotine level in THS

The nicotine content of the prepared THS was assessed by liquid chromatography-mass spectrometry (LCMS, Agilent1260 Infinity II, USA) equipped with a solvent pump, manual injection valve, and diode array detector, as described previously in detail.[21] Six dilutions of nicotine standard were used to calculate the equation and the R^2 value (Supplementary Figure S1 and Supplementary Table 1). The area of the standard peaks was calculated according to the mass values.

Cytotoxicity

A549 human lung epithelial-like cells (ATCC, CCL-185™) were used in cell culture studies. For this purpose, the cells were seeded in a 96-well plate and exposed to different concentrations

of THS (12.5-100%, *v/v*) diluted with DMEM for 24 hours. Since previous data reported increased H_2O_2 levels in expired breath condensates of patients with COPD,[22] and oxidative stress contributes to the development and progression of chronşc airway diseases through numerous pathways, such as mucus hyperproduction, tissue remodeling, and inflammation, *in vitro* oxidative stress in the respiratory system was demonstrated by the co-exposure of H_2O_2 (100 µM) in A549 cells. As a negative control, a 2-hour pretreatment with N-acetylcysteine [(NAC), 1 mM] was used in all studies to observe its ameliorative effects against THS itself and under H_2O_2-driven oxidative stress conditions. After the incubation period, cytotoxicity was assessed using the MTT assay, as previously described.[21]

Oxidative stress

Glutathione (GSH) level

GSH levels were measured in cell lysates according to our previous study.[23] The exposed cell lysate prepared in phosphate-buffered saline (PBS) was mixed with DTNB and then mixed with ethylenediaminetetraacetic acid (EDTA) buffer solution (pH 8.2). After incubation at 37 ˚C in the dark for 30 minutes, the absorbance of the yellow chromophore was measured at 412 nm spectrophotometrically (ThermoScientific, Finland). The results are expressed as µmol/g protein GSH, and each measurement was performed in duplicate.

CAT activity

CAT activity was measured using the correlation between the carbonatocobaltate (III) complex and the CAT enzyme. Briefly, the cell lysate was mixed with H_2O_2 as described in our previous study[21] and incubated at 37 ˚C for 2 minutes. Subsequently, a solution containing phosphate buffer (pH 7.4), sodium bicarbonate, and cobalt (II) nitrate hexahydrate was added to the mixture and vortexed. The reaction tubes were kept in the dark for 10 minutes, and absorbances for the kinetic reaction were recorded at 440 nm spectrophotometrically for 2 minutes in duplicate. CAT activity was expressed as U/mg protein.

ROS level

The oxidative effect of THS in H_2O_2-induced A549 cells was assessed using a cellular ROS assay kit *via* flow cytometry. As described previously,[23] under oxidative conditions, 2,7-dichlorofluorescein diacetate (DCFDA), a fluorescence-sensitive dye, is deacetylated by cellular esterases and forms a non-fluorescent compound, which is oxidized into 2,7-dichlorofluorescein by the produced ROS. Briefly, cells pre-treated with NAC/treated with THS/treated with THS + H_2O_2 were collected from 12-well plates and harvested in PBS solution, followed by 20 mM DCFDA addition to each flow cytometer tube in the dark for 30 minutes at 37 ˚C with 5% CO_2. Cells pre-treated with the medium were used as a negative control, whereas the group exposed to 100 µM of *tert*-butyl hydroperoxide (THBP) for 4 hours was used as the positive control (PC). Data were analyzed in triplicate, and intracellular ROS levels were expressed as relative ROS content compared to the PC.

IL-6 level

The inflammatory response induced by THS exposure in A549 cells co-treated with H_2O_2 was determined using the proinflammatory cytokine IL-6 release as determined using a human IL-6 ELISA kit according to the manufacturer's protocol as previously.[24] Cell supernatants were used to detect IL-6 release in A549 cells, and each group was evaluated in duplicate. The results are expressed as pg/mL.

Statistical analysis

The results of each experiment were analyzed with One-Way ANOVA and Tukey's post hoc tests. The statistical significance was accepted as $p < 0.05$ and determined by GraphPad Prism 9.0 Software (LaJolla, California, USA).

RESULTS

Nicotine level in THS

According to the LCMS analysis of the THS extract prepared from 2 of 3R4F cigarettes (100%, v/v), the nicotine concentration of samples was recorded as 0.287 mg/mL (Supplementary Table 2) according to the prepared nicotine standard calibration curve. The mass spectrums and chromatograms of nicotine standards were also given in Supplementary Figure S2-S7, and for THS sample, given as Supplementary Figure S8.

Cytotoxicity

The cytotoxicity of THS and its co-exposure to H_2O_2 *via* the MTT assay showed that THS induced dose-dependent cytotoxicity in A549 cells, remarkably at 50-100% (*v/v*) ($p < 0.05$) (Figure 1A). Based on this finding, THS 50% (*v/v*) (approximate IC_{50} value) was selected for further assessments of the cytotoxicity of THS under respiratory oxidative conditions *in vitro*.

As a step to assess the exacerbative effect of THS under respiratory oxidative conditions, A549 cells were co-exposed to a selected dose of THS (50%, *v/v*) and 100 µM H_2O_2. The results showed that THS significantly reduced cell viability under oxidative conditions compared with the control group ($p < 0.001$). On the other hand, 2 hours of pre-treatment with a potent antioxidant, NAC (1 mM), a powerful antioxidant, significantly reduced the cytotoxicity induced by THS and H_2O_2 alone, as well as their combination (Figure 1B).

Respiratory oxidative damage by THS in H_2O_2-stimulated cells

The oxidative stress conditions of A549 cells exposed to THS, H_2O_2, and THS + H_2O_2 after pre-treatment with NAC indicated the antioxidant capacity of NAC in the present study. According to our findings, THS led to a significant increase in oxidative stress by reducing GSH levels and elevating CAT activity ($p < 0.01$) (Figure 2). In parallel, lipid peroxidation was significantly increased by THS exposure. The oxidative effect of H_2O_2 exposure used in the *in vitro* modeling of COPD notably upregulated CAT activity and MDA levels, which were also elevated with co-exposure. In addition, pre-treatment with NAC significantly ameliorated the oxidative responses of THS alone and under COPD conditions induced by H_2O_2 (Figure 2).

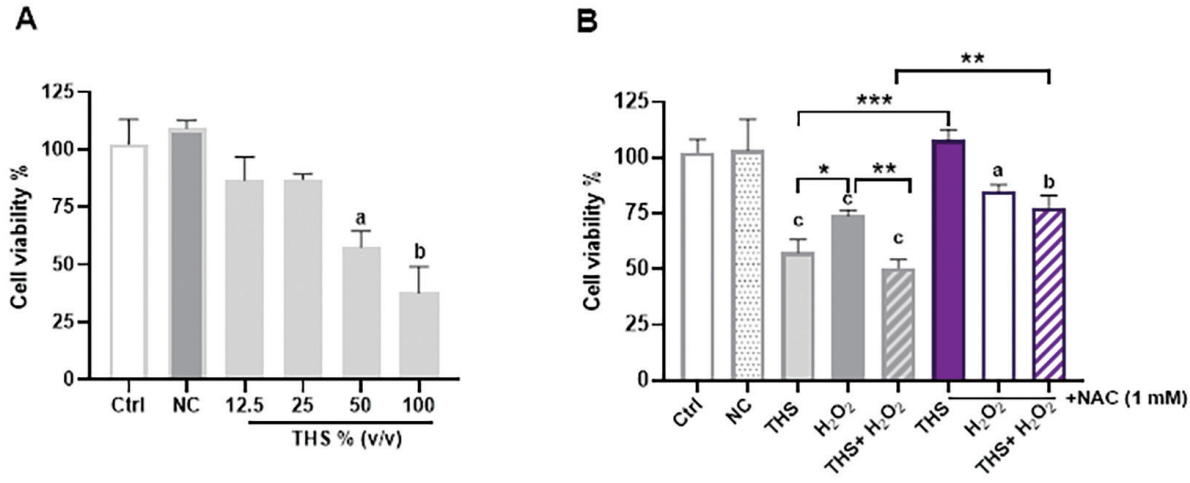

Figure 1. Cell viability of A549 cells exposed to THS with or without H_2O_2. A) Dose-dependent cytotoxicity profile of THS; B) Statistical significance between the Ctrl and groups $^{a}p < 0.05$, $^{b}p < 0.01$, $^{c}p < 0.001$; the significance between the two groups $^{*}p < 0.05$; $^{**}p < 0.01$ and $^{***}p < 0.001$. NAC: (1 mM) applied a 2-hour pre-treatment; THS: extract (50%, *v/v*); H_2O_2: 100 µM. The data were shown as mean ± SD

NAC: N-acetylcysteine, THS: Third-hand smoke, SD: Standard deviation

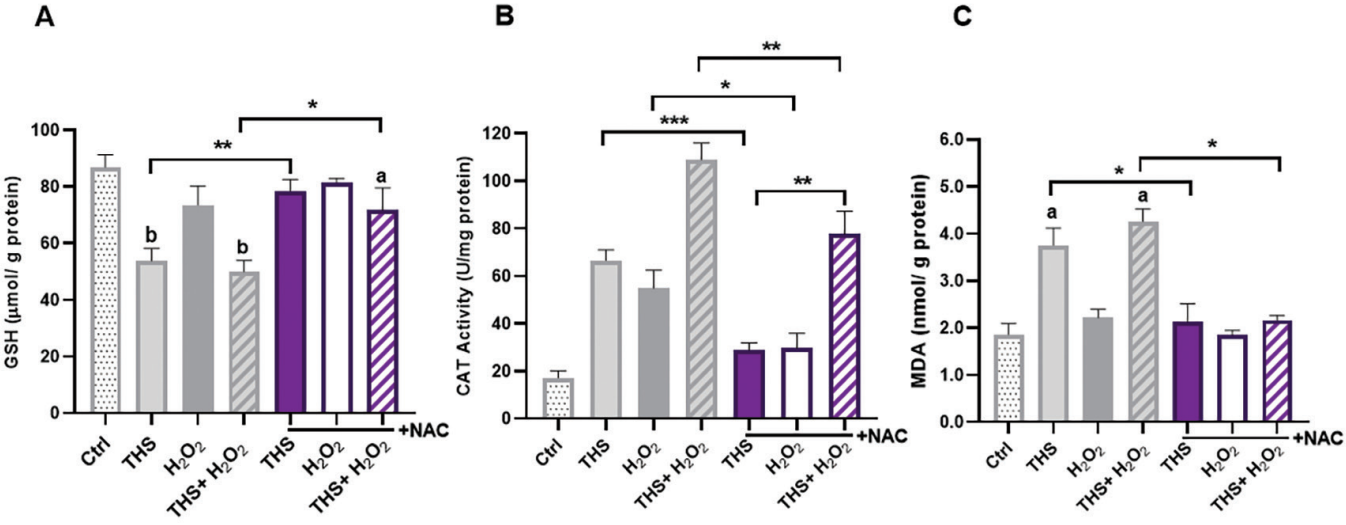

Figure 2. Modulation of oxidative stress and lipid peroxidation by THS and co-exposure with H_2O_2. A) Total GSH level; B) CAT activity; C) MDA level in A549 cells co-treated with THS and H_2O_2. Statistical significance between the Ctrl and groups $^{a}p < 0.05$, $^{b}p < 0.01$; the significance between the two groups $^{*}p < 0.05$; $^{**}p < 0.01$ and $^{***}p < 0.001$. NAC: (1 mM) applied as 2 hours pre-treatment; THS: extract (50%, *v/v*); H_2O_2: 100 µM. The data were shown as mean ± SD

NAC: N-acetylcysteine, THS: Third-hand smoke, SD: Standard deviation, GSH: Glutathione, CAT: Catalase, MDA: Malondialdehyde

Intracellular ROS levels

In the present study, total ROS levels were measured in A549 cells exposed to THS alone or in combination with H_2O_2. Based on our findings, THS exposure itself significantly elevated intracellular ROS production ($p < 0.05$) compared with the control group in A549 cells. Furthermore, this increase in ROS levels was intensified by co-exposure to H_2O_2 ($p < 0.01$) (Figure 3) Similar to the results of the oxidative stress assays, NAC pretreatment improved the elevated ROS production levels and decreased the relative ROS levels significantly in all THS-exposed groups ($p < 0.01$), possibly due to the replenishment of intracellular GSH deposits.

IL-6 level

The present findings revealed that residual THS exposure and its co-exposure to H_2O_2 significantly induced IL-6 release in A549 cells, and this response declined after NAC pre-treatment (Figure 4). The inflammatory response of the THS co-exposed COPD group was notably higher than that of the THS alone group despite NAC pre-treatment.

DISCUSSION

THS, a recent concept in environmental toxicology, can attach to surfaces for long periods, even after the smoke has cleared. Children are particularly susceptible to THS exposure because

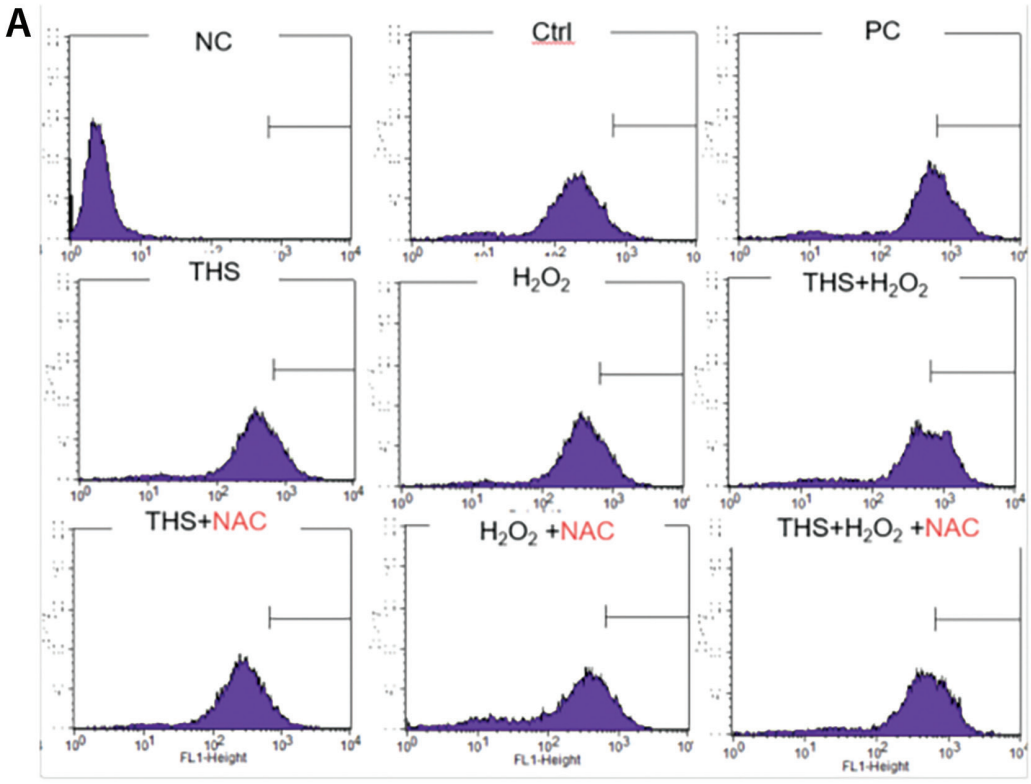

Figure 3. Intracellular ROS levels of A549 cells exposed to THS with or without H_2O_2. A) Representative histograms of the percentage increase in ROS accumulation in the groups. Enhancement of intracellular ROS levels was observed *via* the shift of the signal curve obtained for the THS and H_2O_2 treated cells to the right compared with that of the control. B) Relative ROS percentage of A549 cells exposed to THS with or without H_2O_2. Statistical significance between Ctrl vs. groups $^{a}p < 0.01$; $^{b}p < 0.05$; the significance between the two groups $^{*}p < 0.05$; $^{**}p < 0.01$. NAC: (1 mM) applied as a 2 hours pre-treatment; NC: Cells *w/o* DCFDA; THS: extract (50%, *v/v*); H_2O_2: 100 µM; THBP (100 µM)

THS: Third-hand smoke, PC: Positive control, NAC: N-acetylcysteine, ROS: Reactive oxygen species, DCFDA: 2,7-dichlorofluorescein diacetate, THBP: Tert-butyl hydroperoxide, NC: Negative control

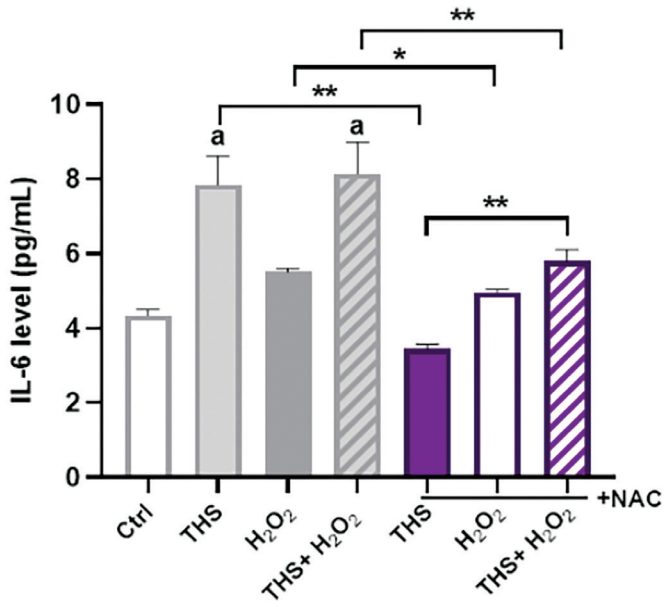

Figure 4. IL-6 release induced by THS and its co-exposure to H_2O_2 in A549 cells. Statistical significance between Ctrl vs. groups $^{a}p < 0.05$; the significance between the two groups $*p < 0.05$; $**p < 0.01$. NAC: (1 mM) applied a 2-hour pre-treatment; THS: extract (50%, *v/v*); H_2O_2: 100 µM. The data were shown as mean ± SD

NAC: N-acetylcysteine, THS: Third-hand smoke, IL-6: Interleukin-6, SD: Standard deviation

they are more likely to come into contact with smoke-embedded surfaces. Although parental precautions might protect this population against residual toxins, people with respiratory conditions, such as asthma and COPD, are still at increased risk of health problems due to involuntary THS exposure. In the present study, we have investigated the accelerative potential of THS in an H_2O_2-induced oxidative stress model of human airway epithelia *in vitro*.

Based on our findings, the present study showed that THS exposure can lead to cytotoxicity, oxidative stress, and an elevated proinflammatory response in human airway epithelia *in vitro*. Increased inflammation and oxidative stress due to tobacco smoke exposure either as second-hand or first-hand smoke are important indicators of chronic airway diseases in general and IL-6 plays a role in several inflammatory and immune responses, including the acute phase response, response to infections, and development of chronic diseases, such as rheumatoid arthritis and COPD.[25-27] In COPD, IL-6 levels are elevated in the blood and airways, contributing to the development and progression of COPD by promoting inflammation, impairing lung function, and increasing the risk of disease exacerbations.[26,27] Based on this context, exposure to THS may be a significant issue that must be addressed for people with respiratory diseases. Recent studies have shown that dose-dependent THS exposure decreases cell survival in human dermal fibroblasts, mouse neural stem cells, human palatal mesenchyme,[4] human hepatocellular carcinoma cells,[28] and male rodent reproductive cells.[29] In the present study, THS extracts reduced the viability of A549 cells, similar to previously reported data,[4,30,31] dose-dependently. Therefore, the complex chemical content of THS may lead to cytotoxicity in human airway epithelia, mostly *via* mitochondrial cell viability. In addition to its cytotoxic potential, co-exposure to H_2O_2 further increased the cytotoxicity response in the human airway epithelia. Moreover, it is well known that intracellular increases in the production of ROS are important parameters for evaluating the imbalance between the oxidative response and the body's ability to neutralize them. Since oxidative stress is believed to play a role in the development and progression of COPD and other respiratory disorders, detecting ROS levels might represent a preliminary marker for further lung tissue damage, which may lead to inflammation and impaired lung function.[12] Based on this finding, THS may interact with other environmental or exogenous oxidant factors to increase its toxicity. Moreover, THS induced the production of intracellular ROS, CAT activity, and depleted GSH deposits, which help detoxify ROS in A549 cells. In addition, THS increased lipid peroxidation, as well. However, these oxidative stress-induced toxicity responses were significantly alleviated by NAC pretreatment. Previously, Boskabady and Gholami Mahtaj[30] reported that the CS-induced COPD model in guinea pigs led to a significant decrease in the level of the thiol group in experimental animals, which was reversed by carvacrol pretreatment by boosting intracellular antioxidant capacity. As reported in our previous study,[21] exposure to CS and its components may lead to an excessive increase in CAT activity in the target organ, probably due to the presence of higher peroxide concentrations. In addition, the decreases in GSH and increased MDA levels in A549 cells clearly indicate that antioxidant defense mechanisms are not sufficient to prevent lipid peroxidation due to THS exposure either alone or in combination with H_2O_2. Similarly, *in vitro* studies using CS suggested a significant deposition of intracellular antioxidant enzymatic/non-enzymatic capacity[23] as well as an elevated inflammatory response.[23,31,32] It has been reported that overproduced free radicals react with cellular and humoral components, permanently impairing their function and triggering inflammatory responses.[33] However, there are limited studies on the residual portion of CS, such as THS, and its possible inflammatory and oxidant potency in respiratory disease conditions. In addition, the exposure and extraction conditions of THS might change the severity of these detrimental effects on the respiratory system under oxidative conditions. In the present study, the prepared THS extract had a nicotine level of approximately 0.28 mg/mL (0.28 mg/g fabric), whereas samples extracted from indoor or outdoor surfaces or under different extraction conditions might change this nicotine level dramatically from 2-12 g nicotine/g fabric.[4] Therefore, the observed toxicity outcomes in the literature might differ in proportion to the accumulation and extraction capacity of other expected chemicals present in THS such as VOCs, TSNAs, and PAHs.

THS in the environment might contribute to the inflammatory and oxidative complications of chronic airway conditions initially mediated by oxidative stress. It is known that the inhalation of

PAHs and various VOCs is responsible for oxidative damage and inflammation through the induction of mitochondrial free radical formation.[34] Furthermore, a major concern may arise due to environmental THS exposure because smoking with COPD has the highest correlation with all types of lung cancer and the development of small-cell lung cancer.[34,35] Therefore, as an indirect source of CS, THS might be a significant contributing risk factor for lung cancer development in this population. As a result, the present preliminary findings are important for elucidating the toxicological key points involved in cell survival/death in target organs with respiratory disease due to THS exposure.

CONCLUSION

Based on the present findings, co-exposure to THS may lead to more detrimental effects in human airways *in vitro*. Hence, it can be concluded that as an environmental residue, THS may play a role in the progression of chronic respiratory diseases, which are mediated through oxidative and inflammatory exacerbations in human airway epithelia. Further studies are needed to confirm these mechanisms by which THS is exerted and to help identify approaches to reduce environmental THS exposure.

Acknowledgment

The study was presented as a poster at the Society of Toxicology 61st Annual Meeting and ToxExpo 2022 (San Diego, California, USA) with a travel grant from The Scientific and Technological Research Council of Türkiye 2224-A program.

Ethics

Ethics Committee Approval: Not required.

Informed Consent: Not required.

Authorship Contributions

Concept: R.R., K.K., Design: R.R., K.K., Data Collection or Processing: R.R., K.K., G.P.C., Analysis or Interpretation: R.R., K.K., Y.Ö., G.P.C., H.S., Literature Search: R.R., K.K., Writing: R.R., H.S.

Conflict of Interest: No conflict of interest was declared by the authors.

Financial Disclosure: The authors declared that this study received no financial support.

REFERENCES

1. Acuff L, Fristoe K, Hamblen J, Smith M, Chen J. Third-hand smoke: old smoke, new concerns. J Community Health. 2016;41:680-687.
2. Matt GE, Quintana PJ, Destaillats H, Gundel LA, Sleiman M, Singer BC, Jacob P, Benowitz N, Winickoff JP, Rehan V, Talbot P, Schick S, Samet J, Wang Y, Hang B, Martins-Green M, Pankow JF, Hovell MF. Thirdhand tobacco smoke: emerging evidence and arguments for a multidisciplinary research agenda. Environ Health Perspect. 2011;119:1218-1226.
3. Liu H, Chen H. The effects of thirdhand smoke on reproductive health. J Appl Toxicol. 2022;42:172-179.
4. Bahl V, Shim HJ, Jacob P 3rd, Dias K, Schick SF, Talbot P. Thirdhand smoke: Chemical dynamics, cytotoxicity, and genotoxicity in outdoor and indoor environments. Toxicol *In Vitro.* 2016;32:220-231.
5. Jacob P 3rd, Benowitz NL, Destaillats H, Gundel L, Hang B, Martins-Green M, Matt GE, Quintana PJ, Samet JM, Schick SF, Talbot P, Aquilina NJ, Hovell MF, Mao JH, Whitehead TP. Thirdhand Smoke: New Evidence, Challenges, and Future Directions. Chem Res Toxicol. 2017;30:270-294.
6. Matt GE, Quintana PJE, Hoh E, Dodder NG, Mahabee-Gittens EM, Padilla S, Markman L, Watanabe K. Tobacco smoke is a likely source of lead and cadmium in settled house dust. J Trace Elem Med Biol. 2021;63:126656.
7. Zhang J, Lin XF, Bai CX. Comparison of clinical features between non-smokers with COPD and smokers with COPD: a retrospective observational study. Int J Chron Obstruct Pulmon Dis. 2014;9:57-63.
8. Yoshida M, Minagawa S, Araya J, Sakamoto T, Hara H, Tsubouchi K, Hosaka Y, Ichikawa A, Saito N, Kadota T, Sato N, Kurita Y, Kobayashi K, Ito S, Utsumi H, Wakui H, Numata T, Kaneko Y, Mori S, Asano H, Yamashita M, Odaka M, Morikawa T, Nakayama K, Iwamoto T, Imai H, Kuwano K. Involvement of cigarette smoke-induced epithelial cell ferroptosis in COPD pathogenesis. Nat Commun. 2019;10:3145.
9. Safiri S, Carson-Chahhoud K, Noori M, Nejadghaderi SA, Sullman MJM, Ahmadian Heris J, Ansarin K, Mansournia MA, Collins GS, Kolahi AA, Kaufman JS. Burden of chronic obstructive pulmonary disease and its attributable risk factors in 204 countries and territories, 1990-2019: results from the Global Burden of Disease Study 2019. BMJ. 2022;378:e069679.
10. Crotty Alexander LE, Shin S, Hwang JH. Inflammatory diseases of the lung induced by conventional cigarette smoke: a review. Chest. 2015;1481307-1322.
11. CDC. What is COPD? Accessed at: https://www.cdc.gov/copd/about/index.html
12. Jiao Z, Zhang Q, Chang J, Nie D, Li M, Zhu Y, Wang C, Wang Y, Liu F. A protective role of sulforaphane on alveolar epithelial cells exposed to cigarette smoke extract. Exp Lung Res. 2013;39:379-386.
13. Schweitzer KS, Hatoum H, Brown MB, Gupta M, Justice MJ, Beteck B, Van Demark M, Gu Y, Presson RG Jr, Hubbard WC, Petrache I. Mechanisms of lung endothelial barrier disruption induced by cigarette smoke: role of oxidative stress and ceramides. Am J Physiol Lung Cell Mol Physiol. 2011;301:836-846.
14. Martins-Green M, Adhami N, Frankos M, Valdez M, Goodwin B, Lyubovitsky J, Dhall S, Garcia M, Egiebor I, Martinez B, Green HW, Havel C, Yu L, Liles S, Matt G, Destaillats H, Sleiman M, Gundel LA, Benowitz N, Jacob P 3rd, Hovell M, Winickoff JP, Curras-Collazo M. Cigarette smoke toxins deposited on surfaces: implications for human health. PLoS One. 2014;9:e86391.
15. Kolci K, Garipkuş SN, Reis R. Thirdhand smoke exposure and its toxicological impacts: A review on target organ based studies. Fabad J Pharm Sci. 2023;48:303-318.
16. Kirkham PA, Barnes PJ. Oxidative stress in COPD. Chest. 2013;144:266-273.
17. Polosa R, Thomson NC. Smoking and asthma: dangerous liaisons. Eur Respir. 2013;41:716-726.
18. Mims JW. Asthma: definitions and pathophysiology. Int Forum Allergy Rhinol. 2015;5(Suppl 1):2-6.
19. BSI. Biological Evaluation of Medical Devices Part 12: Sample Preparation and Reference Materials (ISO 10993-12:2007); 2009.
20. Reis R, Kolci K. Comparative toxicity responses of thirdhand smoke derived from conventional cigarette and heated tobacco products in human bronchial epithelial cells. Experimed. 2023;13:127-132.

21. Reis R, Kolci K, Bahcivan İ, Coskun GP, Sipahi H. Alpha-lipoic acid modulates the oxidative and inflammatory responses induced by traditional and novel tobacco products in human liver epithelial cells. Chem Biodivers. 2023;20:e202200928.

22. Hsu JY, Chu JJ, Chou MC, Chen YW. Dioscorin pre-treatment protects A549 human airway epithelial cells from hydrogen peroxide-induced oxidative stress. Inflammation. 2013;36:1013-1019.

23. Reis R, Orak D, Yilmaz D, Cimen H, Sipahi H. Modulation of cigarette smoke extract-induced human bronchial epithelial damage by eucalyptol and curcumin. Hum Exp Toxicol. 2021;40:1445-1462.

24. Aslani MR, Amani M, Moghadas F, Ghobadi H. Adipolin and IL-6 Serum Levels in Chronic Obstructive Pulmonary Disease. Adv Respir Med. 2022;90:391-398.

25. Mazarakis N, Higgins RA, Anderson J, Toh ZQ, Luwor RB, Snibson KJ, Karagiannis TC, Do LAH, Licciardi PV. The effects of the dietary compound L-sulforaphane against respiratory pathogens. Int J Antimicrob Agents. 2021;58:106460.

26. Fischer BM, Pavlisko E, Voynow JA. Pathogenic triad in COPD: oxidative stress, protease-antiprotease imbalance, and inflammation. Int J Chron Obstruct Pulmon Dis. 2011;6:413-421.

27. Zuo L, He F, Sergakis GG, Koozehchian MS, Stimpfl JN, Rong Y, Diaz PT, Best TM. Interrelated role of cigarette smoking, oxidative stress, and immune response in COPD and corresponding treatments. Am J Physiol Lung Cell Mol Physiol. 2014;307:205-218.

28. Hang B, Sarker AH, Havel C, Saha S, Hazra TK, Schick S, Jacob P 3rd, Rehan VK, Chenna A, Sharan D, Sleiman M, Destaillats H, Gundel LA. Thirdhand smoke causes DNA damage in human cells. Mutagenesis. 2013;28:381-391.

29. Hang B, Wang P, Zhao Y, Sarker A, Chenna A, Xia Y, Snijders AM, Mao JH. Adverse health effects of thirdhand smoke: from cell to animal models. Int J Mol Sci. 2017;18:9321.

30. Boskabady MH, Gholami Mahtaj L. Lung inflammation changes and oxidative stress induced by cigarette smoke exposure in guinea pigs affected by Zataria multiflora and its constituent, carvacrol. BMC Complement Altern Med. 2015;15:39.

31. Tan WSD, Liao W, Peh HY, Vila M, Dong J, Shen HM, Wong WSF. Andrographolide simultaneously augments Nrf2 antioxidant defense and facilitates autophagic flux blockade in cigarette smoke-exposed human bronchial epithelial cells. Toxicol Appl Pharmacol. 2018;360:120-130.

32. Lin XX, Yang XF, Jiang JX, Zhang SJ, Guan Y, Liu YN, Sun YH, Xie QM. Cigarette smoke extract-induced BEAS-2B cell apoptosis and anti-oxidative Nrf-2 up-regulation are mediated by ROS-stimulated p38 activation. Toxicol Mech Methods. 2014;24:575-583.

33. Lugrin J, Rosenblatt-Velin N, Parapanov R, Liaudet L. The role of oxidative stress during inflammatory processes. Biol Chem. 2014;395:203-230.

34. Wu JX, Lau ATY, Xu YM. Indoor secondary pollutants cannot be ignored: third-hand smoke. Toxics. 2022;10:363.

35. Taucher E, Mykoliuk I, Lindenmann J, Smolle-Juettner FM. Implications of the Immune Landscape in COPD and Lung Cancer: Smoking Versus Other Causes. Front Immunol. 2022;13:846605.

Supplementary Document of "Third-Hand Smoke Induces COPD Exacerbations in Human Airway Epithelia *In Vitro*"

Chromatographic conditions

Materials

(-)-Nicotine, acetonitrile, methanol, and glacial acetic acid were purchased from Sigma (USA). Deionized water was obtained from the Sartorius Arium Pro (Germany) water purification system and was used to prepare mobile phase solutions. All other chemicals used were of analytical grade.

Preparation of standard solutions

(-)-Nicotine is freely soluble in methanol. The stock solution was prepared as 9 mg/mL The stock solutions were then diluted with methanol within the concentration range of 0.70-1.62 mg/mL.

Instrumentation and chromatographic conditions

Agilent 1260 Infinity II series of LCMS systems (USA) equipped with a solvent pump, manual injection valve, and a diode-array detector were used. The quantitative analysis of nicotine was performed with the C18 column (particle size: 3 µm, pore size: 100A). The column temperature was adjusted to 30 ºC in the column compartment. The mobile phase consisted of an acetonitrile- 0.1% glacial acetic acid solution (95:5, v/v) mixture and was delivered at a 0.6 mL/min flow rate. The injection volume was 20 µL. The ultraviolet detector was operated at 254 nm.

Calibration curve

The calibration curve was calculated according to area under the curve vs. concentration values. Six dilutions were used for the calculation of the equation and R2 value. The area of the standard peaks were calculated according to their mass values (Supplementary Figure S1, Supplementary Table 1).

Supplementary Table 1. Nicotine standard dilutions were used for the calibration curve.

Dilutions	Concentration (mg/mL)	Area (mAU)
1	0.70	7070.36
2	0.93	10774
3	1.08	13313.3
4	1.25	16146.6
5	1.43	19125,5
6	1.62	22231.2

mAU: Milli-absorbance units

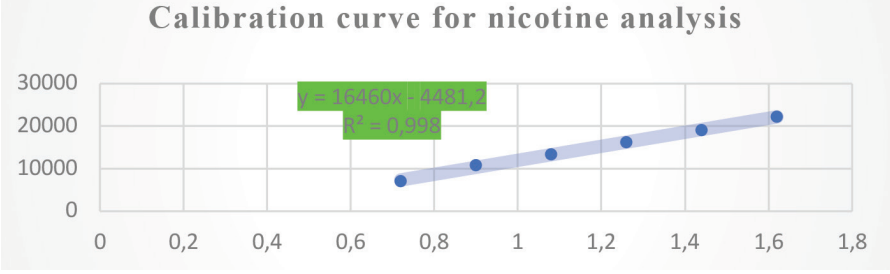

Supplementary Figure S1. Calibration curve of nicotine analysis

Calibration curve equation:

y= 16460x-4481.2

R^2: 0.998

Detection of the nicotine content of third-hand smoke

Nicotine analysis was performed for THS samples prepared from 2 of 3R4F research cigarettes and injected into the liquid chromatography-mass spectrometry system immediately. The area under the curve of the sample is given in Supplementary Table 2.

Supplementary Table 2. Peak area and nicotine concentration of THS

Test sample	Concentration (mg/mL)	Area (MAU)
Control	ND	-
THS sample	0.2872	246.965

THS: Third-hand smoke

Supplementary Mass spectrum and chromatograms of nicotine standards and chromatograms of third-hand smoke samples are given below:

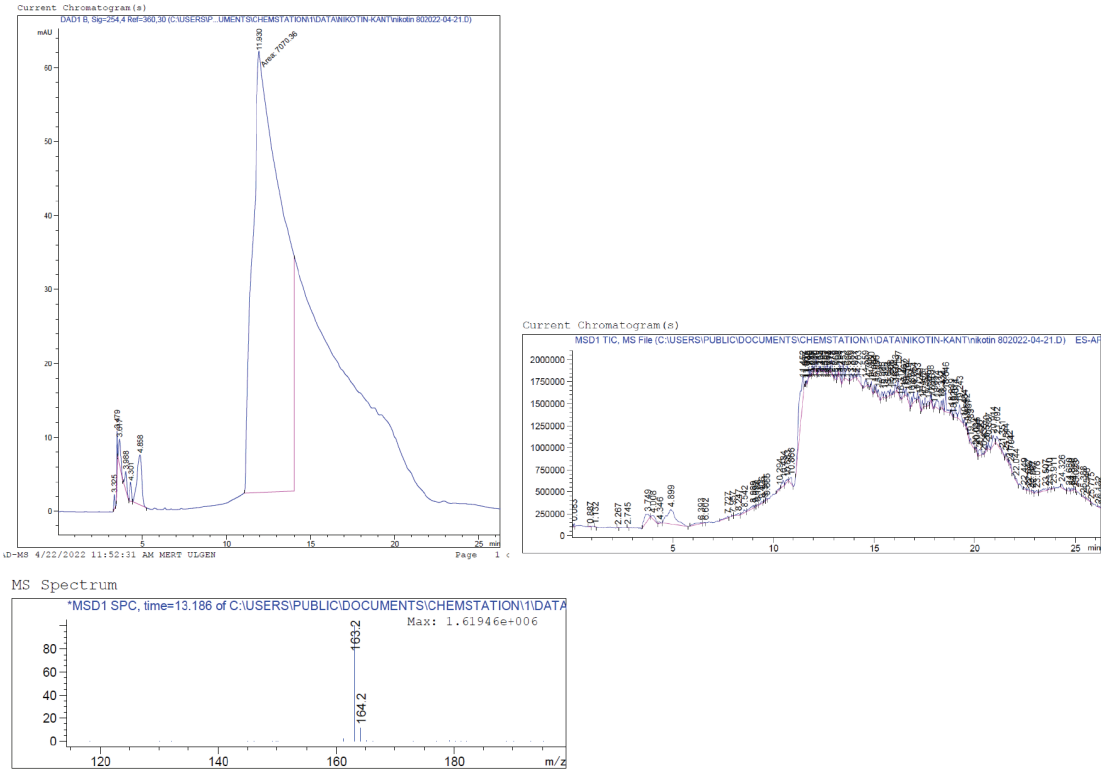

Supplementary Figure S2. AUC, Mass spectrum, and chromatogram of dilution 1

AUC: Area under the curve

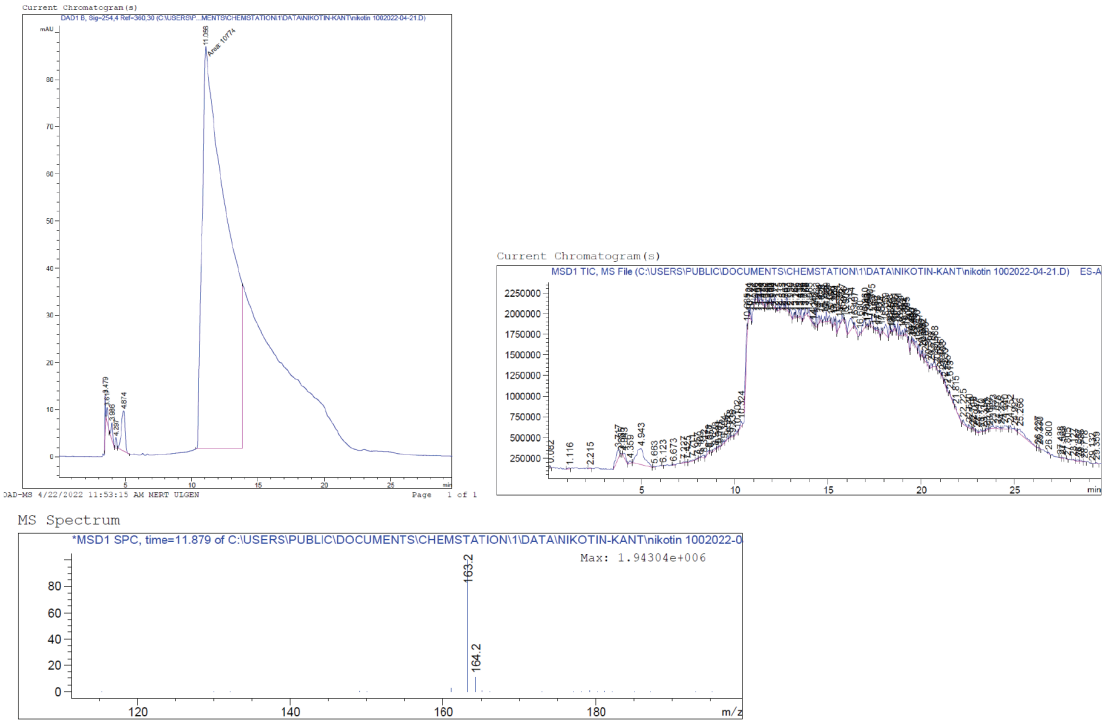

Supplementary Figure S3. AUC, Mass spectrum, and chromatogram of dilution 2
AUC: Area under the curve

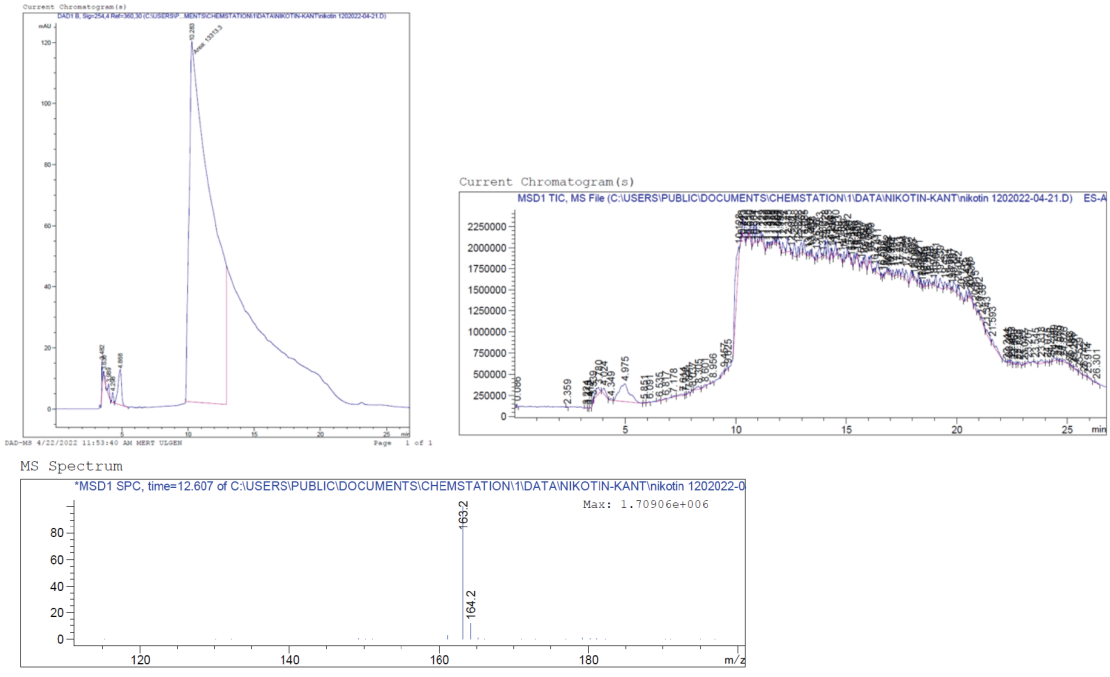

Supplementary Figure S4. AUC, Mass spectrum, and chromatogram of dilution 3
AUC: Area under the curve

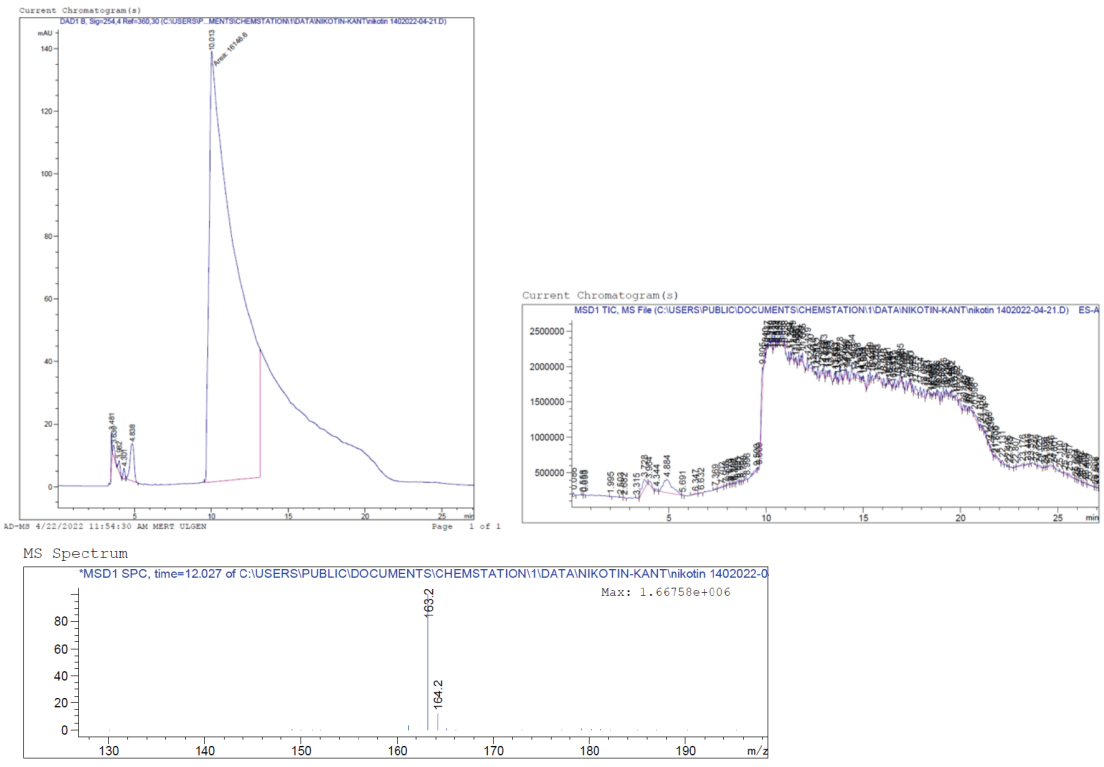

Supplementary Figure S5. AUC, Mass spectrum, and chromatogram of dilution 4
AUC: Area under the curve

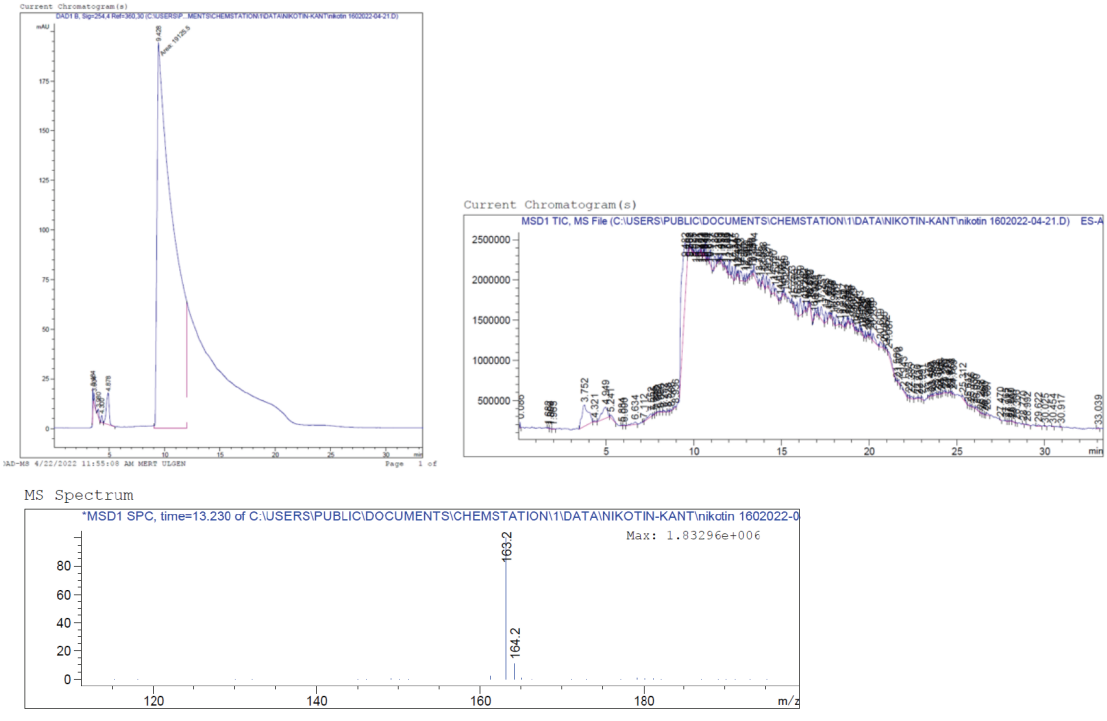

Supplementary Figure S6. AUC, Mass spectrum, and chromatogram of dilution 5
AUC: Area under the curve

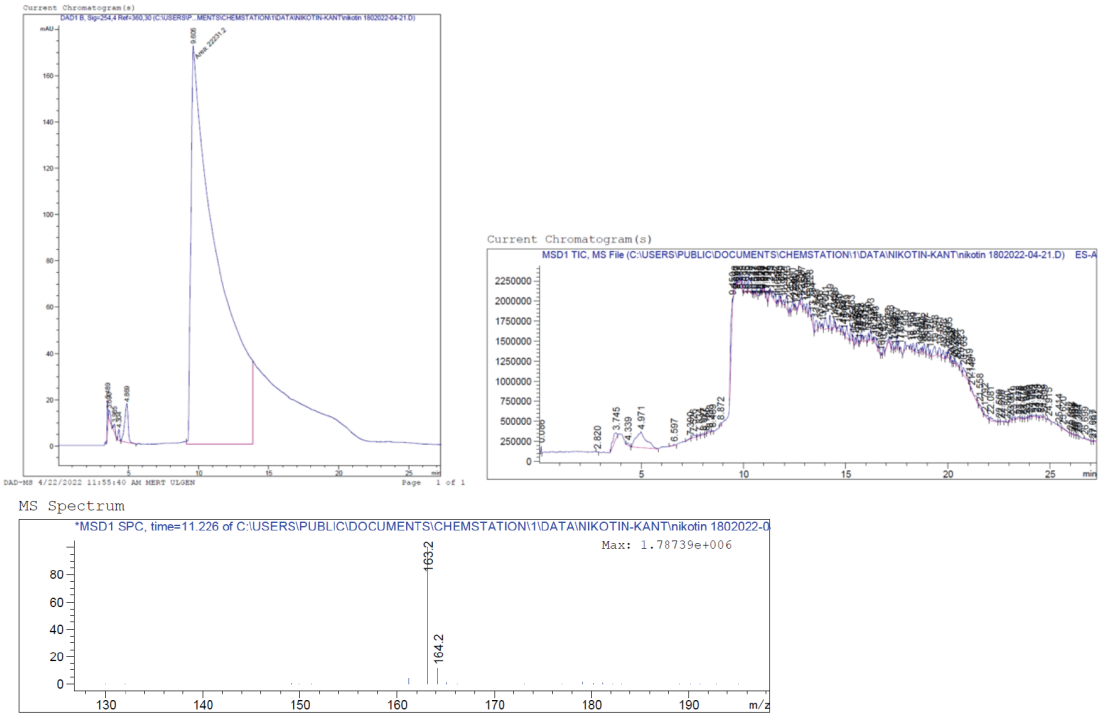

Supplementary Figure S7. AUC, Mass spectrum, and chromatogram of dilution 6

AUC: Area under the curve

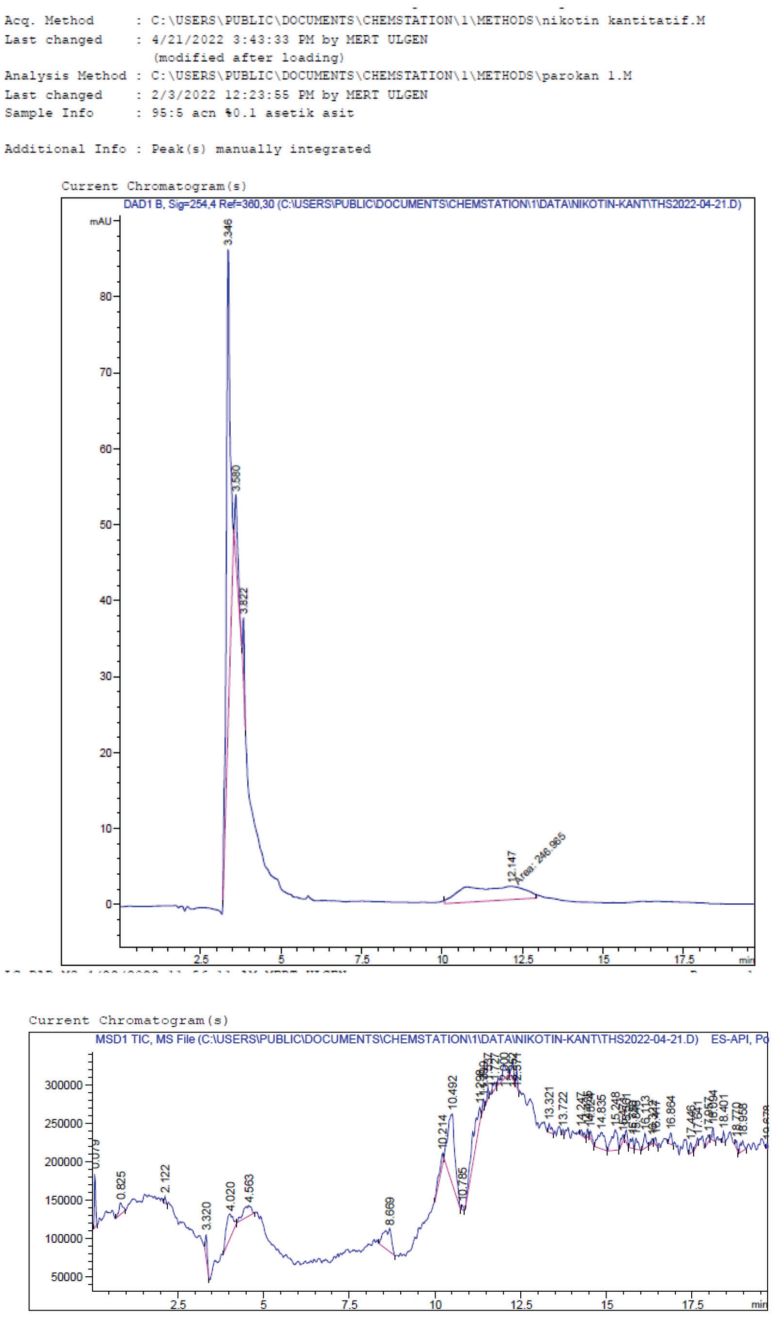

Supplementary Figure S8. Chromatogram and mass spectrum of THS sample
THS: Third-hand smoke

Turk J Pharm Sci 2024;21(5):390-398
DOI: 10.4274/tjps.galenos2024.07944

ORIGINAL ARTICLE

Time-Dependent Relationship Between Endothelial Dysfunction and High Blood Pressure in Fructose Drinking Rats

Abdelrahman HAMAD, Melike Hacer ÖZKAN*

Hacettepe University Faculty of Pharmacy, Department of Pharmacology, Ankara, Türkiye

ABSTRACT

Objectives: This study aims to investigate the duration required for endothelium dysfunction to develop in the fructose drinking-induced hypertension and examine the relative contributions of endothelium-dependent relaxing factors to changes in mesenteric arterial reactivity in male Wistar Albino rats.

Materials and Methods: Metabolic parameters (water intake and food consumption) and hemodynamic parameters systolic blood pressure (SBP) and diastolic blood pressure (DBP)-were monitored *in vivo*. Vascular reactivity was examined in the isolated organ bath. Endothelium-dependent relaxation (EDR) to acetylcholine was observed in the absence and presence of pharmacological inhibitors of endothelial nitric oxide (NO) synthase, cyclooxygenase, and KCa2.3 channels. Contractile responses to phenylephrine and relaxation of sodium nitroprusside (SNP) were also determined.

Results: A significant increase in daily water intake and decrease in food consumption were typically observed in rats treated with 10% fructose for 4 weeks ($p < 0.05$). SBP and DBP increased significantly as early as 2 weeks of induction and continued to rise gradually throughout the induction period ($p < 0.05$). Fructose consumption significantly impaired EDR at week 3 and worsened at week 4 ($p < 0.05$). Impairment of the KCa3.1 channel-mediated component of endothelium-dependent hyperpolarisation (EDH)-type relaxation contributed to worsening EDR, whereas the contribution of NO-mediated relaxation was not apparent compared with the controls. The reduction in EDH-type relaxation in fructose-fed rats appears to be partially compensated by increased NO sensitivity in the smooth muscle region, as fructose induction increased SNP relaxation compared with the control.

Conclusion: These data provide evidence of early endothelial dysfunction developing concurrently with increased blood pressure in 10% fructose-fed rats. Decreased KCa3.1-mediated part of EDH-type relaxation appears to contribute to the impairment of endothelium-dependent vasorelaxation over time in this model.

Keywords: Endothelial dysfunction, fructose, hypertension, mesenteric artery, rat

INTRODUCTION

In The 1970s, it has been seen the introduction of high fructose corn syrup as an affordable alternative for sweetening processed foods and soft drinks. Since then, there has been a progressive global increase in the consumption of packaged food containing fructose and corn syrup.[1-3] However, high fructose consumption in mice and rats has been associated with obesity, type 2 diabetes mellitus, insulin resistance in the liver and extrahepatic tissues, and elevated blood pressure (BP).[4-7] In 1987, Hwang et al.[4] first reported that male Sprague-Dawley rats fed pellets containing 66% fructose for 2 weeks developed systolic hypertension with increased plasma insulin levels and insulin resistance.

*Correspondence: melikeo@hacettepe.edu.tr, Phone: +90 532 691 17 17 , ORCID-ID: orcid.org/0000-0003-1339-2616
Received: 20.12.2023, Accepted: 04.08.2024

Therefore, many investigations have been conducted to elucidate the underlying mechanism(s) of hypertension in this model. In summary, three main mechanisms through which high fructose consumption can raise BP have been reported: increased intestinal Na^+ absorption, central sympathetic outflow, and endothelial dysfunction.[8-10]

The vascular endothelium plays a vital role in regulating the vascular tone by releasing certain autocrine and paracrine factors.[11] In large-sized arteries, endothelium-dependent relaxation is achieved through diffusible factors like endothelium-derived nitric oxide (NO) and prostacyclin. In smaller arterioles and resistant arteries, the-opening of intermediate (KCa3.1)-and/or small (KCa2.3)-conductance calcium-activated potassium channels located on the endothelium triggers endothelial hyperpolarization that spreads toward smooth muscle and leads to vasorelaxation. This type of relaxation is called endothelium-dependent hyperpolarization (EDH)-type relaxation; in this way, the endothelium contributes to the regulation of regional blood flow and total peripheral vascular resistance in the microcirculation. Multiple studies have reported that fructose feeding diminishes NO production by reducing the activity and/or expression of endothelial NO synthase in the aorta, mesenteric artery, cardiac myocyte, and kidney homogenates.[12,13] Moreover, fructose utilization was reported to decrease acetylcholine-induced EDH-type relaxations.[9,14] Although these studies point to a possible link between endothelial dysfunction and the development of hypertension in the fructose-fed rat model, experiments need to be carried out, especially in the early period when fructose-induced endothelial changes begin to become evident and BP increases. Indeed, previous studies have been conducted to determine the inducing time required for endothelium dysfunction to occur in rats fed a 66% fructose diet.[15,16] Yet, these studies have been designed to deliver fructose in the rat's chow pellets,[14-16] and no such studies have been performed on the 10% *w/v* fructose in the drinking water design of the hypertensive rat model. Besides, most of these studies have been done on Sprague-Dawley rats, but not on the Wistar Albino rat strain. Whether Wistar rat strains respond to 10% fructose-water induction with endothelial dysfunction and to what extent they are sensitive to this model have not been previously studied in detail.

Consequently, in this study, it is aimed to determine the time required for the development of early endothelial dysfunction in 10% fructose drinking Wistar Albino rats. The second aim of this study is to examine its effect on the different components of endothelium-derived EDH-type relaxation in terms of increasing the duration of acute fructose consumption.

MATERIALS AND METHODS

Male Wistar Albino rats (8 weeks, 180-200 g) were obtained from Kobay Company (Ankara, Türkiye). Animals were housed for a week before the experiments to acclimatize to the laboratory settings and were maintained on a 12-hour light: 12-hour dark cycle. In compliance with institutional guidelines and the European Convention for the Protection of Vertebrate Animals used for Experimental and Other Scientific Purposes, the animals were handled and cared for as directed.

Animal procedures and protocols were approved by the Animal Ethics Committee of the University of Hacettepe (approval number: 2021/03-06, date: 30.03.2021).

Rats were divided randomly into four groups (n= 6 each). The fructose groups were given 10% fructose water (*w/v*) *ad libitum* for 3 and 4 weeks, whereas the control rats were given tap water for the same periods. All groups were fed standard rat chow. Water intake (mL/kg/day), food consumption (g/kg/day), and body weight (g/kg/day) were tracked twice weekly; systolic blood pressure [(SBP); mmHg], diastolic blood pressure [(DBP); mmHg], and heart rate [(HR); beats/minute] were measured weekly in all groups.

The non-invasive tail-cuff method was used for hemodynamic measurements (Biopac Systems, USA). Rats were habituated to the protocol 3 days before the experiments. Measurements were performed by the same researcher between 12:00 and 15:00. On the measurement day, the animals were kept in the procedure room (30 ± 2 °C) for 45 min and then sedated with isoflurane inhalation and oxygen mixture (5% induction and 1.5% maintenance) (Adeka, Türkiye).[17] Meanwhile, after the tails were warmed under a heat blanket, SBP, DBP, and HR were measured 5-6 times consecutively, and the average of the measurements was calculated.

For the *in vitro* organ bath experiments, rats in both the fructose (3 and 4 weeks) and control groups were euthanized by decapitation under CO_2 anesthesia. The superior mesenteric artery's main branch was cut and placed into a Petri dish with Krebs-Henseleit solution (KHS) at 4 °C. After removing the fat and connective tissues, the artery was divided into 2-mm-long rings. The rings were suspended at 37 °C in 5 mL organ baths filled with KHS gassed with 95% O_2-5% CO_2. One gram was determined as the optimum resting tension for the rings. The change in tension was measured by an isometric force transducer. Following an hour of rest, 80 mM KCl containing KHS was applied to the rings until consistent contractions were achieved.

In the main experiments, the assessment of vascular contractility required determining the total contractions to phenylephrine (10 nM-100 μM) for each group. After 1 h, the same rings were precontracted submaximally using 1 or 3 μM phenylephrine, and endothelium-dependent relaxations to acetylcholine (0.1 nM-10 μM) were then obtained. To examine the EDH-type component of acetylcholine relaxation, the same responses were repeated in the presence of N^w-nitro-L-arginine methyl ester (L-NAME; 100 μM), and indomethacin (10 μM), NO synthase inhibitors, and cyclooxygenase inhibitors, respectively. Moreover, a KCa3.1-mediated component of EDH-type vasorelaxation was also observed in rings incubated with L-NAME, indomethacin plus apamin (50 nM), a KCa2.3 channel blocker. In addition, to examine the NO-mediated component of acetylcholine-induced endothelial vasorelaxation, the same responses were repeated in the presence of indomethacin (10 μM), apamin (50 nM), and

TRAM-34 (1 μM), a KCa3.1 channel blocker. The incubation period was 45 minutes, and antagonist concentrations were selected using data from prior studies.[18-21] Finally, cumulative relaxation responses were obtained using sodium nitroprusside (SNP; 0.1 nM-10 μM), the NO donor.

Reagents

Fructose (Egepak Co., Türkiye) was dissolved in tap water. Acetylcholine chloride (Sigma-Aldrich, Germany, A6625), apamin (Sigma-Aldrich, A1289), L-NAME (Sigma, N-5751), L-phenylephrine hydrochloride (Sigma, P6126), and SNP (Sigma, S-0501) were dissolved in distilled water. Indomethacin (Sigma, I-7378) was dissolved in distilled water containing 0.7% Na_2CO_3 (*w/v*). KHS had the following composition (mM): NaCl 118.0, KCl 4.7, $MgSO_4$ 1.2, $CaCl_2$ 2.5, KH_2PO_4 1.2, $NaHCO_3$ 25.0 and glucose 11.1. NaCl was replaced with equimolar KCl to obtain an 80 mM KCl solution.

Statistical analysis

All data was displayed as the mean ± standard error of the mean. The contractions induced by KCl (80 mM) were used to standardize cumulative phenylephrine contractions, whereas the percentage of precontraction generated by phenylephrine was used to standardize relaxation. pD_2 values [-log(EC_{50})] were expressed as the negative logarithm of the drug concentration, which constitutes the half-maximum response, and the area under the curve (AUC) was expressed as arbitrary units. All analyses were conducted using GraphPad Prism 9.4.1. Comparisons between the two groups were performed using the unpaired *t*-test. $p < 0.05$ was considered significant.

Results

Metabolic characteristics of fructose-fed rats

The addition of 10% fructose to drinking water in rats for 4 weeks resulted in a significant increase in daily water intake and a decrease in food consumption compared with rats fed tap water ($p < 0.05$; n= 6). These changes were significantly different from the control during all weeks of induction. Both groups gained weight during the 4 weeks, but no significant difference was detected between them (Figure 1).

Effects of fructose on hemodynamic parameters

High fructose intake caused a moderate increase in SBP levels starting from week 2 compared with the control [SBP values; control (2 weeks) 116.8 ± 0.98 mm Hg vs. Fructose (2 weeks) 129.4 ± 2.90 mmHg; $p < 0.05$, n= 6]. The increase in SBP continued gradually as the fructose induction was prolonged to week 4 [SBP values; fructose (2 weeks) 129.4 ± 2.90 mmHg vs. fructose (3 weeks) 137.3 ± 3.50 mmHg (n= 6), and vs. fructose (4 weeks) 145.3 ± 5.30 mmHg; $p < 0.05$, n= 6] (Figure 2).

DBP also increased in parallel with the increase in SBP in rats fed high fructose [DBP values; fructose (2 weeks) 88.9 ± 2.40 mmHg vs. fructose (3 weeks) 97.7 ± 1.50 mmHg ($p < 0.01$, n= 6), and vs. fructose (4 weeks) 97.7 ± 1.30 mmHg ($p < 0.01$, n= 6]. However, HR did not differ significantly between the groups (Figure 2).

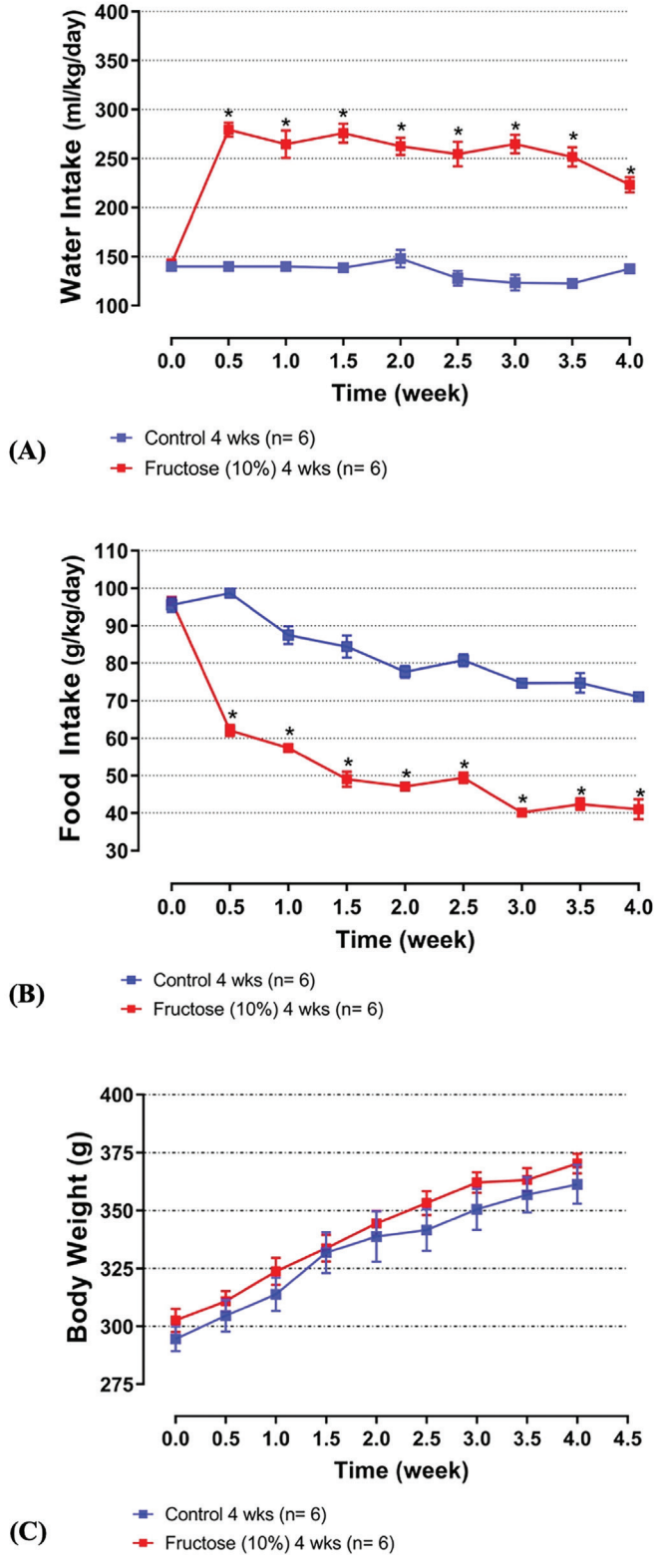

Figure 1. Change over time of daily water intake (A), food consumption (B), and body weight (C) in rats fed fructose (10%) or tap water (control) for 4 weeks (mean ± SEM, *fructose vs. control, unpaired t-test, *$p < 0.05$)

SEM: Standard error of the mean

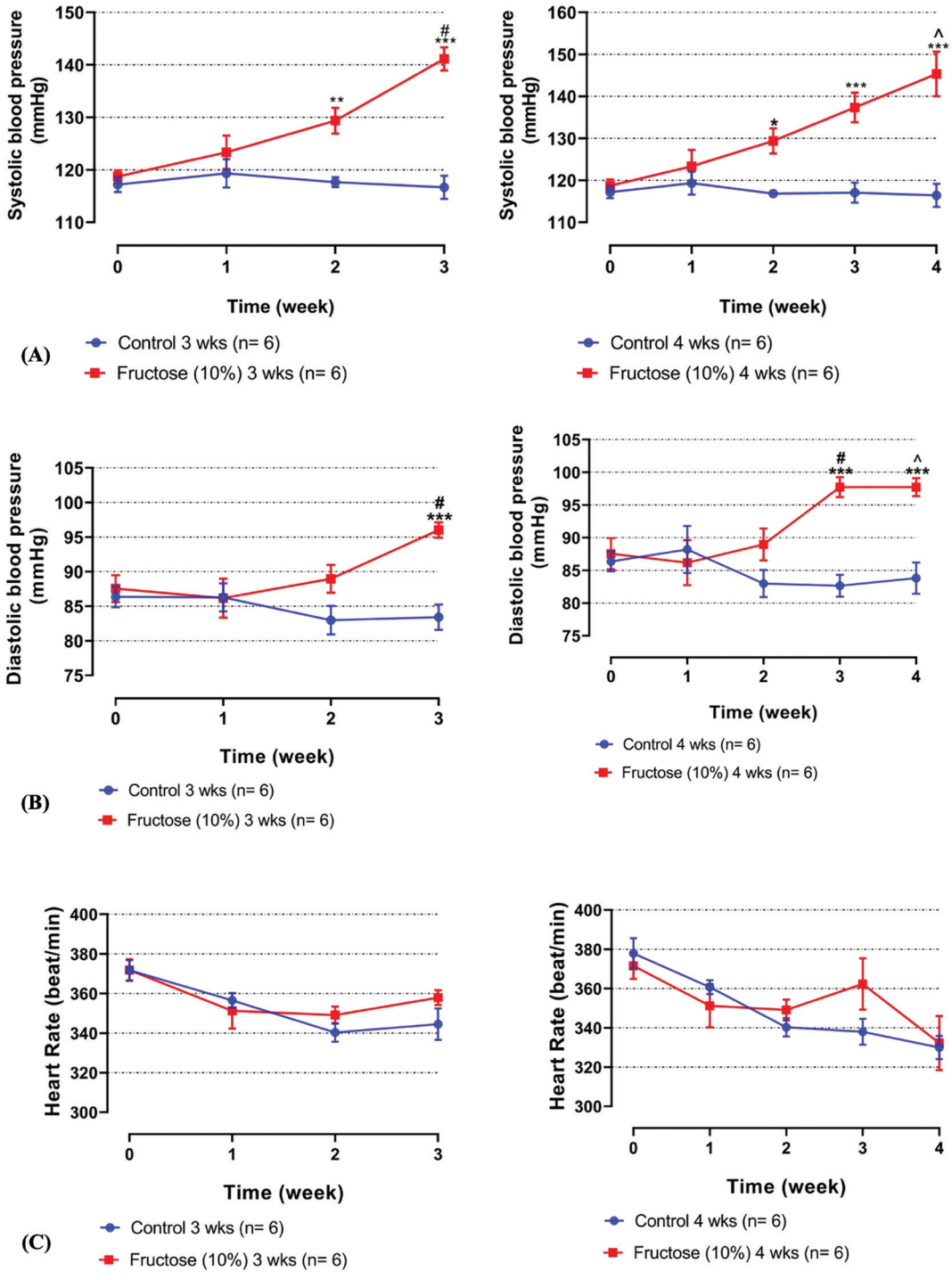

Figure 2. Change over time of SBP (A), DBP (B), and HR (C) in rats fed fructose (10%) or tap water (control) for 4 weeks (mean ± SEM, *fructose vs. control; #fructose 2nd vs. 3rd week; ^fructose 2nd vs. 4th week, unpaired *t*-test, *.#.^$p < 0.05$, ***$p < 0.001$)

SEM: Standard error of the mean, SBP: Systolic blood pressure, DBP: Diastolic blood pressure, HR: Heart rate

Effects of fructose on vascular reactivity

Cumulative contractions of phenylephrine (10 nM-100 µM) were examined in mesenteric arteries isolated from rats in the 3- and 4-week fructose groups. After 3 weeks of fructose induction, phenylephrine contractions were the same as those in the control (n= 6). When the induction period was extended to 4 weeks, a modest decrease in peak phenylephrine concentrations was observed, but the difference was not statistically significant (n= 6) (Figure 3). E_{max}, pD_2, and AUC values of contractile responses to phenylephrine were similar between the fructose groups (data not shown).

To assess endothelial function in fructose-fed rats, cumulative relaxation to acetylcholine (0.1 nM-10 µM) was observed in rings pre-contracted with phenylephrine (1 or 3 µM). Fructose

induction for 3 weeks led to a decrease in endothelium-dependent relaxation as opposed to contractions. The relaxation response curve of acetylcholine slightly but significantly shifted to the right without showing a change in E_{max} values in the 3-week fructose group ($p < 0.05$; n= 6) (Table 1). A similar but significantly higher rightward shift was detected in the rats at 4-week induction compared with that in the 3-week group ($p < 0.05$; n= 5) (Figure 4). The decrease in pD_2 values in the 4-week fructose group resulted in a significant decrease in AUC values compared with the control, which suggests a worsening of endothelium-dependent relaxation in correlation with the duration of fructose induction.

Acetylcholine-induced relaxation was repeated in the presence of L-NAME (100 µM) and indomethacin (10 µM). The remaining relaxation of acetylcholine were considered EDH-mediated and they were diminished in fructose-induced rats (Figure 5). The relaxation-response curves shifted to the right in both induction periods with decreasing pD_2 and AUC values. Moreover, the

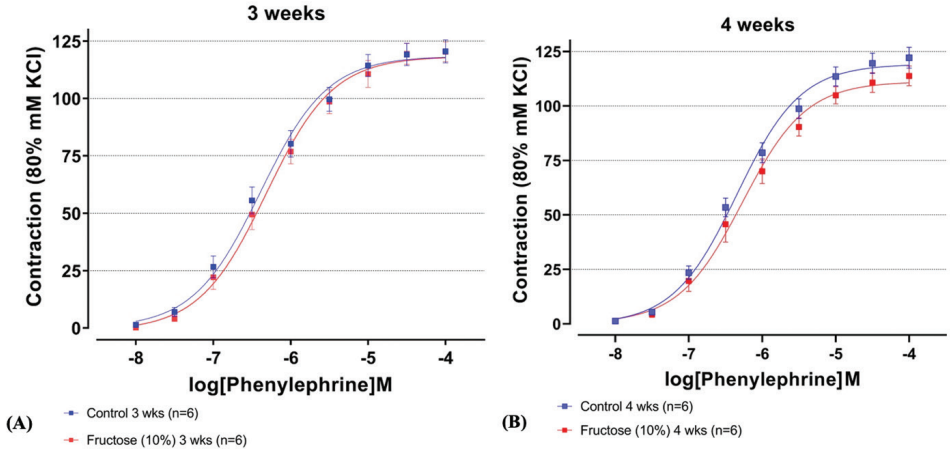

Figure 3. Phenylephrine-induced contractions in superior mesenteric arteries isolated from control and fructose groups at the 3rd (A) and 4th (B) weeks of fructose induction (mean ± SEM)

SEM: Standard error of the mean

Table 1. Comparison of the AUC, pD_2, and E_{max} values for the acetylcholine-induced relaxation response in the superior mesenteric arteries isolated from the control and fructose groups at the 3rd and 4th weeks of fructose induction

Acetylcholine	3rd week			4th week		
	Control (n= 5)	Fructose (n= 6)	*p* value	Control (n= 5)	Fructose (n= 5)	*p* value
AUC	302.30 ± 8.28	276.40 ± 7.15*	0.040	317.40 ± 17.77	255.70 ± 14.79*	0.030
pD_2	7.95 ± 0.05	7.69 ± 0.04*	0.003	8.13 ± 0.10	7.37 ± 0.09*, #	0.001
E_{max}	100 ± 0.00	99.26 ± 0.54	0.247	99.44 ± 0.56	97.24 ± 1.92	0.304
Acetylcholine in the presence of L-NAME + indomethacin	**Control (n= 4)**	**Fructose (n= 6)**	***p* value**	**Control (n= 4)**	**Fructose (n= 6)**	***p* value**
AUC	233.60 ± 15.00	175.20 ± 10.73*	0.012	238.90 ± 14.67	175.40 ± 10.39*	0.007
pD_2	7.22 ± 0.10	6.68 ± 0.07*	0.001	7.46 ± 0.10	6.84 ± 0.07*	0.001
E_{max}	96.40 ± 3.60	93.14 ± 3.97	0.584	93.35 ± 2.89	81.45 ± 2.57*, #	0.012
Acetylcholine in the presence of L-NAME + indomethacin + apamin	**Control (n= 5)**	**Fructose (n= 6)**	***p* value**	**Control (n= 6)**	**Fruktoz (n= 6)**	***p* value**
AUC	132.50 ± 12.41	115.10 ± 11.86	0.354	145.50 ± 16.14	115.20 ± 7.26	0.118
pD_2	6.50 ± 0.10	6.47 ± 0.09	0.827	6.70 ± 0.12	6.56 ± 0.08	0.331
E_{max}	75.42 ± 2.38	68.25 ± 5.16	0.320	77.93 ± 4.52	59.53 ± 3.28*	0.008
Acetylcholine in the presence of indomethacin + TRAM-34 + apamin	**Control**	**Fructose**	***p* value**	**Control (n= 3)**	**Fruktoz (n= 2)**	***p* value**
AUC	-	-	-	234.30 ± 21.42	214.30 ± 17.33	0.540
pD_2	-	-	-	7.45 ± 0.18	7.15 ± 0.14	0.324
E_{max}	-	-	-	92.97 ± 4.62	96.1 ± 2.8*	0.654

*Fructose vs. control, #3 week vs. 4 week fructose, unpaired t-test, *,#$p < 0.05$. AUC: Area under the curve, E_{max}: Maximum response, pD_2: Negative logarithm of drug concentration which constitutes half-maximum response, TRAM-34: Triarylmethane-34, NO: Nitric oxide, EDH: Endothelium-dependent hyperpolarization

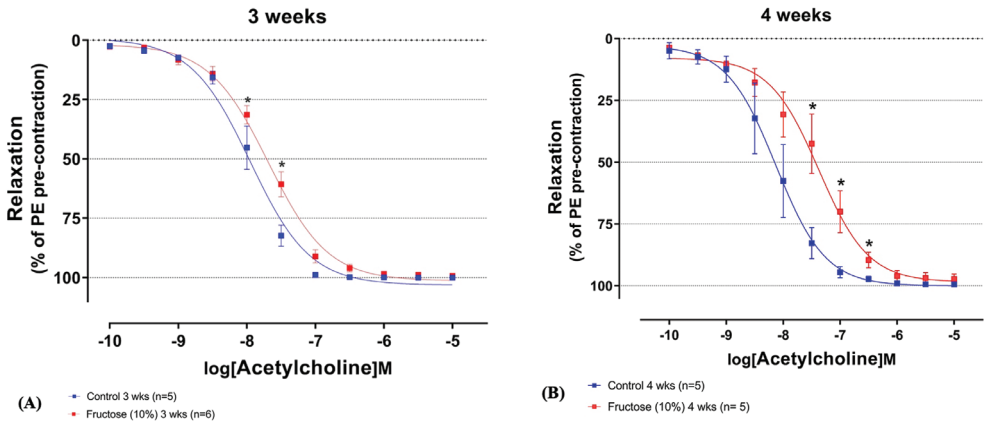

Figure 4. Acetylcholine-induced relaxations in superior mesenteric arteries isolated from control and fructose groups at the 3rd (A) and 4th (B) week of fructose induction (mean ± SEM, *fructose vs. control, unpaired *t*-test, *$p < 0.05$)

SEM: Standard error of the mean

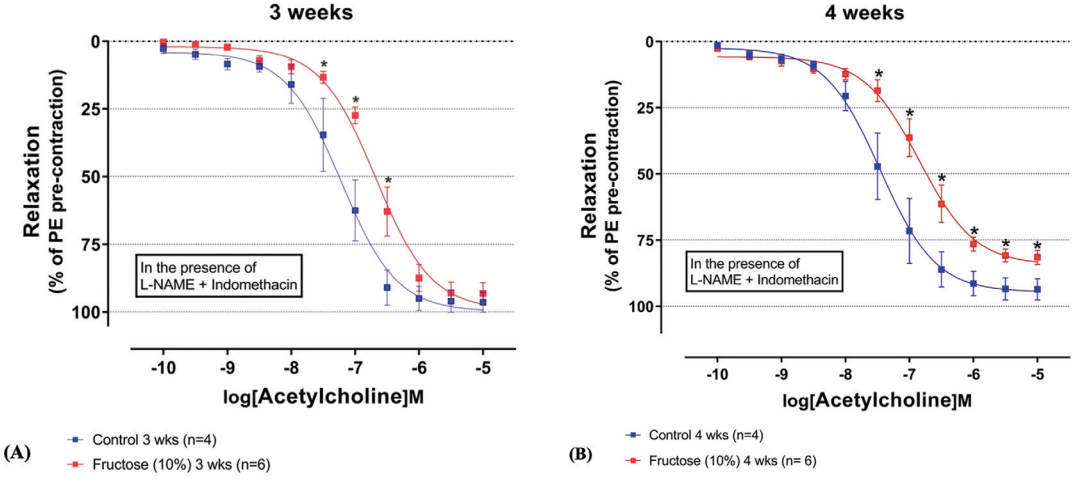

Figure 5. EDH-type relaxations obtained with acetylcholine in the presence of L-NAME and indomethacin in superior mesenteric arteries isolated from control and fructose groups at the 3rd (A) and 4th (B) week of fructose induction (mean ± SEM, *fructose vs. control, unpaired *t*-test, *$p < 0.05$)

EDH: Endothelium-dependent hyperpolarization, SEM: Standard error of the mean

amplitude of EDH-type relaxations decreased significantly only in the 4-week fructose group ($p < 0.05$; n= 6) (Table 1), suggesting that decreasing EDH-type vasorelaxation in time might partly contribute to the development of hypertensive responses in fructose-fed rats.

Because EDH-type relaxations are mediated by the activation of endothelial KCa3.1 and/or KCa2.3 channels, we examined acetylcholine relaxations in the presence of L-NAME (100 µM), indomethacin (10 µM), and apamin (10 nM), which are KCa2.3 channel blockers. The remaining relaxations in response to acetylcholine were considered to be solely mediated by KCa3.1 channels. Acetylcholine relaxations triggered by KCa3.1 activity did not change in the 3-week fructose group; however, as expected, a decrease in the amplitude of these relaxations was detected in the 4-week fructose group compared with the control or 3-week fructose group (Figure 6 and Table 1). These data suggest that impairment of endothelial KCa3.1 channel function contributes to the time-dependent reduction of EDH-type relaxation in fructose-fed rats.

There was significant potentiation in SNP-induced relaxation (0.1 nM-10 µM) in both fructose groups. Both relaxation response curves shifted significantly to the left compared to their controls (Figure 7). [pD_2 values; control (3 weeks) 8.70 ± 0.03 vs. fructose (3 weeks) 8.91 ± 0.04 ($p < 0.001$, n= 6); control (4 weeks) 8.07 ± 0.04 vs. fructose (4 weeks) 8.43 ± 0.06, $p < 0.001$, n= 6). These results indicate that smooth muscle sensitivity to NO and/or other downstream pathways increases under acute fructose induction.

DISCUSSION

The aim of this study was to determine the duration required for early endothelial dysfunction to develop in fructose drinking-induced hypertension in male Wistar Albino rats. BP and HR were measured simultaneously to detect changes in hemodynamic parameters associated with endothelial dysfunction. The second aim of this study is to detect changes in different components of endothelium-dependent relaxation in isolated mesenteric arteries of rats induced by high fructose.

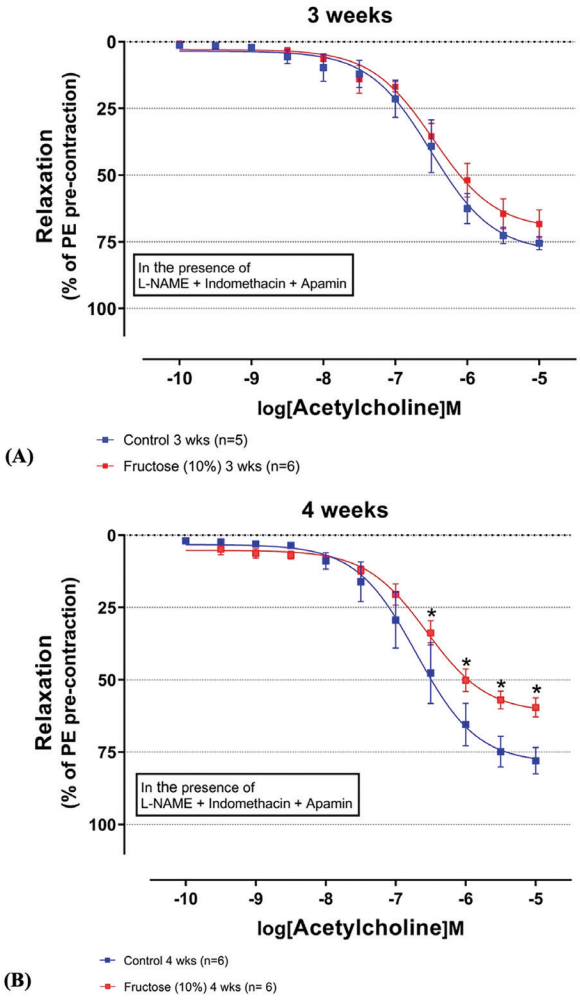

Figure 6. KCa3.1 channel-mediated component of EDH-type relaxations obtained with acetylcholine in the presence of L-NAME, indomethacin, and apamin in superior mesenteric arteries isolated from control and fructose groups at the 3rd (A) and 4th (B) week of fructose induction (mean ± SEM, *fructose vs. control, unpaired *t*-test, *$p < 0.05$)

EDH: Endothelium-dependent hyperpolarization, SEM: Standard error of the mean

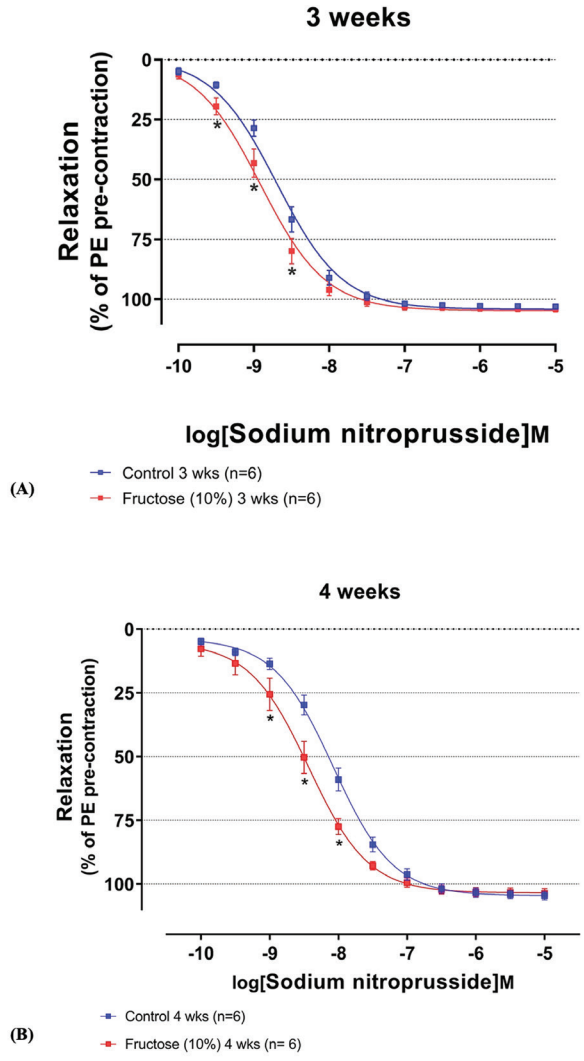

Figure 7. SNP-induced relaxation in superior mesenteric arteries isolated from control and fructose groups at the 3rd (A) and 4th (B) week of fructose induction (mean ± SEM, *fructose vs. control, unpaired *t*-test, *$p < 0.05$)

SNP: Sodium nitroprusside, SEM: Standard error of the mean

The duration of acute fructose exposure was determined as 3 and 4 weeks to evaluate the development phase of high BP and endothelial dysfunction in rats fed 10% fructose water. An increase in water intake and a corresponding decrease in food consumption observed in fructose induction were metabolic characteristics of this model since rats require less calorie intake if they have free access to fructose.[22] Consistent with the literature, these metabolic changes were used as model validation in this study.

Altered hemodynamic parameters during fructose induction are important symptoms of this experimental model and indicate metabolic syndrome development.[23] *In vivo* BP monitoring results showed that SBP began to increase with fructose induction as early as 2 weeks, and this increase continued gradually as the induction period was extended up to 4 weeks. DBP showed a similar increasing trend as SBP, but the rate of increase in DBP was more stable over the induction period. Early development of the increase in SBP has previously been reported in both fructose water and pellet design.[4,22,24] However, the pathophysiological mechanism(s) by which hypertension occurs in the fructose induction model has not been completely clarified, yet many studies have referred to endothelial dysfunction as a common underlying mechanism.[15,25] In a way that supports this, we were able to detect endothelial dysfunction in isolated mesenteric arteries of rats that consumed fructose (10%) for only 3 weeks, and it became more severe as the fructose consumption prolonged to 4 weeks. We also showed that endothelial dysfunction in fructose-fed rats was accompanied by a concomitant increase in SBP and DBP.

In our *ex vivo* organ bath experiments, contractile responses to phenylephrine were comparable between groups provided with or without 10% fructose water. In addition, fructose-related vascular impairment was characterized by decreased

endothelium-dependent relaxation in response to acetylcholine, which refers to dysfunctional endothelium, and increased smooth muscle sensitivity to SNP-induced relaxation. The maximal acetylcholine relaxations in both 3- and 4-week fructose-fed rats were not different from those in the control rats, despite being reported to lessen in other studies performed using the pellet design.[15,16] Nevertheless, the sensitivity of acetylcholine relaxation in our study design declined significantly in week 3 and worsened in week 4. Although not clear, this discrepancy might be due to differences in experimental protocols that might affect the sensitivity of mesenteric arteries to endothelium-dependent relaxant agents.

When the acetylcholine relaxation components were examined separately, it can be said that this inhibition was due to decreased EDH-type relaxation, which is compatible with the studies performed using the pellets.[14] Based on the obtained data, it was suggested that the KCa3.1-mediated component of EDH-type relaxation was decreased. The decrease in EDH-type relaxation in the short-term (3 or 4 weeks) fructose-induced hypertensive rats seems to be partially compensated by the increased NO sensitivity at the site of smooth muscle cells. This deduction was indirectly supported by the increase in sensitivity to SNP relaxations, although no functional increase in NO-mediated vasorelaxation in response to acetylcholine was detected in fructose-fed rats (Table 1). Other studies have reported no change in SNP relaxation with pellet design.[16,25] Furthermore, a long period of fructose consumption has been reported to decrease SNP relaxation,[26] suggesting that long-term exposure to fructose leads to the failure of this compensation mechanism.

Whether endothelial dysfunction is a cause or a consequence of hypertension remains a matter of debate. This paradox can be explained by simultaneously examining whether antihypertensive treatments improve endothelial dysfunction in fructose-induced hypertensive rats. According to our findings, the preservation of phenylephrine contractions in the mesenteric arteries after fructose induction indicates that smooth muscle sensitivity to contractile agents does not change and that the tonic inhibitory effect of endothelial factors against contractions continues. In this case, it can be argued that the two pathophysiologies may operate independently of each other. It has previously been suggested that fructose-mediated hypertension is associated with a central neuro-inflammatory response that triggers increased sympathetic outflow.[27] Blocking this mechanism with centrally acting anti-inflammatory agents can ameliorate hypertension by reducing only the sympathetic outflow without directly targeting endothelial dysfunction or hyperinsulinemia, which usually accompanies hypertension in this model.[24] On the other hand, in the pellet design of the fructose-induced hypertensive rat model, endothelial dysfunction has been reported to precede hypertension.[15] This means that further experiments are needed to conclude that hypertension and dysfunctional endothelium trigger each other.

CONCLUSION

In conclusion, rats subjected to 10% fructose water for only 3 weeks showed decreased relaxation responses to acetylcholine in isolated superior mesenteric arterial rings, supporting increases in SBP and DBP. Hypertensive response and corresponding endothelial dysfunction become more severe as the induction period with fructose increases. Decreased KCa3.1-mediated EDH-type relaxation appears to contribute to impaired mesenteric arterial relaxation in this model.

Ethics

Ethics Committee Approval: Animal procedures and protocols were approved by the Animal Ethics Committee of the University of Hacettepe (approval number: 2021/03-06, date: 30.03.2021).

Informed Consent: Not required.

Authorship Contributions

Concept: A.H., M.H.Ö., Design: A.H., M.H.Ö., Data Collection or Processing: A.H., Analysis or Interpretation: A.H., M.H.Ö., Literature Search: A.H., Writing: A.H., M.H.Ö.

Conflict of Interest: No conflict of interest was declared by the authors.

Financial Disclosure: This study was financially supported by the Hacettepe University Scientific Research Projects Coordination Unit (project ID: THD-2022-19593).

REFERENCES

1. Forshee RA, Storey ML, Allison DB, Glinsmann WH, Hein GL, Lineback DR, Miller SA, Nicklas TA, Weaver GA, White JS. A critical examination of the evidence relating high fructose corn syrup and weight gain. Crit Rev Food Sci Nutr. 2007;47:561-582.
2. Johnson RJ, Segal MS, Sautin Y, Nakagawa T, Feig DI, Kang DH, Gersch MS, Benner S, Sánchez-Lozada LG. Potential role of sugar (fructose) in the epidemic of hypertension, obesity and the metabolic syndrome, diabetes, kidney disease, and cardiovascular disease. Am J Clin Nutr. 2007;86:899-906.
3. Marriott BP, Cole N, Lee E. National estimates of dietary fructose intake increased from 1977 to 2004 in the United States. J Nutr. 2009;139:1228S-1235S.
4. Hwang IS, Ho H, Hoffman BB, Reaven GM. Fructose-induced insulin resistance and hypertension in rats. Hypertension. 1987;10:512-516.
5. Klein AV, Kiat H. The mechanisms underlying fructose-induced hypertension: a review. J Hypertens. 2015;33:912-920.
6. Komnenov D, Levanovich PE, Rossi NF. Hypertension Associated with Fructose and High Salt: Renal and Sympathetic Mechanisms. Nutrients. 2019;11:569.
7. Sukiasyan L. Fructose-Induced Alteration of the Heart and Vessels Homeostasis. Curr Probl Cardiol. 2023;48:101013.
8. Soleimani M, Alborzi P. The role of salt in the pathogenesis of fructose-induced hypertension. Int J Nephrol. 2011;2011:392708.
9. El-Bassossy HM, Dsokey N, Fahmy A. Characterization of vascular complications in experimental model of fructose-induced metabolic syndrome. Toxicol Mech Methods. 2014;24:536-543.
10. Tran LT, MacLeod KM, McNeill JH. Selective alpha(1)-adrenoceptor blockade prevents fructose-induced hypertension. Mol Cell Biochem. 2014;392:205-211.

11. Krüger-Genge A, Blocki A, Franke RP, Jung F. Vascular endothelial cell biology: an update. Int J Mol Sci. 2019;20:4411.

12. Palanisamy N, Venkataraman AC. Beneficial effect of genistein on lowering blood pressure and kidney toxicity in fructose-fed hypertensive rats. Br J Nutr. 2013;109:1806-1812.

13. Miatello R, Risler N, Gonzalez S, Castro C, Rüttler M, Cruzado M. Effects of enalapril on the vascular wall in an experimental model of syndrome X. Am J Hypertens. 2002;15:872-878.

14. Katakam PV, Ujhelyi MR, Miller AW. EDHF-mediated relaxation is impaired in fructose-fed rats. J Cardiovasc Pharmacol. 1999;34:461-467.

15. Katakam PV, Ujhelyi MR, Hoenig ME, Miller AW. Endothelial dysfunction precedes hypertension in diet-induced insulin resistance. Am J Physiol. 1998;275:788-792.

16. Verma S, Bhanot S, Yao L, McNeill JH. Defective endothelium-dependent relaxation in fructose-hypertensive rats. Am J Hypertens. 1996;9:370-376.

17. Hem NA, Phie J, Chilton L, Kinobe R. A volume-pressure tail cuff method for hemodynamic parameters: Comparison of restraint and light isoflurane anesthesia in normotensive male Lewis rats. J Pharmacol Toxicol Methods. 2019;100:106601.

18. Hamad A, Ozkan MH, Uma S. Trimethylamine-N-oxide (TMAO) selectively disrupts endothelium-dependent hyperpolarization-type relaxations in a time-dependent manner in rat superior mesenteric artery. Biol Pharm Bull. 2021;44:1220-1229.

19. Gerber R, Anwar M, Poston L. Enhanced acetylcholine induced relaxation in small mesenteric arteries from pregnant rats: an important role for endothelium-derived hyperpolarizing factor (EDHF). Br J Pharmacol. 1998;125:455-460.

20. Crane GJ, Gallagher N, Dora KA, Garland CJ. Small- and intermediate-conductance calcium-activated K+ channels provide different facets of endothelium-dependent hyperpolarization in rat mesenteric artery. J Physiol. 2003;553:183-189.

21. Ozkan MH, Uma S. β-adrenergic receptor blocker ICI 118,551 selectively increases intermediate-conductance calcium-activated potassium channel (IK_{Ca})-mediated relaxations in rat main mesenteric artery. Basic Clin Pharmacol Toxicol. 2018;122:570-576.

22. Dai S, McNeill JH. Fructose-induced hypertension in rats is concentration- and duration-dependent. J Pharmacol Toxicol Methods. 1995;33:101-107.

23. Tran LT, Yuen VG, McNeill JH. The fructose-fed rat: a review on the mechanisms of fructose-induced insulin resistance and hypertension. Mol Cell Biochem. 2009;332:145-159.

24. Ho CY, Lin YT, Chen HH, Ho WY, Sun GC, Hsiao M, Lu PJ, Cheng PW, Tseng CJ. CX3CR1-microglia mediates neuroinflammation and blood pressure regulation in the nucleus tractus solitarii of fructose-induced hypertensive rats. J Neuroinflammation. 2020;17:185.

25. Miller AW, Hoenig ME, Ujhelyi MR. Mechanisms of impaired endothelial function associated with insulin resistance. J Cardiovasc Pharmacol Ther. 1998;3:125-134.

26. Shaligram S, Sangüesa G, Akther F, Alegret M, Laguna JC, Rahimian R. Differential effects of high consumption of fructose or glucose on mesenteric arterial function in female rats. J Nutr Biochem. 2018;57:136-144.

27. Wu CJ, Cheng PW, Kung MH, Ho CY, Pan JY, Tseng CJ, Chen HH. Glut5 Knockdown in the nucleus tractus solitarii alleviates fructose-induced hypertension in rats. J Nutr. 2022;152:448-457.

Turk J Pharm Sci 2024;21(5):399-412
DOI: 10.4274/tjps.galenos.2024.37632

ORIGINAL ARTICLE

Effect of Vitamin D Supplementation According to Daily Dietary Levels on Biochemical Parameters in 25-Hydroxyvitamin D Deficiency of Women with Obesity

Fatih CESUR[1]*, Zehra Nur GENÇ[2]

[1]Çankırı Karatekin University Faculty of Health Science, Department of Nutrition and Dietetics, Çankırı, Türkiye
[2]Üsküdar University Faculty of Health Science, Department of Nutrition and Dietetics, İstanbul, Türkiye

ABSTRACT

Objectives: This study examined how vitamin D supplementation based on daily dietary intake affects biomarkers in obese women with 25-hydroxyvitamin D deficiency.

Materials and Methods: Group D (n= 14) used vitamin D supplements daily for 2 months, and Group C (n= 16) did not receive supplements. Three blood samples were collected from the volunteers during the initial phase of the study. In this study, blood was collected from the volunteers: first measurement (M1), second measurement (M2), and third measurement (M3).

Results: Compared with Group C, Group D had lower high-density lipoprotein (HDL) levels at M2 and fasting serum glucose (FSG) levels at M3 ($p < 0.05$), and lower HDL levels at M2 and FSG levels in normal-weight individuals at M3 ($p < 0.05$). In addition, 25-hydroxyvitamin D levels were higher in normal-weight women than in obese women according to M3 ($p= 0.043$). There was a higher negative correlation between HDL-C in M1 and FSG in Group D (r= -0.710, $p= 0.004$). 25-hydroxyvitamin D was moderately positively correlated with dietary vitamin D in M2 in Group D (r= 0.559, $p= 0.038$). Significant positive correlations were observed between iodine intake and triiodothyronine (T3) levels, whereas no significant difference was observed between thyroid-stimulating hormone and T3 levels.

Conclusion: Vitamin D intake improves HDL levels in normal-weight individuals and causes an effect on FSG to be at the desired low level, whereas in individuals with obesity, although serum 25-hydroxyvitamin D levels increased in the last measurement, no effect was observed. Women with normal vitamin D levels have higher serum 25-hydroxyvitamin D levels than those who are obese.

Keywords: Vitamin D supplement, fasting serum glucose, high-density lipoprotein, obesity, thyroid hormones,

INTRODUCTION

Two types of vitamin D have a fat-soluble sterol structure known as calciferol. Of these, ergocalciferol is taken from the diet (D2), whereas cholecalciferol is synthesized in the skin by sunlight (D3). The most significant indicator of human vitamin D status is 25-hydroxyvitamin D concentration. While its deficiency or insufficiency is frequently observed worldwide, its excess causes toxic effects. This deficiency, which is common worldwide, can be restored to normal levels with orally supplemented vitamin D.[1]

It has been reported that there is an opposite association between 25-hydroxyvitamin D and fasting blood glucose (FSG), and vitamin D intake improves FSG and HbA1c levels.[2]

Deficiency in 25-hydroxyvitamin D levels is also crucial for lipid profiles, which are markers of cardiovascular disease. It was reported that low or decreased 25-hydroxyvitamin D levels are related to hyperglycemia, high serum triglyceride (TG) levels, high cholesterol, and low high-density lipoprotein (HDL) levels.[3] In another study, vitamin D supplementation helped reduce blood levels of TGs, low-density lipoprotein (LDL), and total cholesterol (TC).[4]

One study stated that vitamin D levels were associated with thyroid-stimulating hormone (TSH).[5] A low vitamin D level in youth has been related to low wandering triiodothyronine (T3) levels.[6] When vitamin D was given to subjects with Hashimoto's thyroid, there was also a significant reduction in TSH hormone compared with the baseline.[7]

*Correspondence: fatihcesr@gmail.com, Phone: +90 553 751 27 37, ORCID-ID: orcid.org/0000-0003-2062-098X
Received: 24.12.2023 , Accepted: 16.09.2024

When the literature is examined, the effects of circulating serum 25-hydroxyvitamin D levels on serum lipids, especially in cross-sectional and experimental studies, provide conflicting results.[8] Thus, further research on the effects of vitamin D supplementation on blood vitamin D levels is required. This study aimed to determine how vitamin D supplementation based on daily dietary intake affects TSH, T3, FSG, and lipid levels in normal-weight and obese women with 25-hydroxyvitamin D deficiency.

MATERIALS AND METHODS

Thirty volunteer women aged between 18 and 23 years who were known to have vitamin D deficiency were involved in this investigation. The research was conducted between February 2023 and April 2023 in the Avrasya University. The participants were divided into two groups (experimental and control groups). The experimental group received 10 mL of vitamin D [a total of 150,000 international units (IU)]. The volunteers consumed vitamin D for 2 months and received 3,200 IU of vitamin D per day. In the control group, no dietary supplementation was recommended. Patients with diabetes, thyroid disorders, and hypertension were not included in the study. The study did not include individuals with FPG levels › 100 or 25-hydroxyvitamin D levels › 20.

After the first measurement (M1, beginning) was obtained from the women, two more measurements were obtained with an average interval of 28 days. Blood was collected from the volunteers three times: M1, second measurement (M2, week four), and third measurement (M3, week eight). 25-hydroxyvitamin D levels were measured at each blood draw. Next, the blood was separated into serum by centrifugation (four thousand rpm for ten minutes) and preserved at 80 °C (Figure 1).

Routine biochemical analysis results

Biochemical parameters were examined by women participating in the study *via* the e-Pulse system (Republic of Türkiye Ministry of Health).

Serum 25-hydroxyvitamin D level

25-hydroxyvitamin D content was measured using an SD Biosensor Fluorescent Immunological device. The temperature was adjusted to 37 °C in the SD Biosensor (F200 Analyzer), and the extractor was activated. The test cassette was then inserted into the device to be read. With a micropipette, 155 microliters of bumper solvent and 35 microliters of serum specimen were added to the reaction tablet. This solution and test tape were placed in the incubator for 30 min, and then the material from reaction tablet two was added to this solution. After homogenization, the solution was completely transferred to the test tape well using a micropipette and then incubated for 15 days. The 25-hydroxyvitamin D level was then determined by scanning the cassette. The proposed method and device have been accepted in the literature.[9]

Fasting serum glucose level

Serum glucose levels during fasting were measured after subjects had fasted for an average of 6 to 8 hours. The American Diabetes Association has determined impaired FSG tolerance to be › 100 mg/dL.[10]

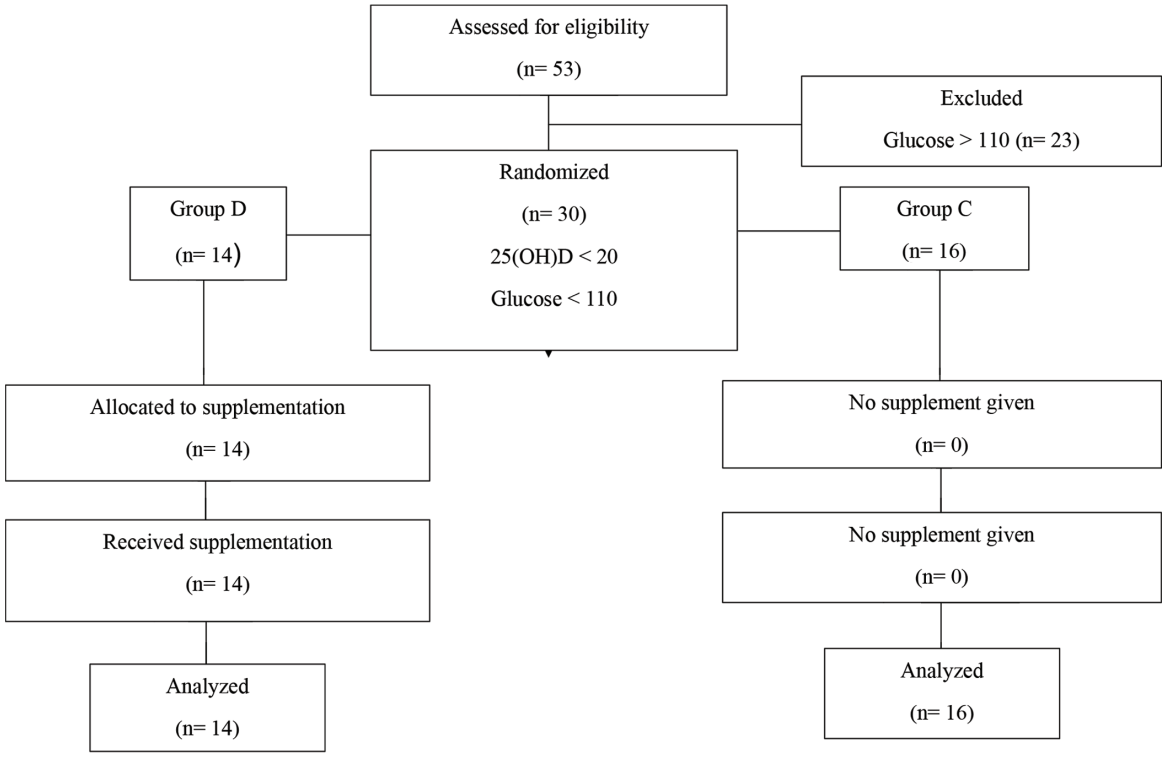

Figure 1. CONSORT flowchart the flow of participants through the trial is represented by a diagram, as suggested by the CONSORT group. Group C: No reinforcement; group D: Vitamin D supplement

FSG measurements were performed using the Accu-Chek Performa Nano device when taking samples.[9] After the device was activated, an unused measuring strip was placed in the device, and 35 microliters of serum specimen were taken from the blood serum using a micropipette. The sample was dripped onto the tip of the strip. The measurement results were taken immediately afterward.

Measurement of serum lipid levels

After the stored serums thawing, LDL, HDL, non-HDL, TC, and TG levels were measured with a Standard LipidoCare Analyzer and a Lipid Profile Test Strip. The SD LipidoCare is an approved device that diagnoses patients rapidly and precisely in a clinical setting.[11]

The device was turned on, and the measurement setting was set to serum. The lid of the device was opened, and 35 L of serum specimen was received with a micropipette and placed into the application hole of the device, and the lid was closed. Results were obtained after a 3-minute waiting period.

Measuring ranges

100-450 mg/dL for TC, 25-95 mg/dL for HDL cholesterol, 0-130 mg/dL for LDL, and 45-650 mg/dL for TGs. This study considered TC ideal for < 200 mg/dL and high for > 240 mg/dL. In HDL-C levels, > 55 mg/dL in women and > 45 mg/dL in men are ideal. TG < 150 mg/dL was accepted as ideal.

Serum TSH level

A 35 µl sample was taken from the serum using a STANDARD Ezi tube and distributed in the extraction buffer. Then, the sample and buffer were mixed 2-3 times with a 100 µL pipette and placed in the test cassette, and the result was obtained after 15 minutes. The normal range for TSH has been determined as 0.45-4.5 mIU/mL.

Serum T3 levels

A standard D-BLOCK incubator device was prepared and its temperature was raised to 37 °C. Using a micropipette, 100 L of serum was obtained. The sample was added to the extraction buffer, and a Spoitte tablet was dissolved. The cells were kept in the incubation device and previously brought to 37 °C for 10 minutes. The tester was placed in the test slot of the analyzer. A hundred µl of the incubated sample mixture was taken and applied to the specimen well of the test device. The result was obtained 15 deeps after the test start button was pressed. The measuring range of the device is 0.3-10.0 nmol/L, and the normal range for T3 is specified as 1.3-3.1 nmol/L.

Anthropometric measurements

Using the bioelectrical impedance analysis (BIA) approach, the TANITA MC-780MA was used to assess weight body fat, protein, muscle, waist-hip ratio, visceral fat level, basal metabolic rate, waist circumference, and mineral levels. A stadiometer was used for height measurement. Women were classified as obese or normal according to the fat ratio determined by the BIA method. Obese (D group = 6, C group = 9), and normal (D group = 8, C group = 7) were determined. A power analysis of obese and normal women was performed, and the effect size was found to be 1.70, and the power was found to be 92% One-Way and 85% Two-Way.

Diet quality calculation

Diet quality was calculated using frequency questionnaires on food consumption among women. Diet quality was assessed using the Diet Quality Index-International scale.[12]

Ethics statement

The ethics committee approval for this study was approved by the Avrasya University Ethics Committee (approval number: 2022-52/14, date: 21.07.2022). Informed consent was obtained from all participants. This study was registered with ClinicalTrials.gov (identifier number: NCT05447065).

Statistical analysis

Data were analyzed using R language and R studio v.0.98.501. The data were evaluated using the Kolmogorov-Smirnov or Shapiro-Wilk tests to determine their normal distribution. Continuous variables are presented as mean ± standard deviation (SD). The Wilcoxon signed rank test and the Mann-Whitney U test were, respectively, used to assess the data of dependent and independent groups that did not exhibit normal distribution. If a Three-Way comparison was made between independent groups, the results were analyzed using Friedman's variance. Food consumption records and food frequency forms were analyzed using CEBEBIS. G-Power v. 3.1.9.4 software was used to calculate the sample size, and statistical significance was determined as $p < 0.05$.

RESULTS

Women with low vitamin D levels were included in this study. The participants consisted of a total of 30 volunteer women, including those who took vitamin D supplements (n= 14) and those who did not take vitamin D supplements (n= 16). The mean ages of groups D and C were 20.07 ± 1.33 and 20.56 ± 1.36, respectively. Frequency of food consumption, anthropometric measurements, FSG levels, serum lipids (LDL, HDL, TG, and TC), serum TSH, and serum T3 levels were measured.

Regarding age and routine biochemical values, there was not a significant difference between Group D and C (except from NEUTROPHIL). A comparison of Group D to Group C revealed significant decreases in the intake of cheese, butter, eggs, sunflower oil, margarine, yogurt, and white bread. The data on the frequency of each person's food consumption was analyzed after one year. Energy, protein, fat, MUFA, PUFA, linolenic acid, linoleic acid, myristic acid, lauric acid, palmitic acid, oleic acid, cholesterol, retinol, folate, vitamin D, vitamin E, and vitamin B 1 values in group D A decreased in vitamin B2, sodium, potassium, phosphorus, and zinc values compared to group C. In addition, in the comparison of Groups D and C, the w-3/w-6 ratio was higher in Group D (Table 1).

When the anthropometric measurements between the groups were analyzed, no difference was observed between the three measurements (Table 2).

When the anthropometric measurements of the women were analyzed, no significant difference was found between the

Table 1. Comparison of the characteristics of healthy volunteers, routine biochemical findings, frequency of food consumption, average daily energy consumption, and food consumption frequencies of the groups[a]

	Group D (n= 14)	Group C (n= 16)	*p*[b]
Routine biochemical findings			
Age (years)	20.07 ± 1.33	20.56 ± 1.36	0.334
PA (met-min./week)	2744.40 ± 2944.13	2473.94 ± 1953.27	0.773
ALT (U/L)	12.57 ± 6.03	13.75 ± 0.95	0.358
AST (U/L)	13.91 ± 3.76	19.29 ± 7.41	0.140
BASOPHIL (10*3/uL)	0.07 ± 0.04	0.06 ± 0.04	0.709
NEUTROPHIL (10*3/uL)	5.22 ± 1.64	4.10 ± 1.18	0.029
EOSINOPHIL (10*3/uL)	0.20 ± 0.13	0.11 ± 0.08	0.259
LYMPHOCYTE (10*3/uL)	2.63 ± 0.75	2.3 ± 0.92)	0.624
MONOCYTE (10*3/uL)	0.70 ± 0.18	0.56 ± 0.27	0.093
RBC (10*6/uL)	4.67 ± 0.39	4.60 ± 0.53	0.311
HGB (g/dL)	12.73 ± 1.55	12.74 ± 1.38	0.732
MCV (fL)	81.14 ± 8.29	85.73 ± 10.18	0.105
MCH (pg)	27.193 ± 0.88	28.34 ± 4.28	0.368
MCHC (g/dL)	33.45 ± 2.20	33.02 ± 2.48	0.471
HCT (%)	37.98 ± 3.21	38.51 ± 3.31	0.857
PLT (10*3/uL)	295.58 ± 94.35	273.01 ± 81.83	0.328
MPV (fL)	8.33 ± 1.09	8.86 ± 1.68	0.328
PDW (fL)	17.23 ± 3.60)	18.04 ± 8.17	0.496
PCT (%)	0.25 ± 0.11	0.24 ± 0.08	0.586
WBC (10*3/uL)	8.89 ± 1.88	8.09 ± 2.56	0.247
Average daily energy and food consumption frequencies			
Energy (kcal)	1225.80 ± 354.43	1763.29 ± 668.78	0.011
CHO (g)	145.98 ± 51.88	194.78 ± 110.20	0.262
Protein(g)	33.57 ± 9.16	53.93 ± 22.72)	0.009
Fat (g)	55.37 ± 25.94	83.88 ± 19.03	< 0.001
Cholesterol (mg)	120.81 ± 67.51	262.86 ± 136.50	0.001
Fiber (g)	13.39 ± 6.10	17.47 ± 10.38	0.271
Alcohol (g)	0.01 ± 0.04	0.05 ± 0.13	0.437
Saturated fatty acid (g)	24.29 ± 8.65	32.63 ± 11.56	0.067
Myristic acid (g)	2.02 ± 1.32	3.30 ± 1.75	0.034
Lauric acid (g)	0.85 ± 0.44	1.34 ± 0.69	0.045
Palmitic acid (g)	11.31 ± 4.11	15.59 ± 5.12	0.029
Monounsaturated fatty acid (g)	20.23 ± 11.20	29.28 ± 7.85	0.002
Oleic acid (g)	18.47 ± 10.55	26.98 ± 7.57	0.002
Polyunsaturated fatty acid (g)	7.11 ± 6.06	14.88 ± 4.54	< 0.001
Linoleic acid (g)	5.76 ± 5.76	12.99 ± 4.49	< 0.001
a-linolenic acid(g)	0.60 ± 0.27	0.98 ± 0.39	0.007

Table 1. Continued

	Group D (n= 14)	Group C (n= 16)	p^b
Average daily energy and food consumption frequencies			
Omega-3/Omega-6	0.14 ± 0.07	0.09 ± 0.05	0.023
Water (g)	934.86 ± 442.41	1097.76 ± 507.08	0.198
Retinol (µg)	330.37 ± 339.90	600.66 ± 557.17	0.013
A (µg)	710.66 ± 487.27	1040.01 ± 746.89	0.088
D (µg)	2.34 ± 1.45	5.01 ± 3.67	0.023
E (mg)	6.19 ± 7.49	14.04 ± 5.77	0.000
Thiamine (mg)	0.54 ± 0.26	0.78 ± 0.38	0.015
Riboflavin (mg)	0.87 ± 0.22	1.41 ± 0.52	0.005
Niacin (mg)	6.44 ± 1.80	8.64 ± 4.08	0.280
B6 vit. (µg)	0.60 ± 0.15	0.80 ± 0.37	0.062
Folate (µg)	168.04 ± 94.18	247.63 ± 126.20	0.025
B12 vit. (µg)	2.09 ± 1.33	3.77 ± 2.41	0.005
C vit. (µg)	63.42 ± 33.81	72.61 ± 47.52	0.678
Sodium (mg)	990.82 ± 388.95	1679.03 ± 843.69	0.009
Potassium (mg)	1416.24 ± 468.59	1877.40 ± 805.27	0.031
Calcium (mg)	465.33 ± 103.96	713.39 ± 312.40	0.051
Phosphorus (mg)	654.05 ± 160.00	964.71 ± 393.95	0.009
Magnesium (mg)	178.59 ± 57.72	235.08 ± 98.39	0.051
Iron (mg)	4.89 ± 1.89	6.51 ± 3.31	0.124
Zinc (mg)	5.25 ± 1.30	7.38 ± 2.89	0.013
Essential amino acid (µg)	17.14 ± 5.07	27.64 ± 10.95	0.006
Comparison of food consumption frequency			
Black tea (%)	3.47 ± 6.03	2.75 ± 2.57	0.447
Turkish coffee (%)	2.03 ± 2.62	3.64 ± 4.48	0.538
Instant coffee (%)	3.79 ± 5.31	2.53 ± 4.91	0.356
Herbal teas (%)	1.93 ± 3.54	4.17 ± 6.28	0.086
Fizzy drinks (cola, soda, etc.) (%)	2.65 ± 4.05	3.18 ± 5.83	0.882
Mineral water (%)	2.97 ± 4.86	3.58 ± 5.85	0.966
Instant juice (%)	2.97 ± 5.73	3.57 ± 6.53	0.717
Alcoholic beverages (%)	0.00 ± 0.00	0.00 ± 0.00	1.000
Bagel/Pastry (%)	1.94 ± 3.07	3.59 ± 6.85	0.292
Rice (%)	2.80 ± 3.06	3.55 ± 4.67	0.830
Bulgur rice (%)	3.30 ± 7.99	2.97 ± 4.12	0.172
Pasta (%)	3.02 ± 4.11	2.36 ± 2.44	0.931
Cake/Biscuit (%)	2.27 ± 3.36	3.71 ± 3.55	0.076
Diet biscuits (%)	6.56 ± 18.17	0.51 ± 1.56	0.442
Dumplings (%)	1.39 ± 2.01	4.06 ± 5.61	0.092
Milky desserts (%)	1.51 ± 1.87	4.51 ± 6.32	0.108

Table 1. Continued

	Group D (n= 14)	Group C (n= 16)	p^b
Comparison of food consumption frequency			
Chocolate (%)	2.92 ± 2.58	1.95 ± 1.46	0.570
Jam, honey, and molasses (%)	3.00 ± 3.77	3.03 ± 7.06	0.657
Olives (%)	2.49 ± 4.26	3.56 ± 3.67	0.208
Butter (%)	0.92 ± 2.92	4.22 ± 8.51	0.026
Margarine (%)	0.00 ± 0.00	4.40 ± 10.87	0.049
Olive oil (%)	2.23 ± 4.15	3.14 ± 3.52	0.146
Sunflower oil (%)	1.44 ± 3.39	4.89 ± 3.73	0.003
Red meat (%)	2.52 ± 1.58	3.38 ± 5.93	0.390
Chicken meat (%)	2.53 ± 3.14	3.84 ± 4.02	0.531
Fish (%)	2.18 ± 2.89	3.72 ± 3.32	0.108
Egg (%)	1.04 ± 1.51	3.97 ± 3.58	0.008
Salami/Sausage etc. (%)	2.57 ± 3.15	3.79 ± 5.83	0.656
Dry beans (%)	2.45 ± 4.12	3.39 ± 3.80	0.186
Oilseeds (%)	1.87 ± 2.10	3.39 ± 3.80	0.086
Offal (%)	2.02 ± 6.54	4.48 ± 12.46	0.701
Yogurt (%)	1.89 ± 1.92	3.97 ± 2.60	0.025
Buttermilk (%)	2.14 ± 2.35	3.73 ± 5.12	0.362
Kefir (%)	1.48 ± 3.10	4.96 ± 14.61	0.757
Cheese (%)	2.42 ± 3.77	3.65 ± 3.33	0.049
Green leafy vegetables (%)	2.60 ± 3.05	3.62 ± 3.28	0.223
Other vegetables (%)	3.00 ± 3.01	3.20 ± 2.75	0.471
Dried fruit (%)	5.96 ± 12.05	1.04 ± 1.25	0.911
Fresh fruit (%)	2.96 ± 3.09	2.94 ± 3.51	0.786
Freshly squeezed fruit juice (%)	2.75 ± 5.24	3.71 ± 7.72	0.565
White bread (%)	0.93 ± 1.35	5.32 ± 8.52	0.020
Whole wheat bread (%)	0.96 ± 2.48	4.84 ± 7.21	0.185
Whole grain bread (%)	4.39 ± 5.21	2.29 ± 4.29	0.128

[a]Data are expressed as mean ± SD, [b]*p* values were determined using a Mann-Whitney U test. D group, vit-D supplemented group; C, no reinforcement. PA: Physical activity, ALT: Alanine aminotransferase, AST: Aspartate transaminase, RBC: Red blood cells, HGB: Hemoglobin, MCV: Mean corpuscular volume, MCH: Mean corpuscular hemoglobin, MCHC: Mean corpuscular hemoglobin concentration, HCT: Hematocrit, PLT: Platelets, MPV: Mean platelet volume, PDW: Platelet distribution width, PCT: Plateletcrit, WBC: White blood cells, vit.: Vitamin, SD: Standard deviation

within-group and between-group analyses (Table 3). The fat values of the obese group were M1 (mean ± SD = 31.05 ± 3.40), M2 (mean ± SD = 30.80 ± 3.24) and M3 (mean ± SD = 31.62 ± 2.94), respectively. The fat values of the normal weight group were M1 (mean ± SD = 19.99 ± 4.24), M2 (mean ± SD = 21.11 ± 4.15) and M3 (mean ± SD = 21.31 ± 3.98).

A significant increase in FSG and TG levels in group C was observed between both the M1-M2 and the M2-M3. In addition, between M2 and M3, HDL values significantly decreased (Table 4).

There were no significant differences between groups for all values in M1. HDL levels were found to be higher in Group D in M2. In M3, although the FSG levels were lower, the vitamin D levels were significantly higher in Group D. However, there were no significant differences in LDL, non-HDL, TC, TSH, T3, and HDL/LDL levels among the M3 (Table 4).

Between M1 and M2 in Group D, FSG levels significantly decreased. A significant increase in HDL levels was observed between stations M2 and M3. A significant increase in TG levels was observed in M1 and M3. A significant increase in

Table 2. Comparison of food consumption record[a]									
	Group D (n= 14)			Group C (n= 16)			p^b	p^c	p^d
	M1	M2	M3	M1	M2	M3			
Energy (kcal)	969.91 ± 342.66	1041.88 ± 403.34	1188.75 ± 353.97	1206.99 ± 438.70	1230.28 ± 426.44	1407.65 ± 530.58	0.105	0.198	0.239
Water (g)	675.62 ± 226.98	677.48 ± 241.73	673.28 ± 232.71	797.57 ± 249.77	863.16 ± 188.24	853.38 ± 245.76	0.170	0.011	0.074
Protein (g)	45.38 ± 15.43	42.69 ± 29.65	43.26 ± 11.97	45.72 ± 17.80	43.84 ± 14.65	53.16 ± 17.37	0.967	0.506	0.111
Fat (g)	47.25 ± 19.47	53.51 ± 21.94	56.85 ± 17.42	60.56 ± 25.65	57.62 ± 22.28	63.91 ± 25.20	0.157	0.547	0.663
CHO (g)	88.91 ± 37.30	92.67 ± 37.53	123.51 ± 53.40	117.19 ± 47.10	131.33 ± 56.59	152.14 ± 68.97	0.135	0.081	0.275
Fiber (g)	9.16 ± 4.87	9.15 ± 4.08	9.98 ± 3.42	10.41 ± 5.18	11.10 ± 4.60	11.29 ± 4.42	0.183	0.158	0.407
Polyunsaturated fatty acid (g)	8.17 ± 3.04	10.36 ± 3.77	10.97 ± 7.14	8.67 ± 3.54	9.34 ± 5.96	11.04 ± 5.61	0.618	0.146	0.663
Cholesterol (mg)	214.52 ± 146.08	264.56 ± 223.31	200.64 ± 101.33	295.72 ± 162.82	236.46 ± 104.11	279.86 ± 142.74	0.124	0.647	0.127
Vitamins									
D (µg)	3.41 ± 4.44	1.50 ± 1.17	2.19 ± 3.03	3.37 ± 3.37	4.04 ± 2.73	4.36 ± 3.32	0.299	0.003	0.023
A (mg)	596.68 ± 429.33	635.98 ± 359.44	1117.49 ± 2070.88	882.76 ± 627.28	707.84 ± 444.92	550.96 ± 234.41	0.124	0.533	0.793
E (mg)	6.18 ± 2.97	6.81 ± 3.96	7.68 ± 4.22	7.54 ± 3.04	7.90 ± 5.33	8.45 ± 3.76	0.190	0.677	0.458
Carotene (mg)	2.07 ± 2.26	1.81 ± 1.31	1.77 ± 1.31	1.88 ± 1.26	1.99 ± 2.52	1.13 ± 0.57	0.533	0.442	0.256
Thiamine (mg)	0.48 ± 0.14	0.46 ± 0.22	0.50 ± 0.14	0.51 ± 0.24	0.54 ± 0.21	0.62 ± 0.21	0.738	0.316	0.142
Riboflavin (mg)	0.69 ± 0.36	0.73 ± 0.36	0.80 ± 0.38	0.92 ± 0.36	0.91 ± 0.22	0.98 ± 0.37	0.151	0.077	0.205
Pyridoxine (mg)	0.85 ± 0.42	0.85 ± 0.43	0.93 ± 0.26	0.83 ± 0.45	0.78 ± 0.38	0.99 ± 0.39	0.851	0.479	0.827
Folate (µg)	152.51 ± 73.06	147.79 ± 69.09	154.86 ± 76.37	175.49 ± 86.60	175.35 ± 92.36	158.68 ± 63.03	0.253	0.406	0.663
Minerals									
Iodine (mg)	249.43 ± 124.36	273.39 ± 117.76	271.29 ± 110.79	337.52 ± 112.59	356.30 ± 144.33	329.21 ± 140.45	0.061	0.135	0.239
Sodium (mg)	1744.81 ± 741.73	1748.40 ± 901.61	2194.08 ± 1041.97	2237.35 ± 738.27	2360.82 ± 814.64	2528.34 ± 912.43	0.081	0.056	0.256
Potassium (mg)	1362.60 ± 450.46	1359.87 ± 660.28	1511.67 ± 412.08	1501.22 ± 600.62	1579.38 ± 527.95	1667.94 ± 542.77	0.480	0.198	0.458
Calcium (mg)	343.79 ± 225.60	307.87 ± 189.17	394.24 ± 112.93	416.61 ± 202.73	460.99 ± 148.62	481.46 ± 195.24	0.360	0.028	0.256
Magnesium (mg)	146.07 ± 45.81	144.94 ± 49.42	163.16 ± 33.97	167.48 ± 73.45	174.99 ± 61.00	195.07 ± 59.87	0.280	0.114	0.127
Iron (mg)	6.04 ± 1.97	5.50 ± 2.54	6.32 ± 1.84	6.38 ± 2.86	6.26 ± 2.13	7.65 ± 2.49	0.693	0.170	0.106
Zinc (mg)	6.16 ± 2.35	6.10 ± 2.76	6.30 ± 2.50	6.69 ± 2.46	6.29 ± 2.28	7.58 ± 2.22	0.350	0.787	0.127

D group, vit-D supplemented group; C, no reinforcement. [a]Data are expressed as mean ± SD. [b-d]*p* values were determined using a Mann-Whitney U test. vit.: Vitamin, SD: Standard deviation, M1: First measurement, M2: Second measurement, M3: Third measurement

Table 3. Comparison of anthropometric measurements of all volunteers[a]

	Group D (n= 14)			Group C (n= 16)			p^b	p^c	p^d
	M1	M2	M3	M1	M2	M3			
Weight (kg)	60.81 ± 10.15	61.50 ± 9.77	62.06 ± 10.30	61.72 ± 11.38	62.10 ± 11.10	62.29 ± 11.10	0.803	0.917	0.861
Height (cm)	161.79 ± 3.24	161.86 ± 3.30	161.79 ± 3.24	162.13 ± 6.73	162.13 ± 6.73	161.53 ± 6.52	0.868	0.917	0.896
BMI (kg/m^2)	23.21 ± 3.64	23.46 ± 3.57	23.69 ± 3.71	23.40 ± 3.48	23.56 ± 3.45	23.79 ± 3.36	0.835	0.901	0.861
Waist/Hip	0.78 ± 0.05	0.78 ± 0.05	0.79 ± 0.05	0.80 ± 0.07	0.78 ± 0.05	0.79 ± 0.05	0.465	0.950	0.948
Waist (cm)	75.29 ± 10.17	75.93 ± 9.98	76.71 ± 10.25	75.88 ± 10.78	76.38 ± 10.29	72.65 ± 22.26	0.851	0.967	0.861
Visceral fat	1.86 ± 1.17	1.79 ± 1.12	2.00 ± 1.24	1.81 ± 1.11	1.81 ± 1.11	2.07 ± 1.16	0.964	0.837	0.814
Muscle (%)	70.85 ± 6.76	70.39 ± 6.39	69.97 ± 6.69	70.55 ± 6.32	70.18 ± 5.46	69.32 ± 5.38	0.934	0.967	1.000
Mineral (%)	4.79 ± 0.98	4.64 ± 0.93	4.83 ± 0.93	4.84 ± 0.90	4.82 ± 0.88	4.93 ± 0.83	0.934	0.519	0.662
Protein (%)	15.97 ± 1.61	15.97 ± 1.62	15.63 ± 1.58	15.69 ± 1.27	15.74 ± 1.35	15.38 ± 1.30	0.493	0.662	0.727
PBF (%)	25.34 ± 7.15	25.84 ± 6.75	26.29 ± 7.04	25.68 ± 6.66	26.06 ± 5.77	26.98 ± 5.66	0.934	1.000	0.983
BMR (Kcal)	1398.6 ± 129.73	1407.07 ± 120.77	1409.21 ± 126.10	1410.25 ± 144.43	1414.38 ± 146.93	1404.27 ± 147.74	0.852	0.983	0.810

D group, vit-D supplemented group; C, no reinforcement. [a]Data are expressed as mean ± SD, [b-d]*p* values were determined using a Mann-Whitney U test. BMI: Body mass index, PBF: Body fat percentage, BMR: Basal metabolic rate, SD: Standard deviation, M1: First measurement, M2: Second measurement, M3: Third measurement

FSG and TG levels was observed between M1 and M2 in Group C. In addition, a significant decrease in FSG and HDL levels was observed between M2 and M3. There was a significant difference in HDL values in M2 between groups D and C. The M3 FSG and LDL levels were lower in the experimental group, whereas the 25-hydroxyvitamin D levels were higher (Table 4).

In group D, a significant difference was observed between the FSG values of obese and normal-weight women in the M2 and M3. In addition, 25-hydroxyvitamin D levels were higher in normal-weight women than in obese women according to M3. In Group C, M2 showed that normal-weight women had lower TG values than obese women (Table 5).

When women were categorized as obese and normal-weight, HDL levels of normal-weight women were found to be lower in group D than in group C in the M2. In M3, 25-hydroxyvitamin D levels of normal women in the D group were significantly higher, whereas FSG levels were significantly lower than in group C. FSG levels in group D were significantly lower in the M2 of obese women than in group C. In the M3 of obese individuals, 25-hydroxyvitamin D levels were significantly higher in the D group than in group C. The M1 showed no significant difference between the obese and normal-weight women's groups (Group C and Group D) (Figure 2).

In M1 of group C, a moderate positive correlation was found between 25-hydroxyvitamin D and TG and LDL, respectively (r= 0.531 p= 0.034, r= 0.516 p= 0.041). In M2 of group C, a moderately strong positive correlation was observed between iodine intake and TSH level (r= 0.594, p= 0.015). M2 of HDL had a moderate positive correlation with □-linolenic acid, linoleic acid, MUFA, PUFA, and fat intake. In contrast, no significant correlation was found between M1 and M2, respectively (r= 0.653 $p < 0.001$, r= 0.571 p= 0.001, r= 0.436 p= 0.016, r= 0.573 p= 0.001, r= 0.536 p= 0.002).

In the M2 and M3 of the D group, a moderately strong positive correlation was observed between iodine intake and T3 values. At the same time, a moderately positive relationship was found between dietary vitamin D and serum 25-hydroxyvitamin D levels. There was no significant relationship between vitamin D intake and other serum 25-hydroxyvitamin D levels (M1, M3). While FSG and HDL in M1 in group D showed a highly negative correlation, no significant correlation was found between other measurements (M2, M3). In the M3 group, a moderate positive association was found between HDL and iodine intake and between T3 and vitamin D intake (Figure 3).

DISCUSSION

The current study investigated the effects of vitamin D supplementation on fasting serum glucose, serum lipid, serum TSH, and T3 levels in obese and normal-weight women with vitamin D deficiency.

Both groups (D and C) were evaluated in detail in terms of anthropometric values, frequency of food consumption, and routine biochemical parameters, and it was determined that the groups were close to each other.

Table 4. Responses of all volunteers to biochemistry parameters between and within groups[a]

	Group D (n= 14)			Group C (n= 16)			p^x	p^b	p^c	p^d	p^e	p^f	p^g	p^h	p^i
	M1	M2	M3	M1	M2	M3									
Fasting serum glucose level (mg/dL)	81.00 ± 5.55	76.71 ± 8.34	78.93 ± 11.98	86.25 ± 8.47	81.69 ± 9.62	87.60 ± 10.88	0.030	0.706	0.624	0.043	0.026	0.865	0.144	0.163	0.044
LDL (mg/dL)	81.21 ± 18.76	77.11 ± 16.48	75.20 ± 17.54	85.36 ± 27.71	79.76 ± 25.69	90.93 ± 24.55	0.109	0.975	0.209	0.423	0.084	0.638	0.835	0.787	0.048
HDL (mg/dL)	48.64 ± 13.79	44.07 ± 10.77	49.57 ± 9.51	52.81± 11.39	56.31 ± 9.10	47.21 ± 10.48	0.102	0.017	0.950	0.352	0.019	0.346	0.441	0.004	0.629
Non-HDL	93.57 ± 22.01	90.00 ± 18.77	89.93 ± 18.12	94.19 ± 30.47	93.44 ± 27.17	105.43 ± 26.50	0.162	0.530	0.432	0.897	0.069	0.278	0.852	0.632	0.161
TC (mg/dL)	142.64 ± 25.46	134.07 ± 21.71	139.50 ± 19.91	147.00 ± 30.91	149.75 ± 25.19	152.64 ± 20.23	0.059	0.132	0.638	0.552	0.249	0.507	0.708	0.088	0.089
TG (mg/dL)	61.50 ± 28.95	64.86 ± 30.19	73.57 ± 34.77	57.38 ± 14.27	67.75 ± 19.13	71.79 ± 21.56	0.700	0.330	0.033	0.035	0.551	0.026	0.950	0.140	0.476
TSH (mIU/mL)	1.83 ± 1.24	1.63 ± 0.82	1.51 ± 0.65	1.43 ± 0.75	1.59 ± 0.90	1.77 ± 1.11	0.925	0.552	0.660	0.918	0.706	0.198	0.360	0.835	0.927
T3 (nmol/L)	2.66 ± 1.17	2.55 ± 0.65	2.64 ± 0.60	2.22 ± 0.60	2.26 ± 0.70	2.41 ± 1.03	0.917	0.346	0.551	1.000	0.184	0.132	0.417	0.119	0.476
25-hydroxyvitamin D (ng/mL)	10.94 ± 2.58	13.66 ± 3.76	24.47 ± 10.13	11.78 ± 2.40	12.11 ± 3.87	15.01 ± 11.12	0.052	0.001	0.001	0.717	0.925	0.331	0.129	0.056	< 0.001
LDL/HDL	1.79 ± 0.61	1.84 ± 0.59	1.56 ± 0.40	1.68 ± 0.458	1.49 ± 0.64	2.04 ± 1.01	-	-	-	-	-	-	0.868	0.074	0.295
TC/HDL	3.10 ± 0.77	3.16 ± 0.75	2.89 ± 0.56	2.87 ± 0.68	2.73 ± 0.71	3.37 ± 3.14	-	-	-	-	-	-	0.647	0.105	0.407

D group, vit-D supplemented group; C, no reinforcement. [a]Data are expressed as mean ± SD. Group D [M1-M2 (p^x)], [M2-M3 (p^b)], and [M1-M3 (p^c)] were determined using the paired Wilcoxon Test for within-group differences. Group C [M1-M2 (p^d)], [M2-M3(p^e)], and [M1-M3(p^f)] were determined using the paired Wilcoxon Test for within-group differences. Differences between groups D and C [M1-M1 (p^g)], [M2-M2 (p^h)], and [M3-M3 (p^i)] were determined using the Mann-Whitney U test. SD: Standard deviation, M1: First measurement, M2: Second measurement, M3: Third measurement, LDL: Low-density lipoprotein, HDL: High-density lipoprotein, TC: Total cholesterol, TSH: Thyroid-stimulating hormone, T3: Triiodothyronine, TG: Triglyceride

Vitamin D deficiency is common nowadays and can lead to many negative consequences. Therefore, to eliminate this deficiency and prevent its effects, vitamin D supplementation should be administered at appropriate doses to reach serological levels. The recommended daily vitamin D supplement level by the WHO is 200-400 IU/day.[13]

Participants in the study by Hirschler et al.[14] received a monthly vitamin D dose of 100,000 IU. In another study, volunteer women with vitamin D deficiency were given 2800 IU of vitamin D daily for 12 weeks.[15] When the studies were examined, it was stated that no side effects were observed. In this study, 75,000 IU vitamin D supplements per month were administered to volunteers with vitamin D deficiency, and no side effects were detected.

Serum 25-hydroxyvitamin D levels were correlated with glucose homeostasis after reviewing experimental and observational studies on the impact of vitamin D supplementation were reviewed.[16] Low serum 25-hydroxyvitamin D levels impair insulin secretion and increase the risk of developing T2DM. Low vitamin D levels are associated with high FSG.[17] In another study, the use of vitamin D3 supplementation did not result in a significantly lower risk of diabetes among individuals with vitamin D deficiency.[18] This study found that fasting serum glucose levels decreased significantly when serum 25-hydroxyvitamin D levels increased concurrently with vitamin D management in women with vitamin D deficiency. A study examining glucose metabolism and lipid profiles in young people, excluding vitamin D, reported a significant negative correlation between FSG and HDL levels.[19] Similarly, in this study, a significant negative correlation was found between FSG and HDL in the M1 in group D. In addition, FSG levels at the M2 in group D significantly decreased compared with the M1.

Body fat distribution is also important for glucose, lipid metabolism, and 25-hydroxyvitamin D levels. In another study, obese children were found to have lower HDL-C and higher TG levels than healthy children. At the same time, glucose, LDL, and TC levels were lower in normal children than in obese children.[20] In this study, the HDL levels of normal individuals in group D were lower at the M2, and the FSG levels were lower at the third. FSG levels of obese subjects in group D were lower in the M2, but there was

a similarity in the M3. At the same time, 25-hydroxyvitamin D levels were higher at the M3 in the D group in both the normal and obese groups.

Results suggest a relationship between 25-hydroxyvitamin D deficiency in the blood and thyroid diseases.[21] In a previous study, serum 25-hydroxyvitamin D levels were significantly negatively correlated with TSH levels. A study by Mansorian et al.[22] reported a decrease in T3 levels with an improvement in vitamin D status. This study found no relationship between 25-hydroxyvitamin D levels and TSH and T3 levels.

Conversely, older people with 25-hydroxyvitamin D deficiency were administered vitamin D supplements. It was found that there was no difference in the TSH and T3 levels of older people.[7] Similarly, no significant difference was found in serum TSH and T3 values between the groups in this study.

Based on the related studies, there were conflicting results on the lipid profile of vitamin D supplementation. Normal vitamin D levels were observed to improve HDL-C levels compared with low levels in the Fraser et al.[23] study. In another study examining the high- and low-dose vitamin D supplement groups, an increase in plasma TGs was noted in the high-dose group at the end of the 6th month.[24,25] In this study, 25-hydroxyvitamin D and HDL cholesterol levels significantly increased between the second and third assessments in group D. In addition, the TG

Table 5. Evaluation of biochemical parameters in obese and normal weight women in the groups[a]

Group D	**Women with obesity (n= 6)**			**Women with normal-weight (n= 8)**					
	M1	**M2**	**M3**	**M1**	**M2**	**M3**	***p*[a]**	***p*[b]**	***p*[c]**
Fasting serum glucose level (mg/dL)	79.17 ± 1.33	71.33 ±4.84	88.33 ± 11.13	82.38 ± 7.13	80.75 ± 8.31	71.88 ± 6.75	0.646	0.030	0.005
LDL (mg/dL)	90.14 ± 20.14	83.93 ± 19.17	78.50 ± 16.48	74.33 ± 15.41	72.00 ± 13.13	72.73 ± 19.01	0.115	0.191	0.563
HDL (mg/dL)	48.33 ± 13.72	44.33 ± 13.20	52.83 ± 10.67	48.88 ± 14.79	43.88 ± 9.54	47.13 ± 8.41	0.945	0.941	0.284
Non-HDL	104.83 ± 25.61	99.17 ± 22.57	93.50 ± 18.77	85.13 ± 15.52	83.13 ± 12.81	87.25 ± 18.41	0.098	0.160	0.545
TC (mg/dL)	153.17 ± 28.27	143.50 ± 20.90	146.33 ± 12.37	134.75 ± 21.61	127.00 ± 20.74	134.38 ± 23.59	0.191	0.168	0.283
TG (mg/dL)	71.67 ± 43.88	75.67 ± 42.94	75.00 ± 47.87	53.88 ± 5.11	56.75 ± 14.14	72.50 ± 24.59	0.897	0.301	0.536
TSH (mIU/mL)	2.87 ± 1.81	1.72 ± 0.99	1.38 ± 0.69	1.50 ± 0.47	1.56 ± 0.74	1.61 ± 0.65	0.352	0.744	0.871
T3 (nmol/L)	2.81 ± 1.52	2.39 ± 0.43	2.67 ± 0.70	2.55 ± 0.94	2.68 ± 0.79	2.62 ± 0.55	0.605	0.442	0.876
25-hydroxyvitamin D (ng/mL)	10.77 ± 1.60	11.68 ± 1.55	18.67 ± 4.34	11.08 ± 3.25	15.14 ± 4.33	28.83 ± 11.25	0.746	0.089	0.043
Group C	**Women with obesity (n= 9)**			**Women with normal-weight (n= 7)**					
	M1	**M2**	**M3**	**M1**	**M2**	**M3**	***p*[a]**	***p*[b]**	***p*[c]**
Fasting serum glucose level (mg/dL)	84.89 ± 7.08	79.56 ± 6.39	89.89 ± 10.59	88.00 ± 10.30	84.43 ± 12.71	88.43 ± 12.05	0.999	0.332	0.800
LDL (mg/dL)	83.51 ± 36.02	80.93 ± 24.56	90.64 ± 25.89	87.74 ± 13.33	78.26 ± 28.99	86.00 ± 24.50	0.115	0.884	0.734
HDL (mg/dL)	49.22 ±12.07	53.78 ± 11.26	49.00 ± 11.28	57.43 ± 9.25	59.57 ± 4.04	46.50 ± 9.97	0.080	0.182	0.668
Non-HDL	95.67 ± 39.20	96.00 ± 26.80	106.78 ± 27.85	92.29 ± 16.27	90.14 ± 29.42	99.17 ± 22.16	0.098	0.684	0.605
TC (mg/dL)	144.89 ± 38.72	149.78 ± 22.07	155.78 ± 18.47	149.71 ± 19.32	149.71 ± 30.62	145.67 ± 22.95	0.266	0.996	0.362
TG (mg/dL)	60.44 ± 17.22	74.78 ± 19.43	80.22 ± 24.63	53.43 ± 9.03	58.71 ± 15.54	64.83 ± 12.67	0.710	0.022	0.238
TSH (mIU/mL)	1.17 ± 0.43	1.25 ± 0.63	1.65 ± 1.03	1.77 ± 0.96	2.03 ± 1.05	1.92 ± 1.31	0.114	0.084	0.656
T3 (nmol/L)	2.36 ± 0.67	2.31 ± 0.81	2.86 ± 1.23	2.06 ± 0.48	2.11 ± 0.57	2.32 ± 0.58	0.315	0.958	0.238
25-hydroxyvitamin D (ng/mL)	11.68 ± 2.63	11.22 ± 3.14	11.76 ± 1.77	11.91 ± 2.29	13.26 ± 4.65	19.47 ± 17.28	0.633	0.265	0.409

D group, vit-D supplemented group; C, no reinforcement. [a]Data are expressed as mean ± SD. Differences between groups D and C [M1-M1 (p^x)], [M2-M2 (p^b)], and [M3-M3 (p^c)] were determined using the independent sample t-test, SD: Standard deviation, M1: First measurement, M2: Second measurement, M3: Third measurement, LDL: Low-density lipoprotein, HDL: High-density lipoprotein, TC: Total cholesterol, TSH: Thyroid-stimulating hormone, T3: Triiodothyronine, TG: Triglyceride

levels of the D group increased significantly, but this increase was associated with a return of the TG value closer to the normal range. Looking at group D in this study, it can be said that the HDL-C profile improved in parallel with the increase in vitamin D levels.

A large-scale cohort study found that increased vitamin D levels were correlated with increased TC and HDL levels but not LDL cholesterol. The meta-analysis revealed no correlation between TC and HDL-C. There was no significant correlation between LDL-C and TC levels in group D in this study.[25]

Considering the relationship between dietary iodine and thyroid hormones, a significant negative correlation was reported between iodine intake and TSH levels, but no significant relationship was found for T3 levels.[21] In another study, lambs were supplemented with iodine, and a significant reduction in T3 levels was found.[26] In the second and M3s of group D, there was a strong positive correlation between iodine intake and T3 levels as a result of this study, but no significant difference in TSH levels was found.

It has been observed that the HDL-C levels of those who eat rich monounsaturated fatty acids increase. It has been stated that feeding with high-oleic acid oils also increases HDL concentrations.[27,28] The serum LDL to HDL ratio was found to be lower in those with oleic acid consumption from the two groups compared with palmitic acid and oleic acid consumption compared with the palmitic acid consumption group in a study by Kien et al.[29] Although there was not a significant difference between the groups (D and C) in the first or last measures, it was found that HDL cholesterol levels decreased in the M2 in the present study.

In addition, no significant difference was found in the LDL: HDL ratio. Furthermore, compared with group D, group C consumed much more vitamin D, calories, protein, fat, cholesterol, linolenic acid, linoleic acid, myristic acid, lauric acid, palmitic acid, oleic

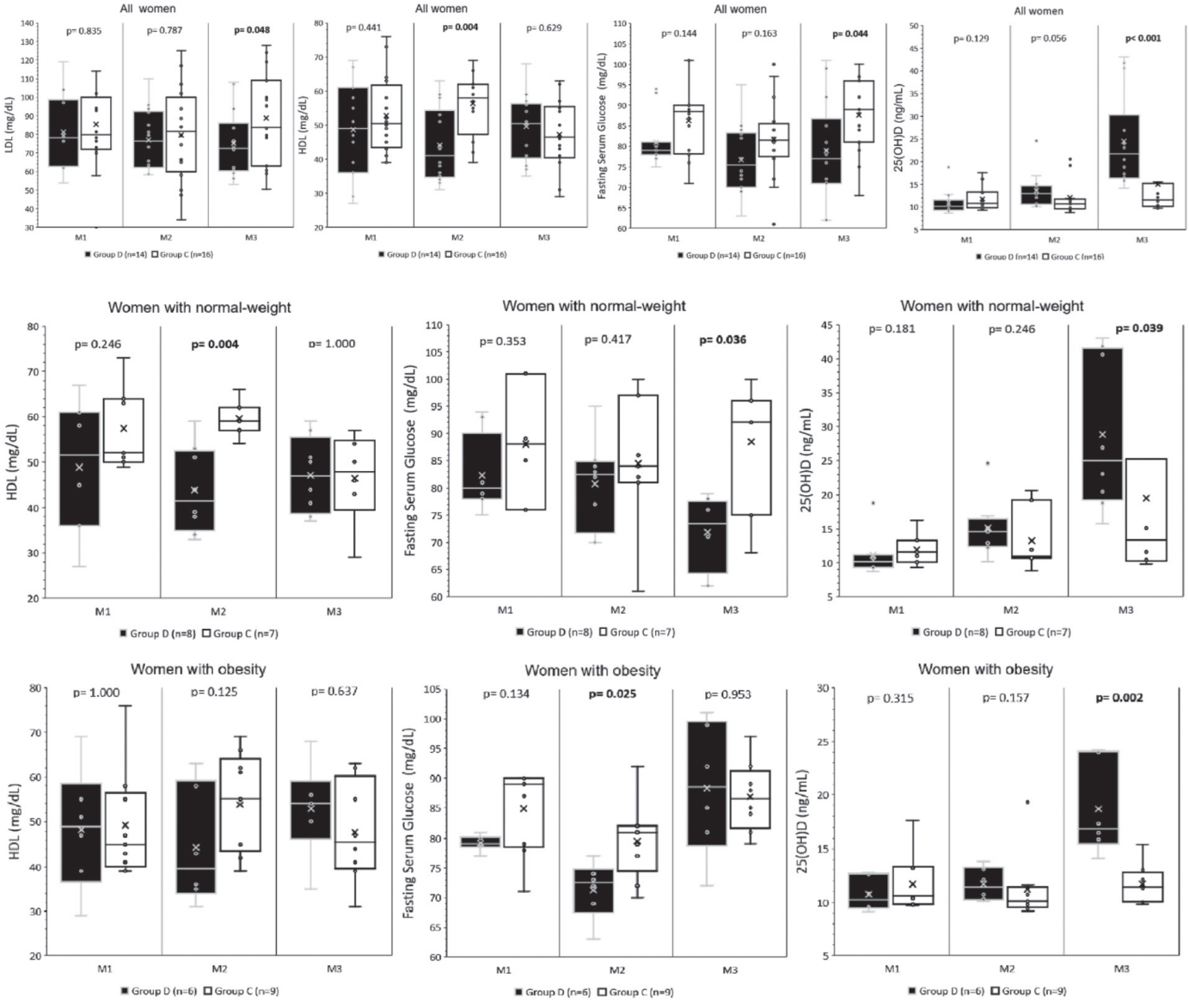

Figure 2. Responses of volunteers to biochemistry parameters between and within groups

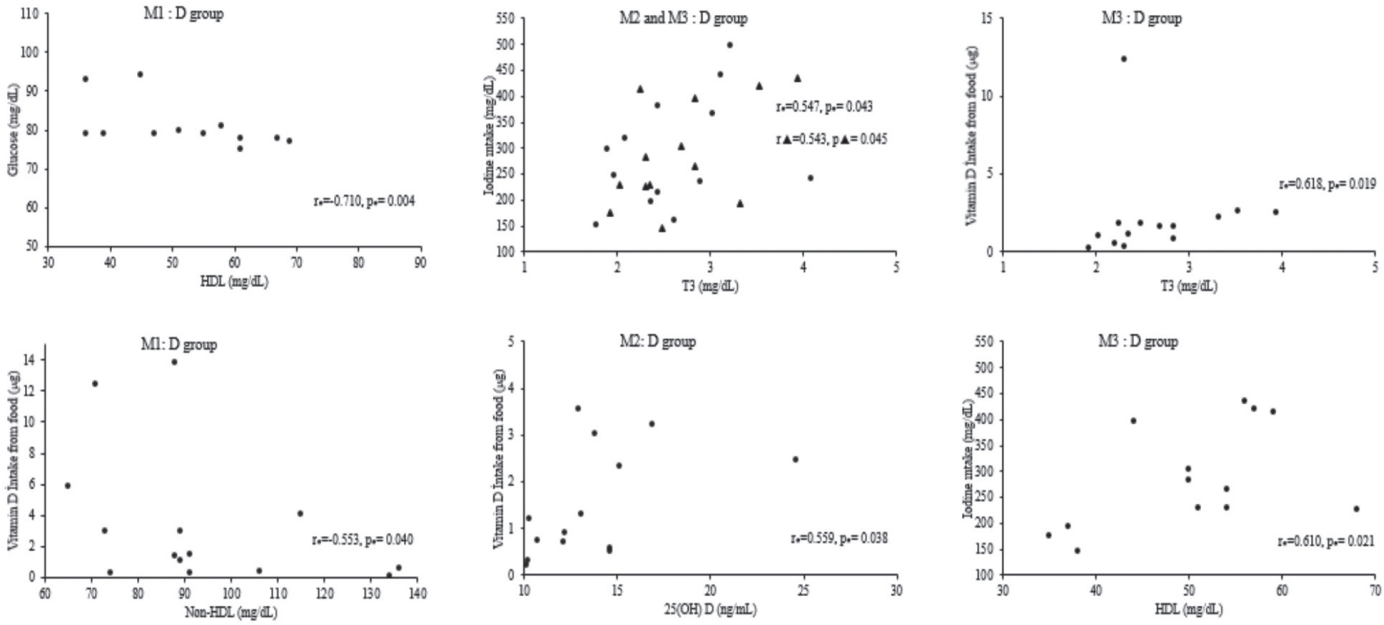

Figure 3. Correlation between group D

acid, MUFA, and PUFA. In the M2 in group C (M2), HDL levels were moderately positively correlated with ⍺-linolenic acid, linoleic acid, MUFA, PUFA, and fat intake. It is thought that the decrease in HDL levels in the M2 was due to the experimental group being fed less in terms of monounsaturated fatty acids, such as olive oil and oilseeds; group C consumed more vitamin D than group D, and they consumed less oleic acid. There were no significant differences in TC, non-HDL, or LDL levels. Although the study included vitamin D supplementation, no dietary intervention was provided, so nutritional differences between the groups may have affected the results.

Studies have indicated that omega-3 fatty acids have advantages for healthy lipid profiles, but omega-6 fatty acids should be avoided. An important consideration for improving lipid profiles is the omega-6 to omega-3 ratio of fatty acids.[24] There are suggestions to decrease the intake of omega-6 fatty acids and increase the intake of omega-3 fatty acid supplements. The World Health Organization recommends keeping the omega-6:3 ratio between 5:1 and 10:1. Omega-3 fatty acids lower plasma TG levels and the lipid profile.[30] A significant correlation was found between LDL-C, TGs, TC, TC/HDL ratio, and omega-6/3 ratio. In the control group in this study, it was observed that there was a decrease in HDL cholesterol levels between the second and M3s, and TG levels increased from the first to the last measurement. It is thought that due to the increase in the intake of white bread, butter, eggs, sunflower oil, omega-6, and saturated fatty acids (palmitic, myristic, and lauric), the omega-6/omega-3 balance is disturbed.

Therefore, HDL-C levels may be reduced.

In summary, although group D received supplementation, dietary vitamin D intake was lower than that of group C. Therefore, no difference was observed in serum 25-hydroxyvitamin D levels between the groups in the M2. In addition, the fact that HDL levels are high in group C may also be because vitamin D intake is very high compared with that in group D. The potential to increase HDL-C levels is related to vitamin D intake. Therefore, in the final measurement, we predict that an increase in vitamin D intake will improve HDL levels and decrease fasting serum glucose levels in addition to vitamin D supplementation.

Study limitations

There are limitations to this study. The volunteers were not given a standard diet. Vitamin D consumption was assessed based on self-reported information, and intake was tracked by requesting a remote photo. Eight weeks are considered a brief duration for the study. The sample size caused the number of volunteer participants to be small due to budget limitations. Therefore, more comprehensive studies are needed to obtain more evident results.

CONCLUSION

Vitamin D intake in the body is believed to improve fasting serum glucose and HDL levels. On the other hand, when examined in more detail, vitamin D intake can be said to improve HDL levels in normal-weight individuals and to cause fasting serum glucose levels to be at the desired low level. In contrast, in individuals with obesity, although serum 25-hydroxyvitamin D levels increased during the last measurement, no effect was observed. As a consequence of vitamin D intake, serum 25-hydroxyvitamin D levels are higher in individuals with normal weight than in those with obesity. Significant positive correlations were observed between dietary vitamin D intake and serum 25-hydroxyvitamin D levels and between iodine intake and T3 levels. In addition, a high omega-6/omega-3 ratio reduces the effect of 25-hydroxyvitamin D intake on biochemical parameters.

Considering these results, it is important to implement nutritional interventions or monitor food consumption, especially when evaluating the effects on serum lipids and thyroid.

Acknowledgments

We thank nurses Muazzez Tüfekçi and dietitian Berat Uygur for their help in the study. I would like to express my deepest gratitude to Harun Gençosmanoğlu (0000-0002-5258-8833) for his invaluable assistance in linguistic editing and refining this article. Their keen insights, constructive feedback, and unwavering support played a crucial role in shaping the final version of this paper. I am truly fortunate to have a dedicated and knowledgeable collaborator.

Ethics

Ethics Committee Approval: The ethics committee approval for this study was approved by the Avrasya University Ethics Committee (approval number: 2022-52/14, date: 21.07.2022).

Informed Consent: Informed consent was obtained from all participants.

Authorship Contributions

Surgical and Medical Practices: F.C., Concept: F.C., Z.N.G., Design: F.C., Data Collection or Processing: F.C., Z.N.G., Analysis or Interpretation: F.C., Literature Search: F.C., Z.N.G., Writing: F.C., Z.N.G.

Conflict of Interest: The authors have no conflicts of interest to declare.

Financial Disclosure: This work was supported by the Research Promotion Program of Avrasya University 2021/02 number.

REFERENCES

1. Akkoyun HT, Bayramoğlu M, Ekin S, Çelebi F. Vitamin D and its importance for the metabolism. Atatürk Üniversitesi Vet Bilim Derg. 2014;9:213-219.
2. Need AG, O'Loughlin PD, Horowitz M, Nordin BE. Relationship between fasting serum glucose, age, body mass index, and serum 25 hydroxyvitamin D in postmenopausal women. Clin Endocrinol (Oxf). 2005;62:738-741.
3. Challoumas D. Vitamin D supplementation and lipid profile: what does the best available evidence show? Atherosclerosis. 2014;235:130-139.
4. Dibaba DT. Effect of vitamin D supplementation on serum lipid profiles: a systematic review and meta-analysis. Nutr Rev. 2019;77:890-902.
5. Chailurkit LO, Aekplakorn W, Ongphiphadhanakul B. Regional variation and determinants of vitamin D status in sunshine-abundant Thailand. BMC Public Health. 2011;11:853.
6. Zhang Q, Wang Z, Sun M, Cao M, Zhu Z, Fu Q, Gao Y, Mao J, Li Y, Shi Y, Yang F, Zheng S, Tang W, Duan Y, Huang X, He W, Yang T. Association of high vitamin d status with low circulating thyroid-stimulating hormone independent of thyroid hormone levels in middle-aged and elderly males. Int J Endocrinol. 2014;2014:631819.
7. Chahardoli R, Saboor-Yaraghi AA, Amouzegar A, Khalili D, Vakili AZ, Azizi F. Can supplementation with Vitamin D modify thyroid autoantibodies (Anti-TPO Ab, Anti-Tg Ab) and thyroid profile (T3, T4, TSH) in Hashimoto's thyroiditis? A double blind, randomized clinical trial. Horm Metab Res. 2019;51:296-301.
8. Rosen CJ. Clinical practice. Vitamin D insufficiency. N Engl J Med. 2011;364:248-254.
9. Cesur F, Seçkiner S, Kucukerdonmez O, Cagindi O, Saygili LF, Meseri R. Can enzyme-resistant starch snack prevent blood glucose fluctuations? A pilot trial in patients with ınsulin-treated type 2 diabetes. Starch. 2023;75:9-10.
10. American Diabetes Association. Classification and diagnosis of diabetes: standards of medical care in diabetes-2021. Diabetes Care 44 (2021): S15-S33.
11. Lee DH, Kim HK, Lee JK, Lim SC. Early diagnosis of chyle fistula with SD LipidoCare after neck dissection. J Laryngol Otol. 2021;135:355-358.
12. Alipour Nosrani E, Majd M, Bazshahi E, Mohtashaminia F, Moosavi H, Ramezani R, Shahinfar H, Djafari F, Shab-Bidar S, Djazayery A. The association between meal-based diet quality index-international (DQI-I) with obesity in adults. BMC Nutr. 2022;8:156.
13. McKinney TJ, Patel JJ, Benns MV, Nash NA, Miller KR. Vitamin D status and supplementation in the critically Ill. Curr Gastroenterol Rep. 2016;18:18.
14. Hirschler V, Molinari C, Maccallini G, Hidalgo M, Gonzalez C. Healthier lipid profiles with vitamin D supplementation in a pilot study in Argentinean children of two ethnicities. Int J Vitam Nutr Res. 2016;86:48-55.
15. Bislev LS, Langagergaard Rødbro L, Bech JN, Pedersen EB, Kjaergaard AD, Ladefoged SA, Rolighed L, Sikjaer T, Rejnmark L. The effect of vitamin D3 supplementation on markers of cardiovascular health in hyperparathyroid, vitamin D insufficient women: a randomized placebo-controlled trial. Endocrine. 2018;62:182-194.
16. Scragg R, Sowers M, Bell C; Third National Health and Nutrition Examination Survey. Serum 25-hydroxyvitamin D, diabetes, and ethnicity in the Third National Health and Nutrition Examination Survey. Diabetes Care. 2004;27:2813-2818.
17. Liu E, Meigs JB, Pittas AG, McKeown NM, Economos CD, Booth SL, Jacques PF. Plasma 25-hydroxyvitamin d is associated with markers of the insulin resistant phenotype in non-diabetic adults. J Nutr. 2009;139:329-334.
18. Pittas AG, Dawson-Hughes B, Sheehan P, Ware JH, Knowler WC, Aroda VR, Brodsky I, Ceglia L, Chadha C, Chatterjee R, Desouza C, Dolor R, Foreyt J, Fuss P, Ghazi A, Hsia DS, Johnson KC, Kashyap SR, Kim S, LeBlanc ES, Lewis MR, Liao E, Neff LM, Nelson J, O'Neil P, Park J, Peters A, Phillips LS, Pratley R, Raskin P, Rasouli N, Robbins D, Rosen C, Vickery EM, Staten M; D2d Research Group. Vitamin D supplementation and prevention of type 2 diabetes. N Engl J Med. 2019;381:520-530.
19. Fernandes AC, Marinho AR, Lopes C, Ramos E. Dietary glycemic load and its association with glucose metabolism and lipid profile in young adults. Nutr Metab Cardiovasc Dis. 2022;32:125-133.
20. Garcés C, Gutierrez-Guisado J, Benavente M, Cano B, Viturro E, Ortega H, de Oya M. Obesity in Spanish schoolchildren: relationship with lipid profile and insulin resistance. Obes Res. 2005;13:959-963.
21. Kim D. The Role of Vitamin D in Thyroid Diseases. Int J Mol Sci. 2017;18:1949.
22. Mansorian B, Mirza-Aghazadeh Attari M, Vahabzadeh D, Mohebbi I. Serum vitamin D level and its relation to thyroid hormone, blood sugar and lipid profiles in Iranian sedentary work staff. Nutr Hosp. 2018;35:1107-1114.
23. Fraser A, Williams D, Lawlor DA. Associations of serum 25-hydroxyvitamin D, parathyroid hormone and calcium with cardiovascular risk factors: analysis of 3 NHANES cycles (2001-2006). PLoS One. 2010;5:e1382.

24. Miao J, Bachmann KN, Huang S, Su YR, Dusek J, Newton-Cheh C, Arora P, Wang TJ. Effects of vitamin D supplementation on cardiovascular and glycemic biomarkers. J Am Heart Assoc. 2021;10:17727.

25. Wang H, Xia N, Yang Y, Peng DQ. Influence of vitamin D supplementation on plasma lipid profiles: a meta-analysis of randomized controlled trials. Lipids Health Dis. 2012;11:42.

26. Boland TM, Hayes L, Sweeney T, Callan JJ, Baird AW, Keely S, Crosby TF. The effects of cobalt and iodine supplementation of the pregnant ewe diet on immunoglobulin G, vitamin E, T3 and T4 levels in the progeny. Animal. 2008;2:197-206.

27. Jenkins DJ, Chiavaroli L, Wong JM, Kendall C, Lewis GF, Vidgen E, Connelly PW, Leiter LA, Josse RG, Lamarche B. Adding monounsaturated fatty acids to a dietary portfolio of cholesterol-lowering foods in hypercholesterolemia. CMAJ. 2010;182:1961-1967.

28. Arapostathi C, Tzanetakou IP, Kokkinos AD, Tentolouris NK, Vlachos IS, Donta IA, Perrea KN, Perrea DN, Katsilambros NL. A diet rich in monounsaturated fatty acids improves the lipid profile of mice previously on a diet rich in saturated fatty acids. Angiology. 2011;62:636-640.

29. Kien CL, Bunn JY, Stevens R, Bain J, Ikayeva O, Crain K, Koves TR, Muoio DM. Dietary intake of palmitate and oleate has broad impact on systemic and tissue lipid profiles in humans. Am J Clin Nutr. 2014;99:436-445.

30. Janczyk W, Socha P, Lebensztejn D, Wierzbicka A, Mazur A, Neuhoff-Murawska J, Matusik P. Omega-3 fatty acids for treatment of non-alcoholic fatty liver disease: design and rationale of randomized controlled trial. BMC Pediatr. 2013;13:85.

Turk J Pharm Sci 2024;21(5):413-420
DOI: 10.4274/tjps.galenos.2023.23428

ORIGINAL ARTICLE

The Inclusion of Sports and Exercise Related Module into Pharmacy Curriculum: Non-Pharmacological Approach on Students' Health Parameters

Ahmad Rashidi MOHAMED TAHIR[1]*, Voon Jia HAW[1], Wan Sazrina Wan ZAİD[2], Mariani Ahmad NİZARUDDİN[1], Fashli Syafiq ABD RAZAK[1], Arimi Fitri Mat LUDİN[3]

[1]University of Cyberjaya Faculty of Pharmacy, Department of Pharmaceutical Technology and Industry, Selangor, Malaysia
[2]Superbig Pharmacy, Selangor, Malaysia
[3]Universiti Kebangsaan Malaysia, Biomedical Science Programme and Center for Healthy Ageing and Wellness, Selangor, Malaysia

ABSTRACT

Objectives: To promote a holistic approach to healthcare, the University of Cyberjaya introduced a unique elective course called sports pharmacy, which incorporates components of lifestyle interventions. Customers increasingly seek guidance about lifestyle factors that impact their health. Pharmacists with expertise in sports and exercise can meet this need. However, there is a lack of studies on the impact of non-pharmacological approaches (NPAs) on health parameters among healthcare professionals and pharmacy students in Malaysia. The objectives of this study were to compare students' health parameters based on NPAs and identify the factors that motivate students to maintain their health.

Materials and Methods: The study comprised 47 Year 4 pharmacy students in the pre- and post-practical phases (September 2018 and November 2018), followed by the post-resting phase (May 2019). The data collection form in the Sport Pharmacy course was used for the data collection.

Results: Nearly half of the students initially displayed a normal body mass index (BMI). However, after the post-resting period, there was a noticeable increase in the number of students categorized as obese and those with elevated total cholesterol (TC) and fasting blood glucose (FBG) levels. Specifically, in the pre-study phase, out of 47 participants, 22 were within the normal BMI (47%), six underweight (13%), nine overweight (19%), and ten obese (21%). The intervention phase showed a slight reduction in the overweight category, while the obese category showed an increase. For TC, the pre-phase had 70% of participants within the normal range, with 26% borderline high and 4% high. Post-study, showed an improvement, likely influenced by controlled dietary intake and physical activity. In the post-resting phase, however, there was a regression as the majority did not adhere to the non-pharmacological regimen. FBG demonstrated significant changes after the intervention, particularly within the normal range (≤ 6.0 mmol/L), showing the only statistically significant change across parameters. While the post-resting phase saw a minor increase, it remained below baseline. Approximately 23% continued diet control, while 32% maintained physical activity. Key motivations included health improvement, visible results, and improved well-being, while lack of motivation, time, and study schedules were primary discontinuation factors.

Conclusion: The 10-week intervention significantly impacted FBG but had limited influence on BMI and TC. Post-resting outcomes highlight that only a small fraction maintained the non-pharmacological approach, resulting in no marked changes in any parameters. Recommendations include further long-term studies to confirm the sustained benefits and the role of educational institutions in supporting such interventions.

Keywords: Non-pharmacological, body mass index, fasting blood glucose, total cholesterol, pharmacy students

***Correspondence:** rashidi@cyberjaya.edu.my, **ORCID-ID:** orcid.org/0000-0002-6983-4084
Received: 02.08.2023, **Accepted:** 12.09.2023

INTRODUCTION

Sports pharmacy is defined as the science and practice of dispensing medication and medical equipment for individuals participating in exercise or sport and the provision of information and advice on exercise programs, treatment, and prevention of simple injuries.[1] A sports pharmacy course is offered by the Faculty of Pharmacy, University of Cyberjaya as an elective course in Year 4 Semester 1 of Bachelor of Pharmacy. This course equips students with knowledge and evidence-based advice on the promotion and maintenance of good health through an active lifestyle.[1] There is a practical session where students need to conduct a non-pharmacological approach of diet control and physical activity (DCPA) for 10 weeks as part of their assessment.

Human health status can be defined by a variety of physiological health parameters, such as body mass index (BMI), fasting blood glucose (FBG), and total cholesterol (TC).[2] According to the World Health Organization (WHO), BMI is defined as a person's weight in kilograms divided by the square of the person's height in meters (kg/m²).[3] Both low BMI (< 22.6 kg/m²) and high BMI (> 27.5 kg/m²) were associated with an increased risk of death from any cardiovascular disease (CVD), cancer, or other causes, resulting in an overall U-shaped association among East Asians but not among Indians and Bangladeshis.[4] According to the Malaysian Clinical Practice Guideline on the management of type 2 diabetes mellitus (2015), FBG is used as a diagnostic tool for type 2 diabetes mellitus based on venous plasma glucose levels in symptomatic individuals.[5] Yiling et al.[6] found that the prevalence of retinopathy began to rise precipitously after FPG levels exceeded 5.8 mmol/L. Based on the Malaysian Clinical Practice Guideline on the Management of Dyslipidemia (2017), TC > 5.2 mmol/L is used as one of the diagnostic tools for dyslipidemia.[7] Raised TC is estimated to cause 2.6 million deaths and 29.7 million disability-adjusted life years (DALYs).[2] In both developed and developing countries, raised TC is a major cause of disease burden as a risk factor for ischemic heart disease (IHD) and stroke.[2]

Non-pharmacological approaches (NPAs) are defined as science-based and non-invasive interventions for human health without involving using of drugs.[8] Examples are physical activity and diet control. Physical inactivity has been identified as the fourth leading risk factor for mortality worldwide (6% of deaths globally).[9] In addition, physical inactivity is predicted to be the main cause of approximately 21-25% of breast and colon cancers, 27% of diabetes, and approximately 30% of IHD burden.[9] The WHO recommends that adults aged 18-64 years should perform at least 150 minutes of moderate-intensity aerobic physical activity throughout the week, at least 75 minutes of vigorous-intensity aerobic physical activity throughout the week, or an equivalent combination of moderate- and vigorous-intensity activities to maintain their health status.[9] Based on the WHO (2018) recommendations, a healthy diet helps protect against malnutrition in all forms, as well as NCDs.[9] An adequate, well-balanced diet together with regular physical activity is a cornerstone of good health.[9] Nybo et al.[10] found that FBG was reduced to a similar extent in the intense interval running and moderate-intensity running groups but remained unchanged in the strength training and control groups.

McManus et al.[11] found that the Mediterranean diet group with moderate fat had significantly reduced weight and BMI at 6, 12, and 18 months, with an average weight loss of 4.8 kg, compared with the low-fat diet group.

Social cognitive theory, including self-efficacy, is defined as the belief that one can organize and execute a course of action to achieve a specific goal and outcome expectations, which are beliefs that if a certain behavior is performed, it will lead to an anticipated outcome.[12] Based on the theory of self-efficacy theory, emphasis on the importance of individuals' perceptions of their personal capabilities as key determinants of successful outcomes is essential for promoting behavioral change to affect others. Pharmacy students need to experience the activities of healthy eating and physical exercise as conceptualized in the 7 pillars of self-care.[13] Pharmacists and pharmacy students recalled limited opportunities for education in sports pharmacy. There is a growing need for specialist pharmacists in the fields of sport and exercise.[13]

Ilow et al.[14] reported that 7.5% of males and 7.1% of females were overweight among 1168 pharmacy students in Poland. In this study, hypertension was diagnosed in 27.2% of males and 7.8% of females.[14] Most of the students did not consume enough fruits and vegetables (female students 61.8%, male students 75%).[14]

Furthermore, 41.9% of female students and 31.9% of male students.[14] Bastardo[15] also reported a similar finding: 106 (62%) pharmacy students did not exercise regularly, and male students (84.1%) were more likely to consume alcohol than female students (59.8%). Physical inactivity and unhealthy diets showed that there is a need for pharmacy students to practice NPAs such as DCPA to maintain their health conditions. The aim of this study is to determine the impacts of NPAs on health parameters, such as BMI, FBG, and TC, among Sports Pharmacy students.

MATERIALS AND METHODS

Participants and study design

This study was divided into pre- and post-resting phases conducted at the University of Cyberjaya in Cyberjaya. The pre- and post-phase phases were conducted from September 2018 to November 2018, and the post-resting phase was conducted in May 2019 after 6 months of resting from the post-study. In the study conducted, a group of 47 Year 4 Pharmacy students who chose to take Sport Pharmacy during their Semester 1 in 2018 were selected as participants. The study protocol was approved by the University of Cyberjaya Research Ethics Review Committee (approval number: CUCMS/CRERC/FR/030, date: 11.07.2019). Informed consent was obtained from all participants.

A data collection form, as used in the Sport Pharmacy course, was administered to participants in the pre-phase, post-phase,

and post-resting phases to document health parameters. Students measured their baseline health parameters during the pre-phase and after conducting the practical session.

In the pre-study phase, respondents' health parameters, such as TC, FBG, and BMI, were measured as baseline health parameters. Subjects were required to fast for at least 8 hours before the measurement of TC and FBG. TC and FBG were measured by withdrawing aseptically two drops of blood sample from the subject's fingertip. BMI was measured using a weighing machine and a stadiometer. Then, the respondents performed 10 weeks of diet control and exercise.

Diet control was defined as the restriction of food calorie intake per day based on the resting metabolism of the respondent as measured in the pre-study. Participants recorded their food intake daily, including breakfast, lunch, dinner, and snacks, and the total food calorie intake. Participants were encouraged to conduct at least 150 min of moderate-intensity aerobic or 75 min of vigorous-intensity aerobic exercise throughout the week. Diet intake and physical activity were submitted as a weekly report online every Sunday. In the 11th week, a post-study phase was conducted in which respondents' health parameters were re-measured. The post-resting phase was conducted 6 months later in May 2019 in which participants' health parameters were re-measured to compare differences in health parameters between the post-resting and post-resting studies.

Statistical analysis

All results were analyzed using the Statistical Package for Social Sciences (SPSS) software (version 25). Results were expressed as mean ± standard deviation for quantitative variables, such as BMI, TC, and FBG in pre-, post, and post-resting periods. Statistical significance was set at $p < 0.05$. A paired samples t-test was performed to compare the mean difference in TC between the pre- and post-studies. The Wilcoxon signed-rank test was used to compare the median difference in BMI and FBG between the pre-and post-resting phases, post- and post-resting phases, and the median difference in TC between the post- and post-resting phases. Multiple Response Analysis was used to study the factors for continuing or not continuing DCPA.

RESULTS

Table 1 presents the health parameters of students in the post and post-resting phase. In the pre-phase, out of 47 participants, 22 were within normal BMI (47%), six were underweight (13%), nine were overweight (19%), and ten were obese (21%). Twelve participants (26%) showed borderline high TC (5.2-6.2 mmol/L) and two participants (4%) showed high TC while the rest (70%) were within normal TC level (< 5.2 mmol/L). Only one respondent had a low FBG level (< 3.9 mmol/L), whereas the remaining (98%) showed normal FBG level (≤ 6.0 mmol/L).

In the post-study, out of 47 students, the same number of participants were within normal BMI (49%) and underweight (13%) categories. Eight participants were overweight (17%) and 11 were obese (21%). Eight participants (17%) showed borderline high TC, two participants (4%) showed high TC, and the remaining participants (79%) were within the normal TC level. Moreover, three participants (6%) had Impaired FBG (6.1-6.9 mmol/L), whereas the rest (94%) showed normal FBG levels.

In the post-resting study, the same number of participants remained in each BMI category. Four participants (9%) showed borderline high TC and six participants (13%) showed high TC, and the remaining (79%) showed normal TC level (≤ 5.2 mmol/L). Two respondents (4%) showed impaired FBG and only one respondent (2%) showed high FBG, whereas the remaining (94%) showed normal FBG levels.

Figure 1 shows that only 11 (23%) students continued their diet control, whereas 36 (77%) students did not continue their

Table 1. Comparison of pre-, post, and post-resting health parameters

		Pre		Post		Post-resting	
n		47		47		47	
Health parameters	Category	n (%)	Mean (SD)	n (%)	Mean (SD)	n (%)	Mean (SD)
BMI	Underweight	6 (13)	23.41 (4.99)	6 (13)	23.13 (4.75)	6 (13)	22.91 (4.83)
	Normal	22 (47)		22 (49)		22 (47)	
	Overweight	9 (19)		8 (17)		8 (17)	
	Obese	10 (21)		11 (21)		11 (23)	
TC	Normal	33 (70)	4.73 (0.81)	37 (79)	4.6 (0.66)	37 (79)	4.35 (1.22)
	Borderline high	12 (26)		8 (17)		4 (9)	
	High	2 (4)		2 (4)		6 (13)	
FBG	Low	1 (2)	5.12 (0.05)	0 (0)	5.09 (0.48)	0 (0)	5.45 (0.52)
	Normal	46 (98)		44 (94)		44 (94)	
	Impaired FBG	0 (0)		3 (6)		2 (4)	
	High	0 (0)		0 (0)		1 (2)	

n: Number, SD: Standard deviation, BMI: Body mass index, TC: Total cholesterol, FBG: Fasting blood glucose

diet control during the post-resting study. The main factors associated with continued diet control in the post-resting study are presented in Table 2. Out of 11 respondents who continued their diet control, the main factors for continuing were health (34.8%), followed by seeing results (getting fitter and healthier) (30.4%) and feeling better (26.1%). Only one respondent chose friends, praise, or rewards (4.3%) as the main factors for continued diet control. The main factors for not continuing diet control in the post-resting study are presented in Table 3. Among the 37 respondents who did not continue their diet control, their main factors were lack of motivation (33.8%), followed by study schedule (24.3%) and lack of time (21.6%). Four students chose financially and did not suit their needs (5.4%) as their main reasons for not continuing their diet control. Only three students chose lack of results (4.1%), whereas two students chose too restrictive and other reasons, such as laziness (2.7%), as their main factors for not continuing their diet control.

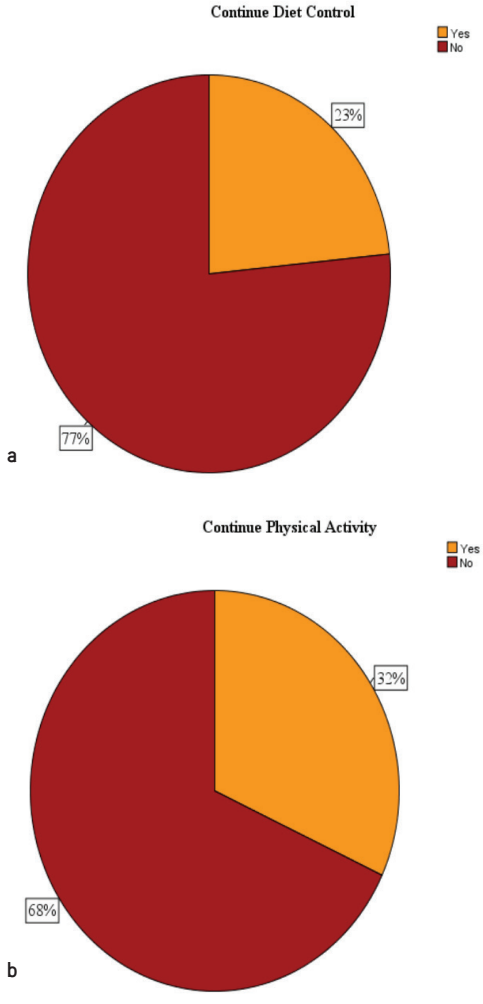

Figure 1. (a) A total of 23% of Year 4 Pharmacy students continued their diet control post-resting. Most Year 4 Pharmacy students (77%) did not continue diet control during the post-resting study. (b) Only 32% of Year 4 Pharmacy students continued physical activity during the post-resting study. Most Year 4 Pharmacy students (68%) did not continue physical activity in the post-resting study

Figure 1 shows that only 15 (32%) students continued physical activity, whereas 32 (68%) students did not continue physical activity in the post-resting study. The main factors associated with continuing physical activity in the post-resting study are presented in Table 4. The top 3 reported factors for continuing physical activity in the post-resting study were health (21.4%), having fun (21.4%), and feeling better (21.4%), respectively. A small proportion of students chose to see results (14.3%) and good appearances (11.9%), respectively. Only three students chose friends, whereas only one student chose praise or rewards as their main motivating factor for

Table 2. Factors for continuing diet control

Factors for continued diet control	Responses (n)	Percentage (%)
Friends	1	4.3
Praise/Rewards	1	4.3
Feeling better	6	26.1
Seeing results (Getting fitter and healthier)	7	30.4
Health	8	34.8
Total	23	100.0

Table 3. Factors for not continuing diet control

Factors associated with not continuing diet control	Responses (n)	Percentage (%)
Too restrictive	2	2.7
Other	2	2.7
Lack of results	3	4.1
Financial	4	5.4
Did not suit needs	4	5.4
Lack of time	16	21.6
Study schedule	18	24.3
Lack of motivation	25	33.8
Total	74	100.0

Table 4. Factors associated with continued physical activity

Factors associated with continued physical activity	Responses (n)	Percentage (%)
Praise/Rewards	1	2.4
Friends	3	7.1
Appearance	5	11.9
Seeing results	6	14.3
Feeling better	9	21.4
Health	9	21.4
Having fun	9	21.4
Total	42	100.0

continuing physical activity. Table 5 shows the main factors for not continuing physical activity in the post-resting study among 33 respondents: lack of motivation (38.5%), followed by lack of time (29.2%) and study schedule (23.1%). Two students chose financial and lack of results (3.1%) as their main factors for not continuing physical activity. Only one student's choice did not suit their needs, and the other was the main reason for not continuing physical activity.

Table 6 shows that there was a significant difference ($p < 0.05$) in FBG levels after 10 weeks of non-pharmacological treatment. However,there were no significant changes in BMI and TC after 10 weeks of NPAs. In addition, Table 6 shows that no significant differences were observed in BMI, TC, and FBG between the post- and post-resting study.

DISCUSSION

After implementing the non-pharmacological approach for 10 weeks, there was a slight decrease in the mean BMI from 23.41 kg/m^2 to 23.13 kg/m^2. A slight increase in the proportion of pharmacy students who were in the normal BMI category (49%) and a slight decrease in the percentage of students who were in the overweight category (17%) after completing 10 weeks of the non-pharmacological approach due to students who might want to control their weight by controlling their diet and conducting physical activity to lose weight. No underweight respondents were able to manage to go into the normal category because all students in this category were female who might want to control their weight to prevent weight gain. At the same time, no respondents in the obese category were able to manage to go into the normal BMI or overweight category due to the physical activity conducted might not be vigorous enough to lose weight or their diet was not well controlled. Although the mean BMI in the post-resting study was lower than that in the post-study, there was a slight decrease in the percentage of students in the normal BMI category and an increase in the proportion of students in the obese category in the post-resting study, which might be due to some participants gained weight as they did not carry out the non-pharmacological approach in the post-resting study.

There was a slight increase in the proportion of pharmacy students (79%) who showed normal TC levels and a decrease in the proportion of borderline TC levels (17%) in the post-study period, which might be due to participants becoming aware of their TC levels by controlling their diets and conducting physical activity regularly during the non-pharmacological approach period. No change in the percentage of participants with high TC levels might be due to some respondents not controlling their diet and conducting physical activity regularly although they knew their TC levels were higher than the normal range. There was a slight reduction in mean TC from 4.73 to 4.6 mmol/L after 10 weeks of the non-pharmacological approach. Although the mean TC in the post-resting study was lower than that in the post-study, the results of the post-resting study showed an increase in the percentage of students who had high TC levels as compared with the post-study (4%) which might be due to the participants not carrying out the non-pharmacological approach in the post-resting study.

They might eat foods high in fat content more frequently because they did not control their diet in the post-resting study.

Table 5. Factors for not continuing physical activity

Factors associated with not continuing physical activity	Responses (n)	Percentage (%)
Did not suit needs	1	1.5
Other	1	1.5
Financial	2	3.1
Lack of results	2	3.1
Study schedule	15	23.1
Lack of time	19	29.2
Lack of motivation	25	38.5
Total	65	100.0

Table 6. Study comparisons for BMI, TC, and FBG

Health parameters	Study comparison	n	Differences	Test statistic	*p* value	Notes
BMI	Comparison of BMI before and after study	47	0 (0)	-1.732	0.083	Wilcoxon signed-rank test
BMI	Comparison of BMI between post- and post-resting study	47	0 (0)	-1.63	0.102	Wilcoxon signed-rank test
TC	Comparison of pre- and post-study TC	47	0.085 (0.62)	0.94 (46)	0.351	Paired *t*-test
TC	Comparison of post- and post-resting TC	47	0 (0)	-0.85	0.396	Wilcoxon signed-rank test
FBG	Comparison of FBG before and after study	47	0 (0)	-2.00	0.046	Wilcoxon signed-rank test
FBG	Comparison of FBG levels between post- and post-resting studies	47	0 (0)	-0.33	0.739	Wilcoxon signed-rank test

TC: Total cholesterol, FBG: Fasting blood glucose, SD: Standard deviation, BMI: Body mass index

In addition, they did not conduct physical activity regularly during the post-resting study.

In the pre-study, only one participant had low FBG, which might be due to the participant being in the underweight category or fasting too long before the measurement of FBG. An increase in the impaired fasting glucose proportion observed in the post-study might be due to the participants not conducting a non-pharmacological approach as instructed in the Sport Pharmacy course as these were self-conducted by respondents. There was a slight decrease in impaired fasting glucose percentage in the post-resting study as compared with the post-study (6%) but one respondent showed high FBG as not observed before in the pre-and post-study, which might be due to the participant not carry out the non-pharmacological approach in the post-resting study. A slight decrease in the mean FBG (5.12 mmol/L to 5.09 mmol/L) was observed from pre to post-study. However, mean FBG levels were increased in the post-resting study, which might be due to the respondents consuming foods high in sugar content more frequently as they did not control their diet in the post-resting study. In addition, they did not conduct physical activity regularly during the post-resting study. Therefore, an increase in mean FBG was observed in the post-resting study.

After 10 weeks, the implementation of non-pharmacological methods resulted in notable changes in the FBG level. However, no substantial variance was observed in the BMI and TC levels. Moreover, no significant differences were observed in BMI, FBG, and TC between the post- and post-resting studies because most students did not continue NPAs in the post-resting study. In neither the diet and physical activity group nor the diet with delayed physical activity group did Goodpaster et al.[16] find any significant change in FBG and TC after a 1-year intervention.

However, the findings of the present study were in contrast to those of this study, which reported a significant difference in body weight and BMI after 1 and 2 years of diet and physical activity interventions.[16] This study concluded that the addition of physical activity, regardless of whether initiated early in the program or delayed, promoted greater weight loss and reduction in BMI.[16] Similarly, Mensink et al.[12] also reported a significant difference in BMI between the intervention group and control group after 1 and 2 years due to changes in body weight. However, this study reported no significant change observed in TC level between the lifestyle intervention and control groups after one and two years of lifestyle intervention, which was similar to the findings of the present study, although a slight increase in TC was observed over time in both groups.[12] In contrast, Zhang et al.[17] found that lifestyle interventions, which included physical activity, diet, and behavioral modification, could significantly improve lipid profiles, including TC. They reported that combined physical activity and diet strategy had the strongest effect on improving CVD profiles compared with diet intervention alone or physical activity alone. Posttests from previous studies were conducted immediately after combined diet and physical activity intervention. There were no resting periods in these studies that could be used to compare the post-resting results of the present study.

Only 23% of participants continued their diet control and 32% continued their physical activity during the post-resting study. Al-Naggar et al.[18] found that more than half of Malaysian university students are physically inactive (53.7%).[19] The percentage of students who practiced physical activity in this study was in contrast to that observed in previous studies.[19-21] The percentage of students practicing diet control was lower than that reported by Yousif et al.[22] who reported that nearly half of students did not control their diet (45.8%), whereas 28.7% controlled their diet and 25.5% were emotional eaters. A low percentage of students continued physical activity and diet control reflects insufficient healthy lifestyle practices among university students despite practicing physical activity and diet control in the Sport Pharmacy course.[20] Being a student in a health university college was found to be associated with a high risk of physical inactivity.[23] Heavy academic study was one of the barriers to university Chinese students' participation in physical activity.[24]

Among the students who continued their diet control in the post-resting study, the main factors for continuing their diet control were health (34.8%), followed by seeing results (30.4%) and feeling better (26.1%). Only a small proportion of students chose friends, praise, or rewards (4.3%), respectively. This coincides with a study conducted by Tok et al.,[25] which reported that the main reasons for practicing diet control in both males and females were health (43.4% and 31.4% respectively). The present study showed that health, having fun, and feeling better were the main three factors for continuing physical activity in the post-resting study. Only a minority of students chose to see results, good appearance, friends, and praise or rewards as their main factors for continuing physical activity. According to Driskell et al.,[26] a study found that health, enjoying themselves, and wanting to lose weight were three factors that impacted students' habits regarding physical activity. A study conducted by Romaguera et al.[21] conducted a study on Spanish university students and found that most students engaged in physical activity to keep themselves fit, and healthy, enjoy themselves, and engage in social interaction (with their friends). The present study noted that participants in this study were pharmacy students who had good knowledge about health and knew that DCPAs were examples of NPAs that could maintain their health. This might be explained by the fact that students chose health, seeing results, and feeling better as their main factors for continuing the non-pharmacological approach in their post-resting study.

For students who did not practice DCPAs, factors for not practicing diet control were lack of motivation, followed by study schedule and lack of time, respectively. A minority of students chose other reasons, such as financial, did not suit their needs, lack of results, too restrictive, and others, such as laziness, as the main factors for discontinuing DCPAs in the post-resting study. This coincides with a study conducted in Saudi Arabia by Majeed[27] who found that the main barriers to diet control were lack of time, followed by lack of access to healthy foods and taste preferences. A similar finding was reported by Silliman et al.,[28] who reported that the most common barriers cited to

practicing diet control were lack of time, followed by lack of money and taste preferences.

Daskapan et al.[29] reported that the most important barrier to not participating in physical activity among Turkish university students was lack of time due to a busy study schedule, followed by parents, social and family responsibilities, and lack of energy. Similarly, barriers to physical activity among Egyptian students reported by El-Gilany et al.[30] included time limitation, lack of friends to encourage them, lack of motivation, financial issues. Awadalla et al.[23] reported that more than half of students chose personal factors as significant barriers of not practicing physical activity, such as time limitation (51.3%). In this study, only 19.6% chose lack of motivation as their significant barrier to not practicing physical activity, which was much lower as compared to the present study.

The present study noted final year pharmacy students who were busy in their studies and had little time for DCPA. This may be explained by the fact that students chose their study schedule and lack of time as their main barriers to DCPA. A busy study schedule and lack of time might cause patients to not be motivated to practice a non-pharmacological approach in their daily lives. They prioritized their academics over DCPA. Another reason for students not practicing diet control might be the wide availability of local traditional cuisines and snacks, such as *nasi lemak*, curry, and *roti canai*, at cafeterias on campus. The emergence of fast food outlets around the campus area and the convenience of transportation systems are believed to be contributing factors for not practicing diet control.[31]

Study limitations

In this study, the respondents might have underestimated their caloric intake or exaggerated the amount of exercise based on response bias because the respondents were self-conducted and self-reported their physical activity and diet intake in their weekly reports.[32] No monitoring of a non-pharmacological approach was conducted by respondents in pre-, post, and post-resting studies. Second, the study subjects consisted of mostly females, which might have contributed to the bias in the results of the present study. Third, the method of measuring health parameters might influence outcome.[32] Based on the Malaysian Clinical Practice Guideline on the Management of type 2 diabetes mellitus (2015), FBG levels should be measured using venous blood samples instead of capillary blood samples.[5] This may affect the accuracy of FBG results. Fourth, the incomplete weekly reports submitted by most respondents resulting in the measurement of food calories per week could not be analyzed for diet control in this study. Fifth, the equipment used in the study, such as a blood glucose meter and weighing scale, were not validated. This could affect the validity of the study results.

CONCLUSION

Significant results for FBG were achieved through a non-pharmacological approach consisting of physical activity and diet control administered over 10 weeks. However, there was no notable influence on BMI or TC. The post-resting phase failed to produce significant changes in BMI, FBG, and TC due to the minority of patients who continued non-pharmacological practices in their daily routine. Barrier identification revealed a lack of motivation, insufficient time, and conflicts with study schedules as hindrances to maintaining non-pharmacological methods among pharmacy students. Long-term follow-up studies should be conducted to

confirm whether pharmacy students continue practicing NPA, and the benefits of these methods should be maintained after the course ceases. The university plays an important role in improving the compliance of pharmacy students with a non-pharmacological approach by reviewing practical assessments of the course to motivate and encourage pharmacy students to practice a non-pharmacological approach in their daily lives. Creating environments conducive to change and promoting healthy habits is also important in the university context.

Pharmacists should be able to discuss the health benefits of exercise, and practical skills in patient counseling should be practiced to encourage appropriate self-care and the dispensing of self-care advice to patients. Maintaining normal health parameters among pharmacy students is important because they are professional students who need to provide pharmaceutical care and patient education to the public. Periodic monitoring through a continuous survey of students' physical and dietary lifestyles can be a wise move to improve their status.

Acknowledgments

We would like to express our gratitude to the University of Cyberjaya Research Ethics Review Committee, for their ethical approval to conduct this study and to Year 4 Sport Pharmacy students who participated in the study.

Ethics

Ethics Committee Approval: The study protocol was approved by the University of Cyberjaya Research Ethics Review Committee (approval number: CUCMS/CRERC/FR/030, date: 11.07.2019).

Informed Consent: Informed consent was obtained from all participants.

Authorship Contributions

Concept: A.R.M.T., A.F.M.L., Design: A.R.M.T., W.S.W.Z., M.A.N., Data Collection or Processing: V.J.H., W.S.W.Z., Analysis or Interpretation: V.J.H., W.S.W.Z., Literature Search: A.R.M.T., V.J.H., M.A.N., F.S.A.R., A.F.M.L., Writing: A.R.M.T., M.A.N., F.S.A.R., A.F.M.L.

Conflict of Interest: The authors have no conflicts of interest to declare.

Financial Disclosure: The authors declared that this study received no financial support.

REFERENCES

1. Mohamed Tahir AR. Student lesson plan. Sports Pharmacy. PHAR 4762. University of Cyberjaya. 2018/2019;1-5. https://drive.google.com/file/d/14InGq6HBbZqCcQJf1kHNxSx1uMZZXDJ1/view?usp=sharing

2. World Health Organization (WHO) (2018). Fact Sheet on Healthy Diet. Geneva: World Health Organization. Access from: https://www.who.int/news-room/fact-sheets/detail/healthy-diet
3. World Health Organization (WHO) (2018). Fact Sheet on Physical Activity. Geneva: World Health Organization. Access from: https://www.who.int/news-room/fact-sheets/detail/physical-activity
4. Zheng W, McLerran DF, Rolland B, Zhang X, Inoue M, Matsuo K, He J, Gupta PC, Ramadas K, Tsugane S, Irie F, Tamakoshi A, Gao YT, Wang R, Shu XO, Tsuji I, Kuriyama S, Tanaka H, Satoh H, Chen CJ, Yuan JM, Yoo KY, Ahsan H, Pan WH, Gu D, Pednekar MS, Sauvaget C, Sasazuki S, Sairenchi T, Yang G, Xiang YB, Nagai M, Suzuki T, Nishino Y, You SL, Koh WP, Park SK, Chen Y, Shen CY, Thornquist M, Feng Z, Kang D, Boffetta P, Potter JD. Association between body-mass index and risk of death in more than 1 million Asians. N Engl J Med. 2011;364:719-729.
5. MOH (2015). Clinical practice guideline (CPG) management of type 2 diabetes mellitus (5th edition). Malaysia Ministry of Health (Vol. 5).
6. Yiling JC, Gregg E, Geiss LS, Imperatore G, Williams DE, Xinzhi Z, Albright AL, Cowie CC, Klein R, Saddin JB. Association of A1C and fasting plasma glucose levels with diabetic retinopathy prevalence in the U.S. population. Diabetes Care. 2009;32:2027-2032.
7. MOH (2017). Clinical practice guideline (CPG) management of dyslipidaemia (5th edition). Malaysia Ministry of Health, 1-107.
8. Ninot G. Defining the concept of non-pharmacological intervention (NPI). Blog en Sante. L16 (Online). http://blogensante.fr/en/2013/09/16/definir-la-notion-dintervention-non-medicamenteuse/html
9. World Health Organization (WHO) (2018). Fact Sheet on Physical Activity. Geneva: World Health Organization. Access from: https://www.who.int/news-room/fact-sheets/detail/physical-activity
10. Nybo L, Sundstrup E, Jakobsen MD, Mohr M, Hornstrup T, Simonsen L, Bülow J, Randers MB, Nielsen JJ, Aagaard P, Krustrup P. High-intensity training versus traditional exercise interventions for promoting health. Med Sci Sports Exerc. 2010;42:1951-1958.
11. McManus K, Antinoro L, Sacks F. A randomized controlled trial of a moderate-fat, low-energy diet compared with a low-fat, low-energy diet for weight loss in overweight adults. Int J Obes Relat Metab Disord. 2001;25:1503-1511.
12. Mensink M, Blaak EE, Corpeleijn E, Saris WH, de Bruin TW, Feskens EJ. Lifestyle intervention according to general recommendations improves glucose tolerance. Obes Res. 2003;11:1588-1596.
13. International Pharmaceutical Federation (FIP). Empowering self-care: A handbook for pharmacists. The Hague: International Pharmaceutical Federation; 2022.
14. Ilow R, Różańska D, Regulska-Ilow B. Prevalence of cardiovascular disease risk factors among pharmacy students from Wroclaw Medical University (Poland). Adv Clin Exp Med. 2017;26:843-850.
15. Bastardo YM. Health status and health behaviors in Venezuelan pharmacy students. Value Health. 2011;14:S122-S125.
16. Goodpaster BH, Delany JP, Otto AD, Kuller L, Vockley J, South-Paul JE, Thomas SB, Brown J, McTigue K, Hames KC, Lang W, Jakicic JM. Effects of diet and physical activity interventions on weight loss and cardiometabolic risk factors in severely obese adults: a randomized trial. JAMA. 2010;304:1795-1802.
17. Zhang X, Devlin HM, Smith B, Imperatore G, Thomas W, Lobelo F, Ali MK, Norris K, Gruss S, Bardenheier B, Cho P, de Quevedo IG, Mudaliar U, Greeg EW. Effect of lifestyle interventions on cardiovascular risk factors among adults without impaired glucose tolerance or diabetes: A systematic review and meta-analysis. PLoS One. 2017;12:1-27.
18. Al-Naggar RA, Bobryshev YV, Mohd Noor NAB. Lifestyle practice among malaysian university students. Asian Pac J Cancer Prev. 2013;14:1895-1903.
19. Haase A, Steptoe A, Sallis JF, Wardle J. Leisure-time physical activity in university students from 23 countries: associations with health beliefs, risk awareness, and national economic development. Prev Med. 2004;39:182-190.
20. Keating XD, Guan J, Piñero JC, Bridges DM. A meta-analysis of college students' physical activity behaviors. J Am Coll Health. 2005;54:116-125.
21. Romaguera, D, Tauler P, Bennasar M, Pericas J, Moreno C, Martinez S, Aguilo A. Determinants and patterns of physical activity practice among Spanish university students. J Sports Sci. 2011;29:989-997.
22. Yousif MM, Kaddam LA, Humeda HS. Correlation between physical activity, eating behavior and obesity among Sudanese medical students Sudan. Nutr. 2019;5:6.
23. Awadalla NJ, Aboelyazed AE, Hassanein MA, Khalil SN, Aftab R, Gaballa II, Mahfouz AA. Assessment of physical inactivity and perceived barriers to physical activity among health college students, south-western Saudi Arabia. East Mediterr Health J. 2014;20:596-604.
24. Yan Z, Sigmund E, Sigmundová D, Yan L. Comparison of physical activity between olomouc and beijing university students using an international physical activity questionnaire. Acta Universitatis Palackianae Olomucensis. Gymnica. 2007;37:107-114.
25. Tok CY, Siti Rohaiza A, Davd Koh SQ. Dietary habits and lifestyle practices among university students in universiti Brunei Darussalam. Malays J Med Sci. 2018;25:56-66.
26. Driskell JA, Kim YN, Goebel KJ. Few differences were found in the typical eating and physical activity habits of lower-level and upper-level university students. J Am Diet Assoc. 2005;105:798-801.
27. Majeed F. Association of BMI with diet and physical activity of female medical students at the University of Dammam, Kingdom of Saudi Arabia. J Taibah Univ Med Sci. 2015;10:188-196.
28. Silliman K, Rodas-Fortier K, Neyman M. Survey of dietary and exercise habits and perceived barriers to following a healthy lifestyle in a college population. Californian Journal of Health Promotion. 2004;2:82-91.
29. Daskapan A, Tuzun EH, Eker L. Perceived barriers to physical activity in university students. J Sports Sci Med. 2006;5:615-620.
30. El-Gilany AH, Badawi K, El Khawaga G, Awadalla N. Physical activity profile of students in Mansoura University, Egypt. East Mediterr Health J. 2011;17:694-702.
31. Nik Hairi O, Tang PL, Lim SJ, Ramaya K. Dietary intake and physical lifestyle of resdential college students in Universiti Kebangsaan Malaysia. Journal Student Personal. 2015;151:10-17.
32. Black DR, Coster DC, Paige SR. Physiological health parameters among college students to promote chronic disease prevention and health promotion. Prev Med Rep. 2017;7:64-73.

Turk J Pharm Sci 2024;21(5):421-427
DOI: 10.4274/tjps.galenos.2023.50246

ORIGINAL ARTICLE

Prospective Drug Utilization Evaluation Analysis in Outpatient Departments with Ear, Nose, and Throat Outpatients: Incorporating Benchmarks and World Health Organization Indicators

Vinodkumar MUGADA*, Blessy JAYAMON, Bindu Krishna KOSIREDDY, Bhagya Sri PALISETTY, Apoorva PINISETTI

Vignan Institute of Pharmaceutical Technology, Department of Pharmacy Practice, Duvvada, India

ABSTRACT

Objectives: Drug utilization studies are tools for determining the effectiveness of drug use. The aim of the study was to evaluate drug usage patterns in ear, nose, and throat (ENT) outpatient settings by incorporating established benchmarks and World Health Organization (WHO) indicators.

Materials and Methods: A cross-sectional study on drug utilization evaluation (DUE) was conducted on 800 patients from the ENT outpatient department. We gathered data on currently prescribed medications and identified any discrepancies with a thorough analysis. Continuing educational activities such as "dear doctor" letters and personal consultations were used to rectify any irrational prescribing patterns among physicians. The WHO/International Network for Rational Use of Drugs core drug use indicators, specifically prescribing and patient care indicators, and established benchmarks were applied to encourage rational prescribing.

Results: The three most common diagnoses were pharyngitis (51.49%), allergic rhinitis (25.11%), and acute suppurative otitis media (21.17%). Montelukast, in combination with levocetirizine (13.77%) and amoxicillin in combination with clavulanic acid (8.81%), was the most frequently prescribed medication. The average number of drugs per prescription was 4.2% (±1.1), with low usage of generic names (33.0%) and suboptimal reliance on the essential drugs list (76.7%). Furthermore, patient care indicators demonstrated room for improvement, particularly concerning consultation times (6 minutes), dispensing times (30 seconds), and drug labeling practices (0% labeled). The DUE improved the prescribing rate of first-line drugs for five diseases and few aspects of prescribing and patient care indicators.

Conclusion: There is an overuse of prescribed drugs, a need for more utilization of generic names, and less than optimal use of the essential drugs list. Additionally, shortcomings in patient care were observed, including issues in consultation, drug dispensing times, and labeling. However, DUE effectively improved WHO patient care metrics and the prescription of first-line drugs warranting its implementation.

Keywords: Drug utilization evaluation, World Health Organization, amoxicillin, suppurative otitis media, benchmarking, montelukast

INTRODUCTION

Drug utilization evaluation (DUE) aims to promote appropriate drug utilization through continuous, authorized, and systematic quality improvement processes, including reviewing prescriptions, providing clinicians feedback, developing optimal drug use standards, and educating patients to optimize therapeutic benefits and reduce adverse effects.[1] The doctor of Pharmacy (PharmD) students' experiences offer the invaluable opportunity to observe and understand the complex aspects of healthcare in real-world settings. A noticeable lack of first-line drug prescriptions was observed during a visit to the ear, nose, and throat (ENT) outpatient department (OPD).

A literature review on DUE within ENT OPDs revealed a significant research gap. Previous studies[1-12] have not included post-DUE analysis, an essential part of the DUE process. These studies did not employ the World Health Organization (WHO)/

*Correspondence: mugadavinodkumar18@gmail.com, ORCID-ID: orcid.org/0000-0002-9364-9874
Received: 10.07.2023, Accepted: 23.09.2023

International Network for Rational Use of Drugs (INRUD) patient care indicators.[13] These indicators provide a comprehensive framework for assessing rational drug use and monitoring the performance of health systems.[13] Therefore, our study aimed to evaluate drug usage patterns in ENT outpatient settings by incorporating established benchmarks and WHO/INRUD core drug use indicators.

MATERIALS AND METHODS

Study design and setting

A cross-sectional study with intervention to improve drug prescribing using established benchmarks was conducted in the ENT OPD. The study duration was six months (November 2022 to April 2023).

Study participants and sampling technique

We included outpatients visiting the ENT department aged <65, whereas patients with comorbidities, severe ailments, and elderly were excluded. A combination of convenience and purposive sampling methods was used to select participants.

Sample size

The sample size was calculated using the Roasoft sample size calculator with a 5% margin of error and 95% confidence level. The recommended sample size is 377 for a population size of 20,000 members.

Data collection

Demographic data, including age, sex, weight, area of residence, occupation, and marital status, were collected from the patients. Patients' past medication history, current medication, history of the present illness, and diagnosis were collected.

Prescription analysis

We used WHO/INRUD core drug use indicators, namely prescribing and patient care indicators. Prescribing indicators will assess medication prescribing patterns, whereas patient care indicators evaluate the quality of care delivered to patients.[13] These indicators will help to evaluate the hospital's support in promoting rational drug use.

Benchmark set-up

We established a benchmark of 90% for increasing the prescription rate of first-line drugs. We conducted a one-month follow-up to monitor the progress.

Interventions to promote the prescribing rate of first-line drugs

Dear Doctor letter

A "Dear Doctor" letter, or a "Dear Healthcare Professional" letter, is a written communication typically sent by a researcher, pharmaceutical company, medical device manufacturer or regulatory authority to healthcare professionals, including doctors, nurses and pharmacists. The purpose of a Dear Doctor letter is to provide important information about a product or medication, such as new safety concerns, updated prescribing guidelines and recalls. These letters are typically used to inform healthcare professionals about significant changes or new findings related to a particular drug or medical device. The letter aims to ensure that healthcare professionals are aware of important updates and can take appropriate action to ensure patient safety.[14]

Personal consultation with the treating physicians

Personal consultations are essential to effective healthcare communication, offering clarity and depth to treatment guidelines. Facilitate information exchange, resolve doubts, and provide context-specific advice that may not be fully conveyed through written communication. Such consultations address individual queries, present real-life cases, discuss potential obstacles, and provide specific guidance. They supplement written communication by reinforcing its content and offering continual support. Personal consultations are integral to a comprehensive and personalized educational experience in healthcare, promoting understanding and support.

Statistical analysis

We calculated the mean and standard deviation or median and interquartile range (whichever is appropriate) for quantitative data. We calculated frequencies and percentages for qualitative data.

Ethical approval

The study was approved by the Institutional Human Ethics Committee (approval number: VIPT/IEC/159/2022, date: 20.10.2022). We obtained written informed consent from the participants who were willing to participate.

RESULTS

Table 1 represents the most common diagnoses of ENT OPD. Ear-related conditions primarily comprised acute suppurative otitis media (ASOM) (21.17%), impacted ear wax (20.39%), and chronic suppurative otitis media (CSOM) (17.25%). Nose-related diagnoses were allergic rhinitis (25.11%), upper respiratory tract infections (17.94%), sinusitis (17.48%), and rhinosinusitis (16.14%). Throat conditions were predominantly pharyngitis (51.49%), with tonsillitis (19.15%) and adenotonsillitis (18.30%).

Table 2 shows the most commonly prescribed drugs for ENT patients in our study. Montelukast combined with levocetirizine appears to be the most commonly prescribed drug, accounting for 13.77% of all prescriptions, followed by amoxicillin and clavulanic acid (8.81%). There is a high level of levocetirizine, both in combination with other drugs and as a standalone treatment.

Table 3 outlines the WHO/INRUD prescribing indicators. The average number of drugs prescribed per prescription was 4.2%, in contrast to the WHO reference value of less than 2%. Similarly, the percentage of drugs prescribed by generic names was 33.0%, notably lower than the WHO's ideal standard of 100%. Regarding encounters with an antibiotic prescribed, the percentage was 17.5%, which remained within the acceptable range set by the WHO of 30%. The percentage of encounters with an injection prescribed was 0%, significantly lower than the WHO benchmark of 20%. Moreover, the percentage of drugs prescribed by the Essential Drug List (EDL) was 76.7%, less than the WHO reference value of 100%.

Table 1. Distribution of diagnoses in the OPD

ENT	Diagnoses	n (%)
Ear-related disease	ASOM[a]	54 (21.17)
	Impacted ear wax	52 (20.39)
	CSOM[b]	44 (17.25)
	Otomycosis	29 (11.37)
	Otitis externa	20 (7.84)
	Others	56 (21.9)
Nose-related disease	Allergic rhinitis	56 (25.11)
	URTI[c]	40 (17.94)
	Sinusitis	39 (17.48)
	Rhinosinusitis	36 (16.14)
	Post-op FESS[d]	26 (11.66)
	Epistaxis	9 (4.04)
	Others	17 (7.62)
Throat-related disease	Pharyngitis	121 (51.49)
	Tonsillitis	45 (19.15)
	Adenotonsillitis	43 (18.30)
	Tonsillopharyngitis	10 (4.26)
	Others	16 (6.80)

[a]ASOM: Acute suppurative otitis media, [b]CSOM: Chronic Suppurative Otitis Media, [c]URTI: Upper respiratory tract infection, [d]FESS: Functional endoscopic sinus surgery, OPD: Outpatient department, ENT: Ear, nose, and throat

Table 2. The most commonly prescribed ENT-related drugs during the study

Commonly prescribed drugs	Frequency	%
Montelukast + Levocetirizine	469	13.77
Amoxicillin + Clavulanic acid	300	8.81
Levocetirizine	117	3.44
Sodium chloride nasal drops	96	2.82
Azelastine + fluticasone nasal spray	91	2.67
Ambroxol + Levocetirizine + Montelukast	72	2.12
Xylometazoline nasal drops	70	2.06
Ciprofloxacin	61	1.79
Paradichlorobenzene + Chlorbutol + Turpentine oil + Lidocaine ear drops	53	1.56
Levodropropizine + Chlorpheniramine maleate	53	1.56
Others Pantoprazole	500	14.68
Acetaminophen	350	10.28
Thiamine, riboflavin, niacin, pyridoxine, pyridoxal, biotin, pantothenic acid, folic acid, and vitamin B12	219	6.43

Investigating WHO patient care indicators (Table 4) yielded some significant findings. The average consultation time was six minutes, considerably shorter than the WHO reference value of 30 minutes or more. The average dispensing time was 30 seconds, significantly below the WHO-recommended minimum of 60 seconds. Regarding medication-related indicators, the percentage of drugs dispensed was 95.6%, slightly below the WHO standard of 100%. The study found that none of the drugs were adequately labeled, in stark contrast to the WHO reference value of 100%.

Table 5 illustrates the influence of DUE on first-line drug prescriptions for various ENT diseases assessed one month after DUE. The percentage of first-line drug prescriptions for sinusitis increased from 53.4% to 81.9%. Similarly, the rate of first-line drugs used for pharyngitis increased from 43.8% to 82.7%. For patients diagnosed with ASOM, the percentage of first-line drug prescriptions increased from 55.6% to 80.6%, whereas the percentage of first-line drugs prescribed for CSOM increased from 47.8% to 87.4%. For otitis externa, an increase from 45.0% to 84.2% was noted. Table 6 shows an improvement in a few aspects of WHO/INRUD prescribing and patient-care indicators. There was an increase in the percentage of drugs prescribed generically (33.0% to 45.3%) and those from the EDL (76.6% to 82.1%). The average consultation time improved slightly from 6 to 7 minutes.

Table 3. WHO/INRUD prescribing indicators

Indicator	Percentage prescription	WHO reference values
Average number of drugs prescribed per prescription	4.2%	< 2%
Percentage of drugs prescribed according to generic names	33.0%	100%
Percentage of encounters with antibiotic-prescribed drugs	17.5%	< 30%
Percentage of encounters with prescribed injections	0%	< 20%
Percentage of drugs prescribed by EDL*	76.7%	100%

*EDL: Essential drugs list, WHO: World Health Organization

Table 4. WHO/INRUD patient care indicators

Indicator	Frequency/ percentage	WHO reference value
Average consultation time (in minutes)	6 minutes	≥ 30 minutes
Average dispensing time (in seconds)	30 seconds	≥ 60 seconds
Percentage of drugs dispensed	95.6%	100%
Percentage of adequately labeled drugs	0%	100%

Table 5. Improvement in prescribing rate of first-line drugs post-DUE analysis

Disease	Baseline percentage of prescribed drugs	DUE impact on prescribed drugs after 1 month
	Percentage of first-line drugs	Percentage of first-line drugs
Sinusitis	53.4	81.9
Pharyngitis	43.8	82.7
ASOM[b]	55.6	80.6
Otitis externa	45.0	84.2
CSOM[c]	47.8	87.4

[a]DUE: Drug utilization evaluation, [b]ASOM: Acute suppurative otitis media, [c]CSOM: Chronic suppurative otitis media

Table 6. Impact of DUE on WHO core prescribing and patient care indicators

WHO core indicators	Baseline	Post DUE
Prescribing indicators		
Percentage of drugs prescribed by generic name	33.0%	45.3%
Percentage of drugs prescribed by EDL	76.6%	82.1%
Patient care indicator		
Average consultation time (in minutes)	6 minutes	7 minutes

DISCUSSION

Key results

Our study evaluated the prevalence of ENT diseases, identifying ASOM, allergic rhinitis, and pharyngitis as the most common, whereas Otitis externa, epistaxis, and tonsillopharyngitis were the least frequent. A combination of montelukast and levocetirizine was prescribed, with amoxicillin clavulanic acid as the most commonly used antimicrobial agent. However, the study identified concerns regarding prescription practices, including a high mean number of medicines prescribed, limited use of generic names and subpar reliance on the EDL. Additionally, the findings indicated potential areas for improvement in patient care, particularly consultation and dispensing times and drug labeling practices. This study underscores the need to enhance these practices to optimize patient care and safety in treating ENT diseases.

The study's findings align with and differ from previous research, demonstrating the impact of regional environmental factors. ASOM was identified as the most common ear condition, while otitis externa was the least common, a trend similar to one study.[5] Regarding nasal disorders, allergic rhinitis was the most prevalent, and epistaxis was the least frequent, consistent with findings in other research[15] and reflective of region-specific allergens. Among throat conditions, pharyngitis was the most frequent, while tonsillopharyngitis had the lowest prevalence, showing some variation from other studies.[5,16] These variations underscore the importance of considering local factors in evaluating ENT conditions.

Our study revealed a high prevalence of the combination of montelukast and levocetirizine, contrasting with findings from other studies. One study demonstrated that antimicrobials were the most frequently prescribed drugs, a notable difference from the current findings.[17] Another study reported levocetirizine as the most commonly prescribed single drug, and this study similarly observed a high prescription rate for it, often combined with montelukast.[6] This suggests a regional preference for combination therapy. Additionally, some research found non-steroidal anti-inflammatory drugs to be the most frequently prescribed drugs, highlighting possible variations due to differences in prevalent conditions or prescribing habits among the study populations.[1]

The study identified amoxicillin-clavulanic acid as the most frequently prescribed antimicrobial agent, accounting for 8.81% of all drug prescriptions. This finding aligns with previous research,[7,18] reinforcing the reliability of the results. However, a contrasting outcome was observed in another study,[19] where cefpodoxime and clavulanic acid were the most commonly prescribed antibiotics. This variation may reflect differences in prescription patterns influenced by several factors, including patient needs, physician preferences, antibiotic availability, and local microbial resistance patterns.

Research has highlighted the prevalence of specific pathogens in ENT infections. Analysis of bacterial samples from patients with these infections shows that the predominant organisms are *Streptococcus* spp., including *Streptococcus pneumoniae*, *Staphylococcus* spp., and *Haemophilus influenzae*.[20] These microorganisms are generally susceptible to amoxicillin, supporting its use in current prescribing practices.[21] Consequently, amoxicillin is widely recognized as the primary treatment for most ENT infections requiring antibiotic therapy, consistent with findings from other studies.[22] This study thus provides valuable insights into effective management strategies for ENT infections, adding to existing literature on the topic.

Using WHO/INRUD core drug use indicators, this study assessed rational drug use, finding that a total of 3,405 drugs were prescribed, with an average of 4.2 (±1.1) drugs per prescription. This average was lower than other studies, such as those reporting higher values,[23,24] but it still exceeded the benchmark recommendation of fewer than two drugs per prescription. The observed average reflects a balanced approach to drug therapy, aiming to minimize polypharmacy, defined as using more than five drugs[25] to help reduce healthcare costs, improve patient adherence, and lower the risk of adverse drug events. The association between the number of prescribed drugs and an increased risk of drug interactions highlights the importance of reducing prescription quantities to improve patient outcomes and healthcare efficiency.[17,26]

Only 33% of medications were prescribed using generic names, while most were issued as brand names, a trend higher than observed in other studies.[2] Prescribing generic drugs could significantly reduce therapy costs and minimize the risk of medication errors. Healthcare providers need to focus on prescribing generics. Additionally, they should prioritize

clear and legible handwriting or adopt electronic prescribing systems to ensure the highest safety and quality standards in medication administration.[27] Similar findings were observed in studies showing a strong preference for brand names over generics in prescriptions.[7]

The study reported a lower rate of antibiotic usage (17.5%) compared to prior research.[5,6] This could be due to the high prevalence of self-limiting viral infections, with antibiotics prescribed only for severe cases.[22] Notably, the study did not use injections, significantly below the WHO reference of less than 20%. This finding is consistent with previous studies[3,6] and may be attributed to the focus on OPD patients or increased physician awareness about the potential adverse effects of overusing injections. Additionally, 76.7% of prescriptions in the study included drugs from the EDL, which is higher than in previous studies.[17,23,28] This reflects a growing acceptance of essential medicines, which promote health equity and cost-effectiveness.[29] However, there is still room for improvement in optimizing EDL utilization.

The study also incorporated patient care indicators as defined by the WHO/INRUD, offering valuable insights into various aspects of healthcare services. Previous studies on drug utilization in the OPD for ENT have not used these indicators, and by applying them in this context, the study provided new insights into drug use in this specialized area of healthcare. Our investigation reported a brief six-minute average consultation time, significantly lower than the WHO/INRUD recommended 30 minutes, likely due to high patient-to-doctor ratios and multiple responsibilities in OPD settings, especially in teaching hospitals. Although a half-hour consultation might be impractical, there is scope for a moderate increase in the duration.

Our study recorded an average dispensing time of merely 30 seconds, significantly less than the WHO/INRUD recommended minimum duration of 60 seconds. This marked deviation might indicate the existence of time constraints in the medication dispensing process, potentially increasing the risk of errors or contributing to inadequate patient understanding of their medication regimen and management. Our study revealed 95.6% of prescribed medications were successfully dispensed to patients. Although this percentage is slightly less than the WHO/INRUD perfect benchmark of 100%, it nevertheless signifies a remarkable achievement in efficiently dispensing medication. Such an accomplishment sets a robust platform for future endeavors to align fully with the WHO's ideal standards, promoting enhanced patient satisfaction and enriched health outcomes in the healthcare system.

Our research identified a stark deficiency in drug labeling, with an alarming 0% compliance with WHO guidelines, which mandate the inclusion of dosage regimens, patient names, and drug dosage.[30] The absence of critical information poses substantial risks to patients, possibly causing usage or dosage mistakes, thereby affecting safety and treatment outcomes. These findings highlight the need for substantial improvements in consultation, dispensing, and labeling processes.

Amoxicillin is the primary medication for sinusitis, pharyngitis, and ASOM. The American Academy of Otolaryngology's updated 2015 guidelines for adult sinusitis also recommend amoxicillin, with or without clavulanate, as the first-line therapy for most adults for 5-10 days.[31] Similarly, penicillin or amoxicillin is the treatment of choice for pharyngitis, particularly in cases caused by group A *streptococcus*.[35] For acute otitis media, a typical middle ear infection, amoxicillin is the drug of choice.[34] These recommendations highlight the efficacy of amoxicillin for managing a range of ENT conditions.

Current treatment guidelines emphasize topical antibiotics as the preferred choice for otitis externa.[36] These guidelines also recommend a combination of topical antibiotics with steroids and pain medications as the first-line treatment. Oral antibiotics have been found to lack substantial evidence of benefits. Undoubtedly, their misuse may increase resistance among common otitis externa pathogens, leading to more complicated treatment in the future.[32] Topical quinolones are the preferred treatment for persistent ear conditions such as CSOM.[33] Post-implementation of continuing education programs improved the prescribing of first-line drugs for five different diseases. Furthermore, a few aspects of prescribing and patient care indicators increased slightly. Continuing education is pivotal in improving medical practices, promoting more informed, rational decision-making, and optimizing patient treatment strategies.

Study limitations

The strength of our study was implementing a one-month post-DUE analysis and including interventions that improve the prescribing patterns of first-line drugs. Another strength of the study is evaluating WHO/INRUD patient-care indicators to evaluate the quality of care delivered to the patients. Despite providing valuable insights, our study has a few limitations, such as chances of selection bias due to convenience and purposive sampling, a single-centre design restricts the generalizability of the findings to other settings, and a short one-month follow-up may not capture the long-term effects.

Recommendations and scope of further research

Healthcare professionals should update the information on prescribing practices for ENT diseases and should use generic drug names while prescribing. A need for an increase in consultation and dispensing times should be addressed. Future studies should include post-DUE analysis over longer intervals. This approach will help identify discrepancies in prescribing practices and enable timely corrections.

CONCLUSION

The study identified a few discrepancies through post-DUE analysis. The study interventions: "dear doctor" letters and "personal consultations" improved the prescribing rate of first-line drugs. There is a need to conduct post-DUE analysis in DUE studies by establishing benchmarks and including appropriate interventions to improve prescribing rates of first-line drugs.

Ethics

Ethics Committee Approval: The study was approved by the Institutional Human Ethics Committee (approval number: VIPT/IEC/159/2022, date: 20.10.2022).

Informed Consent: A written informed consent was obtained.

Authorship Contributions:

Concept: V.M., Design: V.M., Data Collection and Processing: B.J., B.K.K., B.S.P., A.P., Analysis or Interpretation: V.M., B.J., B.K.K., B.S.P., A.P., Literature Search: V.M., B.J., B.K.K., B.S.P., A.P., Writing: V.M., B.J., B.K.K., B.S.P., A.P.

Conflicts of Interest: The authors have no conflicts of interest to declare.

Financial Disclosure: The authors declared that this study received no financial support.

REFERENCES

1. Vijay R, Atray M. Drug utilization pattern in ENT outpatient department in tertiary care teaching hospital in Southern Rajasthan. Natl J Physiol Pharm Pharmacol. 2022;12:1725-1734.
2. Kumari N, Mishra SK, Kumar M, Shakur AA, Mishra H, Dikshit H. Prescription pattern of drugs prescribed in the outpatient department of ENT and adverse drug reactions reported from ENT department in a tertiary care hospital of Bihar. Int J Pharm Sci Rev Res. 2022;73:178-183.
3. Joshi U, Banjara H, Hishikar R, Chandrakar R. Prescription pattern of drugs in ENT outpatient department of tertiary care teaching hospital. Int J Basic Clin Pharmacol. 2018;7:9.
4. Daniel M, Bharathi DR, Nataraj GR, Jinil AL. Drug utilization trends in ENT outpatients. Int J Sci Healthc Res. 2018;3:166-171.
5. Anandhasayanam A, Kannan S, Sajir M, Zachariah N. Drug prescription pattern observation at an ENT OPD department in a tertiary care hospital at Malappuram district of Kerala. Int J Pharm Sci Res. 2016;7:4157-4163.
6. Suman RK, Kumar R, Garje YA, Wagh AR, Satpathy A, Ray IM. Drug usage patterns in ent out patients department of teaching hospital. Int J Sci Res. 2014;3:341-343.
7. Padwal S, Kulkarni M, Deshmukh V, Patil J, Jadhav S, Jadhav A. Drug use pattern in the ear, nose, throat outpatient department of a rural tertiary-care teaching hospital. Nat J Physiol Pharm Pharmacol. 2015;5:3.
8. Kesari SP, Pandey SK, Shekhar S, Singhal S. Drug utilisation trends in ENT outpatient department in a tertiary care hospital of Sikkim. J Evolution Med Dent Sci. 2017;6:6047-6055.
9. Kishore Kumar Y, Cheekavolu C, Obulesu G. Drug utilization pattern in ENT OPD of government tertiary care teaching hospital in Raigarh. Int J Otorhinolaryngol Head Neck Surg. 2017;3:1042-1045.
10. Sumalatha R, Nagabushan H, Prasad HM. Drug utilization study in otorhinolaryngology outpatient department in a tertiary care teaching hospital. Int J Basic Clin Pharmacol. 2017;6:572-576.
11. Any OH, Banu LA, Sultana R, Khan NT, Hossain M, Akhtar S. Drug utilization trends in ENT out patient department in a private teaching hospital in Bangladesh. Bangladesh J Physiol Pharmacol [Internet]. 2015;30:41-45.
12. Pramila Y, Vanita K, Preety L, Siddharth J. Drug Utilization Trends in ENT outpatient department in a teaching hospital. Int J Pharma Bio Sci. 2010;1:153-160.
13. Narayana G, Joackim S, Bhavana Reddy B, Durga Prasad T, Veerbhadrappa Kasturi V, Joseph Obeizu CE, Sarad Pawar Naik B. Evaluation of rational drug use based on WHO/ INRUD core drug use indicators in a secondary care hospital: A cross-sectional study in Western Uganda. Drug Healthc Patient Saf. 2023;15:125-135.
14. Weatherby LB, Walker AM, Fife D, Vervaet P, Klausner MA. Contraindicated medications dispensed with cisapride: temporal trends in relation to the sending of 'Dear Doctor' letters. Pharmacoepidemiology and drug safety. 2001;10:211-218.
15. Dhanasekharan SV, Rajaram S, Jayan M, Sargunan A, Shankar R. Trends of antimicrobial prescription in department of Otorhinolaryngology in a Teritiary Care Teaching Hospital. Med Res Chronicles. 2015;2:44-50.
16. Phukan S, Das S. A study on the prescribing pattern of antimicrobial drugs in patients attending the ear, nose, throat department of a tertiary care teaching hospital. Asian J Pharm Clin Res. 2020;13:197-199.
17. Chandra S, Bhosle D, Ubale A. Prescription pattern at outpatient department in a tertiary care hospital at central Maharashtra, India. Int J Comprehensive Adv Pharmacol. 2019;4:56-58.
18. Naqvi S, Ahmad M, Akhter M, Yadav A, Singh A, Ahmad J, SHAMS AR. Drug utilization pattern and adverse drug reaction monitoring of antibiotics use in ear, nose and throat infection at tertiary care hospital, Lucknow, India. Authorea Pre-prints. 2023;4:71-81.
19. Srinivasa J, Rajendran V, Nadig P, Swamy S. Prescribing pattern of antibiotics in ENT outpatient department in a tertiary care teaching hospital. Int J Basic Clin Pharmacol. 2020;9:1892-1896.
20. Olzowy B, Kresken M, Havel M, Hafner D, Körber-Irrgang B, Working Party 'Antimicrobial Resistance'of the Paul-Ehrlich-Society for Chemotherapy. Antimicrobial susceptibility of bacterial isolates from patients presenting with ear, nose and throat (ENT) infections in the German community healthcare setting. Eur J Clin Microbiol Infect Dis. 2017;36:1685-1690.
21. Akhavan BJ, Khanna NR, Vijhani P. Amoxicillin. 2023 Nov 17. In: StatPearls [Internet]. Treasure Island (FL): StatPearls Publishing; 2024.
22. Cohen R, Haas H, Lorrot M, Biscardi S, Romain O, Vie Le Sage F, Hentgen V, Grimprel E. Antimicrobial treatment of ENT infections. Arch Pediatr. 2017;24:S9-S16.
23. Geetha P, Vijayalakshmi P, Tilak S, Maheswaran A, Naray N. Prescription analysis to evaluate the rational use of drugs using who health care indicators. Int J Multidiscipl Res Dev. 2015;2:358-360.
24. Gupta S, Poudel S, Gupta A, Bashyal B, Baskota B, Sah A, Pandaya S, Shrestha D. A prospective cross-sectional study on prescribing pattern of antibiotics on patients suffering from ENT infections in tertiary care hospital, Pokhara, Nepal. Int J Basic Clin Pharmacol. 2017;6:2303.
25. Varghese D, Ishida C, Haseer Koya H. Polypharmacy. [Updated 2022 Sep 9]. In: StatPearls [Internet]. Treasure Island (FL): StatPearls Publishing; 2023.
26. Sridevi SA, Janagan T, Rathnasamy P, Rajarajeswari R. Drug utilization study in the otorhinolaryngology department in a tertiary care hospital. Int J Basic Clin Pharmacol. 2013;2:306-310.
27. Andrade C, Rao TS. Prescription writing: Generic or brand?. Indian J Psychiatry. 2017;59:133.
28. Chandra S, Khan IN, Mateenudin M, Chandrakapure A, Maaz S, Mubin F. Drug utilization study in OPD of a tertiary care hospital in a rural area of Jalna, Maharashtra, India by using WHO prescribing indicators. Int J Basic Clin Pharmacol [Internet]. 2017;7:52-54.

29. Kar SS, Pradhan HS, Mohanta GP. Concept of essential medicines and rational use in public health. Indian J Community Med. 2010;35:10-13.

30. World Health Organization (WHO). How to investigate drug use in health facilities: selected drug use indicators. WHO; 1993.

31. DeBoer DL, Kwon E. Acute Sinusitis. 2023 Aug 7. In: StatPearls [Internet]. Treasure Island (FL): StatPearls Publishing; 2024.

32. Hajioff D, MacKeith S. Otitis externa. BMJ Clin Evid. 2015;2015:0510.

33. Rosario DC, Mendez MD. Chronic Suppurative Otitis. 2023 Jan 31. In: StatPearls [Internet]. Treasure Island (FL): StatPearls Publishing; 2024.

34. Le Saux N, Robinson JL; Canadian Paediatric Society, Infectious Diseases and Immunization Committee. Management of acute otitis media in children six months of age and older. Paediatr Child Health. 2016;21:39-50.

35. Pharyngitis (Strep Throat): Information for Clinicians. CDC [Internet]. Atlanta (GA): Centers for Disease Control and Prevention; [2023 Jun 1]. Available from: https://www.cdc.gov/groupastrep/diseases-hcp/strep-throat.html

36. Medina-Blasini Y, Sharman T. Otitis Externa. [Updated 2023 Feb 12]. In: StatPearls [Internet]. Treasure Island (FL): StatPearls Publishing; 2023.

Turk J Pharm Sci 2024;21(5):428-439
DOI: 10.4274/tjps.galenos.2023.68054

ORIGINAL ARTICLE

Development of Cyclosporine A Nanosuspension Using an Experimental Design Based on Response Surface Methodology: *In Vitro* Evaluations

Sıla GÜLBAĞ PINAR[1]*, Nevin ÇELEBİ[2]

[1]Süleyman Demirel University Faculty of Pharmacy, Department of Pharmaceutical Technology, Isparta, Türkiye
[2]Başkent University Faculty of Pharmacy, Department of Pharmaceutical Technology, Ankara, Türkiye

ABSTRACT

Objectives: This study aimed to develop nanosuspensions (NSs) of cyclosporine A (CycA) using a top-down technology [high-pressure homogenization-(HPH)] for oral administration.

Materials and Methods: Formulas were prepared using different ratios of hydroxypropyl methylcellulose (HPMC) (1% and 0.5%) and sodium dodecyl sulfate (SDS) (1%) to improve the solubility of CycA. The HPH method was optimized by investigating the effects of critical formulation parameters (stabilizer ratio) and critical process parameters (number of homogenization cycles) on the particle size (PS), polydispersity index (PDI), and zeta potential (ZP) of NS using the Design of Experiment (DoE). After lyophilization, differential scanning calorimetry, X-ray diffraction, fourier-transform infrared spectroscopy, and morphological evaluation with scanning electron microscopy were performed. Stability studies were conducted at 4 ˚C and 25 ˚C storage conditions. The solubility of the optimum CycA NS was investigated by comparing it with a coarse CycA powder and a physical mixture (PM). *In vitro* dissolution studies were conducted in four media using United States Pharmacopeia apparatus I.

Results: PS, PDI, and ZP values for the NS were approximately 250 nm, 0.6, and 35 mV, respectively. Under storage conditions, the CycA NS exhibited significant physical stability at both 4 ˚C and 25 ˚C for 9 months. The solubility of CycA was improved 1.9 and 1.4 times by NS in the presence of CycA powder and PM, respectively. CycA NS exhibited higher dissolution than CycA coarse powder in 0.1 N HCl, fasted simulated intestinal fluid, and fed simulated intestinal fluid.

Conclusion: CycA NS was successfully developed using the DoE approach with the HPH method with HPMC:SDS combination in a 1:0.5 ratio, and the solubility and dissolution of CycA in the NS were improved.

Keywords: Cyclosporine A, nanosuspension, high pressure homogenization, solubility, dissolution

INTRODUCTION

Approximately 60% of drugs have low solubility. This condition affects the pharmacokinetics and pharmacodynamics of these drugs, resulting in low dissolution and bioavailability when they are taken into the body. The low solubility of the active substance in water causes changes in the absorption of the drug in the gastric medium in both fasting and fed situations, causing variation in fasting-fed states. Low solubility also leads to impaired dose-response proportionality of the drug, unexpected collapse after administration, decreased patient compliance, and, as a result, low bioavailability.[1]

Cyclosporine A (CycA), one of the above-mentioned low solubility active substances that have been used for many years, is a neutral cyclic non-ribosomal peptide composed of 11 amino acids that was first isolated from the fungal extract of *Tolypocladium inflatum* in 1973.[2] CycA, one of the calcineurin inhibitors, is an immunosuppressant widely used to prevent organ rejection after transplantation, just like the other calcineurin inhibitor tacrolimus.[3] CycA shows its immunosuppressant activity by forming a cyclosporine-cyclophilin complex after binding to cyclophilin, thereby inhibiting T-cell activation and calcineurin phosphatase, which, under normal circumstances,

*Correspondence: silagulbag@sdu.edu.tr, ORCID-ID: orcid.org/0000-0001-6743-3474
Received: 26.07.2023, Accepted: 14.10.2023

is responsible for activating the transcription of interleukin-2 (IL-2).[4] The molecular formula of CycA is $C_{62}H_{111}N_{11}O_{12}$, and the unsaturated chain at position 1 and amino acids at positions 2, 3, and 11 are responsible for the immunosuppressive effect.[5] The solubility of CycA in water at 25 ˚C is 0.04 mg/mL, and its solubility in n-hexane is 1.6 mg/g.[6] When CycA is evaluated in terms of solubility and permeability properties; it is classified as Class II (low solubility, high permeability) according to the Biopharmaceutical Classification System (BCS) created by Amidon et al.[7] CycA was first introduced to the market as a conventional oil-based formulation under the name Sandimmun®, and then the microemulsion formulation was developed with the trade name Sandimmun Neoral® because the gastrointestinal system effect was evident in CycA pharmacokinetics.[3] Although partial improvement was achieved in pharmacokinetic parameters with the microemulsion formulation; studies with CycA are continuing to reduce side effects (an undesirable plasma peak above 1000 ng/mL is thought to cause nephrotoxicity), prepare products at a lower cost, and reduce inter-and intravariation and fasting-fed variability. Many studies with current opinions and different drug delivery systems have been included in the literature to improve the solubility and dissolution of CycA, to provide higher blood concentrations, and to decrease toxicity.[3,8,9]

There are many opinions on how to improve the solubility of drugs to improve oral bioavailability. Nanosuspension (NS) technology is an attractive approach that aims to improve the solubility, dissolution rate, and bioavailability of BCS Class II and IV drugs by decreasing the particle size (PS) of drugs to nanometer sizes without the use of carriers.[10,11] When NSs are dried, they are called nanocrystals, but these nanocrystals do not necessarily indicate that the structure is physicochemically crystalline.[12] When drugs are reduced to nanometer size, the saturation solubility improves according to the Noyes-Whitney equation; therefore, nanocrystals/NSs can significantly improve the oral absorption and bioavailability of drugs.[13-16]

The techniques used for preparing NSs are classified into two main approaches; "top-down" and "bottom-up" technologies. In bottom-up technology, the molecule is first dissolved in a solvent, and then an insoluble solution is added to form a precipitate, resulting in particles in nanometer sizes.[16] Top-down technologies include wet milling (WM) and high-pressure homogenization (HPH), while bottom-up technologies include precipitation. In the WM or pearl milling/ball milling method, the drug macrosuspension is placed in a milling container, which is rotated with the addition of beads prepared with special polymers such as glass, zirconium oxide, or hard polystyrene derivatives. Depending on the size, amount, or rotational speed of the beads in the container, NSs are obtained. The second most commonly used top-down method is the HPH method. Microfluidization and piston-gap homogenization are two homogenization principles currently used. Microfluidization is a jet stream principle; the suspension is accelerated and passes at high speed through a specially designed "Y" or "Z" type homogenization chamber. In the "Z" type chamber, the flow direction of the macrosuspension is changed several times while the particles are collided and cut; while in the "Y" type chamber, the macrosuspension is divided into two flows by the obstacle in front of it.[17] In the piston-gap homogenization method; the macrosuspension is forced to pass through a small size gap so that the particles can be reduced to smaller sizes. Top-down NS production methods have many advantages, such as minimum solvent content, high drug loading, easy preparation methods, and rapid production. Due to these advantages of NSs; many studies have been performed with NS (or nanocrystal) formulations prepared by WM[9,18-22] and HPH[23-26] methods, which are top-down methods.

NSs are prepared using surfactants such as sodium dodecyl sulfate (SDS), tween 80, vitamin ED-α-Tocopherol polyethylene glycol 1000 succinate, poloxamer, and polymeric stabilizers such as hydroxypropyl methylcellulose (HPMC), polyvinylpyrrolidone (PVP), and polyvinyl alcohol. These stabilizers can be used individually or as a combination; furthermore, there are many studies in which both surfactants and polymeric stabilizers are used together to improve the stability of NSs.[23,27-29]

In the last 20 years, opinions aimed at ensuring the quality of pharmaceutical products and achieving the most proper formulation have gained interest in the pharmaceutical industry. The effects of critical formulation and/or process parameters can be determined by optimizing the formulation and/or process requirements using the design of experiment (DoE), which is one of these approaches. Therefore, the effects of the independent variables, which are thought to be effective in the formulation, on the dependent variables can be successfully investigated experimentally.[30] In addition to many drug delivery system studies using DoE, studies on NS preparation have become common in the literature.[8,14,23,25,26] In Figure 1, the parameters that affect PS, polydispersity index (PDI), PDI and zeta potential (ZP) in NS formulations obtained by HPH technology are shown by the fishbone diagram.

As mentioned above, there remains a need for a novel formulation of CycA to be developed for oral administration. The Sandimmun Neoral® microemulsion formulation is expensive and requires many excipients, and Cremophor®RH40, which is included as a surfactant in its composition, has a toxic effect; complicates its use in therapy. Thus, studies on increasing the solubility and dissolution rate of CycA with nanoparticles, lipid nanoparticles, and liposome carrier systems that do not contain Cremophor®RH40 are available in the literature; however, studies on the preparation of CycA NS are limited. This research article describes the preparation of CycA NS by HPH using the DoE approach. One of the unique values of this article is to improve the product quality as a result of the developed formulation requiring fewer process parameters and providing a nanotechnology-based, innovative, and creative approach suitable for scale-up in a shorter time using the DoE approach in the formulation development process.

Numerous results have been obtained in our previous studies on CycA NSs. In the first of these studies, CycA was prepared using the HPH method with HPMC and Soluplus®, and after DoE, the ratio of CycA: HPMC: Soluplus® 1:1:0.5 *(w/w)* was

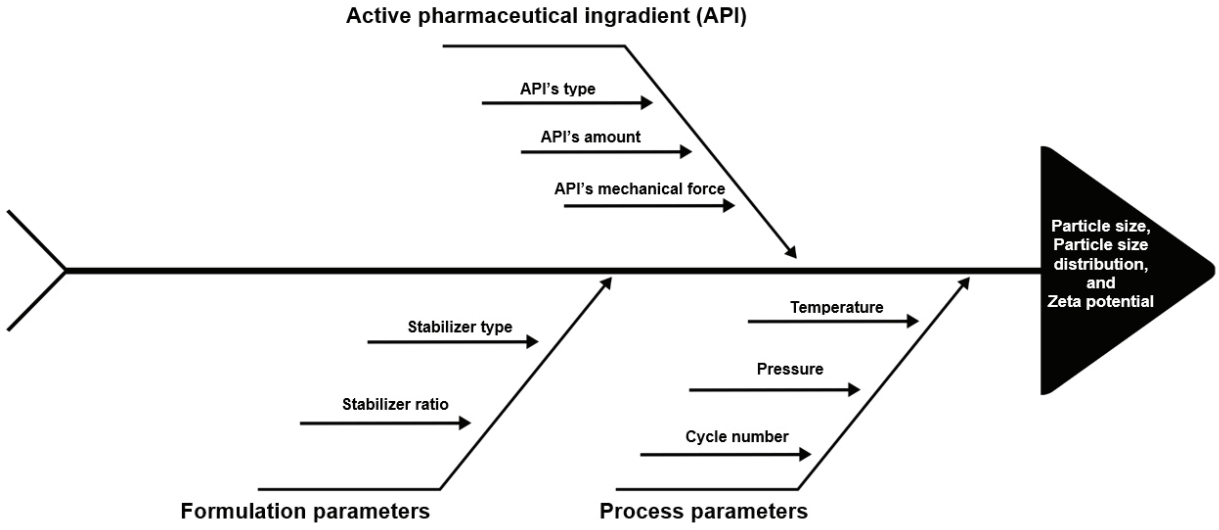

Figure 1. Fishbone diagram showing the process and formulation parameters of HPH
HPH: High-pressure homogenization

found to be the most appropriate ratio. Characterization studies showed that the solubility improved by 2.1-fold compared to the coarse powder.[8] In order to further this study, CycA NSs were prepared using the WM method in the second step, which is another NS preparation method. The ratio of CycA: HPMC: SDS® 1:1:0.5 *(w/w)* was determined as the optimal ratio after DoE and formulation were examined *in vivo*. The solubility improved 4.5-fold compared to the coarse powder and was higher in the *in vitro* fed simulated intestinal fluid (FeSSIF) medium than in the trade product. The pharmacokinetic study indicated that area under the curve $(AUC)_{0-24}$ values of CycA NS were 2.09- and 5.51-fold higher than those of coarse powder in fasted and fed situations, respectively.[18] When the permeability of this formulation in Caco-2 cells was examined, NS showed improved CycA transport by 5 and 1.5 times, respectively, compared with coarse CycA powder and trade product (Sandimmun Neoral®).[19]

Based on this information, this study aimed to prepare CycA NSs using HPH technology by using a polymer (HPMC) and surfactant (SDS) combination based on previous knowledge and to determine the optimum ratio using the DoE approach. HPMC was selected because it was previously proven to be an efficient stabilizer for NSs.[21,23] SDS with a surfactant structure is an electrostatic stabilizer that allows high ZP loading on the surface of particles and therefore is widely used.[13,20,23] SDS can migrate to the solid-liquid intersurface and provide an electrostatic barrier against the aggregation of nanometer-sized particles.[10] One of the main objectives of this study was to examine the effect of the surfactant ratio on PS, PDI, and ZP in formulations prepared when a polymeric stabilizer (HPMC) and surfactant (SDS) were used together with an experimental design approach.

The effects of formulation parameters (HPMC: SDS ratio) and process parameters (cycle number of homogenization) as independent variables on dependent variables (PS, PDI, and ZP) were evaluated using the DoE approach. As a result of the DoE analysis, the optimum formulation was determined, and characterization studies were conducted using this formulation. The physical stability (PS and ZP results) of the optimum formulation for 9 months at 4 °C and 25 °C was evaluated. The solubility of the optimum CycA NS were was compared with those of coarse powder and physical mixture (PM). For CycA dissolution medium, fasted simulated intestinal fluid (FaSSIF) and FeSSIF dissolution studies, NSs were compared with coarse powder, PM, and a trade product (Sandimmun Neoral®).

MATERIALS AND METHODS

Materials

CycA was provided as a gift by the Deva Drug Company (Türkiye). HPMC was obtained from Colorcon (USA). SDS and D (-) mannitol were purchased from Merck (Germany). SIF® Powder was purchased from Biorelevant© (UK).

Preparation of the CycA NS

The HPH method (microfluidization technique) involved 0.2 g (1%) HPMC and 0.1 or 0.05 g (0.5% or 0.25%) SDS dissolved in distilled water. In the second step, CycA powder (1% *w/w*) was dispersed in this solution using a magnetic stirrer at 1000 rpm for 20 minutes. To prevent chamber blockage of the high-pressure homogenizer (Microfluidics LV1 with a Z-type 84 µm chamber), UltraTurrax (Heidolph® Silent Crusher) was used at 15000 rpm for 10 minutes to reduce the PS of this suspension. Finally, this suspension was transported to Microfluidics LV1 (Microfluidizer®) and homogenized for different homogenization cycles at 30,000 psi.

Different homogenization cycles (X_1) (5, 10, 15, and 30 cycles) and different amounts of surfactant (SDS) (X_2) (0.5% and 0.25%) were defined as critical process parameters (independent variables) in preformulation studies on the HPH method, and their impacts on dependent variables [PS (Y_1), PDI (Y_2), and ZP (Y_3)] were assessed using DoE. The process

parameter consisted of four levels with two replicates. After conducting trials in random order using the Design Expert 9.0 software, the results were evaluated using this software. The interactions between independent variables were investigated using the DoE approach, and the optimal CycA NS formulation was determined for characterization.

PS, PDI, and ZP studies

PS, PDI, and ZP measurements, which are prominent results regarding nanodrug delivery systems, were conducted at 25 ˚C by dynamic light scattering method using a particle sizer (Malvern Instruments® ZetaSizer-Nano ZS). For PS and PS measurement, the first 750 µL of NS was added to the sample measuring cup and topped with up to 1500 µL of distilled water. At the end of this dilution, the diluted sample was placed in the PS and ZP measurement cuvettes. Each sample was measured at least three times, and the results were calculated as the mean ± standard deviation (SD).

Preparation of the PM

The PM was prepared by stirring the coarse CycA powder for approximately 5 minutes with the same HPMC and SDS ratios used in the optimum NS formulation.

Lyophilization of the CycA NS

Lyophilization of NS is essential for long-term stability and the generation of solid dosage forms. Lyophilization was performed after the PS, PDI, and ZP measurements of the NS were prepared by HPH. Mannitol was chosen as the cryoprotectant for the formulations, and the CycA: mannitol ratio was 1:1 (% *w/w*) after preformulation studies.[8] Approximately 2 g of the NS was frozen at 80 ˚C for 2 hours and lyophilization was performed at -50 ˚C under 0.021 mbar pressure for 48 hours with Christ Alpha® 1-2 LD Plus.

In vitro characterization studies

Morphology study

The surface morphologies of the powder samples (CycA coarse powder, PM, and lyophilized NS) were observed by scanning electron microscopy (SEM). The samples were placed on carbon specimen holders and air-dried. The samples were then covered with gold-palladium composition prior to experiments, and morphological images were monitored using a microscope (Quanta® 400F).

X-ray powder diffraction (XRD) study

The XRD spectral analysis of the CycA coarse powder, stabilizers, PM, and lyophilized NS was carried out by Rigaku Ultima® IV (Japan). The scan rate was adjusted at 1° per minute, and the scan range was 2θ in the range of 3-90˚.

Fourier transform infrared (FTIR) spectroscopy

The FTIR spectra of CycA coarse powder, PM, and CycA NS were examined using a spectrometer (Perkin Elmer® Spectrum 400 Attenuated Total Reflectance-FTIR). A scanning range of 650-4000 cm^{-1} and the discrimination power of 1 cm^{-1} were selected for the measurements.

Physical stability assessment

After preparing the optimal CycA NS, PS, PDI, and ZP values were initially measured. The physical stability studies for the optimal CycA NS were initiated by storing the formulation at two temperatures (4 ˚C and 25 ˚C), and the measurements were repeated for 9 months after each month of storage. PS, PDI, and ZP values at designated time points were measured using a Malvern ZetaSizer-Nano ZS (Malvern Instruments®) with the same protocol described in the preceding sections. Studies were conducted in triplicate, and results were determined as the mean ± SD.

Solubility studies

For the solubility study, an excess amount of CycA coarse powder, PM, and lyophilized CycA NS was added to the flasks and dispersed in distilled water. The flasks were agitated for 48 hours at 37 ± 0.5 ˚C. The samples were filtered with 0.22 µm nylon filters and were investigated using an ultraviolet (UV) spectrophotometer (Agilent Technologies® Cary 60 UV-visible spectroscopy) at 207 nm. Analysis was performed thrice, and the mean results and SDs were calculated.

In vitro dissolution studies

In vitro dissolution studies were conducted using CycA coarse powder, PM, and NS. They were weighed to 10 mg and placed in hard gelatin capsules with number 00. The study was conducted using a USP Apparatus I Basket (Agilent Technologies® 708-DS) rotating at 150 rpm and a temperature of 37 ± 0.5 ˚C, according to the USP dissolution method.[31] The USP dissolution medium was 1000 mL of 0.1 N HCl containing 0.5% SDS, and the study was repeated with 1000 mL of 0.1 N HCl without SDS to investigate the efficacy of SDS on the dissolution rate. In addition, dissolution studies were performed in 500 mL of FaSSIF or FeSSIF media, which included several amounts of sodium taurocholate and phospholipids, to simulate the *in vivo* fasting and feeding state, respectively. Samples were withdrawn from the dissolution medium at predetermined intervals (5, 10, 20, 30, 45, 60, 90, and 120 min), and then the same amount of fresh medium was added to the dissolution medium (for sink condition). The experiment was repeated three times. The samples were filtered with a 0.22 µm membrane filter, and the quantitative analysis of CycA was performed using a validated HPLC method at 205 nm. The mean results and standard deviations (SD) were determined.

Analytical methods

For quantification in solubility and dissolution studies, analyses were performed using both UV spectrophotometric and HPLC chromatographic methods.

UV spectrophotometry was used to determine CycA concentration in the solubility study. The proposed method was validated according to validation parameters.

The HPLC method was used to determine the CycA concentrations in the four dissolution media.

Chromatographic separation was performed using an Agilent® 1220 Infinity LC HPLC system with a C18 RP column (150 mm x 4.6 mm, 5 µm). The mobile phase consisted of acetonitrile:

water (75:25 *v/v*), the flow rate was set to 1 mL per minute and the column temperature was 60°C. The injection volume of the samples was 20 µL and the detection of the drug was conducted at 205 nm. The HPLC method was validated for specificity, linearity, range, accuracy, precision, and robustness.

Statistical analysis

Statistical analysis was performed using SPSS software (version 22.0, IBM Corp., USA). A One-Way analysis of variance followed by Tukey's HSD post-hoc test was used to analyze statistical data at a significance level (α) of 0.05. All results are presented as mean ± standard deviation (SD).

RESULTS

Preparation of the CycA NS

The HPH method for preparing drug powders in stabilizer solutions is a suitable method for preparing NS formulations. While the process parameters determining the final dispersion are the homogenization pressure and the number of homogenization cycles (pass number), the formulation parameters are the stabilizer types and ratios. Stabilizers influence the long-term physical stability but do not influence the form of the produced NSs.

The appropriate stabilization of NSs is determined by trial and error depending on the active ingredient.[29,32] For NSs, it has been reported that the type of stabilizer, as well as its amount, is crucial, and stability problems may occur when using an insufficient stabilizer.[29] Many studies have reported the use of stabilizers in combination to ensure and maintain thermodynamic stability in the preparation of NSs.[28,33-35]

In our study, HPMC (a polymer) and SDS (a surfactant) were used as combined stabilizers, and their ratios were investigated to determine the PS, PDI, and ZP values of NSs. The PS, PDI, and ZP results of NSs are shown in Figure 2.

ANOVA and interaction results for PS, PDI, and ZP of CycA NSs prepared using the HPH method and the HPMC: SDS combination in two ratios (1: 0.5 and 1: 0.25) with the experimental design are presented in Table 1, and contour plots are given in Figure 3.

Surface morphology study

After preparation of the NS, CycA NSs obtained after 5 passes, 10 passes, 15 passes, and 30 passes of the CycA: HPMC: SDS 1:1:0.5 formulation were lyophilized to examine the effects of the homogenization cycle (pass number) on the internal structure (Figure 4).

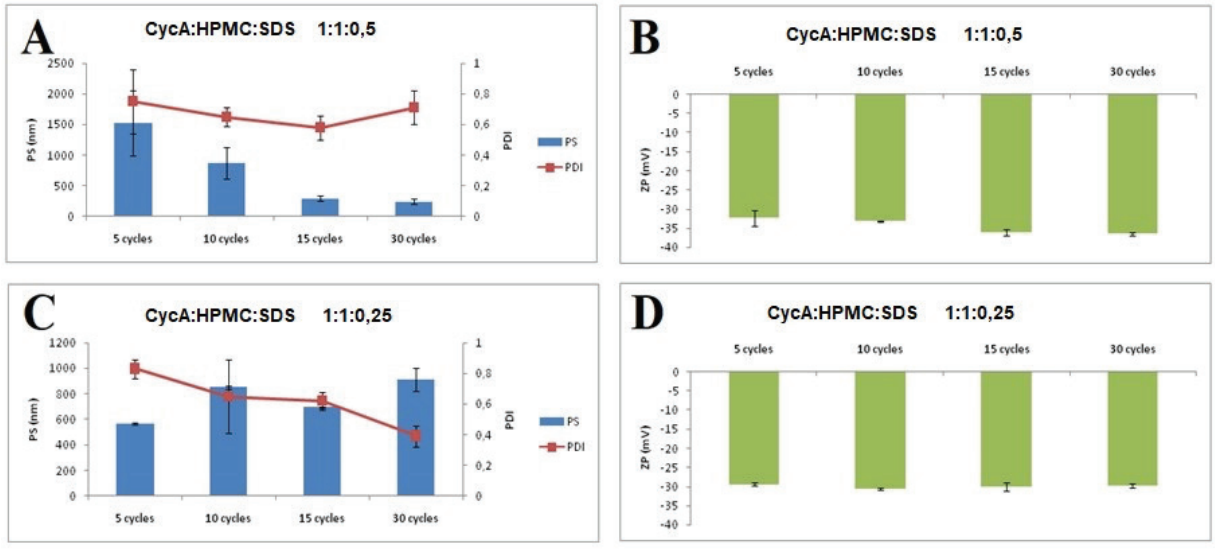

Figure 2. PS, PDI, and ZP results for the CycA NS stabilized with HPMC: SDS (1:0.5 and 1:0.25) (mean ± SD; n= 3)

PS: Particle size, PDI: Polydispersity index, ZP: Zeta potential, CycA: Cyclosporine A, NS: Nanosuspension, HPMC: Hydroxypropyl methylcellulose, SDS: Sodium dodecyl sulfate, SD: Standard deviation

Table 1. ANOVA and interaction for PS, PDI, and ZP of CycA: HPMC: SDS NS

Source	PS		PDI		ZP	
	f value	*p* value	*f* value	*p* value	*f* value	*p* value
Model	5.46	0.0133	4.36	0.0269	27.21	< 0.0001
A-SDS ratio	1.09	0.3175	1.90	0.1937	73.62	< 0.0001
B-homogenization cycle	4.54	0.0546	6.31	0.0273	7.60	0.0174
AB	11.83	0.0049	6.20	0.0284	8.00	0.0152

ANOVA: Analysis of variance, CycA: Cyclosporine A, HPMC: Hydroxypropyl methylcellulose, SDS: Sodium dodecyl sulfate, NS: Nanosuspension, PS: Particle size, PDI: Polydispersity index

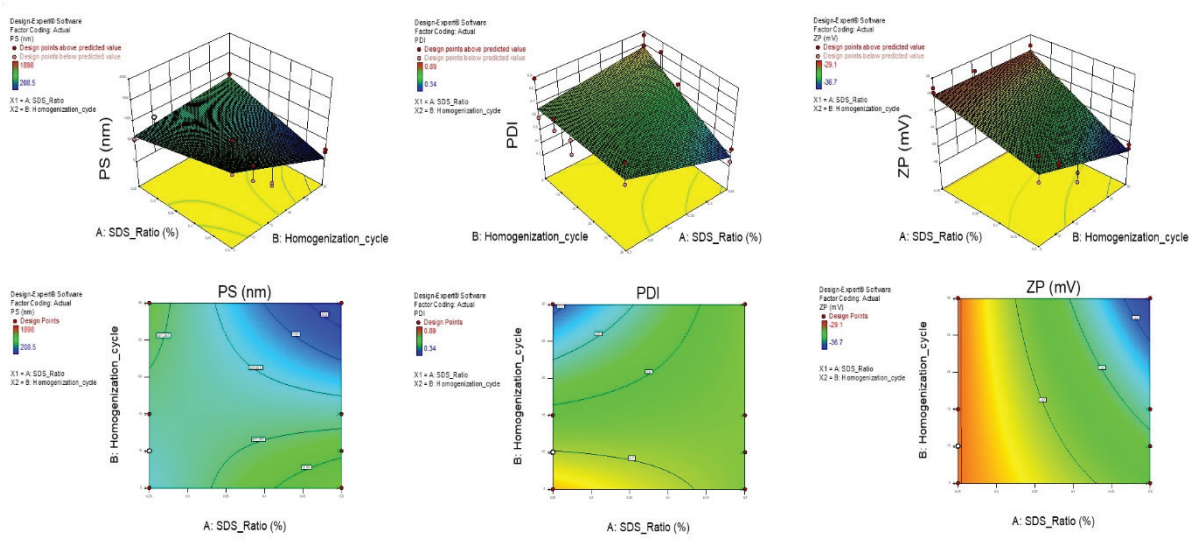

Figure 3. 3D surface (top) and contour (down) graphs illustrating the effects of the SDS ratio and homogenization cycle on PS, PDI, and ZP
PS: Particle size, PDI: Polydispersity index, ZP: Zeta potential, SDS: Sodium dodecyl sulfate

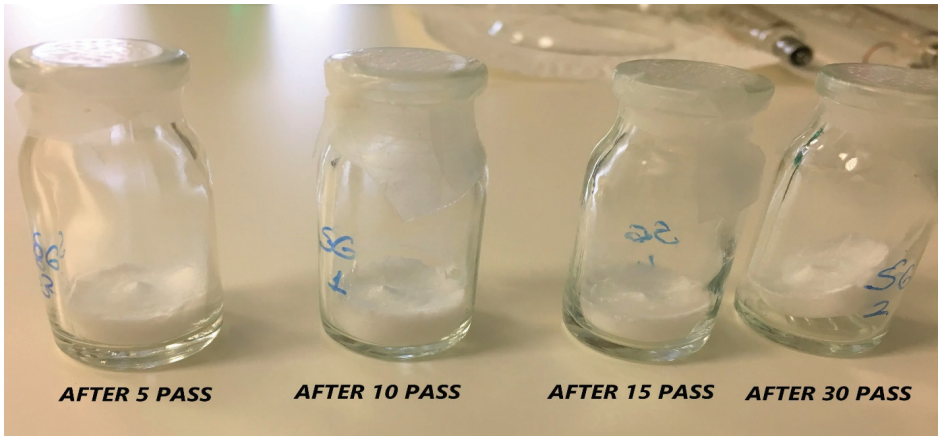

Figure 4. Lyophilized CycA NSs composed of CycA: HPMC: SDS (1:1:0.5) after different homogenization cycles (pass number)
CycA: Cyclosporine A, NSs: Nanosuspensions, HPMC: Hydroxypropyl methylcellulose, SDS: Sodium dodecyl sulfate

The surface morphologies of CycA coarse powder, HPMC, SDS, mannitol, PM, and the optimal CycA NS were investigated using SEM (Figure 5). The SEM images showed that the CycA coarse powder was in a crystalline state with sharp edges (Figure 5A). The PM consists of coarse powder, HPMC, SDS, and mannitol, and these components should be observed in the morphological examination of the PM after SEM. According to Figure 5E, HPMC was shown as long fibers, SDS was seen to be spherical, and mannitol was found to be crystalline and spiky. CycA in the NS exhibited a sharp surface (Figure 5F).

XRD study

XRD analysis is a method that is frequently used to explain the crystalline or amorphous structure of substances. XRD studies were conducted to evaluate the crystal properties of CycA, HPMC, SDS, mannitol, PM, and the optimal CycA NS (Figure 6).

FTIR spectroscopy

FTIR measurements were performed in addition to XRD analysis to evaluate possible changes in CycA under the applied pressure during the preparation of the formulations by the HPH method. The FTIR spectroscopy results of the samples are shown in Figure 7.

Physical stability assessment

The stability evaluation of the optimal CycA NS was carried out by measuring the PS, PDI, and ZP at 4 °C and 25 °C (Figure 8). There were no major alterations in the PS and ZP results of CycA NSs for 9 months at 4 °C and 25 °C (Figure 8A-D). In accordance with the results of all stability studies, the ZP value was › 20 mV at 4 °C and 25 °C, indicating that the formulation was physically stable.

Solubility study

Saturation solubility studies were conducted in distilled water with CycA coarse powder, PM, and lyophilized CycA NS at 37 °C. In Table 2, the water solubility was found to be 6.48 ± 0.88 µg/mL with CycA coarse powder and 8.78 ± 0.38 µg/mL with the PM.[8,18,19] These results demonstrate that PM improved the water solubility of CycA by approximately 1.4-fold. Furthermore, the

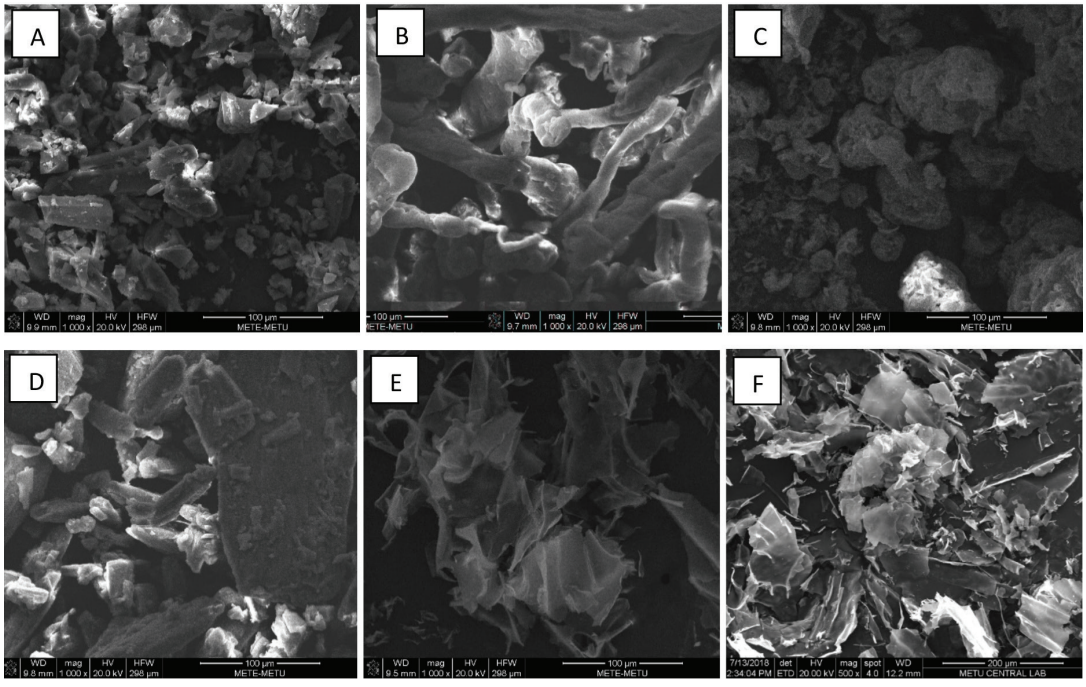

Figure 5. SEM images of (A) CycA coarse powder (mag. 1000x), (B) HPMC (mag. 1000x), (C) SDS (mag. 1000x), (D) mannitol (mag. 1000x), (E) the PM (mag. 1000x), (F) the CycA NS (mag. 500x)

CycA: Cyclosporine A, NSs: Nanosuspensions, HPMC: Hydroxypropyl methylcellulose, SDS: Sodium dodecyl sulfate, PM: Physical mixture, mag.: Magnification, SEM: Scanning electron microscopy

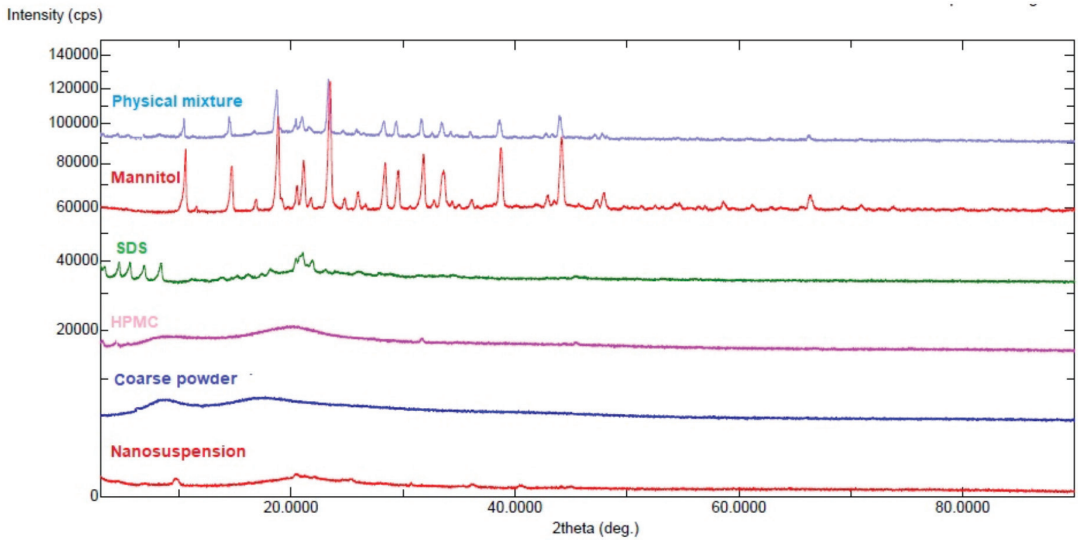

Figure 6. XRD patterns of CycA NS, CycA coarse powder, HPMC, SDS, mannitol, and the PM

XRD: X-ray powder diffraction, CycA: Cyclosporine A, NS: Nanosuspension, HPMC: Hydroxypropyl methylcellulose, SDS: Sodium dodecyl sulfate, PM: Physical mixture

solubility of CycA NS was 12.61 ± 1.48 µg/mL, and the solubility of CycA improved 1.9-fold compared to the coarse powder. According to Beauchesne et al.,[6] the solubility of CycA in water at 25 ˚C is 0.04 mg/mL, but in our study, the solubility was obtained to be 6.48 ± 0.88 µg/mL. The reason for this difference may be that the sources of the active substances used in the studies were different or that the analysis was performed in different ways.

Table 2. Saturation solubility of the CycA coarse powder, the PM, and the CycA NSs (mean ± SD; n= 3)

Sample	Saturation solubility (µg/mL)
CycA coarse powder	6.48 ± 0.88
PM	8.78 ± 0.38
CycA NS	12.61 ± 1.48

CycA: Cyclosporine A, PM: Physical mixture, NS: Nanosuspension, SD: Standard deviation

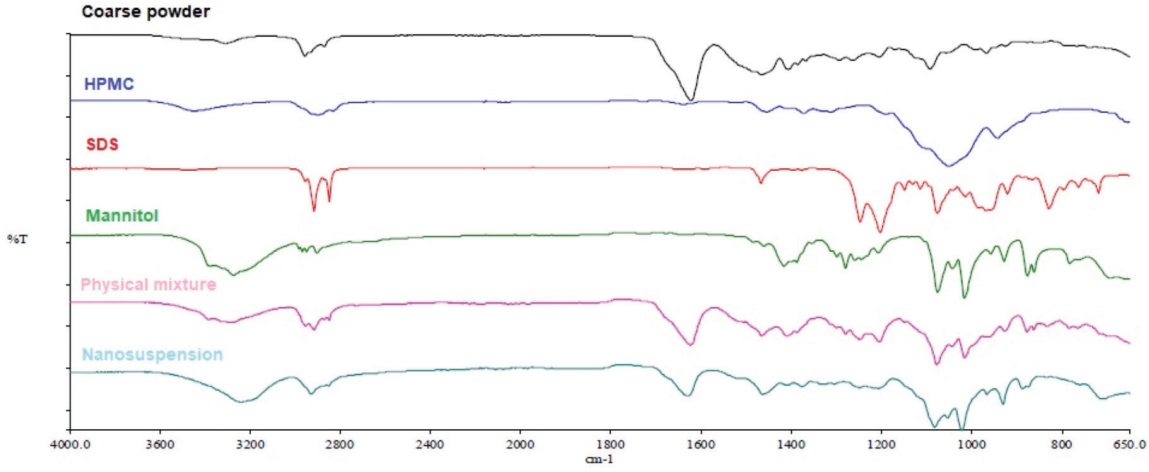

Figure 7. FTIR spectra of the CycA coarse powder, HPMC, SDS, mannitol, PM, and CycA NS

FTIR: Fourier transform infrared radiation, CycA: Cyclosporine A, HPMC: Hydroxypropyl methylcellulose, SDS: Sodium dodecyl sulfate, NS: Nanosuspension, PM: Physical mixture

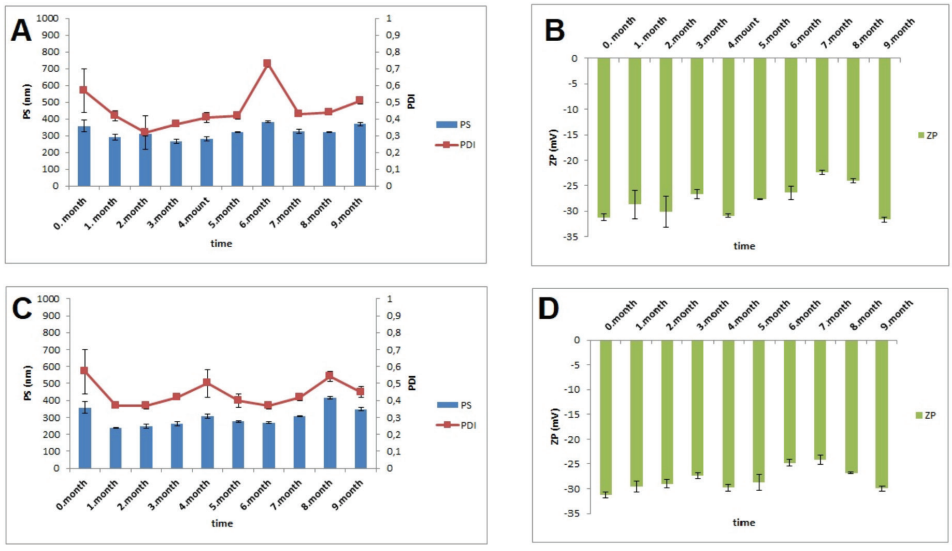

Figure 8. Physical stability results of CycA NS; 4 °C (A and B) and 25 °C (C and D) (not statistical significant)

CycA: Cyclosporine A, NS: Nanosuspension

In vitro dissolution studies

Dissolution studies were conducted in various dissolution media containing CycA coarse powder, PM, a trade product (Sandimmun Neoral®), and CycA NS. In dissolution studies, first, 0.1 N HCl medium containing 0.5% sodium lauryl sulfate, as suggested by the and USP for Sandimmun Neoral®, was used,[31] and then to examine the effects of SLS in this medium on dissolution, the study was repeated with 0.1 N HCl medium without SLS.

In 0.1 N HCl medium containing 0.5% SLS; CycA coarse powder, PM, and CycA NS showed dissolution over 70%, CycA coarse powder showed no dissolution, and CycA NS showed 40% dissolution in the study performed in 0.1 N HCl medium. The trade product showed more than 90% dissolution in both media (Figure 9A and B).

Furthermore, dissolution studies were conducted with FaSSIF and FeSSIF media that simulate fasting and feeding. The physiological conditions (such as bile salts and lecithin) can be simulated *in vitro*, and *in vivo* predictions can be provided for drugs such as BCS Class II drugs using these irrelevant media. Figure 10 shows the dissolution profiles of CycA coarse powder, the trade product PM, and CycA NS in the FaSSIF and FeSSIF media.

CycA coarse powder and PM showed a 15% in 120 minutes in FaSSIF medium. While NS showed 70% dissolution, the trade product showed higher dissolution in all samples, with 80% dissolution at 120 minutes (Figure 10A).

While CycA coarse powder and PM showed almost 40% dissolution; the NS prepared using the HPH method showed 60% dissolution in 120 minutes in FeSSIF medium and other

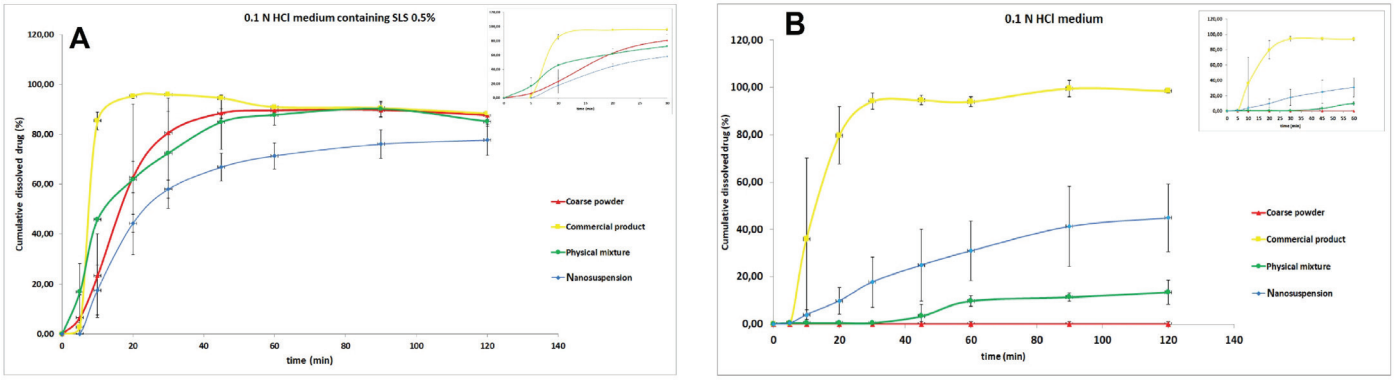

Figure 9. Dissolution profiles of CycA coarse powder, a commercial product, and a PM of CycA NS in (A) 0.1 N HCl containing 0.5% SDS and (B) 0.1 N HClCycA: Cyclosporine A, HPMC: Hydroxypropyl methylcellulose, SDS: Sodium dodecyl sulfate, NS: Nanosuspension, PM: Physical mixture, HCl: Hydrochloric acid

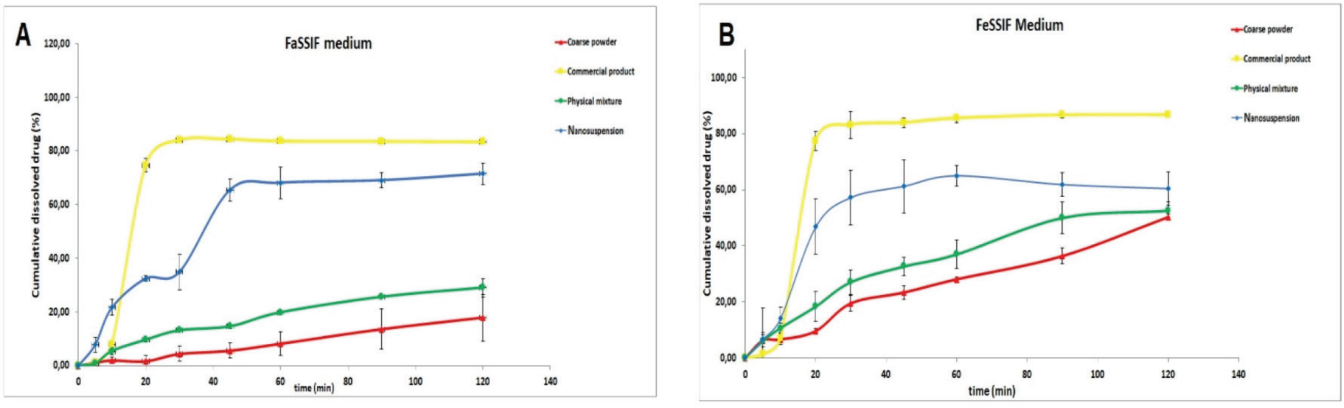

Figure 10. Dissolution profiles of the CycA coarse powder, commercial product, and PM as well as the CycA NS in (A) FaSSIF medium and (B) FeSSIF medium

CycA: Cyclosporine A, PM: Physical mixture, FaSSIF: Fasted simulated intestinal fluid, FeSSIF: Fed simulated intestinal fluid

irrelevant media. Similar to the FaSSIF results, the trade product exhibited 80% dissolution in the FeSSIF medium (Figure 10B).

DISCUSSION

In the preparation of CycA NS, the model was found to be significant (p= 0.0133) as shown in Table 1, where the interaction between the SDS ratio and homogenization cycle in terms of PS was examined. The effects of the SDS ratio (p= 0.3175) and homogenization cycle (p= 0.0546) were not significant individually. the SDS ratio*homogenization cycle interaction was found to be significant (p= 0.0049).

The interaction equation for the model affecting PS, A: SDS ratio, B: homogenization cycle, and AB: interaction of A and B, is shown in equation (Eq) 1.

PS = +699.87 82.59*A 217.67*B 351.56*AB (1)

The model was found to be significant (p= 0.0269) when the interaction of the SDS ratio and homogenization cycle was evaluated in terms of PDI, as reported in Table 1. Although the SDS ratio (p= 0.1937) was not significant individually; the homogenization cycle and SDS ratio homogenization cycle interaction were found to be significant (p= 0.0273 and p= 0.0284, respectively).

The interaction equation for the model affecting the PDI, A: SDS ratio, B: homogenization cycle, and AB: interaction of A and B, is shown in Eq 2.

PDI = +0.63+0.043*A 0.10*B +0.10*AB (2)

The model was found to be significant ($p < 0.0001$), when the interaction between the SDS ratio and homogenization cycle was evaluated in terms of ZP, as reported in Table 1. The SDS ratio, homogenization cycle, and SDS ratio homogenization cycle interaction were found to be significant ($p < 0.0001$, p= 0.0174 and p= 0.0152, respectively).

The interaction equation for the model affecting the ZP, A: SDS ratio, B: homogenization cycle, and AB: interaction of A and B, is shown in Eq 3.

ZP = 32.41 2.49*A 1.03*B 1.06*AB (3)

According to the obtained data and contour plots, as the SDS ratio and homogenization cycle decrease, PS values increase; as the SDS ratio decreases and the homogenization cycle increases, PDI values decrease. In all NSs, ZP values were above -20 mV, which is acceptable, indicating the stability of the NS. Hence, the ratio of CycA: HPMC: SDS was determined as 1:1:0.5, and homogenization cycles of 30 were found to be suitable process parameters to achieve the optimum NS with the HPH method.

In this study, ritonavir NSs were prepared using the HPH method. The DoE approach was used to explain the impact of the critical formulation parameters. After the DoE analysis, the optimal formulation was selected with 4% HPMC and 20 passes.[23] To enhance the water solubility of ziprasidone hydrochloride monohydrate (ZHM), which is a BCS Class II drug, the impacts of the formulation and process parameters in NSs prepared using microfluidization were evaluated using the DoE approach. NSs showed the lowest PS value ($p < 0.05$) after 30 homogenization cycles, and the optimal NSs were ZHM: vitamin E TPGS 2:1 at 30 passes and ZHM: PVP K30 1:1 at 20 passes.[26] Our results and those of previous studies have shown that increasing the number of passes through the homogenizer decreases the PS of the NS.

When the morphological images of NSs are evaluated; it is thought that CycA coarse powder was covered with stabilizers and that high energy was applied in the high-pressure NS production process. The observed morphological results were similar to those reported in the literature.[8,26]

The XRD patterns of SDS and mannitol showed obvious diffraction peaks although the peaks of SDS were weaker. This suggests that they were in a crystalline state. Also, the PM was found to be crystalline, confirming that the PM possessed the same properties as CycA, HPMC, SDS, and mannitol. As shown in Figure 6, the CycA coarse powder, HPMC, and lyophilized CycA NS were in an amorphous state. It has been shown by others[36,37] that CycA exists in an amorphous state, and our results also showed this state. It is known that the amorphous structure of NSs can have positive effects on solubility and dissolution.[38]

In FTIR studies, Figure 7 shows that the characteristic bands of the active substance were the amide carbonyl band at 1623 cm^{-1} and the amide N-H band at 3314 cm^{-1}. When the FTIR results of the CycA coarse powder were examined, characteristic CycA bands similar to those observed in the study of Bertacche et al.[39] were observed at 2960 cm^{-1}. In the HPMC spectrum, the characteristic band was the band belonging to the C-O group at 1052 cm^{-1}; it was the band of RO-SO_2-OR sulfate at 1203 cm^{-1} in the SDS spectrum. The bands that were considered characteristic of mannitol were O-H bands at 3277 cm^{-1}, C-O bands at 1077 cm^{-1}, and 1016 cm^{-1}. In the FTIR spectrum of the PM, the band at 1624 cm^{-1} belongs to CycA, while the bands at 1248 cm^{-1} and 1206 cm^{-1} belong to SDS. Since the bands observed around 1000 cm^{-1} were thought to belong to HPMC and mannitol, it has been proven that there is no interaction in the PM spectrum. In the FTIR spectrum of NSs prepared using the HPH method; characteristic bands of CycA at 1630 cm^{-1}, SDS at 1249 cm^{-1}, mannitol at 1083 cm^{-1}, and HPMC at 1021 cm^{-1} were seen. When this spectrum of NS was evaluated together with the XRD results; it proved that there was no polymorphic change between the active substance and the excipients and that the pressure applied while preparing the formulation and the lyophilization process did not change the physicochemical structure. In a study by Attari et al.,[40] characteristic bands of the active substance were observed in olmesartan medoxomil NSs, and no interaction was found.

Stability issues, known as Ostwald ripening, that result in the growth of nanosized particles are critical for NS formulations. It is important to maintain the PS, PDI, and ZP values in the evaluation of the physical stability of NSs. The small PDI value in the stable NSs indicates that the particles are of similar size and have less tendency to coalesce and grow; also high ZP values indicate that due to the high electrical charge in the stabilizers, the aggregation of the particles is prevented.[41]

The obtained results of solubility study prove that the purpose of increasing the solubility of CycA was achieved by the NS preparation. The reason for this improvement is based on the Ostwald-Freundlich equation. According to this equation, the solubility and dissolution of the NPs improve by increasing the surface area by reducing the PS to nano-size.[42] In a study, a 2.13-fold improvement in water solubility was found in CycA NSs prepared using the HPH method using a combination of HPMC and Soluplus® stabilizer after 30 homogenization cycles.[8] In another study, the solubility of CycA was improved by 4.5-fold by wet-milled NSs.[18]

As a result of the dissolution studies, it was seen that the dissolution profile change between the two media was caused by SLS. In the literature review, it was found that similar results supported this result.[26,43]

Many studies have suggested that NSs can diminish the dissolution variation of drugs with low water solubility in fasting and feeding states. It was found that ZHM NS stabilized with PVP and vitamin E TPGS exhibited > 95% dissolution in FeSSIF medium and > 80% dissolution in FaSSIF medium.[26] In a dissolution study conducted in FaSSIF medium with NSs prepared using the HPH method for five active substances (albendazole, fenofibrate, itraconazole, probucol, and revaprazan hydrochloride) with low water solubility, it was found that NSs showed higher dissolution than microsuspensions for all five active substances. In a pharmacokinetic study with free access to food and water in Male Wistar rats with the same NS formulations; NSs were found to have higher AUC and C_{max} than microsuspensions (for albendazole approximately 2- and 3.2-times, for fenofibrate approximately 2.2- and 3.5-times, for itraconazole approximately 7- and 8.6-times, for probucol approximately 6.4- and 2.9-times, and revaprazan hydrochloride approximately 1.4-and 2.1-times, respectively) at the end of administration at a dose of 100 mg/kg.[44]

In a study to investigate the impact of PS on the absorption of aprepitant, a single-pass method of intestinal perfusion in the rat jejunum was used with phosphate buffer, FaSSIF, FeSSIF as perfusion medium. The results showed that the absorption of aprepitant from the NSs was equal to that from all perfusion media (phosphate buffer = FaSSIF = FeSSIF), but food had a noticeable impact on absorption from the microsuspensions (FeSSIF > FaSSIF > phosphate buffer).[45]

In summary, dissolution studies performed in fasting, feeding, or both media are important to predict the oral absorption of new formulations in the gastrointestinal fluids. Thanks to these studies, preliminary data for *in vivo* studies can be obtained, and *in vitro/in vivo* correlations can be determined as a result

of supporting *in vitro* dissolution studies with fasting and fed *in vivo* studies.

CONCLUSION

In conclusion, CycA NS was successfully obtained by the HPH method, which is one of the top-down production technologies, and the DoE approach took into account the impact of critical formulation and process parameters on the dependent variables. The optimum CycA NS was obtained with a CycA: HPMC: SDS 1:1:0.5 ratio and 30 homogenization cycles after statistically determining the interactions. According to the stability results at 4 °C and 25 °C, it was found that the NSs remained physically stable for 9 months. CycA NSs improved the water solubility of CycA 1.9- and 1.4-fold compared to coarse powder and PM, respectively. CycA NS showed higher dissolution than CycA coarse powder in 0.1 N HCl, FaSSIF, and FeSSIF media. When the characterization, solubility, and dissolution results were evaluated together, it was found that CycA NS prepared using the HPH method was successful, and this study proved that the NS could be an encouraging strategy for improving the solubility and dissolution of CycA for oral administration.

Acknowledgments

This research was financially supported by the Gazi University Scientific Research Project Foundation [Grant number: 02/2017-14]. The authors are grateful to Deva Pharmaceuticals Company (İstanbul, Türkiye) for providing CycA and to Alptuğ Eren Karaküçük for the design expert analysis.

Ethics

Ethics Committee Approval: Not required.

Informed Consent: Not required.

Authorship Contributions

Concept: S.G.P., N.Ç., Design: S.G.P., N.Ç., Data Collection or Processing: S.G.P., Analysis or Interpretation: S.G.P., N.Ç., Literature Search: S.G.P., N.Ç., Writing: S.G.P., N.Ç.

Conflict of Interest: The authors have no conflicts of interest to declare.

Financial Disclosure: The authors declared that this study received no financial support.

REFERENCES

1. Kumar R, Thakur AK, Chaudhari P, Banerjee N. Particle size reduction techniques of pharmaceutical compounds for the enhancement of their dissolution rate and bioavailability. J Pharm Innov 2022;17:333-352.
2. Borel JF, Kis ZL. The discovery and development of cyclosporine (Sandimmune). Transplant Proc. 1991;23:1867-1874.
3. Guada M, Beloqui A, Kumar MN, Préat V, Dios-Viéitez Mdel C, Blanco-Prieto MJ. Reformulating cyclosporine A (CsA): More than just a life cycle management strategy. J Control Release. 2016;225:269-282.
4. Survase SA, Kagliwal LD, Annapure US, Singhal RS. Cyclosporin A--a review on fermentative production, downstream processing and pharmacological applications. Biotechnol Adv. 2011;29:418-435.
5. Wenger RM, Payne TG, Schreier MH. Cyclosporine: chemistry, structure activity relationships and mode of action. Anonymous metabolic control in diabetes mellitus beta adrenoceptor blocking drugs nmr analysis of cancer cells ımmunoassay in the clinical laboratory cyclosporine. Springer. 1986;157-191.
6. Beauchesne PR, Chung NS, Wasan KM. Cyclosporine A: a review of current oral and intravenous delivery systems. Drug Dev Ind Pharm. 2007;33:211-220.
7. Amidon GL, Lennernas H, Shah VP, Crison JR. A theoretical basis for a biopharmaceutic drug classification: the correlation of *in vitro* drug product dissolution and *in vivo* bioavailability. Pharm Res. 1995;12:413-420.
8. Gülbağ Pınar S, Çelebi N. Optimization and evaluation of cyclosporine A nanosuspension stabilized by combination stabilizers using high pressure homogenization method. J Res Pharm. 2019;23:1009-1021.
9. Kobayashi M, Kondo K, Nakashima C, Kida Y, Niwa T. Design of self-dispersible microsponge containing cyclosporine through wet milling and drop freeze-drying processes to improve dissolution behavior. J Drug Deliv Sci Technol. 2020;57:101577.
10. Gao L, Zhang D, Chen M. Drug nanocrystals for the formulation of poorly soluble drugs and its application as a potential drug delivery system. J Nanopart Res. 2008;10:845-862.
11. Zhang H, Chen W, Zhao Z, Dong Q, Yin L, Zhou J, Ding Y. Lyophilized nanosuspensions for oral bioavailability ımprovement of ınsoluble drugs: preparation, characterization, and pharmacokinetic studies. J Pharm Innov. 2017;12:271-280.
12. Guan W, Ma Y, Ding S, Liu Y, Song Z, Liu X, Tang L, Wang Y. The technology for improving stability of nanosuspensions in drug delivery. J Nanopart Res. 2022;24:14.
13. Mauludin R, Müller RH, Keck CM. Kinetic solubility and dissolution velocity of rutin nanocrystals. Eur J Pharm Sci. 2009;36:502-510.
14. Medarevic D, Djuris J, Ibric S, Mitric M, Kachrimanis K. Optimization of formulation and process parameters for the production of carvedilol nanosuspension by wet media milling. Int J Pharm. 2018;540:150-161.
15. Pu X, Sun J, Han J, Lian H, Zhang P, Yan Z, He Z. Nanosuspensions of 10-hydroxycamptothecin that can maintain high and extended supersaturation to enhance oral absorption: preparation, characterization and *in vitro/in vivo* evaluation. J Nanopart Res. 2013;15:2043.
16. Jahangir MA, Imam SS, Muheem A, Chettupalli A, Al-Abbasi FA, Nadeem MS, Kazmi I, Afzal M, Alshehri S. Nanocrystals: characterization overview, applications in drug delivery, and their toxicity concerns. J Pharm Innov. 2022;17:237-248.
17. Yadav KS, Kale K. High pressure homogenizer in Pharmaceuticals: understanding ıts critical processing parameters and applications. J Pharm Innov. 2020;15:690-701.
18. Gülbağ Pınar S, Canpınar H, Tan C, Celebi N. A new nanosuspension prepared with wet milling method for oral delivery of highly variable drug Cyclosporine A: development, optimization and in vivo evaluation. Eur J Pharm Sci. 2022;171:106123.
19. Gülbağ Pınar S, Pezik E, Mutlu Ağardan N, Celebi N. Development of cyclosporine A nanosuspension: cytotoxicity and permeability on Caco-2 cell lines. Pharm Dev Technol. 2021;27:52-62.
20. Liu Q, Mai Y, Gu X, Zhao Y, Di X, Ma X, Yang J. A wet-milling method for the preparation of cilnidipine nanosuspension with enhanced dissolution and oral bioavailability. J Drug Deliv Sci Technol. 2020;55:101371.
21. Koradia KD, Sheth NR, Koradia HD, Dabhi MR. Ziprasidone nanocrystals by wet media milling followed by spray drying and lyophilization: Formulation and process parameter optimization. J Drug Deliv Sci Technol. 2018;43:73-84.

22. Gulsun T, Borna SE, Vural I, Sahin S. Preparation and characterization of furosemide nanosuspensions. J Drug Deliv Sci Technol. 2018;45:93-100.

23. Karakucuk A, Celebi N, Teksin ZS. Preparation of ritonavir nanosuspensions by microfluidization using polymeric stabilizers: I. A Design of Experiment approach. Eur J Pharm Sci. 2016;95:111-121.

24. Karakucuk A, Teksin ZS, Eroglu H, Celebi N. Evaluation of improved oral bioavailability of ritonavir nanosuspension. Eur J Pharm Sci. 2019;131:153-158.

25. Oktay AN, Karakucuk A, Ilbasmis-Tamer S, Celebi N. Dermal flurbiprofen nanosuspensions: Optimization with design of experiment approach and in vitro evaluation. Eur J Pharm Sci. 2018;12:254-263.

26. Tashan E, Karakucuk A, Celebi N. Optimization and *in vitro* evaluation of ziprasidone nanosuspensions produced by a top-down approach. J Drug Deliv Sci Technol. 2019;52:37-45.

27. George M, Ghosh I. Identifying the correlation between drug/stabilizer properties and critical quality attributes (CQAs) of nanosuspension formulation prepared by wet media milling technology. Eur J Pharm Sci. 2013;48:142-152.

28. He J, Han Y, Xu G, Yin L, Ngandeu Neubi M, Zhou J, Ding Y. Preparation and evaluation of celecoxib nanosuspensions for bioavailability enhancement. RSC Adv. 2017;7:13053-13064.

29. Malamatari M, Taylor KMG, Malamataris S, Douroumis D, Kachrimanis K. Pharmaceutical nanocrystals: production by wet milling and applications. Drug Discov Today. 2018;23:534-547.

30. Politis SN, Colombo P, Colombo G, Rekkas DM. Design of experiments (DoE) in pharmaceutical development. Drug Dev Ind Pharm. 2017;43:889-901.

31. Xu X, Gupta A, Faustino P, Sathe PM, Sayeed VA, Khan MA. Development and validation of a HPLC method for dissolution and stability assay of liquid-filled cyclosporine capsule drug products. AAPS PharmSciTech. 2013;14:959-967.

32. Lestari MLAD, Müller RH, Möschwitzer JP. Systematic screening of different surface modifiers for the production of physically stable nanosuspensions. J Pharm Sci. 2015;104:1128-1140.

33. Bose S, Schenck D, Ghosh I, Hollywood A, Maulit E, Ruegger C. Application of spray granulation for conversion of a nanosuspension into a dry powder form. Eur J Pharm Sci. 2012;47:35-43.

34. Sun W, Ni R, Zhang X, Li LC, Mao S. Spray drying of a poorly water-soluble drug nanosuspension for tablet preparation: formulation and process optimization with bioavailability evaluation. Drug Dev Ind Pharm. 2015;41:927-933.

35. Wang Y, Li X, Wang L, Xu Y, Cheng X, Wei P. Formulation and pharmacokinetic evaluation of a paclitaxel nanosuspension for intravenous delivery. Int J Nanomed. 2011;6:1497-1507.

36. Iyama Y, Mineda M, Sei S, Hirasawa W, Matahira Y, Seto Y, Sato H, Onoue S. Cyclosporine a-loaded UniORV(R): Pharmacokinetic and safety characterization. Int J Pharm. 2019;570:118630.

37. Yamasaki K, Kwok PC, Fukushige K, Prud'homme RK, Chan HK. Enhanced dissolution of inhalable cyclosporine nano-matrix particles with mannitol as matrix former. Int J Pharm. 2011;420:34-42.

38. Kanaujia P, Poovizhi P, Ng WK, Tan RBH. Amorphous formulations for dissolution and bioavailability enhancement of poorly soluble APIs. Powder Technol. 2015;285:2-15.

39. Bertacche V, Pini E, Stradi R, Stratta F. Quantitative determination of amorphous cyclosporine in crystalline cyclosporine samples by Fourier transform infrared spectroscopy. J Pharm Sci. 2006;95:159-166.

40. Attari Z, Bhandari A, Jagadish PC, Lewis S. Enhanced ex vivo intestinal absorption of olmesartan medoxomil nanosuspension: Preparation by combinative technology. Saudi Pharm J. 2016;24:57-63.

41. Wang Y, Zheng Y, Zhang L, Wang Q, Zhang D. Stability of nanosuspensions in drug delivery. J Control Release. 2013;172:1126-1141.

42. Müller RH, Gohla S, Keck CM. State of the art of nanocrystals - special features, production, nanotoxicology aspects and intracellular delivery. Eur J Pharm Biopharm. 2011;78:1-9.

43. Huang S, Zhang Q, Li H, Sun Y, Cheng G, Zou M, Piao H. Increased bioavailability of efonidipine hydrochloride nanosuspensions by the wet-milling method. Eur J Pharm Biopharm. 2018;130:108-114.

44. Li W, Quan P, Zhang Y, Cheng J, Liu J, Cun D, Xiang R, Fang L. Influence of drug physicochemical properties on absorption of water insoluble drug nanosuspensions. Int J Pharm. 2014;460:13-23.

45. Roos C, Dahlgren D, Sjögren E, Sjöblom M, Hedeland M, Lennernäs H. Jejunal absorption of aprepitant from nanosuspensions: Role of particle size, prandial state and mucus layer. Eur J Pharm Biopharm. 2018;132:222-230.

Turk J Pharm Sci 2024;21(5):440-448
DOI: 10.4274/tjps.galenos.2023.37807

ORIGINAL ARTICLE

Formulation and Evaluation of Triamcinolone Acetonide-Loaded Oral Disintegrated Film with Different Polymers *via* Solvent Casting Method

Özlem ÇOBAN[1]*, Kutsal ÖZCAN[1], Seçkin ENGİN[2], Buse TATAR[3], Mihriban SOYLU[3]

[1]Karadeniz Technical University Faculty of Pharmacy, Department of Pharmaceutical Technology, Trabzon, Türkiye
[2]Karadeniz Technical University Faculty of Pharmacy, Department of Pharmacology, Trabzon, Türkiye
[3]Karadeniz Technical University Faculty of Pharmacy, Trabzon, Türkiye

ABSTRACT

Objectives: The study aimed to investigate the effect of different polymers and plasticizers on oral disintegrating films (ODFs) containing triamcinolone acetonide (TA), a glucocorticosteroid indicated for the treatment of oral wounds.

Materials and Methods: Thirteen different formulations with the same amount of polymer and plasticizer were prepared by solvent casting. Briefly, the solutions containing polymer, plasticizer, and other ingredients were poured into Petri dishes and kept at room temperature for 20 hours to obtain ODFs. Physical properties of ODFs such as visual appearance, weight and thickness uniformity, pH, mechanical durability (tensile strength, elongation at break and folded insurance), and disintegration time were assessed and drug content analysis was performed on ODFs.

Results: Suitable ODFs were produced with hydroxypropyl methylcellulose (HPMC), polyvinyl alcohol, carboxymethylcellulose, gelatin, and pectin, while film integrity was not achieved with polyethyleneglycol 4000 (PEG 4000), chitosan and starch. Glycerin made ODFs more transparent, reduced their thickness, and improved their mechanical properties. On the other hand, PEG 400 reduced the weight variation. Regarding drug content, PEG-containing gelatin-based ODF (ODF10) and pectin-based ODF (ODF12) complied with pharmacopeial limits. In addition, all ODFs except HPMC-based ODFs had an appropriate pH range.

Conclusion: When all features were evaluated together in terms of the applicability of an ODF to the patient, the most convenient formulation was found to be gelatin-based with PEG 400 ODF (ODF10). In short, patients will benefit from ease of application and transportation and effective therapy with correct dosing with the development of ODF forms of TA for which there are no preparations except for cream, gel, and pomade forms for topical use in Türkiye.

Keywords: Triamcinolone acetonide, oral disintegrating films, solvent casting method, PEG 400, glycerin

INTRODUCTION

Oral mucositis is an acute ulceration and inflammation of the oral mucosa caused by various factors, such as cancer, infectious diseases, immunologic diseases, and trauma lesions.[1,2] It occurs in 20-100% of patients with cancer, depending on the dose of chemotherapeutics received, and significantly reduces the patient's quality of life as it causes pain, bleeding, ulcers, and difficulty in eating, drinking, and even speaking. Although many different approaches, such as zinc, aloe vera, and amifostine, have been used to treat oral mucositis, progress of oral mucositis can be serious enough to require hospitalization.[3]

Triamcinolone is a moderate-potency corticosteroid with a chemical structure of 9α-fluoro-11β, 16α, 17α, 21-tetrahydroxy-1, 4-pregnadiene-3, 20-dione and is used in the treatment of mouth sores.[4] Triamcinolone acetonide (TA) is a more potent derivative of triamcinolone, a synthetic glucocorticosteroid, with antiallergic, immunosuppressive, anti-inflammatory, and anti-scarring activities. TA can be administered systemically or

*Correspondence: o.coban88@gmail.com, ORCID-ID: orcid.org/0000-0003-1154-7602
Received: 10.08.2023, Accepted: 21.10.2023

topically, but its systemic use at high doses for a long time causes many adverse reactions that limit its clinical use.[5] It is indicated for the temporary relief of symptoms of oral inflammatory and ulcerative lesions and is used as mouthwashes, buccal formulations, or ointments.[6] Fast-acting products are needed to treat oral mucositis due to the painful process; furthermore, the concentration of corticosteroids in the oral mucosa must be increased by preventing systemic absorption as much as possible to treat effectively.[6,7] However, due to saliva flow and mechanical effects, the contact time of mouthwashes with the oral mucosa and their action time are short.[8]

Buccal formulations may decrease patient comfort due to their large size and prolonged stay in the oral cavity. In ointments, on the other hand, the active substance may be released from the dosage form during storage, and its efficacy may decrease because the drug is administered at insufficient doses. It can also be separated easily from the drug administration site during speaking and by salivation, which may lead to treatment failure.[6] In addition, TA has been shown to have low chemical stability in ointment forms.[9] Orally disintegrating films (ODFs) are a novel drug delivery system in which a stable solid film form is quickly disintegrated and absorbed in contact with saliva in the oral cavity. Therefore, ODFs containing TA may be a therapeutic option because of dispersing quickly due to their large surface areas along with its rapid onset of action. They exhibit high stability due to their solid form. Packing is also easier because they are not fragile, unlike orally disintegrating tablets.[10,11] Additionally, ODFs allow easy and safe application, especially in pediatric, geriatric, and dysphasia patients. These systems can be applied without water, which is very important when there is no access to water.[12,13]

ODFs have been prepared using various methods, including solvent casting, hot-melt extrusion, semisolid casting, solid dispersion extrusion, rolling, solvent spraying, and new technologies (Soluleaves™, XGel™, Wafertab™, etc.).[13,14] Among them, solvent casting is a highly preferred method with high reproducibility, a simple procedure, and no equipment requirement. Using organic solvents is one of the limitations of solvent casting, which can be eliminated by using distilled water (DW).[10,15] In the formulation of ODFs, water-soluble polymers are usually used to ensure rapid oral disintegration and makeup at least 45% of the film weight. They also contain plasticizers (increase film flexibility), saliva stimulants, super disintegrants, and surfactants (facilitate film disintegration), sweeteners and flavorings (better taste), and coloring agents in certain proportions to give the formulation various properties.[10,11] The polymers used may have natural or synthetic structures. Natural polymers include pectin, pullulan, maltodextrin, sodium alginate, sodium starch glycolate and gelatin; synthetic polymers include cellulose derivatives [hydroxypropyl methylcellulose (HPMC), carboxymethylcellulose (CMC), methylcellulose], vinyl polymers [polyvinylpyrrolidone, polyvinyl alcohol (PVA) and polyethylene oxide (PEO)], and acrylic polymers (Eudragit) are widely used.[10]

The purpose of this study was to compare TA-loaded ODFs prepared using different polymers (synthetic or natural) and plasticizers, which are frequently preferred in the preparation of ODFs, in terms of organoleptic properties, weight and thickness variation, mechanical strength, pH, disintegrating time, and drug amount. ODFs were prepared using the solvent casting method. Several characterization studies were conducted on TA-loaded ODFs for comparative evaluations.

MATERIALS AND METHODS

Materials

Materials used for the preparation of the formulation: HPMC (ShinEtsu, Japan), PVA (85-124 kDa, 99% + hydrolyzed, Sigma, USA), polyethyleneglycol 4000 (PEG 4000) (Merck, USA), CMC (Doğa İlaç, Türkiye), chitosan (190-375 kDa, Sigma, USA), starch (Yasin Teknik, Türkiye), gelatin (Doğa İlaç, Türkiye), pectin (Doğa İlaç, Türkiye), PEG 400 (Merck, Germany), glycerin (99.5%, Farma Kalite, Türkiye), monopotassium phosphate (KH_2PO_4, ≥ 99.5%, Isolab, Germany), disodium phosphate dihydrate ($Na_2HPO_4.2H_2O$, Merck, Germany), sodium chloride (NaCl, ≥ 99.5%, Merck, Denmark), phosphoric acid (Sigma, USA), citric acid (anhydrous) (› 99.5%, Tekkim Kimya, Türkiye), sodium saccharin (Na-saccharin, ≥ 98%, Sigma, USA), vanillin (≥ 99%, Merck, Germany), ethanol (absolute) (EtOH; ≥ 99.9%, Isolab, Germany). DW was obtained using a Millipore Milli-Q ultrapure water system in the laboratory.

TA-loaded ODFs

Eight different polymers were used to prepare the TA-loaded ODFs. Four of them were HPMC, PVA, PEG 4000, and CMC as the synthetic polymers, and the others were chitosan, starch, gelatin, and pectin as natural polymers. Furthermore, two different plasticizers (PEG 400 and glycerin) were selected to evaluate their effectiveness on the properties of ODFs. The active substance (TA) and excipients used in the formulations and their amounts are given in Table 1. The ODF preparation process for HMPC, PEG 4000, CMC, and gelatin, which are easily water-soluble polymers, was briefly described as follows: The polymer (0.68 g) was added part by part onto 20 mL of DW on a magnetic stirrer (Heidolph Instruments, Germany), and mixing was continued until it was completely dissolved at room temperature. The citric acid (0.05 g) as a saliva stimulant, Na-saccharin (0.05 g) as a sweetener, PEG 400 or glycerin (0.2 g) as a plasticizer for film flexibility, and vanillin (0.01 g) as a flavor were added to the polymer solution. Since TA is not water-soluble, 0.01 g of TA was first dissolved in 1 mL EtOH using bath sonication (Weightlab Instruments, Türkiye), followed by its addition to the polymer mixture.

The amounts of TA and excipients were kept constant in all formulations (Table 1). However, the preparation method had to be modified for PVA, chitosan, starch, which are not freely water-soluble polymers, and pectin. For example, PVA dissolves in hot water. Therefore, for the PVA-based ODFs, PVA was added to 20 mL of DW, heated to about 100-120 °C,

Table 1. Formulation of the TA-loaded ODFs

Formulations	Quantity in 20 mL dw (g)	ODF1	ODF2	ODF3	ODF4	ODF5	ODF6	ODF7	ODF8	ODF9	ODF10	ODF11	ODF12	ODF13
Polymer	0.68													
HPMC	Synthetic	+	+											
PVA	Synthetic			+	+									
PEG 4000	Synthetic					+								
CMC	Synthetic						+	+						
Chitosan	Natural								+					
Starch	Natural									+				
Gelatin	Natural										+	+		
Pectin	Natural												+	+
Plasticizer	0.2													
PEG 400		+		+		+	+		+	+	+		+	
Glycerin			+		+			+				+		+
Citric acid	0.05	+	+	+	+	+	+	+	+	+	+	+	+	+
Na-saccharin	0.05	+	+	+	+	+	+	+	+	+	+	+	+	+
Vanillin	0.01	+	+	+	+	+	+	+	+	+	+	+	+	+
Triamcinolone acetonide	0.01	+	+	+	+	+	+	+	+	+	+	+	+	+

ODF: Oral disintegrating film, HPMC: Hydroxypropyl methylcellulose, PVA: Polyvinyl alcohol, PEG 4000: Polyethylene glycol 4000, CMC: Carboxymethylcellulose, PEG 400: Polyethylene glycol 400, Na-saccharin: Sodium saccharin, Dw: Distilled water

and stirred vigorously until all the PVA had dissolved. After cooling to room temperature, the volume was increased to 20 mL with DW. Excipients (citric acid, Na-saccharin, PEG 400 or glycerin, vanillin) and then 1 mL ethanolic solution of TA were added to the PVA solution at room temperature, as mentioned above.

For chitosan-based ODFs, since chitosan dissolves in an acidic environment, citric acid was first dissolved in DW, and then chitosan in parts was added to this solution under a magnetic stirrer at room temperature. Subsequently, Na-saccharin, PEG 400 or glycerin, and vanillin were added to the polymer solution, respectively, and mixing continued. Finally, 1 mL of the TA solution in ethanol was added to the solution.

For starch-based ODFs, a plasticizer (PEG 400 or glycerin) was first added to the DW under a magnetic stirrer to decrease the phase-transition temperature of the starch and protect it from temperature-related degradation.[16]

Starch was added to this solution and mixed for 30 minutes to disperse it. Afterwards, the temperature was turned on and the mixture was mixed at 80 °C for 30 minutes to gel. After cooling to room temperature, the volume was increased to 20 mL with DW. Citric acid, Na-saccharin, and vanillin were added to the polymer solutions, and the mixing was continued. Finally, 1 mL of the TA solution in ethanol was added to the solution.

For pectin-based ODFs, pectin was added to 20 mL of DW and left at room temperature for one day without mixing to prevent bubble formation. The next day, citric acid, Na-saccharin, PEG 400 or glycerin, and vanillin were added to the polymer solution under gentle stirring with a glass rod. Subsequently, 1 mL of TA solution in ethanol was added to the solution.

Each final polymer solution containing TA, prepared as mentioned above, was mixed under a magnetic stirrer for 10 minutes, and then it was rested outside for a further 10 minutes without mixing to remove the formed bubbles. After that, it was poured into a 10 cm Petri dish. Petri dishes wrapped in aluminum foil with holes punched on them were placed in a fume hood (second-degree) and left to dry for 20 hours at room temperature.

Characterization of TA-loaded ODFs

Film-forming capacity and physical appearance

The film-forming capacity is the ability of a polymer to form films that can be separated

from the surface on which they are cast. The films were characterized as easy-moderate-difficult-very difficult depending on the difficulty level of getting out of the mold. The film's appearance was evaluated by visual observation. The parameters like homogeneity and transparent/blurry images of the films were evaluated.[17]

Weight and thickness variation

After the prepared ODFs were cut into 2 x 2 cm^2 dimensions, the weight and thickness of 3 samples for each formulation were measured with an analytical balance (Ohaus Corporation, USA) and a caliper, respectively.

Mechanical strength

Two different methods (folding endurance and tensile strength) were used to determine the mechanical strength of the films. For folding endurance, the prepared ODFs were cut in 2 x 2 cm^2 dimensions and folded manually on top of each other from the same place. The number before the fold number at which the first break occurs was accepted as the fragility parameter.[14] In the tensile strength analysis, a TA-XT Plus Texture Analyzer (Stable Micro Systems, UK) equipped with a 5 kg load cell in TPA mode was used. Films with dimensions of 1 x 3 cm^2 were held between two clamps of the TA-XT probe positioned at a distance of 1 cm. The lower clamp was held stationary, and the ODF strips were stretched by the upper clamp at a rate of 1 mm/s until the strip tore. The tensile work performed during this process and the tensile deformation/elongation of the film at the moment of tearing were measured.[18]

pH analysis

2 x 2 cm^2 cut films were added to 2 mL of artificial saliva. After they were completely dissolved, their pH was measured using a digital pH meter (Ohaus Starter 3000, USA).[14] Three samples were tested for each formulation. Films containing only PVA had to be heated at high temperatures to dissolve after expulsion into the salivary fluid.

Disintegrating time

There are no official guidelines for determining the degradation time of ODFs. 2 x 2 cm^2 cut films were placed in 10 mL of artificial saliva at 37 °C, and the stirring rate was set to 100 rpm. The time taken for complete film disintegration was determined using a stopwatch.[19] Three samples were tested for each formulation.

Drug content

A certain amount of TA was weighed on an analytical balance and dissolved in EtOH. After sonication, the same volume of DW as EtOH was added to this solution to prepare a stock solution. Calibration samples were prepared at concentrations of 1000, 800, 400, 200, 100, and 50 µg/mL using the stock solution. Dilutions were made using an EtOH: DW mixture (1:1 *v/v*). Spectrum scanning was performed in the 200-800 nm range using an ultraviolet-visible (UV-Vis) spectrophotometer (Thermo Scientific Multiskan G0, USA), and the maximum absorbance was observed at 286 nm. 20 mL of DW was added to the films cut in 2 x 2 cm^2 size, and their weights were measured. The films were homogenized *via* Ultraturrax (Heidolph Instruments, Germany) at 15,000 rpm for 5 minutes in an ice bath. A certain volume of the samples obtained as a result of this process was taken, and the same volume of EtOH was added to it. After filtering through a 0.45 µm filter, absorbance was measured at 286 nm wavelength using a UV-Vis spectrophotometer. Measurements were performed in triplicate for each formulation.

Statistical analysis

Data were presented as mean ± standard deviation (SD) and analyzed using GraphPad Prism Version 5.0 (GraphPad Software Inc., USA). Statistical analyses were performed using Student's t-test or One-Way analysis of variance followed by Tukey's test, as appropriate.

RESULTS

The results of the film-forming capacity and physical appearance are listed in Table 2. Among the formulations in which the film can be removed from the Petri dish; HPMC (ODF1), PVA (ODF3), CMC (ODF6), and gelatin (ODF10) formulations prepared with PEG 400 had homogeneous, semi-transparent, easy-to-remove properties (Figures 1a, c, e, and 2a), while HPMC (ODF2), PVA (ODF4), CMC (ODF7), and pectin (ODF13) formulations prepared

Table 2. Results of the film-forming capacity, physical appearance analysis and total score of ODF formulations

Formulations	Film-forming capacity	Physical appearance	Total score
ODF1	Easy to remove from the mold	Homogeneous, semi-transparent	++++
ODF2	Easy to remove from the mold	Homogeneous, transparent	+++++
ODF3	Easy to remove from the mold	Homogeneous, semi-transparent	++++
ODF4	Easy to remove from the mold	Homogeneous, transparent	+++++
ODF5	Do not remove from the mold	Homogeneous, semi-transparent, sticky	+
ODF6	Easy to remove from the mold	Homogeneous, semi-transparent	++++
ODF7	Easy to remove from the mold	Homogeneous, transparent	+++++
ODF8	No film formation was observed.		
ODF9	Very difficult to remove from the mold	Non-homogeneous, non-transparent, fragmentary, brittle	+

Table 2. Continued

Formulations	Film-forming capacity	Physical appearance	Total score
ODF10	Easy to remove from the mold	Homogeneous, semi-transparent	++++
ODF11	Difficult to remove from the mold	Homogeneous, transparent, fragmented	++
ODF12	Easy to remove from the mold	Homogeneous, transparent but bubble view	+++
ODF13	Easy to remove from the mold	Homogeneous, transparent	+++++

ODF: Oral disintegrating film, +++++: Very good, ++++: Good, +++: Average, ++: Poor, +: Very poor

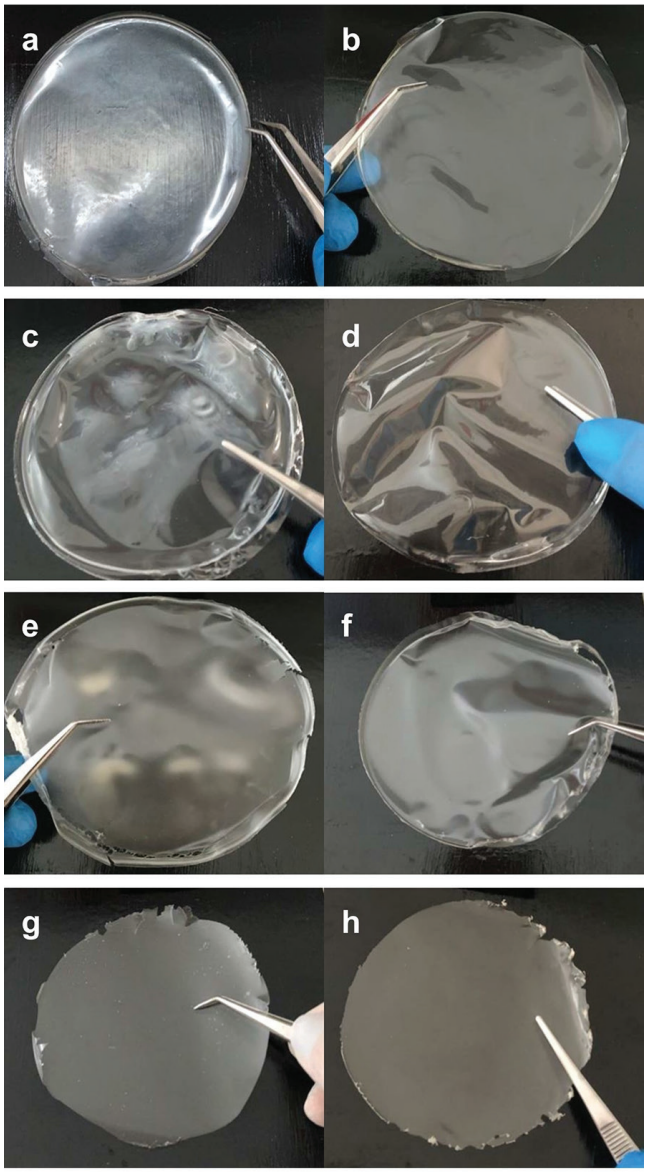

Figure 1. Images of HPMC formulation prepared with PEG 400 (ODF1) (a) and glycerin (ODF2) (b); PVA formulation prepared with PEG 400 (ODF3) (c) and glycerin (ODF4) (d); CMC formulation prepared with PEG 400 (ODF6) (e) and glycerin (ODF7) (f); pectin formulation prepared with PEG 400 (ODF12) (g) and glycerin (ODF13) (h)

HPMC: Hydroxypropylmethyl cellulose, PEG 400: Polyethylene glycol 400, ODF: Oral disintegrating film, PVA: Polyvinyl alcohol, CMC: Carboxymethylcellulose

with glycerin exhibited homogeneous, transparent, and easy-to-remove properties (Figure 1b, d, f, h). Films containing pectin plus PEG 400 (ODF12) exhibited a homogeneous and transparent appearance, were easily demolded, and contained bubbles (Figure 1g). On the other hand, ODF11 films prepared with gelatin and glycerin exhibit homogeneous and transparent properties; however, they break up when removed from the mold (Figure 2b). Finally, no film formation was observed in the formulation in which PEG 4000 (ODF5) or chitosan (ODF8) were used as the polymer, and PEG 400 was used as the plasticizer (Figure 3a, b). In addition, although starch formulations prepared with PEG 400 (ODF9) can be removed from the mold, it cannot be asserted that a film has been formed (Figure 3c).

The values obtained as a function of weight, thickness, folding endurance, tensile strength, pH, *in vitro* disintegration time, and drug content of ODFs prepared using different polymers and plasticizers are shown in Table 3. The weights of the ODFs ranged from 28.6 ± 3.2 mg to 75.6 ± 4.0 mg, and the highest film weight was obtained using HPMC plus PEG 400 film (ODF1). The general trend in films other than those prepared with CMC is that lower-weight films are formed when glycerin is used as a plasticizer. In the ODFs with glycerin as the plasticizer, the film thickness was similar to or lower than that of PEG 400. When the mechanical properties were examined, the films with HPMC exhibited low mechanical strength. The pH values of the ODFs differed between 4.02 ± 0.18 and 6.11 ± 0.06. Only four ODFs (ODF1, ODF2, ODF7 and ODF10) dispersed within 5 minutes, and the shortest disintegration time was observed in the ODF1 formulation containing HPMC plus PEG 400, with a value of 59.43 ± 15.12 s. Although the formulations prepared with PVA

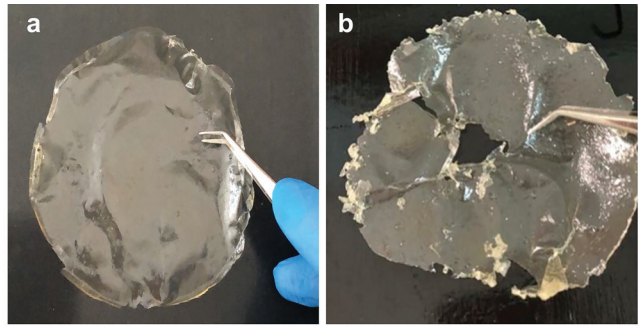

Figure 2. Images of gelatin formulations prepared with PEG 400 (ODF10) (a) and glycerin (ODF11) (b)

PEG 400: Polyethylene glycol 400, ODF: Oral disintegrating film

were kept for more than five minutes, no disintegration was observed, and the film remained intact (data not shown). In addition, ODFs exhibited high drug loading capacity overall; only ODFs with PVA had the lowest drug content with 58.8 ± 2.1% and 51.0 ± 1.0% (Table 3).

DISCUSSION

ODF formulations have several advantages, such as an effective therapeutic response that can be achieved as a result of the active substance being released in a shorter time and improved patient compliance. In this regard, ODFs are expected to have a suitable appearance, sufficient mechanical strength, short disintegration time, and high drug content.[15,20] In the present study, we found that PEG 4000, chitosan or starch-containing fomulates did not form films. On the contrary, easily demoldable films with a homogeneous appearance were obtained when HPMC, PVA, CMC, gelatin, and pectin were used as polymers. Furthermore, more transparent films were produced when glycerin was used as the plasticizer, which is similar to the results presented by Okonogi et al.[21] (Table 2). PEG has been mentioned as a polymer that can be used in ODFs in the literature; however, its high molecular weight version, PEO, has been used rather than PEG.[22] Similarly, there are ODFs prepared with chitosan and starch in the literature; however, the amounts of the polymers and the contents of the formulations used are quite different from those in our study.[23-25] In addition, polymers and plasticizers were compared in this study, and polymers were used at a fixed ratio; thus, film formation was not observed due to insufficient solubility at the concentration determined for chitosan and starch.

In this study, ODFs with glycerin generally had a lower average film weight than those with PEG 400; however, the difference was not significant ($p > 0.05$), except for PVA-based ODFs ($p < 0.001$). On the other hand, CMC-based ODFs did not show a

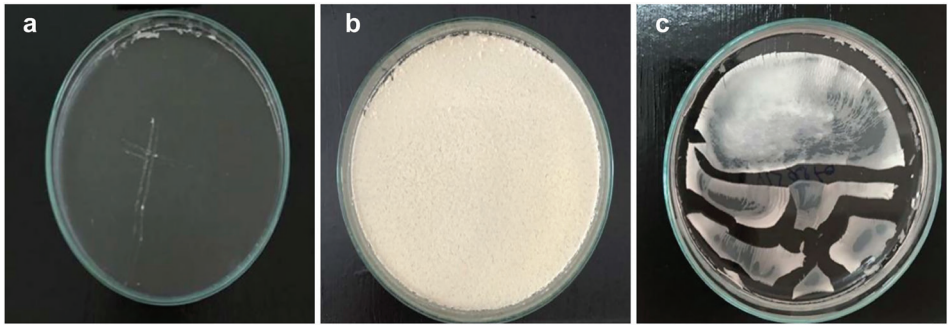

Figure 3. Images of PEG 4000 (ODF5) (a), chitosan (ODF8) (b) and starch (ODF9) (c) formulation prepared with PEG 400
PEG 4000: Polyethylene glycol 4000, ODF: Oral disintegrating film, PEG 400: Polyethylene glycol 400

Table 3. Characterization analysis results in terms of weight variation, thickness variation, mechanical strength, pH, disintegration time, and drug content of ODF formulations

Formulations	Weight (mg ± SD)	Thickness (mm ± SD)	Tensile strength (mPa)	Elongation at break (%)	Folding endurance	pH ± SD	Disintegration time (s ± SD)	Drug content (% ± SD)
ODF1	75.6 ± 4.0	0.33 ± 0.03	4.62 ± 1.01	11.31 ± 4.70	40 ± 18	4.08 ± 0.08	59.43 ± 15.12	115.6 ± 0.5
ODF2	65.3 ± 6.4	0.23 ± 0.03	8.76 ± 1.33	17.91 ± 3.47	73 ± 22	4.02 ± 0.18	147.68 ± 51.9	115.2 ± 0.2
ODF3	68.3 ± 5.5	0.35 ± 0.09	25.66 ± 5.71	276.74 ± 37.13	> 300	4.92 ± 0.19	**	58.8 ± 2.1
ODF4	32.0 ± 4.4	0.20 ± 0.00	4.44 ± 0.48	342.00 ± 185.76	> 300	6.11 ± 0.06	**	51.0 ± 1.0
ODF5*	-	-	-	-	-	-	-	-
ODF6	39.0 ± 1.0	0.23 ± 0.03	6.76 ± 0.60	18.50 ± 3.08	> 300	5.13 ± 0.14	≥ 300	74.3 ± 0.3
ODF7	46.6 ± 6.7	0.22 ± 0.03	5.68 ± 1.14	67.73 ± 25.51	> 300	5.06 ± 0.05	271.6 ± 4.04	78.3 ± 3.3
ODF8*	-	-	-	-	-	-	-	-
ODF9*	-	-	-	-	-	-	-	-
ODF10	63.3 ± 4.2	0.33 ± 0.03	10.38 ± 5.19	8.35 ± 6.39	> 300	4.84 ± 0.10	121.71 ± 21.16	109.8 ± 0.3
ODF11	53.0 ± 3.6	0.26 ± 0.03	2.46 ± 0.23	46.91 ± 15.02	> 300	4.65 ± 0.17	≥ 300	63.8 ± 1.0
ODF12	32.0 ± 1.7	0.20 ± 0.00	11.20 ± 1.25	27.62 ± 5.59	> 300	5.53 ± 0.09	≥ 300	85.6 ± 0.7
ODF13	28.6 ± 3.2	0.20 ± 0.00	4.52 ± 0.40	41.06 ± 9.74	> 300	5.98 ± 0.11	≥ 300	77.4 ± 0.3

*Analysis results are not available as they could not be removed from the mold. **Analysis results were not measured. SD: Standard deviation, ODF: Oral disintegrating film

trend like the other films. The slightly higher average weight obtained in CMC-based ODFs containing glycerin ($p > 0.05$) may be because glycerin films retained more water.[26]

It was concluded that PEG 400 improved the weight variation of ODFs, including HPMC, CMC or pectin, with lower SD values observed (Table 2). Moreover, ODFs with HPMC had significantly higher weights even though they contained the same amount of polymer (ns vs. ODF3, ODF10, and ODF11; $p < 0.01$ vs ODF7; $p < 0.001$ vs. ODF4, ODF6, ODF12, and ODF13). The differences between the weights of ODFs may be related to the viscosity of the polymers used, such that the weight of the ODF may increase as the viscosity of the polymer increases.[27]

Since dose accuracy is directly related to film thickness, it is important to ensure uniform film thickness. Considering that an ideal ODF should exhibit a thickness between 0.05 and 1 mm, the thickness of all ODFs prepared in our study (0.20 ± 0.00 mm to 0.35 ± 0.09 mm) was within these limits. However, the thickness of the ODFs containing glycerin was lower than that of the other formulations, including PEG 400, which is similar to other studies.[23,28,29] The difference between the thickness values of PEG 400 and glycerin was not significant ($p > 0.05$), except for the PVA-based ODFs ($p < 0.01$). For ODFs containing HPMC, PVA, pectin, or gelatin, a linear relationship between the weight and thickness of the films was observed, as expected.[30]

ODFs are expected to have sufficient tensile strength, high elongation at break, and good folding endurance to demonstrate the desired flexibility and stretchability during transportation, handling, and application. However, an excessively high tensile strength is undesirable as it delays drug release from the ODF.[28,31] There is no limit value for the tensile strength and elongation at break, whereas formulations with folding endurance exceeding 300 are considered durable and flexible.[31] In line with the data in the literature, the ODFs had tensile strength values from 2.46 ± 0.2 Mpa to 25.66 ± 5.71 Mpa and elongation at break values from 8.35 ± 6.39% to 342.00 ± 185.76% (Table 3).[28,32] One of the factors affecting the durability of ODFs is the type and amount of plasticizer in the formulation. In our study, two different plasticizers (PEG 400 and glycerin) were used in fixed amounts. In all ODFs except HPMC, glycerin slightly decreased the tensile strength compared with PEG ($p > 0.05$), however; the effect of glycerin on the tensile strength was more prominent in PVA-based ODFs ($p < 0.001$). In addition, according to the elongation at break values, glycerin gave more elasticity to the film than PEG 400 in all ODFs, the difference was not statistically significant ($p > 0.05$), though. Although no plasticizer effect was observed in formulations with a fold number ≥ 300, the elasticity-increasing effect of glycerin was observed in ODF1 and ODF2 formulations prepared with HPMC. Similar results have been obtained in various studies, and this effect of glycerin has been attributed to the effective insertion of its molecules into polymer chains due to its hydroxyl groups and smaller molecular size, as well as the replacement of the intermolecular bonds in the polymer matrix by hydrogen bonds formed between polymer and glycerin.[28,33] The highest tensile strength was obtained with ODF3, and the highest elongation percentage was obtained with ODF4, which may be due to the use of high molecular weight PVA, and the disintegration time results also support this situation.

The surface pH of ODFs is a crucial parameter that should be considered when predicting the stability of dosage forms and mucosal irritation. The pH values of ODFs should be close to the pH value of the oral mucosa (6.2-7.6) so that they do not irritate the oral mucosa and facilitates their administration to patients.[31] However, films developed by Visser with a surface pH of 4.5-6.5 were also found not to cause local irritation (Visser, J. C. Orodispersible films as pharmacy preparations: Let's get flexible, University of Groningen, 2017). In this respect, it was observed in this study that, except for HPMC-based ODF1 and ODF2, the other films had a suitable pH range (Table 3).

A time limit of three minutes has been reported for the *in vitro* disintegration times of ODFs.[34] The ODF1, ODF2, and ODF10 formulations were disintegrated in less than three minutes, whereas ODF1 had the minimum disintegration time (59.43 ± 15.12 s), which is in agreement with the literature.[35] Besides, PEG decreased the disintegration time of HPMC- and gelatin-based ODFs ($p < 0.05$ and $p < 0.001$, respectively). Although PVA is a water-soluble polymer, the disintegration time of films prepared with PVA (ODF3 and ODF4) was more than five minutes, which may be due to the very high molecular weight (MW) of PVA, since PVA with a 16,000 Da MW is generally used in ODF formulations and the disintegration time of these products is less than 127.36 s.[36]

According to the Pharmacopeia, the content uniformity limit is 85-115%.[37] The drug contents of the prepared ODFs varied between 115.6 ± 0.5% and 51.0 ± 1.0%. However, ODF10 and ODF12 met the criteria in terms of pharmacopeial standards (Table 3). The formulation with the highest drug content was ODF1 with 115.6 ± 0.5% (not-significant vs. ODF2; $p < 0.01$ vs. ODF10; $p < 0.001$ vs. the others), whereas the formulation with the lowest drug content was ODF4 with 51.0 ± 1.0%. The difference between these values may be due to the use of different types of polymers and plasticizers. In addition, higher drug content was observed in PEG-containing films, except for CMC-based ODFs. This effect of PEG was not significant for HPMC-based ODFs and CMC-based ODFs ($p > 0.05$), but was highly significant for the other ODFs ($p < 0.001$) and may be due to its higher solubility-enhancing effect.[38]

Study limitations

Although different polymers and plasticizers were used in the study, their amounts were kept constant. Therefore, whereas ODFs could not be obtained with some polymers, unacceptable ODF results, such as higher disintegration time and lower pH, were obtained with some polymers. Further studies are required to obtain formulations with more suitable properties that can be obtained using DoE design. In addition, the superiority of the developed formulation over the marketed product in terms of effectiveness can be evaluated by *in vitro* oral mucositis cell culture or *in vivo* animal models.

CONCLUSION

ODFs of TA, a glucocorticosteroid indicated for treating oral wounds, have been successfully developed using various polymers and plasticizers. In general, successful results were obtained with HPMC, PVA, CMC, gelatin, and pectin, whereas film integrity was not achieved with PEG 4000, chitosan, and starch. The most suitable formulations were obtained for HPMC-based ODF1 and ODF2 and gelatin-based ODF10 in terms of ease of demolding, homogeneous weight and thickness variation, high mechanical durability, suitable pH value, short disintegration time, and high drug content. However, considering that the oral flora can tolerate low values, such as pH 4.5, we conclude that ODF10 is the most appropriate formulation for assessing pH, mechanical durability, disintegration time, and drug content. To summarize, PEG-containing gelatin-based ODF-containing TA is a promising candidate for patients with oral mucositis, and the efficacy of this formulation should be evaluated in future studies.

Acknowledgements

This work was supported by a grant from The Scientific and Technological Research Council of Türkiye 2209/A University Projects Support Program (1919B012104610).

Ethics

Ethics Committee Approval: Not required.

Informed Consent: Not required.

Authorship Contributions

Concept: Ö.Ç., K.Ö., M.S., Design: Ö.Ç., K.Ö., B.T., Data Collection or Processing: Ö.Ç., K.Ö., B.T., M.S., Analysis or Interpretation: Ö.Ç., K.Ö., S.E., B.T., Literature Search: Ö.Ç., K.Ö., S.E., Writing: Ö.Ç., K.Ö., S.E.

Conflict of Interest: The authors have no conflicts of interest to declare.

Financial Disclosure: The authors declared that this study received no financial support.

REFERENCES

1. Nguyen H, Sangha S, Pan M, Shin DH, Park H, Mohammed AI, Cirillo N. Oxidative stress and chemoradiation-induced oral mucositis: a scoping review of *in vitro*, *in vivo* and clinical studies. Int J Mol Sci. 2022;23:4863.
2. Akbaş S, Karabulut E, Sutas Bozkurt AP, Aydın Ö, Düzgün Ergün D. Effects of glutamine on healing of traumatic oral mucosal lesions: an experimental study. J Acad Res Med. 2019;9:6-13.
3. Ferreira AS, Macedo C, Silva AM, Delerue-Matos C, Costa P, Rodrigues F. Natural products for the prevention and treatment of oral mucositis-a review. Int J Mol Sci. 2022;23:4385.
4. Gupta SK, Kumar B, Sharma PK. Development and validation of a spectrophotometric method for estimation of triamcinolone in solid dosage form. Asian J Pharm Ana. 2013;3:42-43.
5. Sağıroğlu AA, Özsoy Y, Özer Ö. Design, optimization, and characterization of novel topical formulations containing triamcinolone acetonide. J Drug Deliv Sci Technol. 2020;58:101594.
6. Hamishehkar H, Nokhodchi A, Ghanbarzadeh S, Kouhsoltani M. Triamcinolone acetonide oromucoadhesive paste for treatment of aphthous stomatitis. Adv Pharm Bull. 2015;5:277-282.
7. Hadjieva T, Cavallin-Ståhl E, Linden M, Tiberg F. Treatment of oral mucositis pain following radiation therapy for head-and-neck cancer using a bioadhesive barrier-forming lipid solution. Support Care Cancer. 2014;22:1557-1562.
8. Said Z, Murdoch C, Hansen J, Siim Madsen L, Colley HE. Corticosteroid delivery using oral mucosa equivalents for the treatment of inflammatory mucosal diseases. Eur J Oral Sci. 2021;129:e12761.
9. van Heugten AJ, de Vries WS, Markesteijn MM, Pieters RJ, Vromans H. The role of excipients in the stability of triamcinolone acetonide in ointments. AAPS Pharm SciTech. 2018;19:1448-1453.
10. Özakar RS, Özakar E. Current overview of oral thin films. Turk J Pharm Sci. 2021;18:111-121.
11. Mahboob MBH, Riaz T, Jamshaid M, Bashir I, Zulfiqar S. Oral films: a comprehensive review. Int Curr Pharm J. 2016;5:111-117.
12. Ekpa ED, Asuquo UR, Elijah AA, Ime SNA, Ini UA. The oral film delivery application of nanotechnology and potential in medication adherence. GSC Biol Pharm Sci. 2020;11:034-051.
13. Bala R, Pawar P, Khanna S, Arora S. Orally dissolving strips: a new approach to oral drug delivery system. Int J Pharm Investig. 2013;3:67-76.
14. Panda BP, Dey NS, Rao MEB. Development of innovative orally fast disintegrating film dosage forms: a review. IJPSN. 2012;5:1666-1674.
15. He M, Zhu L, Yang N, Li H, Yang Q. Recent advances of oral film as a platform for drug delivery. Int J Pharm. 2021;604:120759.
16. Singh GP, Bangar SP, Yang T, Trif M, Kumar V, Kumar D. Effect on the properties of edible starch-based films by the incorporation of additives: a review. Polymers (Basel). 2022;14:1987.
17. Sowjanya JN, Rao PR. Development, optimization, and invitro evaluation of novel fast-dissolving oral films (FDOFs) of Uncaria tomentosa extract to treat osteoarthritis. Heliyon. 2023;9:e14292.
18. Landová H, Vetchý D, Gajdziok J, Doležel P, Muselík J, Dvořáčková K, Jekl V, Hauptman K, Knotek Z. Evaluation of the influence of formulation and process variables on mechanical properties of oral mucoadhesive films using multivariate data analysis. Biomed Res Int. 2014;2014:179568.
19. Chandra A, Chondkar AD, Shirodkar R, Lewis SA. Rapidly dissolving lacidipine nanoparticle strips for transbuccal administration. J Drug Deliv Sci Technol. 2018;47:259-267.
20. Palezi SC, Fernandes SS, Martins VG. Oral disintegration films: applications and production methods. J Food Sci Technol. 2023;60:2539-2548.
21. Okonogi S, Khongkhunthian S, Jaturasitha S. Development of mucoadhesive buccal films from rice for pharmaceutical delivery systems. Drug Discov Ther. 2014;8:262-267.
22. Shivani NS. Polymers used in mouth dissolving formulations: a review. Indo Am J P Sci. 2022;09:400-412.
23. Ibrahim YHY, Regdon G Jr, Kristó K, Kelemen A, Adam ME, Hamedelniel EI, Sovány T. Design and characterization of chitosan/citrate films as carrier for oral macromolecule delivery. Eur J Pharm Sci. 2020;146:105270.
24. Takeuchi I, Togo C, Makino K. Rebamipide-containing film using chitosan and HPMC for oral mucositis ınduced by cancer chemotherapy. Anticancer Res. 2019;39:6531-6536.

25. Pacheco MS, Barbieri D, da Silva CF, de Moraes MA. A review on orally disintegrating films (ODFs) made from natural polymers such as pullulan, maltodextrin, starch, and others. Int J Biol Macromol. 2021;178:504-513.

26. Arik Kibar EA, Us F. Starch-cellulose ether films: microstructure and water resistance. J Food Process Eng. 2017;40:e12382.

27. Roy A, Arees R, Blr M. Formulation development of oral fast-dissolving films of rupatadine fumarate. AJPCR. 2020;13:67-72.

28. Elshafeey AH, El-Dahmy RM. Formulation and development of oral fast-dissolving films loaded with nanosuspension to augment paroxetine bioavailability: *in vitro* characterization, *ex vivo* permeation, and pharmacokinetic evaluation in healthy human volunteers. Pharmaceutics. 2021;13:1869.

29. Hamza M. Development and evaluation of orodispersible films of lamotrigine: hydroxypropyl β cyclodextrin inclusion complex. AJPS. 2017;56:31-46.

30. Junmahasathien T, Panraksa P, Protiarn P, Hormdee D, Noisombut R, Kantrong N, Jantrawut P. Preparation and evaluation of metronidazole-loaded pectin films for potentially targeting a microbial infection associated with periodontal disease. Polymers. 2018;10:1021.

31. Koland M, Sandeep VP, Charyulu NR. Fast dissolving sublingual films of ondansetron hydrochloride: effect of additives on *in vitro* drug release and mucosal permeation. J Young Pharm. 2010;2:216-222.

32. Takeuchi Y, Ikeda N, Tahara K, Takeuchi H. Mechanical characteristics of orally disintegrating films: comparison of folding endurance and tensile properties. Int J Pharm. 2020;589:119876.

33. Davoodi MN, Milani JM, Farahmandfar R. Preparation and characterization of a novel biodegradable film based on sulfated polysaccharide extracted from seaweed Ulva intestinalis. Food Sci Nutr. 2021;9:4108-4116.

34. Panraksa P, Tipduangta P, Jantanasakulwong K, Jantrawut P. Formulation of orally disintegrating films as an amorphous solid solution of a poorly water-soluble drug. Membranes. 2020;10:376.

35. Abdelbary A, Bendas ER, Ramadan AA, Mostafa DA. Pharmaceutical and pharmacokinetic evaluation of a novel fast dissolving film formulation of flupentixol dihydrochloride. AAPS Pharmscitech. 2014;15:1603-1610.

36. El-Setouhy DA, El-Malak NSA. Formulation of a novel tianeptine sodium orodispersible film. AAPS Pharmscitech. 2010;11:1018-1025.

37. Bhyan B, Jangra S, Kaur M, Singh H. Orally fast dissolving films: innovations in formulation and technology. Int J Pharm Sci Rev Res. 2011;9:9-15.

38. Nayak AK, Panigrahi PP. Solubility enhancement of etoricoxib by cosolvency approach. ISRN Org Chem. 2012;2012:1-5.

Turk J Pharm Sci 2024;21(5):449-455
DOI: 10.4274/tjps.galenos.2023.72430

ORIGINAL ARTICLE

Evaluation of a Synthetic Polyethyleneimine Based Polymeric Vector for *ING4* Gene Delivery to MCF-7 Breast Cancer Cells

Uğur KARAGÖZ[1]*, Remant Bahadur KC[2], Elif ISEL[3], Ayşe Gülten KANTARCI[3], Hasan ULUDAĞ[2]

[1]Trakya University Faculty of Pharmacy, Department of Pharmaceutical Biotechnology, Edirne, Türkiye
[2]Alberta University Faculty of Engineering, Department of Chemical and Materials Engineering, Alberta, Canada
[3]Ege University Faculty of Pharmacy, Department of Pharmaceutical Biotechnology, İzmir, Türkiye

ABSTRACT

Objectives: Breast cancer is the most common type of cancer among women and the second most common cause of death after lung cancer. The inhibitor of growth (ING) transcript levels are often suppressed in cancer cells, making it a promising candidate for cancer therapy. In this study, we aimed to formulate a polyplex that effectively carries and delivers pING4 to breast cancer cells.

Materials and Methods: Polyethyleneimine (PEI)-based non-viral vectors were synthesized and characterized for plasmid DNA delivery. Complexation was achieved *via* electrostatic interactions between the synthesized polymeric vectors and plasmid DNA. Characterization studies were conducted by testing Sodium dodecyl sulfate-induced complexation, Deoxyribonuclease I protection, and serum stability of the polyplexes. Subsequently, polyplexes were tested on MCF-7 cells for anticancer activity using the XTT cell viability assay. Western blot analysis was performed for the ING4 protein.

Results: Polyplexes carrying the *ING4* gene exhibited significantly lower cell viability than control polyplexes (p=0.0067). During the 5-day viability assay, the lowest cell viability was observed on day 4. Approximately 69.11±2.18% cell viability was observed with ING4 treatment and the control group showed no cell death on day 4 (101.53±5.06%). The prepared delivery systems did not show a toxic effect on MCF-7 cells treated alone. In addition, the MCF10A normal mammary cell line was used as a positive control. Western blotting was performed to confirm the overexpression of ING4 protein in the treatment groups. Unlike in the control groups, the overexpression of ING4 was clear in the wells of the treatment group.

Conclusion: Our findings suggest that *ING4* gene delivery using prepared PEI-based nonviral delivery systems is a promising approach for breast cancer treatment.

Keywords: *ING4*, polyethyleneimine, gene delivery, breast cancer

INTRODUCTION

Breast cancer is the most common cancer in women globally, and the number of cases is still increasing, according to the World Health Organization. In particular, patients with metastasis have a very low survival rate.[1] Currently, there are several methods exist for the treatment of breast cancer: chemotherapy, immunotherapy, hormone therapy, surgery, and radiotherapy. Surgery is the first choice, mostly because it makes sense to remove most of the tumor tissue. Chemotherapy and radiotherapy applications follow surgery for clearing remnant cancer cells.[2,3] However, treatment using these methods is not recommended. Furthermore, all of these methods have a low level of patient compliance and cause a decrease in the patients' quality of life.[3] However, advanced technology has brought novel techniques to the clinic. Gene therapy is one such therapy.

The basic definition of gene therapy is the transfer of DNA to the patient to cure diseases. Gene therapy can be used to trigger

*Correspondence: ugurkaragoz@trakya.edu.tr, ORCID-ID: orcid.org/0000-0002-3983-0410
Received: 26.07.2023, Accepted: 07.12.2023

the expression of desired proteins within cells. Viral and non-viral vectors can be used for this purpose. The physiological nature of viruses allows them to pack and efficiently deliver specific genes to target cells. To date, most gene therapy trials have been conducted using viral vectors for this reason. However, there are serious concerns regarding viral gene therapy, including immunogenicity and insertional mutagenesis. Both have a high risk of death. In addition, large-scale virus production is not very cost-effective. All of the aforementioned disadvantages can be discarded using non-viral vectors. Non-viral vectors are capable of carrying genes, protecting them from several nucleases, and delivering the genes to desired locations effectively.[4-7]

Peptides, lipids, and polymers can be used to formulate non-viral vectors. All non-viral vector types have their advantages. However, polymer-based vectors can be considered one step ahead because of their high transfection ability.[8] In addition, polymers can be synthesized desirably because they can be modified. Polyethyleneimine (PEI) has been used extensively for designing nonviral vectors.[6,7] PEI is a commercially available synthetic polymer with a repeating unit composed of the amine group and two carbons aliphatic CH_2CH_2 spacer. PEI exhibits remarkable efficacy in the formation of polyanionic complexes with plasmid DNA. Polyplex formation between PEI and pDNA occurs *via* electrostatic interactions, and PEI can protect the pDNA from nuclease degradations.[9] Moreover, PEI is recognized for its ability to induce the "proton sponge" effect owing to its robust buffering capacity under acidic pH conditions.[6] High cytotoxicity is the only major disadvantage of PEI-based vectors.[7] However, there are different types of PEI available (linear or branched, different molecular weights, *etc.*), and their toxic effects can be reduced with modifications. In recent years, advancements in non-viral gene delivery have led to a variety of methods and materials. PEI stands out as a gold standard, ensuring superior transfection efficacy due to its effective DNA binding, protection, and high endosomolytic competence, particularly through lPEI/pDNA polyplexes, which enhance DNA translocation to the nucleus and exhibit improved cell viability and transfection efficiency.[10]

The Inhibitor of Growth (ING) family genes were identified in 1996. INGs are evolutionarily conserved proteins located in the nucleus.[11] ING4 is a constituent of a tumor suppressor protein family comprising five members (ING1-5). ING4, with a molecular weight of 29 kDa, functions as a type II tumor suppressor protein and holds crucial significance as an integral member of the ING protein family. It has two Nuclear Localization Signals and is located in the cell nucleus. It exerts tumor suppressor activity by regulating angiogenesis, metastasis, invasion, cell cycle arrest, and apoptosis. Additionally, ING4 plays a role in chromatin remodeling. It contains a plant homeodomain finger motif that facilitates chromatin-mediated gene regulation.[12,13] ING4 is also linked with p53, NF-B, and HIF-1B and regulates their activities. ING4 exhibits predominant loss or downregulation at the RNA level across various cancer types. Furthermore, multiple studies reported the loss of ING4 protein expression in breast cancer.[11-17] The *ING4* gene has been used as a biomarker for breast cancer.[18] Unfortunately, the mechanism underlying the loss of the *ING4* gene remains unclear.[13] The ability of ING4 to inhibit neoangiogenesis and cell migration resulted in its label as "gatekeeper".[19] It has been reported that pING4 (a pDNA that encodes ING4 protein) can suppress tumor growth and with that exhibit prolonged survival time.[20,21]

The utilization of PEI-based polymeric vectors for plasmid DNA delivery has emerged as a pivotal advancement in gene therapy research. These vectors, owing to their cationic nature and excellent condensation properties, play a critical role in enhancing the stability and protection of DNA cargos during transportation. In the context of *ING4* gene delivery, the use of PEI-based polymeric vectors not only ensures efficient and targeted transfer of the therapeutic gene into cancer cells but also offers a promising avenue for the development of precise and potent treatments for breast cancer and other malignancies. In recent years, the exploration of innovative gene delivery strategies has become paramount in cancer research. This study focused on the delivery of the *ING4* gene to breast cancer cells through PEI-based polymeric vectors, indicating the beginning of a new phase in the creation of reliable and efficient therapeutic interventions. We aimed to formulate a polyplex that effectively carries and delivers pING4 to breast cancer cells.

MATERIALS AND METHODS

Materials

The pcDNA3-ING4 plasmid was obtained from Addgene as a bacterial stab (USA). Additionally, pcDNA3 plasmid DNA was generously provided as a gift by Prof. Dr. Zeki Topçu from the Pharmaceutical Biotechnology Department, Faculty of Pharmacy, Ege University, İzmir, Türkiye. Both plasmids were expanded and purified using an Invitrogen maxipen DNA proliferation kit (USA). For the cell-based experiments, Dulbecco's Modified Eagle's Medium (DMEM) F12 medium, fetal bovine serum (FBS), and XTT cell proliferation kits were obtained from Biological Industries (USA). Phosphate buffered saline (PBS) tablets were purchased from Sigma-Aldrich (USA). RIPA Lysis and Extraction Buffer were obtained from ThermoFisher Scientific (USA). MCF10A and MCF-7 cell lines were obtained from the American Type Culture Collection (USA). Deoxyribonuclease I (DNase I) was obtained from New England Biolabs (USA). The 1.2-kDa branched polyethylenimine was procured from Polysciences Inc. (Warrington, PA, USA). Linoleyl chloride (LA) was obtained from NU-CHEK PREP (Elysian, MN, USA). Propionic acid, acryloyl chloride, 1-ethyl-3-(3-dimethylaminopropyl) carbodiimide (EDC), N-hydroxysuccinimide (NHS), chloroform, and methanol were purchased from Sigma-Aldrich (St. Louis, MO, USA).

Synthesis and characterization of PEI-based polymeric vectors

Hydrophobically modified PEI1.2tLA6 polymers were synthesized via N-acylation using carboxyl end-capped aliphatic lipids.[22] The synthesis process is explained in detail in the aforementioned paper.[22] In summary, LA and mercaptopropionic acid (MPA) were individually dissolved in trifluoroacetic acid.

The MPA solution was cautiously added dropwise to the LA solution under light-protected conditions. The resulting product was the carboxyl end-capped LA, hereafter referred to as tLA. PEI-tLA was obtained by grafting tLA to branched PEI1.2. The grafting process was carried out with EDC/NHS activation. Obtained PEI1.2tLA was characterized by H-NMR spectroscopy (Bruker 300 MHz, Billerica, MA).

Polyplex formation

Polyplexes were formulated at room temperature by combining an aqueous solution of pDNA (0.4 µg/µL) with the pre-synthesized polymer solution. The polymer/DNA ratio was adjusted to 5 (*w/w*). The polyplex suspension was left at room temperature (25 °C) for 30 minutes before transfection.

Sodium Dodecyl Sulfate (SDS)-induced DNA release (decomplexation)

Agarose gel electrophoresis was used to assess the release profile of DNA from polyplexes.[23] Polyplexes were incubated with SDS for 5 min at 25 °C. The samples were then loaded onto a 1% agarose gel for electrophoresis. Final SDS ratios between 1% and 8 were assessed to determine the optimal release. After subjecting the samples to electrophoresis at 90 V for 1 hour, visualization was conducted under ultraviolet (UV) light following a 10-minute staining period with ethidium bromide (EtBr).

DNase I protection

1 U of DNase I enzyme was used for each 2.5 µg DNA in this study.[24] DNase I was added after polyplex formation. Tubes containing DNase I were incubated at 37 °C in a water bath for 30 minutes. Following the incubation period, SDS, the quantity previously determined (as described in the preceding section), was introduced to facilitate DNA release from the polyplexes. The resulting samples were then loaded onto a 1% agarose gel and subjected to electrophoresis for 1 hour at 100 volts. After 10 minutes of EtBr staining, the gel was photographed under UV light.

In vitro serum stability assessment

The stability of DNA integrity can be tested in vitro using FBS containing various nucleases.[25] Serum stability testing was performed to determine the degree of protection from the enzymes found in serum.[26] Resistance of DNA within polyplexes to serum degradation was assessed in a serum stability study at 37 °C using both 10% and 50% FBS to mimic *in vitro* blood conditions. The experiments were performed at distinct time intervals of 1, 6, and 24 hours. After each incubation period, a release solution consisting of SDS at the rate determined in the complexation study and Proteinase K at a concentration of 2 mg/mL was added to the samples. The DNA integrity was subsequently analyzed using agarose gel electrophoresis under the aforementioned conditions.

Cell culture

XTT was performed to determine cell proliferation.[27] MCF10A and MCF-7 cells were used in cell culture studies. The cells were cultured in DMEM F12 medium supplemented with 10% FBS and 100 U/mL penicillin/streptomycin. The cell culture was maintained in a humidified atmosphere with 5% CO_2 at 37 °C throughout the study period.

Cells were seeded into 48-well plates at a density of 25,000 cells/well and incubated for 24 hours before transfection. Subsequently, polyplexes were added at a volume of 20 µl/well. The cells were rinsed with PBS following the incubation period. Cell viability was assessed using the XTT reagent according to the manufacturer's instructions. The untreated cells served as the baseline cells with 100% viability. All experimental treatments were performed in triplicate for statistical rigor. Cell viability in treated wells was expressed as a percentage and calculated using the following formula:

$$\text{Cell viability (\%)} = [(Abs_{sample}/Abs_{control})\text{-}Abs_{blank}] \times 100$$

Protein extraction and western blot analysis

Following the transfection process, protein extraction was performed for western blot analysis.[28,29] Polyacrylamide gels and buffers were prepared according to the protocols of Sambrook et al.[30]. The cells were harvested and lysed using modified RIPA buffer containing protease and phosphatase inhibitors. Protein concentrations were determined using the bicinchoninic acid assay (Sigma, UK). Subsequently, SDS-polyacrylamide gel electrophoresis and western blot analyses were conducted under standard conditions using 50 µg of protein lysate per Lane. The proteins were separated on 12% gels and transferred to polyvinylidene fluoride (PVDF) membranes (Sigma, UK) using a wet transfer blotter.

To prevent non-specific binding, the PVDF membrane was blocked with 5% dry milk in tris-buffered-saline [(TBS-T) TBS-T solution containing 0.1% tween 20]. Primary antibody incubation was performed using an ING4 polyclonal antibody from Elabscience (E-AB-33309), followed by Horseradish peroxidase (HRP)-conjugated secondary antibody incubation, both conducted in TBS-T containing 0.5% dry milk either at room temperature for 1 hour or at 4 °C overnight.

For visualization, the membranes were developed using the chemiluminescent HRP substrate ECL reagent at a 1:1 ratio (Thermo Fisher Scientific, USA) for 4 minutes and then photographed using an image analyzer equipped with a charge-coupled device camera. Subsequently, a densitometric band intensity analysis was performed using ImageJ software.

Statistical analysis

Statistical analysis was conducted using the GraphPad Prism 6.0 software. The cell culture results were analyzed using Student's t-test, and a p value less than 0.05 was considered statistically significant.

RESULTS

SDS-induced polyplex decomplexation

It is important that polymers can successfully release DNA as well as form polyplexes. The SDS-induced release study was conducted to observe the ability of the polyplexes. Another aim of this study was to determine the optimal SDS

amount for releasing DNA, which will be necessary in future studies. SDS concentrations of 1-8% were tested. Figure 1 illustrates successful DNA release by polyplexes at all SDS concentrations. Optimal release was achieved at 5% SDS (Lane 7). Furthermore, it can be concluded that the DNA release is intact since the band luminosityis close to that of control DNA (Lane 1).

DNase I protection ability of polyplexes

SDS-induced decomplexation showed that the polymers can release intact DNA. Nevertheless, it is important that a delivery system can protect its cargo from DNase I. Effective gene expression requires protection of the DNA inserted into the cell from nuclease degradation.[31] Figure 2 shows a gel image of a DNase I protection study.

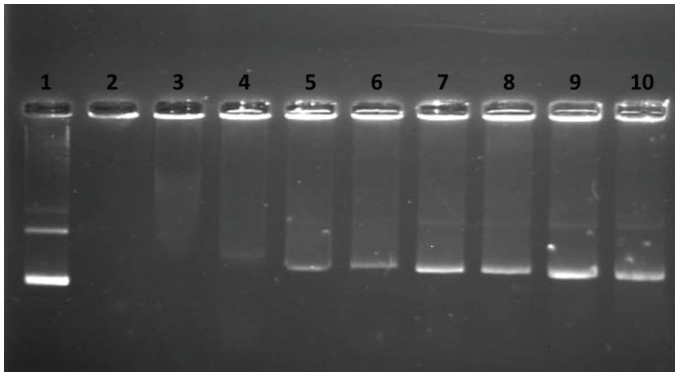

Figure 1. Agarose gel image of the decomplexation study. Lane 1: Naked DNA as control, Lane 2: Polyplex control, Lane 3-10: SDS% with pDNA respectively; 1-8%

SDS: Sodium dodecyl sulfate

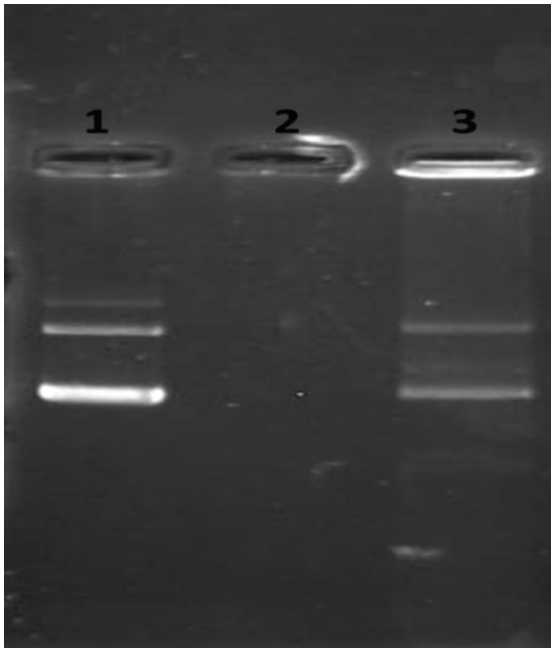

Figure 2. Agarose gel image of a DNase I protection study. Lane 1: Naked DNA control, Lane 2: Naked DNA + DNase I, Lane 3: Polyplex + DNase I + SDS 5%

SDS: Sodium dodecyl sulfate

The presence of serum proteins poses a significant challenge to DNA integrity. Abundant nuclease enzymes in serum can cleave the phosphodiester bonds between sugar and phosphate moieties of DNA, leading to its degradation. In addition, serum opsonin causes opsonization resulting in phagocytosis.[25] Therefore, it is important to protect the cargo DNA from serum proteins. DNA digestion by serum nucleases is shown in Figure 3A. Lane 1 shows the naked DNA as a positive control. Digested DNA at different time intervals can be observed in Lane 2, Lane 3, and Lane 4. Figure 3B-D shows the serum protection ability of the synthesized polymer at three intervals of time (1, 6, and 24 hours) as the bands are visible. Lane 1 is the positive control, as mentioned before. Lanes 2 and 3 represent 10% and 50% FBS protection, respectively.

Cell culture

The cell growth curves demonstrated that proliferation was inhibited in the pcDNA3-ING4-transfected group in a time-dependent manner (Figure 4). There was a significant difference between the pcDNA3 control and pcDNA3-ING4 treatment group in the days following 2nd day ($p < 0.05$). Maximum inhibition was spotted on day 4 as 32.42%.

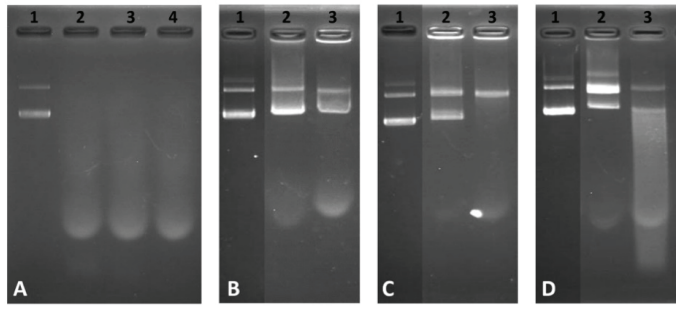

Figure 3. Agarose gel images of serum stability measurements. A: DNA without polymer (Lane 1: Naked DNA control, Lane 2: DNA + FBS - 1 hour, Lane 3: DNA + FBS - 6 hours, Lane 4: DNA + FBS - 24 hours), B-D: 1-6-24 hours (Lane 1: Naked DNA control, Lane 2: Polyplex + FBS 10%, Lane 3: Polyplex + FBS 50%)

FBS: Fetal bovine serum

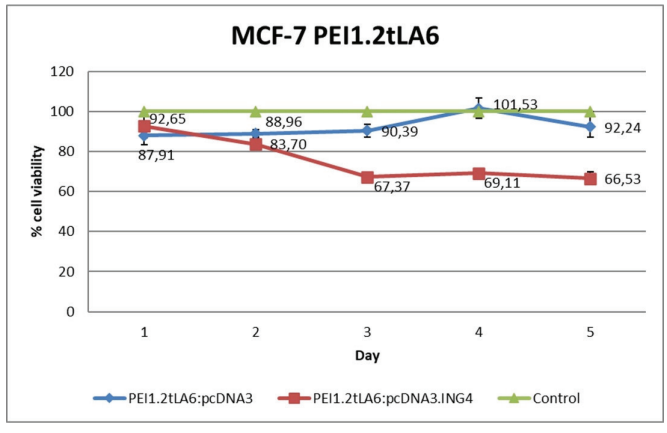

Figure 4. MCF-7 breast cancer cell line 5-day cytotoxicity study

MCF10A cell line is used as a normal human mammary cell line for positive control against the MCF7 cancerous cell line.[32] On day 4, the cell lines treated with pcDNA3 and pcDNA3-ING4 showed no statistically significant difference ($p > 0.05$), as illustrated in Figure 5.

Overexpression of ING4 in MCF-7 cells via polyplex-induced transfection

Western blotting was used to assess ING4 overexpression following polyplex transfection. Increased overexpression was detected in pcDNA3-ING4-transfected cells compared with the control groups based on the densitometric band intensity analysis, suggesting that the synthesized polymer successfully transfected the ING4 plasmid. ING4 expression levels were normalized against β-actin expression. Figure 5 shows significantly elevated ING4 expression.

DISCUSSION

The successful release of DNA from polyplexes, especially at the optimal 5% SDS concentration determined in our study, not only validates the efficiency of our designed polymeric vectors but also ensures the integrity of the released genetic material.

Figure 2 presents a gel image from the DNase I protection study, demonstrating in Lane 3 that the polyplexes effectively protect DNA from DNase I digestion and enable its successful release. Lane 2 shows the absence of discernible bands, indicating the digestion of plasmid DNA by DNase I in the absence of a delivery system. The DNase I protection study without a doubt demonstrates the polymers' ability to shield encapsulated DNA from enzymatic degradation. The polyplexes in Lane 3 effectively protected and released DNA, in stark contrast to Lane 2, where naked DNA succumbs to DNase I digestion.

PEI-based vectors can protect nucleic acids at high (50%) serum concentrations.[33] Furthermore, it is known that PEI exerts successful endosomal escape ability via the proton sponge effect.[6,34] According to the findings of this study, in contrast to naked plasmid DNA, which undergoes rapid degradation by serum nucleases, our designed polymeric vector exhibits remarkable stability, effectively protecting the encapsulated DNA cargo from enzymatic degradation.

A considerable number of *in vitro* studies focused on breast cancer consisting of MCF7 cells considering their estrogen-responsive characteristics. This specialty of MCF7 cells makes them a useful model for breast cancer biology studies.[35] The ability to inhibit proliferation in cancer cells, while not affecting normal cells is a critical step toward developing targeted and effective cancer treatments. Furthermore, western blot results align with those of previous studies in the field, corroborating the importance of these proteins in cancer biology.[29]

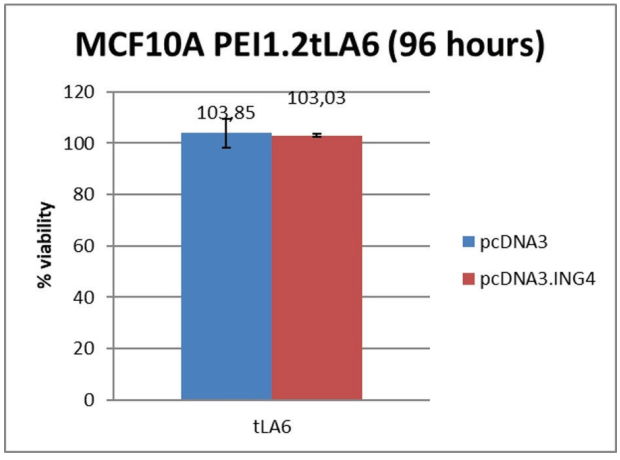

Figure 5. Cytotoxicity of the MCF10A cell line cytotoxicity study as positive control

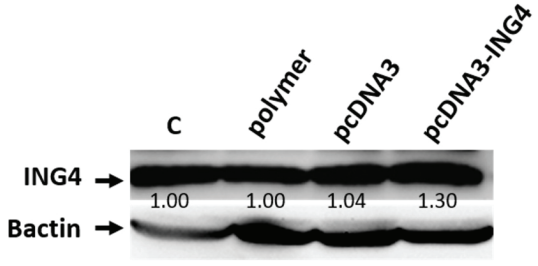

Figure 6. Protein expression of ING4 with western blot analysis

CONCLUSION

In conclusion, a PEI-based non-viral vector was synthesized and complexed with a plasmid that encodes the ING4 protein. It is also an important feature that the formulation can protect DNA from serum proteins.[36] Notably, our polyplexes exhibited potent cytotoxicity against cancer cells while maintaining non-toxicity in control DNA. Western blotting confirmed the presence of the ING4 protein, affirming the efficacy of our approach. These findings strongly support the potential of our formulation as a promising candidate for non-viral gene therapy in breast cancer treatment, emphasizing its viability for further preclinical and clinical investigations.

Acknowledgment

Uğur Karagöz acknowledges the support from the Scientific and Technological Research Council of Türkiye (TUBITAK) 2214/A scholarship. The cell culture studies were conducted at the University of Alberta (Albany, Alberta, grant number 1059B141700163.

Ethics

Ethics Committee Approval: There is no requirement for ethical approval.

Informed Consent: There is no requirement for informed consent to be obtained.

Authorship Contributions

Concept: U.K., Design: U.K., A.G.K., H.U., Data Collection or Processing: U.K., E.I., Analysis or Interpretation: U.K., R.B.KC., E.I., A.G.K., H.U., Literature Search: U.K., Writing: U.K.

Conflict of Interest: The authors have no conflicts of interest to declare.

Financial Disclosure: The authors declared that this study received no financial support.

REFERENCES

1. Wu J, Zhou Z. MicroRNA-432 acts as a prognostic biomarker and an inhibitor of cell proliferation, migration, and invasion in breast cancer. Clin Breast Cancer. 2021;4:462-470.
2. Liu T, Song S, Wang X, Hao J. Small-molecule inhibitors of breast cancer-related targets: Potential therapeutic agents for breast cancer. Eur J Med Chem. 2021;210:112954.
3. Noruzi S, Vatanchian M, Azimian A, Niroomand A, Salarinia R, Oroojalian F. Silencing SALL-4 Gene by transfecting small interfering RNA with targeted aminoglycoside-carboxyalkyl polyethylenimine nano-polyplexes reduced migration of MCF-7 breast cancer cells. Avicenna J Med Biotechnol. 2021;13:2-8.
4. Mohammadinejad R, Dehshahri A, Madamsetty VS, Zahmatkeshan M, Tavakol S, Makvandi P, Khorsandi D, Pardakhty A, Ashrafizadeh M, Afshar EG, Zarrabi A. *In vivo* gene delivery mediated by non-viral vectors for cancer therapy. Journal of Controlled Release. 2020;325:249-275.
5. Santana-Armas ML, Tros de Ilarduya C. Strategies for cancer gene-delivery improvement by non-viral vectors. Int J Pharm. 2021;596:120291.
6. Haladjova E, Rangelov S, Tsvetanov C. Thermoresponsive polyoxazolines as vectors for transfection of nucleic acids. Polymers (Basel). 2020;12:2609.
7. Jana P, Ghosh S, Sarkar K. Low molecular weight polyethyleneimine conjugated guar gum for targeted gene delivery to triple negative breast cancer. Int J Biol Macromol. 2020;161:1149-1160.
8. Halama A, Kuliński M, Librowski T, Lochyński S. Polymer-based non-viral gene delivery as a concept for the treatment of cancer. Pharmacol Rep. 2009;61:993-999.
9. Wang H, Liu X, Ai X, Remant-Bahadur KC, Dick TA, Yan B, Lu T, Zhou X, Luo R, Liu M, Wang X, Li K, Wang W, Uludag H, Fu W. Safe and effective delivery of mRNA using modified PEI-based lipopolymers. Pharmaceutics. 2023;15:410.
10. Lungwitz U, Breunig M, Blunk T, Göpferich A. Polyethylenimine-based non-viral gene delivery systems. Eur J Pharm Biopharm. 2005;60:247-266.
11. Tallen G, Riabowol K. Keep-ING balance: Tumor suppression by epigenetic regulation. FEBS Lett. 2014;588:2728-2742.
12. Byron SA, Min E, Thal TS, Hostetter G, Watanabe AT, Azorsa DO, Little TH, Tapia C, Kim S. Negative regulation of NF-□B by the ING4 tumor suppressor in breast cancer. PLoS One. 2012;7:e46823.
13. Yuan S, Jin J, Shi J, Hou Y. Inhibitor of growth-4 is a potential target for cancer therapy. Tumour Biol. 2016;37:4275-4279.
14. Shatnawi A, Ayoub NM, Alkhalifa AE, Ibrahim DR. Estrogen-related receptors gene expression and copy number alteration association with the clinicopathologic characteristics of breast cancer. Breast Cancer (Auckl). 2022;16:11782234221086713.
15. Tapia C, Zlobec I, Schneider S, Kilic E, Güth U, Bubendorf L, Kim S. Deletion of the inhibitor of growth 4 (ING4) tumor suppressor gene is prevalent in human epidermal growth factor 2 (HER2)-positive breast cancer. Hum Pathol. 2011;42:983-990.
16. Colla S, Tagliaferri S, Morandi F, Lunghi P, Donofrio G, Martorana D, Mancini C, Lazzaretti M, Mazzera L, Ravanetti L, Bonomini S, Ferrari L, Miranda C, Ladetto M, Neri TM, Neri A, Greco A, Mangoni M, Bonati A, Rizzoli V, Giuliani N. The new tumor-suppressor gene inhibitor of growth family member 4 (ING4) regulates the production of proangiogenic molecules by myeloma cells and suppresses hypoxia-inducible factor-1 alpha (HIF-1alpha) activity: involvement in myeloma-induced angiogenesis. Blood. 2007;110:4464-4475.
17. Zhang X, Wang KS, Wang ZQ, Xu LS, Wang QW, Chen F, Wei DZ, Han ZG. Nuclear localization signal of ING4 plays a key role in its binding to p53. Biochem Biophys Res Commun. 2005;331:1032-1038.
18. Shatnawi A, Ayoub NM, Alkhalifa AE. ING4 expression landscape and association with clinicopathologic characteristics in breast cancer. Clin Breast Cancer. 2021;21:e319-e331.
19. Gournay M, Paineau M, Archambeau J, Pedeux R. Regulat-INGs in tumors and diseases: Focus on ncRNAs. Cancer Lett. 2019;447:66-74.
20. Vetter VC, Wagner E. Targeting nucleic acid-based therapeutics to tumors: Challenges and strategies for polyplexes. J Control Release. 2022;346:110-135.
21. Wang S, Huang R. Non-viral nucleic acid delivery to the central nervous system and brain tumors. J Gene Med. 2019;21:e3091.
22. Bahadur RKC, Cezary K, Hasan U. Additive nanocomplexes of cationic lipopolymers for improved non-viral gene delivery to mesenchymal stem cells. J Mater Chem B 2015;3:3972-3982.
23. Karagöz U, Kotmakçı M, Akbaba H, Bozok V, Kantarcı G. Preparation and characterization of non-viral gene delivery systems with pEGFP-C1 plasmid DNA. Braz J Pharm Sci. 2018;54.
24. Apaolaza PS, Del Pozo-Rodríguez A, Solinís MA, Rodríguez JM, Friedrich U, Torrecilla J, Weber BH, Rodríguez-Gascón A. Structural recovery of the retina in a retinoschisin-deficient mouse after gene replacement therapy by solid lipid nanoparticles. Biomaterials. 2016;90:40-49.
25. Chandrasekaran AR. Nuclease resistance of DNA nanostructures. Nat Rev Chem. 2021;5:225-239.
26. Karagöz U, Kantarci AG. Preparation, characterization and evaluation of solid lipid nanoparticles and niosomes for ING4 gene delivery to MCF-7 cells. Journal of Research in Pharmacy. 2019;23:935-943.
27. Ergul M, Bakar-Ates F. A specific inhibitor of polo-like kinase 1, GSK461364A, suppresses proliferation of Raji Burkitt's lymphoma cells through mediating cell cycle arrest, DNA damage, and apoptosis. Chem Biol Interact. 2020;332:109288.
28. Zhang L, Wang Y, Zhang F, Wang Y, Zhang Q. Correlation between tumor suppressor inhibitor of growth family member 4 expression and microvessel density in breast cancer. Hum Pathol. 2012;43:1611-1617.
29. Wei Q, He W, Lu Y, Yao J, Cao X. Effect of the tumor suppressor gene ING4 on the proliferation of MCF-7 human breast cancer cells. Oncol Lett. 2012;4:438-442.
30. Sambrook J, Fritsch EF, Maniatis T. Molecular cloning: A laboratory manual. Cold Spring Harbor Laboratory Press. 1982;545.
31. Kashkouli KI, Torkzadeh-Mahani M, Mosaddegh E. Synthesis and characterization of a novel organosiLane-functionalized chitosan nanocarrier as an efficient gene delivery system: Expression of green fluorescent protein. Int J Biol Macromol. 2019;125:143-148.
32. Bahadur KCR, Uludağ H. PEI and its derivatives for gene therapy. Polymers and Nanomaterials for Gene Therapy. 2016;29-54.
33. Sezlev Bilecen D, Rodriguez-Cabello JC, Uludag H, Hasirci V. Construction of a PLGA based, targeted siRNA delivery system for treatment of osteoporosis. J Biomater Sci Polym Ed. 2017;28:1859-1873.

34. Qu Y, Han B, Yu Y, Yao W, Bose S, Karlan BY, Giuliano AE, Cui X. Evaluation of MCF10A as a reliable model for normal human mammary epithelial cells. PLoS One. 2015;10:e0131285.

35. Vantangoli MM, Madnick SJ, Huse SM, Weston P, Boekelheide K. MCF-7 human breast cancer cells form differentiated microtissues in scaffold-free hydrogels. PLoS One. 2015;10:e0135426.

36. Moret I, Esteban Peris J, Guillem VM, Benet M, Revert F, Dasí F, Crespo A, Aliño SF. Stability of PEI-DNA and DOTAP-DNA complexes: effect of alkaline pH, heparin and serum. J Control Release. 2001;76:169-181.

Turk J Pharm Sci 2024;21(5):456-462
DOI: 10.4274/tjps.galenos.2023.78006

ORIGINAL ARTICLE

Development and Evaluation Essential Oils Nanoemulgel as Human Skin Sanitizer Using Novel Method

Hayder Kadhim DRAIS

Al-Mustaqbal University College of Pharmacy, Department of Pharmaceutics, Babil, Iraq

ABSTRACT

Objectives: The increase in epidemic diseases and frequent use of alcoholic disinfectants, despite their side effects, prompt scientists to develop new sterilization products that do not contain alcoholic materials. The aim of this study was to develop, prepare, and evaluate a nanoemulgel skin sanitizer using essential oils (EOs) as active substances.

Materials and Methods: A microwave-based technique was used to prepare nanoemulsion. The pseudo-ternary phase plots were constructed to contain three ingredients: EOs, polyoxyethylene (80) sorbitan monooleate, and a propylene glycol mixture (1:0:75) % *(w/w)* and double distilled. Five samples of nanoemulsion (NE1-NE5) were selected for the characterization and preparation of nanoemulgel (HN1-HN5). Blank gel (HN6) was also prepared to compare the antibacterial activity against HN1-HN5 formulations. Various evaluation processes were achieved for HN1-HN6 formulations. The statistical test was a One-Way analysis of variance at $p \leq 0.05$ as significant data.

Results: The characterization process indicates that NE1-NE5 formulations had nanosized droplets, a homogenous distribution, and an acceptable charge. The evaluation process for HN1-HN6 formulations indicates clear, homogenous, with distinctive EO odor and no phase separation, slightly acidic pH, spreadability (128.22 to 124.22 g cm/sec), plastic rheological flow, no skin lesions after application, and conspicuous antimicrobial activity.

Conclusion: Laboratory characterization and evaluation demonstrated the existence of a promising product for sanitizing human skin and could be a successful alternative to alcoholic products based on the growing demand for EO products.

Keywords: Essential oils, nano-emulsion, nanoemulgel, microwaves based method

INTRODUCTION

Health service providers are among the most vulnerable groups to bacterial attack, due to their reception of various and many disease cases at clinics and hospitals. In addition, all different groups of society, from workers and employees to those sitting at home, remain vulnerable to bacterial attacks. Therefore, scientists must develop, innovate, and diversify various defensive and preventive methods against these harmful microbes. Alcohol-based hand gel is an antiseptic or hand rub, a product that removes common pathogens after hand application. They are used to destroy the infection chain, making them one of the most important protocols for diminishing the burden on healthcare.[1] It is preferable to use it when soap and water are not available, or due to frequent dealing with diseases, such as those experienced by health service providers, or due to the presence of special skin diseases, such as cracks on the skin. Exposure to alcohol-based hand gel deprives the skin of water and sebum that cause skin dryness, destroy lipid barriers, and eventually cause hand eczema and dermatitis, associated symptoms like dryness, acne, wrinkles, burning, swelling, erythema, and cracking.[2] Non-alcoholic essential oils (EOs) hand gel is an advanced and desirable alternative for fighting various

*Correspondence: deera2020@gmail.com, ORCID-ID: orcid.org/0000-0002-2143-1817
Received: 02.10.2023 , Accepted: 12.12.2023

germs. EOs are aromatic liquids with an oil structure that is obtained naturally from plants. Several reports show that EOs have antiseptic, antibacterial, antifungal, antiviral, antioxidant, antiparasitic, and insecticidal activities. The antimicrobial activity of EOs is achieved by destroying the cell membrane and bacterial cell wall, resulting in microbial cell disruption.[3-5] Peppermint oil and myrtle oil are medicinal EOs with many studies confirming their antimicrobial activity.[6-8] Peppermint oil and myrtle oil are hydrophobic materials that are unstable when mixed with aqueous gel components. Nanoemulsions, an oil-in-water type, represent an advanced delivery system consisting of an internal oil phase and an external aqueous phase, suitable for skin application. When a nanoemulsion combines with a gelling agent, it results in a more convenient nanosystem called a nanoemulgel that provides many advantages, such as better patient compliance, better loading capacity, better stability, and controlled release.[9,10] Various techniques are present in preparing a nanoemulsion as a part of a nanoparticulated drug delivery system but it is related to a large number of negative marks, principally more expense, invested high time and energy, and stability issues of the final dosage form. Recently developed microwave-based strategies are cheap, conservative, stable, and quickly handling on both little and enormous scopes and avoid the appearance of impurities. The radiation of microwaves is a type of electromagnetic non-ionizing radiation that has frequencies of about one meter to one millimeter with frequencies of 300 MHz to 300 GHz. Microwaves have three fundamental ascribes that work with them to be utilized in dosage form development: reflection by metal substances, absorption by substances, and ready to go through plastic, glass, paper, and comparable ingredients.[11] The aim of this research was to develop, prepare, and evaluate an antimicrobial EO nanoemulgel skin sanitizer and compare its efficacy against two bacterial strains: *Staphylococcus aureus* and *Escherichia coli*.

MATERIALS AND METHODS

Materials

The EOs of peppermint and myrtle were purchased from BAR-SUR-loup Grasse A. The M Franc and Nanjing Duly Biotech Co., Ltd. China, respectively. Polyoxyethylene (80) sorbitan monooleate, carbopol 940, and propylene glycol were purchased from Beijing Yibai Biotechnology Co., Ltd. China. All solvents and reagents used in the experiments were of analytical grade.

Methods

Preparation of EO nanoemulsions and construction of pseudoternary phase diagrams using microwave-based methostructures

Peppermint oil and myrtle oil were used to mix with hydrophilic components of double-distilled water, polyoxyethylene (80) sorbitan monooleate, and propylene glycol. Blend prepared under 1000 rpm for 5 min using a magnetic stirrer contained hydrophilic and hydrophobic phases according to the amounts described in Table 1. The mixture was inserted into a microwave device for 10-15 seconds, then a magnetic stirrer device at 1000 rpm was used for adequate time (seconds to minutes according to a final volume of dosage form) until the feature of nanoemulsion (NE1-NE5) was observed.[11] The construction process of pseudo ternary phase diagrams, which contain three components, including EO, a surfactant mixture of polyoxyethylene (80) sorbitan monooleate and propylene glycol (1:0:75) % *(w/w)*, and an aqueous phase, is developed. To determine the borderline of phases for each phase graphing, a visual inspection was performed to assess the transparency of the formulations during the magnetic stirrer process. The pseudo-ternary phase plot was drawn using triplet V4 software 4.1.2. Version. The diagramed area of the nanoemulsion is represented by the shaded area.[10]

Preparation of EO hand nanoemulgels

The carbomer 940 hydrogel was formulated by adding 0.6% *(w/w)* of the gelling agent to double-distilled water by stirring using an electric homogenizer until the mixture was completely dissolved. A few drops of triethanolamine were added to obtain a pH of about (6.2-7.4). The previously prepared nanoemulsion (NE1-NE5) formulations were mixed with hydrogel at a concentration of 15%, and the two were continuously and slowly stirred until a clear EO hand nanoemulsion (HN1-HN5) formulations were formed. Blank gel (HN6) was also prepared by adding a polyoxyethylene (80) sorbitan monooleate and propylene glycol mixture to the gel base with a continuous slow stirring rate to avoid the formation of bubbles (500 rpm for 15 minutes) to obtain a clear blank gel (HN6). The EO nanoemulgel (HN1-HN5) formulations and blank gel (HN6) were stored in tightly closed containers at 25 ˚C temperatures for assessment and study.[9-11]

Characterization of nanoemulsion (NE1-NE5) formulations through the determination of particle size, polydispersity index (PDI), and zeta potential (ZP)

Dynamic light scattering is a technique used to determine particle size in addition to the PDI and surface charge of globules of nanoemulsion (NE1-NE5) formulations using a Horiba Instrument, Ltd. Kyoto, Japan. When a laser beam passes through a sample, a variation in scattering light intensity is observed that is time-dependent in the presence of Brownian motion of the dispersed nanoglobules in a nanosystem. This technique is highly accurate, and the measures were achieved in three trials.[11]

Atomic force microscopy (AFM)

The nanocarrier morphology was determined by AFM Angstrom Advanced Inc. AA3000 USA. It was scanned over the range of 100 MV/s. The study was conducted with 2-3 drops of the nanoemulsion on an experimental glass slide and then measured after 3 hours.

Evaluation of EO hand nanoemulgel (HN1-HN5) formulations Organoleptic determination

Organoleptic tests are important for determining the physical stability of pharmaceutical preparations. The color, smell, homogeneity, and syneresis can be noticed for EO hand

nanoemulgel (HN1-HN5) formulations can be noticed at 0, 7, 14, 21, and 28 days. The data were obtained in triplicate.[12-14]

pH determination

It is an important parameter that can predict the stability of formulation and skin suitability. A digital pH meter was used to determine the pH by collecting a 10 g sample of EO hand nanoemulgel (HN1-HN5) formulations. The optimum human skin pH is in the range of 4.5-6.5. The experiment was conducted in three trials.[9,10]

Measurement of spreadability

It is a parameter related to patient compliance that leads to achieving therapeutic aims. The procedure was performed using two separated glass slides with dimensions (10 x 2.5 cm). The lower slide was tied to a wooden base containing 0.5 g of the EO hand nanoemulgel (HN1-HN5) formulations. The second piece of glass slide was tied to a weight of 25 g when applied to the first glass slide, resulting in the pulling process to a distance of 7.0 cm before it detached. The weight in grams and time in seconds that needed to move the second glass slide was recorded, and the spreadability parameter was determined from Equation 1:

$S = M \times L / T$ ..... Equation 1

S = Spreadability, M = Weight that tide to first slide, L = Length of slide

Here, T = T is the time required to separate two sides. The study was conducted in three trials.[12-14]

Viscosity measurement

In addition to the analysis and development of new formulations, this parameter is crucial for pharmaceutical formulation assessment. Using a rotational digital viscometer with a spindle number (2) from Biobase Meihua Trading Co., Ltd. at 25 °C to measure the viscosity of EO hand nanoemulgel (HN1-HN5) formulations. The samples were subjected to different rotating speeds which are (0.1, 0.3, 0.6, 1.5, 3, 6, 12, 30, and 60 rpm). The experiment was performed in three trials.[12-14]

Skin irritation study

The study was conducted on 30 volunteers and was ethically approved by the Research Ethics Committee of Al-Mustaqbal University/College of Pharmacy (approval number: pHa2/2023, date: 10.02.2023). None of the volunteers had clinical signs of dermal abrasion or infection. The volunteers were asked to sign consent forms after explaining the research protocol with probable adverse effects. The evaluation was performed by applying 1 g of EO hand nanoemulgel (HN1-HN5) formulations on each intact area of the volunteer's hand skin and then allowed to wait for 10-15 min. A questionnaire was administered to the participants of the study to determine skin irritation and acceptability. The formulation was rated according to the characteristics of the EO hand nanoemulgel (HN1-HN5) formulations in terms of the formulation texture, appearance, smell, redness, and irritation or burning sensation after the product application.[12-14]

In vitro antimicrobial activity determination

The *in vitro* antimicrobial activity of the prepared EO hand nanoemulgel (HN1-HN5) formulations and blank gel (HN6) against two pathogenic bacterial species, Gram-negative *E. coli* and Gram-positive *S. aureus*, were studied using the agar disc diffusion method. The Gram-negative *E. coli* and Gram-positive *S. aureus* bacterial strains were obtained from Ali Obais Hospital, Babil Health Directorate, Ministry of Health, Iraq. All experimental conditions were performed under aseptic conditions. From each study sample, 10 µL was added to a sterile filter paper disc. Seven discs from each formula described in Table 1 were placed on each culture plate. Antibacterial activity was assessed by calculating the inhibition zone diameters in millimeters using a sliding caliper. The study was performed in triplicate.

Statistical analysis

The data of the study were obtained as the mean and standard deviation of three experimental trials. Statistical analysis was performed using Excel. One-Way analysis of variance (ANOVA) was used as a statistical test, where the level at ($p \leq 0.05$) was considered significant.[10,11]

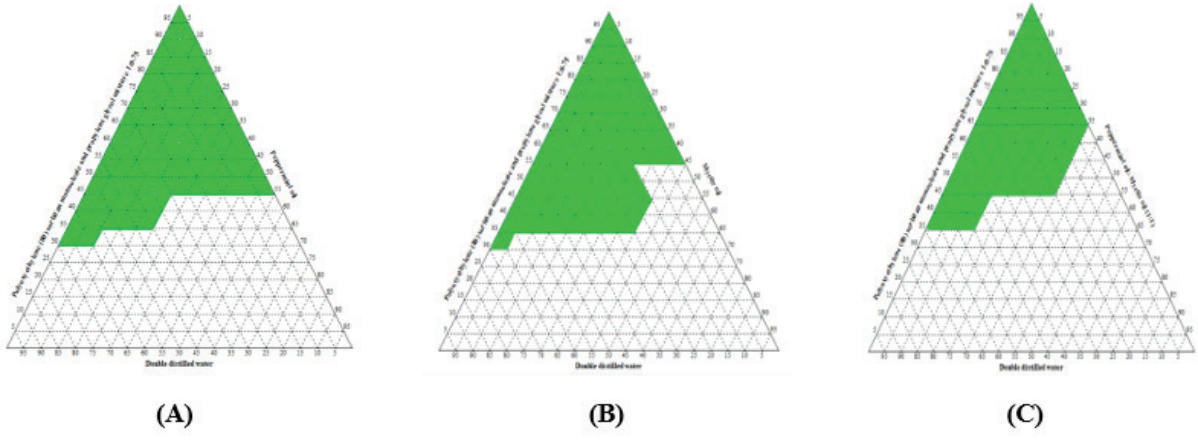

(A) (B) (C)

Figure 1. Pseudoternary phase diagrams containing polyoxyethylene (80) sorbitan monooleate: propylene glycol mixture 1:0.75 *(w/w)* % double-distilled water and oil components: peppermint oil, myrtle oil, peppermint oil: myrtle oil (1:1) mixture in plots (A), (B), and (C), respectively

RESULTS

Measurement of globule size, PDI, and ZP for nanoemulsion (N1-N5) formulations

The pseudo-ternary phase diagrams contained three structural components: EOs, a surfactant mixture (1:0.75) % *(w/w)*, and double-distilled water (Figure 1). A nanoemulsion of EO was prepared successfully using a microwave-based method and was characterized by ease, speed, and flexibility in preparation. The nanoemulsion is represented by a shaded area of pseudo-ternary phase diagrams, while the other area represents the emulsion. From the phase diagrams, five formulas were selected, namely, NE1, NE2, NE3, NE4, and NE5, for characterization of the globule size, PDI, and ZP. The particle size results were NE1 = 25.83 nm, NE2 = 45.96 nm, NE3 = 29.83 nm, NE4 = 49.83 nm, and NE5 = 55.86 nm, as shown in Table 2. The PDI experiment for nanoemulsion (NE1-NE5) formulations was from (0.26 to 0.385) as shown in Table 2. The outcomes of the mean absolute ZP value for nanoemulsion (NE1-NE5) formulations were (12.61 to 19.6 mV) as shown in Table 2.

AFM

The results show that the NE5 formula contains particles with regular smooth surfaces and nearly spherical shapes with nanometer-sized pores, as shown in Figure 2.

Evaluation of EO hand nanoemulgel (HN1-HN5) formulations
Organoleptic assay

The organoleptic test was performed through naked-eye observations of the EO hand nanoemulgel (HN1-HN5) formulations. All HN1-HN5 formulations show clear, homogenous, with the characterized odor of EOs represented by peppermint oil and myrtle oil. No syneresis was observed.[12-14]

pH determination

pH evaluation is an important parameter that can be used to prevent unsuitable properties in nanoemulgels that are related to patient comfort. The pH values of the EO hand nanoemulgel (HN1-HN5) formulations were slightly acidic (5.4 to 5.89) as shown in Table 3.

Measurement of spreadability

The spreadability of EO hand nanoemulgel (HN1-HN5) formulations. The results were (128.22 to 124.22 g cm/sec).

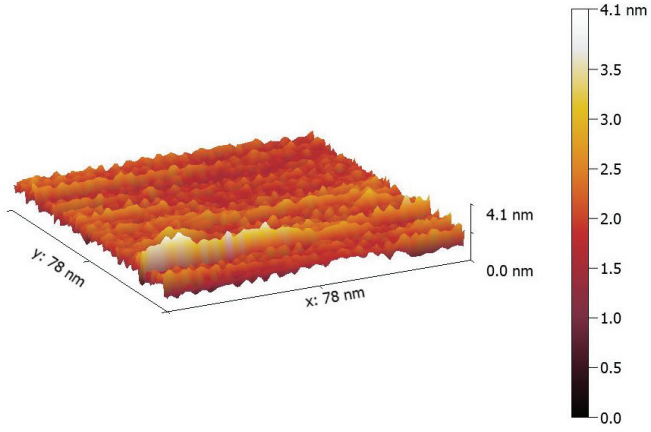

Figure 2. AFM 3D image of EO nanoemulsion (N5) formulation with a scanning area of 78 nm*78 nm

AFM: Atomic force microscopy, EO: Essential oil

Table 1. EO hand nanoemulgel (HN1-HN5) formulations and blank gel (HN6) for optimization

Code	Peppermint oil *(w/w)*	Myrtle oil *(w/w)* %	Peppermint oil: myrtle oil (1:1) *(w/w)* %	Polyoxyethylene (80) sorbitan monooleate/propylene glycol mixture [1:0.75 *(w/w)*]	Carbopol 940 *(w/w)* %	Double-distilled water up to *(w/w)* %
HN1	5			4	0.6	100
HN2	10			4	0.6	100
HN3		5		4	0.6	100
HN4		10		4	0.6	100
HN5			10	4	0.6	100
HN6				4	0.6	100

EO: Essential oil

Table 2. Characterization results of nanoemulsion (NE1-NE5) formulations

Formulation code	Globule size (nm)*	PDI*	ZP*
NE1	25.83 ± 1.04	0.260 ± 0.015	12.61 ± 0.28
NE2	45.96 ± 1.00	0.368 ± 0.035	17.53 ± 0.43
NE3	29.83 ± 1.26	0.292 ± 0.006	15.69 ± 0.34
NE4	49.83 ± 0.85	0.385 ± 0.006	18.43 ± 0.23
NE5	55.86 ± 1.09	0.380 ± 0.013	19.60 ± 0.28

*Values are expressed as mean ± SD (n= 3), SD: Standard deviation, PDI: Polydispersity index, ZP: Zeta potential

Viscosity measurement

A viscometer with a spindle number (2) of a rotational digital type (Biobase Meihua Trading Co., Ltd. was exploited to measure the viscosity and study the rheology behavior of EO hand nanoemulgel (HN1-HN5) formulations as shown in Table 3.

Skin irritation study

A skin irritation experiment was conducted using 30 volunteers with EO hand nanoemulgel (HN1-HN5) formulations. It was found that all formulations did not produce a sense of skin itching, irritation signs, or any painful skin effect after the application of gel to the participants in the experiment.

In vitro antimicrobial activity determination

The experiment of *in vitro* antimicrobial activity was conducted successfully for EO hand nanoemulgel (HN1-HN5) formulations and blank gel (HN6) against Gram-negative *E. coli* and Gram-positive *S. aureus*. We found that increasing the EO concentration increased the bacterial growth inhibition for *S. aureus* and *E. coli*, as shown in Figure 3.

DISCUSSION

Particle size is a cornerstone of nanotechnology, influencing drug delivery, bioavailability, and cellular interactions. Smaller particles offer increased surface area, enhancing dissolution and absorption. Precise size control ensures targeted delivery and reduced side effects, optimizing therapeutic outcomes. In nanotechnology, mastering particle size transforms materials into powerful tools for innovation and healthcare. The results indicates the colloidal features of NE1-NE5 formulations. It was

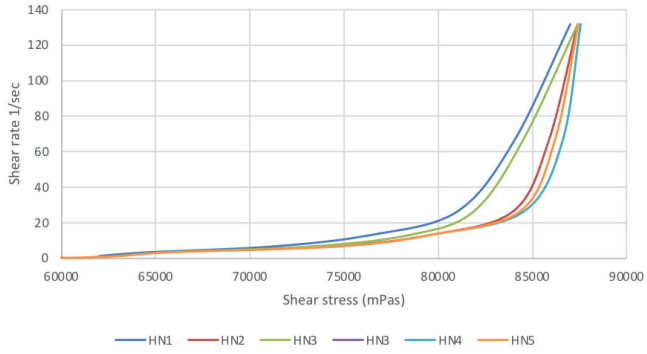

Figure 3. Shear stress against a shear rate of EO hand nanoemulgel (HN1-HN5) formulations

EO: Essential oil

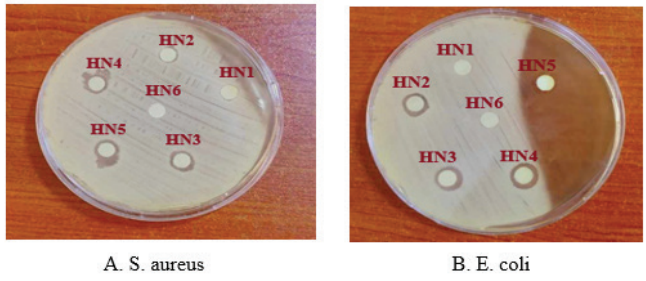

Figure 4: Inhibition zone of the prepared EO hand nanoemulgel (HN1-HN5) formulations compared to blank gel (HN6) formulation (A): *Staphylococcus aureus* and (B): *Escherichia coli*

EO: Essential oil

Table 3. Evaluation of EO hand nanoemulgel (HN1-HN5) formulations

Code	Color	Odor	Syneresis	Homogeneity	pH*	Mean spreadability (gcm/sec)*	Viscosity at 12 rpm (mP.s)*
HN1	Colorless	Aromatic smell	No	Homogeneous	5.60 ± 0.10	128.22 ± 0.12	3074.68 ± 2.54
HN2	Colorless	Aromatic smell	No	Homogeneous	5.89 ± 0.09	124.52 ± 0.09	3186.55 ± 2.50
HN3	Colorless	Aromatic smell	No	Homogeneous	5.40 ± 0.29	127.28 ± 0.14	3107.33 ± 2.08
HN4	Colorless	Aromatic smell	No	Homogeneous	5.62 ± 0.12	124.45 ± 0.12	3203.41 ± 2.53
HN5	Colorless	Aromatic smell	No	Homogeneous	5.85 ± 0.05	124.22 ± 0.11	3195.26 ± 2.40

*Values are expressed as mean ± SD (n= 3), $p \leq 0.05$. SD: Standard deviation, EO: Essential oil

Table 4. Antibacterial activity of different EO hand nanoemulgels (HN1-HN5) formulations compared with the blank gel (HN6) formulation

Formulation code	Inhibition zone of *Staphylococcus aureus* (mm)	Zone of inhibition of *Escherichia coli* (mm)
HN1	0.00 ± 0.00	0.00 ± 0.00
HN2	10.63 ± 0.15	12.33 ± 0.25
HN3	11.27 ± 0.25	12.70 ± 0.20
HN4	11.50 ± 0.20	13.76 ± 0.15
HN5	12.56 ± 0.15	37.03 ± 1.66
HN6 (BlanK)	0.00 ± 0.00	0.00 ± 0.00

*Values are expressed as mean ± SD (n= 3), $p \leq 0.05$. SD: Standard deviation, EO: Essential oil

found that as the concentration of EOs increased, the globule size increased at a constant surfactant: co-surfactant blend concentration. The particle size values have the following ascending order for NE1 < NE2 in formulations containing peppermint oil while NE3 < NE4 in formulations containing myrtle oil. In comparison with similar quantities of EO of different types, it had the following ascending order for NE2 < NE4 < NE5. The globule size increased as the lipid content increased due to an increase in the colloidal dispersion viscosity that made the dispersed globules more resistant to the breakdown of large droplets into smaller droplets during the emulsification process.[9,11] The polydispersity index reflects particle size uniformity, ensuring stability and consistent performance in nanotechnology applications. Low PDI enhances reliability, enabling precise drug delivery, controlled release, and reproducible therapeutic outcomes in advanced formulations. The outcom of PDI experiment indicates a high homogeneous and constricted size distribution for nanosystems.[9-11] Zeta potential determines nanocarrier stability by indicating surface charge, preventing aggregation. High zeta potential enhances colloidal stability, prolongs shelf life, and ensures efficient drug delivery through improved bioavailability and targeted interactions. The outcomes of the mean absolute ZP value indicates the stability of the nanoemulsions. There should be a higher electrical charge on the surface particles of the nanoemulsions to prevent their aggregation in the solutions due to the strong resistance violence among the particles. Globular surface charge values according to the thumb rule are: the range-5 mV to mV shows fast aggregation, about 20 mV supplies only short-term stability, above 30 mV offers good stability, and above 60 mV excellent stability. The thumb rule can apply to ionic stabilizers, but not for large or large molecular weight surfactants such as tween 80, which are nonionic stabilizers that provide steric stability.[9,11] The ANOVA confirmed and accepted the alternative hypothesis and rejected the null hypothesis due to there being a significant relationship between oil content and particle size as a dependent variable, where the p value ≤ 0.05. AFM enables precise characterization of nanocarriers, revealing surface morphology, size, and mechanical properties. Its high-resolution imaging ensures quality control, advancing nanocarrier development for effective drug delivery and targeted therapies. The results show that the NE5 formula contains particles with regular smooth surfaces and nearly spherical shapes with nanometer-sized pores, as shown in Figure 2. There was no particle aggregation, indicating the physical stability of the preparation. Organoleptic assays assess nanoemulgel's sensory attributes like color, odor, and texture, ensuring patient acceptance. These evaluations enhance product appeal and compliance, crucial for the success of innovative pharmaceutical and cosmetic formulations. It was performed that HN1-HN5 formulations show clear, homogenous, with the characterized odor of EOs represented by peppermint oil and myrtle oil. No syneresis was observed, which indicates high physical stability.[12-14] The pH is critical in nanoemulgel formulations, ensuring stability, compatibility with skin, and therapeutic effectiveness. Proper pH balance minimizes irritation, enhances drug delivery, and preserves the formulation's integrity during storage and application. It was found that an increment in the EO concentration slightly increased the pH. The outcomes provided suitable pH that guaranteed patient comfort and prevented skin allergic reactions and dermatitis.[12-14] The ANOVA showed a significant relationship between the dependent factor, which was pH, and the quantity of EO at the level ($p \leq 0.05$). Spreadability measures the ease of application of a nanoemulgel, ensuring uniform distribution on the skin. Optimal spreadability enhances user comfort, drug penetration, and overall efficacy of the therapeutic formulation. It was found that formulations containing peppermint oil had greater spreadability than formulations that contained myrtle oil for a similar quantity of oil at a constant concentration of surfactant mixture (1:0.75), this is because peppermint oil that has been used in the experiment was less viscous than myrtle oil. Also, it was found that the quantity of peppermint oil and myrtle oil increased at the constant quantity of polyoxyethylene (80) sorbitan monooleate, propylene glycol, and carbomer 940, leading to decreased spreadability parameter due to increased viscosity of EO hand nanoemulgel (HN1-HN5) formulations. Generally, the outcome indicates low spreadability time for all EO hand nanoemulgel (HN1-HN5) formulations that enhance patient compliance upon application on the skin.[12-14] The ANOVA indicates a significant relationship between the spreadability and experimental oil (peppermint and myrtle oil) at the level ($p \leq 0.05$). Viscosity determines the nanoemulgel's consistency, impacting application, stability, and drug release. An optimal viscosity ensures smooth spreading, prevents phase separation, and enhances the formulation's performance, making it suitable for therapeutic and cosmetic applications. The obtained data include the shear rate, shear stress, and viscosity. The outcome of viscosity as shown in Table 3 indicates that the quantity of EO increase leads to increase viscosity at a constant concentration of polyoxyethylene (80) sorbitan monooleate and propylene glycol mixture 1:0.75 (*w/w*) %; therefore, it was found the value of viscosity at 12 rpm in (mP.s) units were HN1 = 3074.68, HN2 = 3186.55, HN3 = 3107.33, HN4 = 3203.41, and HN5 = 3195.26. This is due to the increase in the volume concentration of nanoglobules, which makes the colloidal dispersion system more resistant to flow. In addition, decreasing the aqueous phase volume will reduce the continuous phase volume and make the nanosystem more viscous. The rheogram chart was obtained by plotting the shear rate (1/sec) against the shear stress (mP.s), as shown in Figure 3. All EO hand nanoemulgel (HN1-HN5) formulations show plastic flow, which is a non-Newtonian flowing system because there is no gel flowing related to shear stress until it reaches a specific transition point. This plastic flow made formulations easier to wipe on infected skin or membranes and provided additional stability to EO hand nanoemulgel (HN1-HN5) formulations. ANOVA confirmed a significant relationship ($p \leq 0.05$) between viscosity and EO.[12-14] Skin irritation studies are essential in nanoemulgel formulation to ensure safety and patient comfort. By assessing potential skin reactions, these studies help optimize ingredients, prevent adverse effects, and guarantee that the formulation is suitable for sensitive skin. Ultimately, they enhance the therapeutic effectiveness and

consumer acceptability of the product. It was found that all formulations did not produce a sense of skin itching, irritation signs, or any painful skin effect after the application of gel to the participants in the experiment. This indicates that all EO hand nanoemulgel (HN1-HN5) formulations are comfortable and well-tolerated. *In vitro* antimicrobial activity determination is crucial in nanoemulgel formulations to evaluate their effectiveness against pathogens. This testing ensures the formulation's therapeutic potential, supporting its use in treating infections and promoting skin health. It was found no *S. aureus* activity in the HN1 and blank gel (HN6) formulations. The comparability profile of bacterial susceptibility for *S. aureus* was in the following ascending order: HN2 < HN3 < HN4 < HN5. The bacterial susceptibility profiles were significantly higher ($p < 0.05$) for HN5 and significantly lower ($p < 0.05$) for HN2, as shown in Table 4. It was found that *S. aureus* was relatively more sensitive to formulations containing myrtle oil as HN3 and HN4 than those containing peppermint oil as HN1 and HN2 at the same concentrations. It was found that EO hand nanoemulgel (HN1-HN5) formulations had higher microbial activity against *E. coli* than *S. aureus*, as shown in Figure 4. There was no *E. coli* activity in the HN1 and blank gel (HN6) formulations. The comparability profile of bacterial susceptibility for *E. coli* was in the following ascending order: HN2 < HN3 < HN4 < HN5. The bacterial susceptibility profile was significantly higher in microbial growth inhibition for HN5 and significantly lower ($p \leq 0.05$) in microbial growth inhibition for HN2, as shown in Table 4. It was found that a mixture of EOs increased activity against microbial growth, as shown by the HN5 formulation was significantly higher ($p \leq 0.05$) in microbial susceptibility for *S. aureus* and *E. coli*.

CONCLUSION

The new method, which is based on microwaves, proved the success of the task in preparing nanoemulsions NE1-NE5,which were used in EO nanoemulgel HN1-HN5 formulations that makes it the most high-level technique for nanocarrier preparation. The great trend toward the use of skin antiseptics and the presence of some side effects of alcoholic antiseptics enhances the status of vegetable EOs and their use as successful alternatives in the process of cleansing the skin and combating germs for various groups of human society. This study proved the effectiveness of vegetable EOs in combating germs, and that mixing these EOs gives additional strength and motivation toward combating germs, as in the HN5 formulation that contains peppermint oil: myrtle oil (1:1) % *w/w*, which shows greater antimicrobial activity against *S. aureus* and *E. coli*.

Acknowledgements

The authors would like to thank Prof. Dr. Hasan Shakir Majdi, President of Al-Mustaqbal University for scientific research support.

Ethics

Ethics Committee Approval: The study was ethically approved by the Research Ethics Committee of Al-Mustaqbal University/ College of Pharmacy (approval number: pHa2/2023, date: 10.02.2023).

Informed Consent: Informed consent was obtained.

Conflict of Interest: The authors have no conflicts of interest to declare.

Financial Disclosure: This project was made possible with financial support from Al-Mustaqbal University (grant number: MUC-M-0222).

REFERENCES

1. Golin AP, Choi D, Ghahary A. Hand sanitizers: A review of ingredients, mechanisms of action, modes of delivery, and efficacy against coronaviruses. Am J Infect Control. 2020;48:1062-1067.
2. Prajapati P, Desai H, Chandarana C. Hand sanitizers as a preventive measure in COVID-19 pandemic, its characteristics, and harmful effects: a review. J Egypt Public Health Assoc. 2022;97:6.
3. Chouhan S, Sharma K, Guleria S. Antimicrobial activity of some essential oils-present status and future perspectives. Medicines (Basel). 2017;4:58.
4. Vostinaru O, Heghes SC, Filip L. Safety profile of essential oils. In Essential OilsBioactive Compounds, New Perspectives and Applications. Intech Open. 2020;27:1-13.
5. Booq RY, Alshehri AA, Almughem FA, Zaidan NM, Aburayan WS, Bakr AA, Kabli SH, Alshaya HA, Alsuabeyl MS, Alyamani EJ, Tawfik EA. Formulation and Evaluation of alcohol-free hand sanitizer gels to prevent the spread of infections during pandemics. Int J Environ Res Public Health. 2021;18:14-26.
6. Mohamadi Y, Lograda T, Ramdani M, Figuérédo G, Chalard P. Chemical composition and antimicrobial activity of Myrtus communis essential oils from Algeria. Biodiversitas. 2021;22:933-946.
7. Tiwari RK, Tripathi D, Singh L, Sharma V, Verma S. Development and antibacterial characterization of mint handwash. Int J Res Publ. 2018;9:25-32.
8. El-Sheikh MA. El-Sharary A. Preparation, characterization, and antibacterial efficacy of green aromatic soap. Egypt J Chem. 2022:385-393.
9. Kadhim DH, Hussein AA. Formulation and characterization of carvedilol nanoemulsion oral liquid dosage form. Int J Pharm Sci. 2015;7:209-216.
10. Kadhim DH, Hussein AA. Formulation characterization and evaluation of meloxicam nanoemulgel to be used topically. Iraqi J Pharm. Sci. 2017;26:9-16.
11. Drais HK, Ahmed AH. Lipid-polymer hybrid nanocarriers for oral delivery of felodipine: formulation, characterization and ex vivo evaluation. Adv Pharm Bull. 2022;12:791-800.
12. Eid AM, Issa L, Al-Kharouf O, Jaber R, Hreash F. Development of coriandrum sativum oil nanoemulgel and evaluation of its antimicrobial and anticancer activity. Biomed Res Int. 2021;2021:5247816.
13. Booq RY, Alshehri AA, Almughem FA, Zaidan NM, Aburayan WS, Bakr AA, Kabli SH, Alshaya HA, Alsuabeyl MS, Alyamani EJ, Tawfik EA. Formulation and Evaluation of alcohol-free hand sanitizer gels to prevent the spread of infections during pandemics. Int J Environ Res Public Health. 2021;18:14-26.
14. Diviyagahage CM, Thuvaragan S, Gnanakarunyan T, Srikaran R. Formulation and characterization of essential oils based antibacterial hand sanitizer gels. Pharmaceutical Journal of Sri Lanka. 2021;11:14-26.

Turk J Pharm Sci 2024;21(5):463-473
DOI: 10.4274/tjps.galenos.2023.26243

ORIGINAL ARTICLE

Evaluation of Anticancer and Antioxidant Activities (*In Vitro* Studies) of Coffee Stem Parasite Extract [*Scurrula ferruginea* (Roxb. ex Jack) Danser] and *In Silico* Studies of its Isolate

Destria ROZA[1]*, Gianna FADHILAH[2], Eka INDRIANI[1], Yuli Asih WILIRANTI[1], Tita JUWITANINGSIH[1]

[1]Medan State University Faculty of Mathematics and Natural Sciences, Chemistry Study Program, Medan, Indonesia
[2]National Taiwan University of Science and Technology, Department of Chemical Engineering, Taipei, Taiwan

ABSTRACT

Objectives: The coffee parasite *Scurrula ferruginea* (Roxb. ex Jack) Danser has been shown to exhibit various biological activities. Based on previous pharmacological studies, coffee parasites are effective for treating cancer or cytotoxicity and are vasorelaxant. The aim of this study was to examine the potential of the worm *S. ferruginea* (Roxb. ex Jack): danser on coffee stems as a natural anticancer.

Materials and Methods: *In silico* and *in vitro* studies have been conducted on coffee stem parasite extracts to analyze compounds that have the potential to act as human epidermal growth factor 2 (HER2) inhibitors, the antioxidant activity of the extract, and the extract's ability to act as an anticancer agent against HeLa and MCF-7 cells.

Results: The results show that several components of the coffee stem parasite extract, including flavonoids and fatty acids, have the potential to act as HER2 inhibitors. The coffee stem parasite extract has strong antioxidant activity with an IC_{50} of 59,736 ppm and it is inactive against cancer cells. Characterization using gas chromatography-mass spectrometry revealed the presence of bis (2-Ethylhexyl) phthalate (C24H38O4) in the coffee stem parasite extract, which is toxic as an anticancer drug.

Conclusion: Although coffee stem parasite extract does not function as an anti-cancer agent, its strong antioxidant activity has potential for other applications.

Keywords: Anticancer, antioxidant, bis (2-Ethylhexyl) phthalate, coffee parasite, HER2 inhibitors

INTRODUCTION

The *Loranthaceae* family includes the coffee parasite stems [*Scurrula ferruginea* (Roxb. ex Jack) Danser], also known as *Loranthus ferrugineus*, which is hemiparasitic, whose roots attach to the host plant to access nutrients and water (Table 1). The community traditionally uses the coffee parasite as cough medicine for tonsillitis, measles, diabetes, and cancer.[1] Coffee parasites have been shown to exhibit various biological activities, including antioxidant, neuroproactivity, anti-nephrotoxic, antiviral, anti-inflammatory, antihepatotoxic, anti-inflammatory, antidiabetic, antimicrobial, antihypertensive, antioxidant, antidiarrheal, and anti-inflammatory properties. Immunomodulatory and hypolipidemic.[2-5] Based on previous pharmacological studies, coffee parasites are effective for treating cancer or cytotoxicity and are vasorelaxant.[6-8]

The parasite belonging to the Loranthus family comprises 82% crude fiber, 9% water, 3% crude protein, 2% ash, 1% crude fat, and 3% other substances.[2] The total phenolic content, which

*Correspondence: destriaroza@unimed.ac.id, ORCID-ID: orcid.org/0000-0002-7528-260X
Received: 04.08.2023 , Accepted: 17.12.2023

includes phenolic acids, anthocyanins, tannins, and flavonoids, was also the highest in the water fraction.[8] Secondary metabolites in coffee parasites that have been identified include fatty acids: oleic acid, linoleic acid, linolenic acid, octadic-8-10 dinoic acid, (Z)-octade-12-ene-8-10-dioate acid, and octadeca-8-10-12-trinoic acid; quercitrin, quercetin, rutin, icariside B2, aciculin, (+)-catechin, (-)-epicatechin, (-)-epicatechin-3-O-gallate and (-) epigallocatechin-3-O-gallate, choline, isoleucine, catechins, leucine, sesquiterpenes, and chlorogenic acid.[9,10] Three natural flavonol compounds, including quercetin and quercitrin, a flavonol glycoside, have been isolated from the ethyl acetate fraction of coffee parasite stems.[8]

The aim of this study was to examine the antioxidant bioactivity of the coffee parasite stem extract and its effect on MCF-7 and HeLa breast cancer cells. The polar and stem fractions of the coffee parasite contained the highest levels of phenolic chemicals and bioactivity.[6-8] Based on these findings, this study was first conducted *via in silico* studies to predict compounds of coffee stem parasites that are active as anti-cancer. The study continued with the *in vitro* method to determine its antioxidant and anticancer. Isolation of secondary metabolites from coffee stem parasites was also performed.

MATERIALS AND METHODS

In silico study

The three-dimensional structure of the human epidermal growth factor 2 (HER2) receptor with protein data bank code 3PP0 was prepared by separating the structure from the ligand and water attached to the receptor using the Discovery Studio device. The chemical data from PubChem (https://pubchem.ncbi.nlm.nih.gov) provided the chemical structures of all the ligands in the form of bioactive chemicals for coffee parasites. Then, the ligands used for molecular docking are parameterized using AutoDock Tools. According to Lipinski's rules, the bioavailability and prediction of toxicity ligands were analyzed for their bioavailability by accessing the website http://www.scfbioiitd.res.in/software/drugdesign/lipinski.jsp. Ligands that have complied with Lipinski's rules are then predicted for their toxicity by accessing the http://lmmd.ecust.edu.cn/admetsar2 page. Validation of the molecular docking method, the tethered ligand 2-{2-[4-({5-chloro-6-[3-(trifluoromethyl) phenoxy]pyridine-3-yl}amino)-5H-pyrrolo[3,2-d] pyrimidine-5-yl]ethoxy}ethanol attached to the chain was separated first and prepared. Then, the AutoDock Tools application was used for directed molecular docking. The grid box has 8 x 16 x10 dimensions with center points x= 16,564, y= 17,282, z= 26,889, and space= 1.00. Molecular docking was performed ten times to obtain a root mean square deviation (RMSD) < 2.5 Å at least three times. Molecular docking was performed using a command prompt program. The molecular docking results can be seen in an out document with the *.pdbqt format opened using the Discovery Studio Visualizer application. A log file is a document that contains data on affinity energy values (ΔG/binding affinity) in kcal/mol units. 2D visualization was performed using the Ligplot+ application.

Sample preparation

The plant material used was the stem of *S. ferruginea* (Roxb. ex Jack) *Danser* obtained it in Sidikalang District, Dairi Regency. Plant identification was carried out at the Herbarium Medanese in December 2020. This study was conducted to determine whether the taxonomy of the plants used in the study was the same as that in the reference, resulting in more accurate results.

The mashed sample, which weighed 2 kg, was macerated by immersion in acetone for three consecutive days. A Buchner funnel was used to filter the resulting macerate before it was evaporated.

Antioxidant activity measurement using the 2,2 diphenyl-1-picrylhydrazyl (DPPH) method

A standard Roswell Park Memorial Institute Medium liquid culture medium was utilized for the anti-cancer test; it contained 10% fetal bovine serum and 50 µL/50 mL of antibiotics. Cisplatin was introduced as a positive control. A dimethyl sulfoxide solvent, which is not hazardous to cells, was used to dissolve materials at various concentrations of 7.81, 15.63, 31.26, 62.50, 125, 500, and 1000 µg/mL. PrestoBlueTM Cell Viability Reagent is the appropriate working solution. HeLa cervical cells and MCF-7 breast cancer cells were cultured in 96-well plates and incubated at 37 ˚C in an atmosphere containing 5% CO_2 until 70% of the cells had grown. Presto blue working reagent was applied to the cells, which were then incubated for 48 hours at 37 ˚C in an atmosphere of 5% CO_2. The absorbance of the cells was then measured using a multimode reader.

For isolation, the extract was fractionated with vacuum column chromatography, and thin-layer chromatography (TLC) was used to identify each fraction. The resulting fractions upon separation were purified using column chromatography with an appropriate eluent until pure isolates were obtained. Pure isolates were characterized by the presence of a single spot in the TLC test for different eluents. Pure isolates were identified using gas chromatography-mass spectrometry (GC-MS).

RESULTS

Findings of in silico test

First, the molecular docking method was validated using natural receptors and ligands attached to the structure. The HER2 3PP0 receptor has a natural ligand, namely the molecule 2-{2-[4-({5-chloro-6-[3-(trifluoromethyl) phenoxy] pyridine-3-yl} amino)-5H-pyrrolo[3,2-d] pyrimidine-5-yl] ethoxy} ethanol. The natural ligand molecules were redocked ten times to validate their molecular docking. The average of the RMSD values from the ten conformations is 1.17 Å (Figure 1).

Accordig to Lipinski's rule, the ligand bioavailability of the coffee parasite's active ingredient was predicted (Table 2). Based on Lipinski's rule, several ligands such as Hexadecanoic acid, methyl ester; hexanedioic acid, bis(2-ethylhexyl) ester; Oleic acid; Linoleic acid; Linolenic acid; Quercitrin; Aviculin; (-)- Epicatechin-3-O-gallate; and (-) Epigallocatechin-3-O-gallate violate one of the five Lipinski rules. While Rutin violates

four of the five Lipinski rules. Further testing was then carried out without using the Rutin ligand because it was predicted to have poor bioavailability.

The study was then continued with toxicity testing. Based on the parameters of human Ether-a-go-go-related gene (herG), carcinogenicity, and toxicity, ligands such as 2,6-bis(1,1-dimethylethyl)-4-methyl phenol; 1,2-benzene-dicarboxylic acid, 2-butoxy-2-oxoethyl butyl ester; Quercetin; Aviculin; (-)-Epicatechin-3-O-gallate; and (-)Epigalocatechin-3-O-gallate are toxic ligands, so they cannot be used for further studies (Table 3).

Table 1. Coffee stem parasite classification

Kingdom	Plantae
Division	Spermatophyta
Class	Dicotyledonea
Order	Santalales
Family	Loranthaceae
Genus	Scurrula
Botanical name	*Scurrula ferruginea* (Roxb. ex Jackie) Danser
Synonym	*Loranthus ferrugineus*
Common name	Coffee stem parasites
Herbarium voucher	RG4664

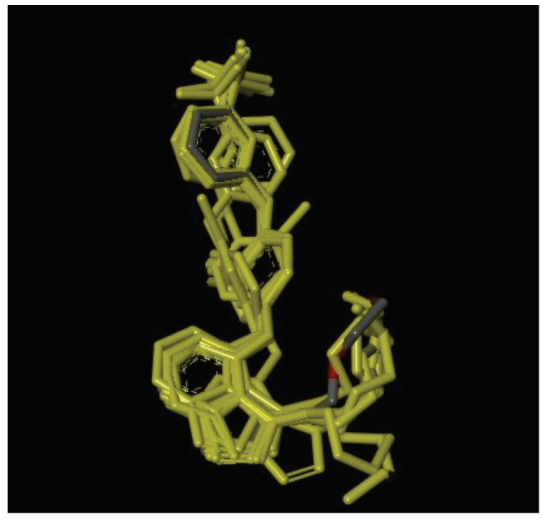

Figure 1. Molecular docking validation results. The average RMSD value is 1.17 Å

RMSD: Root mean square deviation

Table 2. Prediction of ligand bioavailability

Ligand name	Atomic mass	Hydrogen bond donor	Hydrogen bond donor	logP	Molar refractivity
2-Methoxy-4-vinyl phenol	150	1	2	2,044	44,750
2,6-bis(1,1-dimethyl ethyl)-4-methyl phenol	220	1	1	4,296	70,244
Hexadecanoic acid, methyl ester	270	0	2	5,641*	82,328
1,2-benzene dicarboxylic acid, 2-butoxy-2-oxoethyl butyl ester	336	0	6	3,144	87,782
Hexanedioic acid, bis(2-ethylhexyl) ester	370	0	4	6,066*	106,998
Oleic acid	282	1	2	6,109*	87,088
Linoleic acid	280	1	2	5,885*	86,994
Linolenic acid	280	1	2	5,885*	86,994
Octadeca-8-10-dinoic acid	276	1	2	4,779	84,266
Octadeca-8-10-12-trinoate	272	1	2	4,002	82,808
Quercitrin	448	7	11*	0,297	104,862
Quercetin	302	5	7	2,011	74,050
Rutin	610*	10*	16*	-1,879*	137,496
Aviculin	506	6*	10	0,640	126,305
(+)- Catechin	290	5	6	1,546	72,623
(-)- Epicatechin	290	5	6	1,546	72,623
(-)- Epicatechin-3-O-gallate	442	7*	10	2,528	107,256
(-) Epigallocatechin-3-O-gallate	458	8*	11	2,233	108,921

*Lipinski rule violation

Natural ligands in the molecular docking process have the lowest energy than other ligands. Cyclophosphamide, which is commonly used to treat breast cancer, has the greatest energy when interacting with HER2 receptors. Compared with cyclophosphamide and other active compounds of the coffee parasite, catechins and epicatechin have the most negative energy (Table 4). In addition, there are several amino acids related to catalytic activity (yellow highlights in Table 4) detected in all visualized ligands (Figure 2).

Antioxidant activity

The investigation continued with an antioxidant test before an anticancer test to directly demonstrate its effectiveness. Figure 3 and Table 5 present the results of the antioxidant activity test performed on the ethanol extract of the parasitic coffee stem, revealing that the IC_{50} value was 59.736 ppm.

Anticancer activity

The extract activity test was continued for cancer testing, namely on HeLa cervical cancer cells and MCF-7 breast cancer cells, based on the coffee parasite stem's substantial IC_{50} antioxidant strength. The IC_{50} values of the coffee parasite extract against HeLa cervical cancer cells and MCF-7 breast cancer cells were 11825.83 µg/mL and 9084.37 µg/mL, respectively (Figure 4). The majority of HeLa and MCF-7 cells were harmed or dead at a dosage of 1000 µg/mL, despite the fact that the ethanol extract of the coffee parasite was weak or ineffective against the two cancer cells (Figure 5).

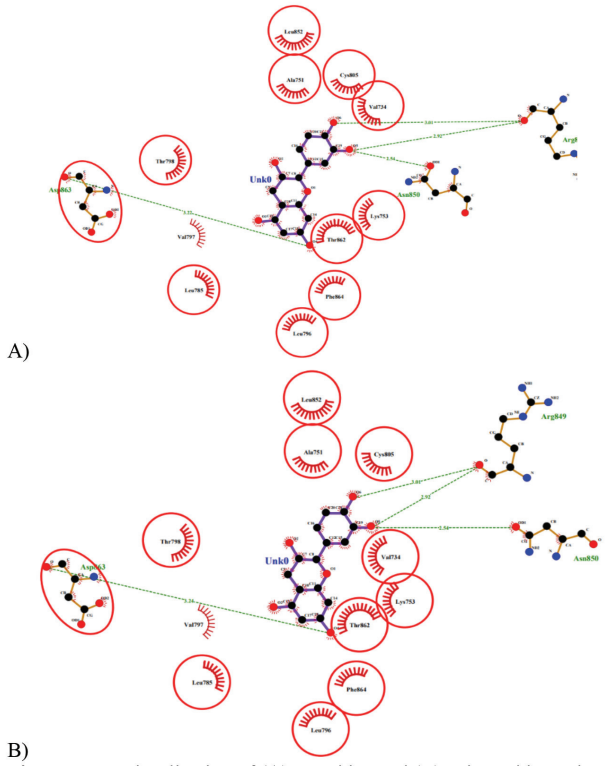

Figure 2. 2D visualization of (A) catechins and (B) epicatechin against receptors. The red circle indicates hydrophobic interactions between amino acids and ligands that interact on the same side of the receptor as the natural ligand. The dashed green line indicates hydrogen interactions between amino acids and ligands that interact on the same side of the receptor as that of the natural ligand.

Table 3. Prediction of ligand toxicity

Ligand name	herG		Carcinogenicity		Acute oral toxicity	
	Category	Score	Category	Score	Category	Score
2-Methoxy-4-vinyl phenol vinyl phenol	Weak inhibitor	0.719	Non-carcinogenic	0.630	III	0.860
2,6-bis(1,1-dimethylethyl)-4-methyl phenol	Weak inhibitor	0.749	Carcinogenic*	0.629	III	0.827
Hexadecanoic acid, methyl ester	Weak inhibitor	0.408	Non-carcinogenic	0.600	III	0.859
1,2-benzene-dicarboxylic acid, 2-butoxy-2-oxoethyl butyl ester	Strong inhibitor*	0.785	Non-carcinogenic	0.729	IV	0.792
Hexanedioic acid, bis(2-ethylhexyl) ester	Weak inhibitor	0.621	Non carcinogenic	0.671	IV	0.772
Oleic acid	Weak inhibitor	0.394	Non-carcinogenic	0.671	IV	0.829
Linoleic acid	Weak inhibitor	0.461	Non-carcinogenic	0.671	IV	0.829
Linolenic acid	Weak inhibitor	0.360	Non-carcinogenic	0.671	IV	0.639
Octadeca-8-10-dinoic acid	Weak inhibitor	0.580	Non-carcinogenic	0.671	IV	0.448
Octadeca-8-10-12-trinoate	Weak inhibitor	0.689	Non-carcinogenic	0.671	IV	0.448
Quercitrin	Weak inhibitor	0.635	Non-carcinogenic	0.986	III	0.518
Quercetin	Weak inhibitor	0.841	Non-carcinogenic	1.000	II*	0.735
Aviculin	Strong inhibitor*	0.726	Non-carcinogenic	0.971	III	0.618
(+)-Catechins	Weak Inhibitor	0.468	Non-carcinogenic	0.929	IV	0.643
(-)-Epicatechin	Weak Inhibitor	0.468	Non-carcinogenic	0.929	IV	0.643
(-)-Epicatechin-3-O-gallate	Strong Inhibitor*	0.855	Non-carcinogenic	0.986	IV	0.376
(-)Epigalocatechin-3-O-gallate	Strong Inhibitor*	0.892	Non-carcinogenic	0.986	IV	0.376

*Lipinski rule violation

Table 4. Molecular docking results

Ligand name	Energy affinity (kcal/mol)	Amino acid residues	Number of hydrophobic bonds	Number of hydrogen bonds	Hydrogen bond length
Natural ligand	-11.4	leu800; gly804; **leu726**; leu852; ala751; cys805; ser728; **val734**; **lys753**; **thr862**; **phe864**; **leu796**; **met774**; **leu785**; **ser783**; **gly729**; **asp863**; thr729; **met801**; gln799	18	2	Met801 3.03; Asp863 3.28
Cyclophosphamide (breast cancer therapy drug)	-5.4	**met801**; **leu726**; leu852; ala751; cys805; ser728; **val734**; **thr862**; **gly729**; gly727	10	0	
2-Methoxy-4-vinylphenol	-7.1	thr798; **ser783**; **lys753**; **thr862**; **phe864**; **leu796**; **met774**; **leu785**; **asp863**; ala 771	7	3	asp863 3.22; ser783 2.70; thr862 2.97
Hexadecanoic acid, methyl ester	-6.8	thr798; **asp863**; **lys753**; thr863; **phe864**; **leu796**; **met774**; **leu785**; **ser783**; arg784; ala771	8	3	asp863 3.24; thr863 2.93; ser783 2.71
Hexanedioic acid, bis(2-Ethylhexyl) ester	-7.6	**leu726**; leu852; ala751; cys805; ser728; **val734**; **lys753**; **thr862**; **phe864**; **leu796**; **met774**; **leu785**; **ser783**; **asp863**; thr798; **met801**; arg784; ile752; glu770; ala771	20	0	
Oleic acid	-7.2	leu800; **leu726**; leu852; ala751; **val734**; **lys753**; **thr862**; **phe864**; **leu796**; **met774**; **leu785**; **ser783**; **asp863**; thr798; **met801**; glu770; ala751	16	1	met801 2.79
Linoleic acid	-7.6	leu800; **leu726**; leu852; ala751; **val734**; **lys753**; **thr862**; **phe864**; **leu796**; **met774**; leu785; **asp863**; thr798; **met801**; glu770; ala751	15	2	met801 2.79 and 3.04, respectively
Linolenic acid	-7.6	leu800; gly804; **leu726**; leu852; **val734**; **lys753**; **thr862**; **phe864**; **leu796**; **met774**; **leu785**; **asp863**; thr798; **met801**; ala771	14	2	met801 2.79 and 2.92, respectively
Octadeca-8-10-dinoic acid	-7.5	leu800; **leu726**; leu852; ala751; **val734**; **lys753**; **thr862**; **phe864**; **leu796**; **leu785**; **asp863**; thr798; **met801**; ala771; glu770	14	2	met801 2.92 and 2.97, respectively
Octadeca-8-10-12-trinoate	-7.5	**met801**; leu800; gly804; **leu726**; leu852; ala751; **val734**; **lys753**; **thr862**; **phe864**; **leu796**; **met774**; leu785; **asp863**; glu770; ala771	16	0	
Quercitrin	-8.1	leu800; gly804; leu852; ala751; cys805; **leu726**; ser728; **val734**; **lys753**; **thr862**; **leu796**; **asp863**; **gly729**, thr798; **met801**; gly727	13	3	met801 2.54; asp863 3.21; leu726 2.86
(+)-Catechins	-9.3	thr798; ala751; leu852; cys805; **val734**; asn850; **lys753**; **thr862**; **phe864**; **leu796**; leu785; **asp863**; arg849; val797	11	4	asp863 3.22; asn850 2.54; arg849 2.92 dan 3.01
(-)-Epicatechin	-9.3	thr798; ala751; leu852; cys805; **val734**; asn850; **lys753**; **thr862**; **phe864**; **leu796**; leu785; **asp863**; arg849; val797	11	4	asp863 3.24;asn850 2.54; arg849 2.92 dan 3.01

Bold part: Amino acids on the binding site

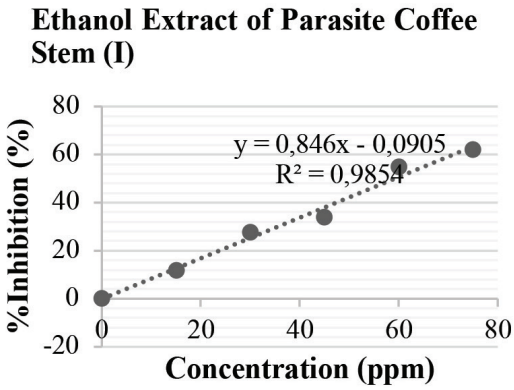

Figure 3. Diagram of antioxidant activity (DPPH) of the ethanol extract of parasite coffee stem. The IC50 value of 59,736 ppm indicates strong antioxidant activity

Isolation of secondary metabolites

After isolation of the extract of the coffee stem parasite in the polar fraction, it was found that the compound was classified as pure, which was shown as one spot in the TLC test. Identification using the GC-MS instrument (Figure 6 and Table 6) contained one main peak. At a retention time of 16.073 min, the peak was the highest in the analytical spectrum with the highest 100% abundance.

The identification results indicated that the compound was a bis (2-Ethylhexyl) phthalate compound with a relative molecular mass (m/z) of 149 and a molecular formula of $C_{24}H_{38}O_4$. The peak also provided a lib score (similarity) of 94.9%. The fragmentation peak (Figure 7) indicates that the fragmentation of the bis (2-Ethylhexyl) phthalate compound indicates the presence of a base peak at m/z 149, which is the peak of the molecular ion itself.

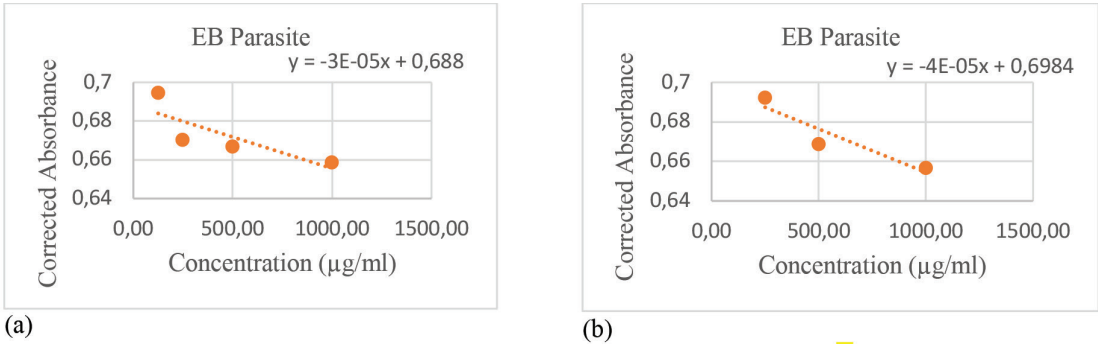

Figure 4. Parasite extract test results against (a) HeLa and (b) MCF-7 cells. The IC50 value of this coffee parasite extract against cancer cells was low or inactive

Table 5. Antioxidant activity test data (DPPH) of the ethanol extract of coffee stem parasites

Concentration (ppm)	Absorbance		Inhibition (%)	
	1st repetition	2nd repetition	1st repetition	2nd repetition
0	0.873	0.873	0.000	0.000
15	0.770	0.797	11.798	8.740
30	0.632	0.676	27.629	22.520
45	0.578	0.559	33.837	35.956
60	0.396	0.455	54.685	47.846
75	0.333	0.300	61.856	65.601

DPPH: 2,2 diphenyl-1-picrylhydrazyl

Table 6. Identification of compounds detected by GC-MS in fraction

Retention time (minute)	16,073
Area	4303860.41
Concentration (%)	100%
Probability (%)	100%
Compound Name	Bis (2-Ethylhexyl) phthalate
Score lib	94.9%

GC-MS: Gas chromatography-mass spectrometry

DISCUSSION

Findings of in silico test

The Lipinski's rule states that the log *p* value must be less than 5, the relative atomic mass value must be less than 500 Da, the hydrogen bond acceptor value must be less than 10, and the molar refractivity value must be in the range of 40-130.[11] Bioavailability analysis was carried out according to Lipinski's rule. This test is used as a guide for evaluating the drug design. Compounds that are ideal drugs must be adequately absorbed, distributed, metabolized, and excreted by the body. Compounds with an atomic mass exceeding 500 Da can reduce the passive diffusion ability of molecules because large molecules are difficult to penetrate cell membranes and take a long time to absorb.[11] Rutin compounds are predicted to have difficulty penetrating cell membranes and being absorbed by the body.

The quantity of hydrogen bond acceptors and donors also affects the capacity of a compound to cross the lipid bilayer membrane. Quercetin, rutin, aviculin, (-)-epicatechin-3-O-gallate, and (-) epigallocatechin-3-O-gallate are predicted to require more energy for absorption across the lipid bilayer membrane due to hydrogen bonding. In addition, the high hydrogen capacity requires more energy for the absorption process.[11]

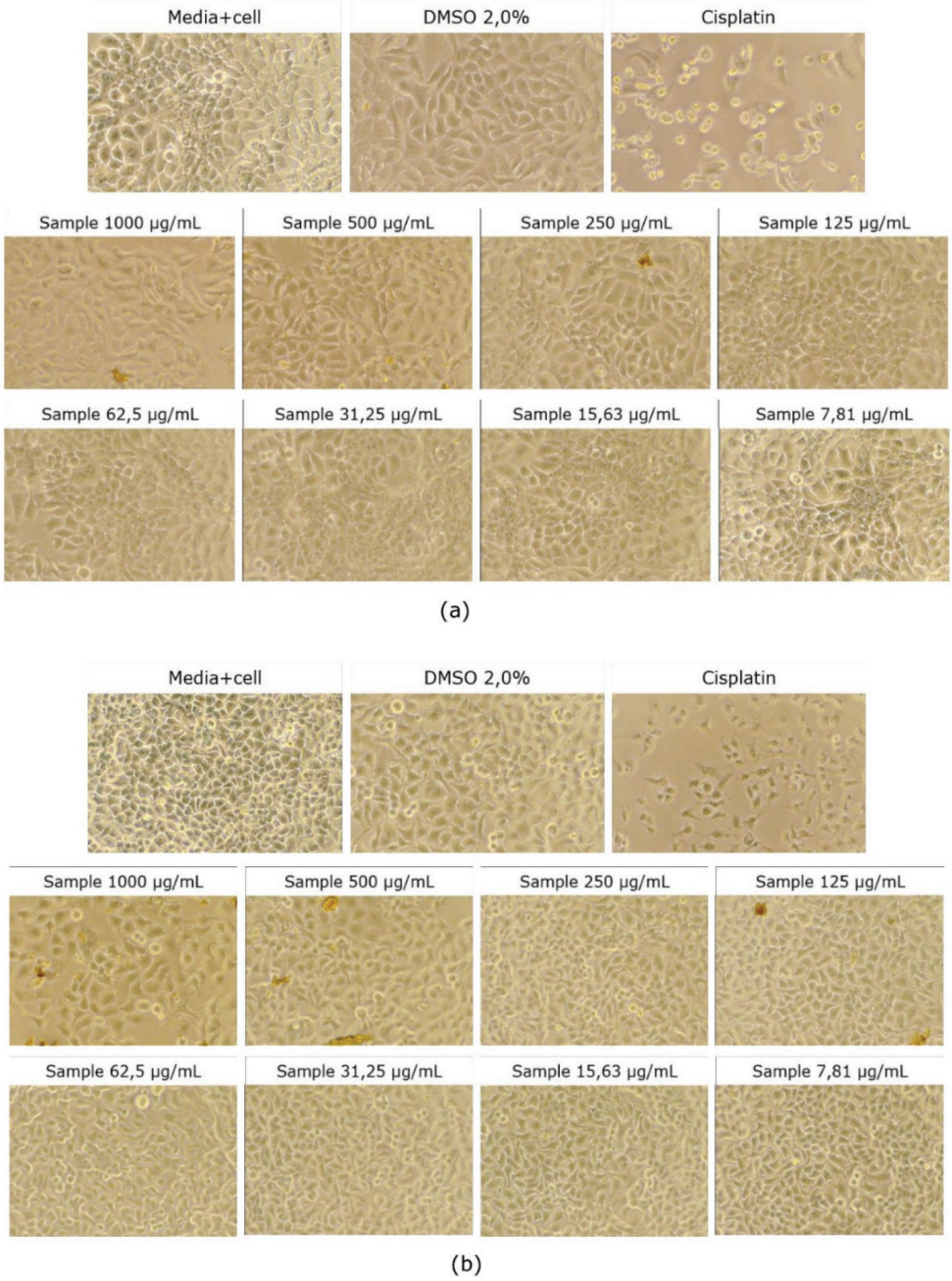

Figure 5. Documentation of the morphology of parasite extract test results (a) Hela cells (b) MCF-7 cells

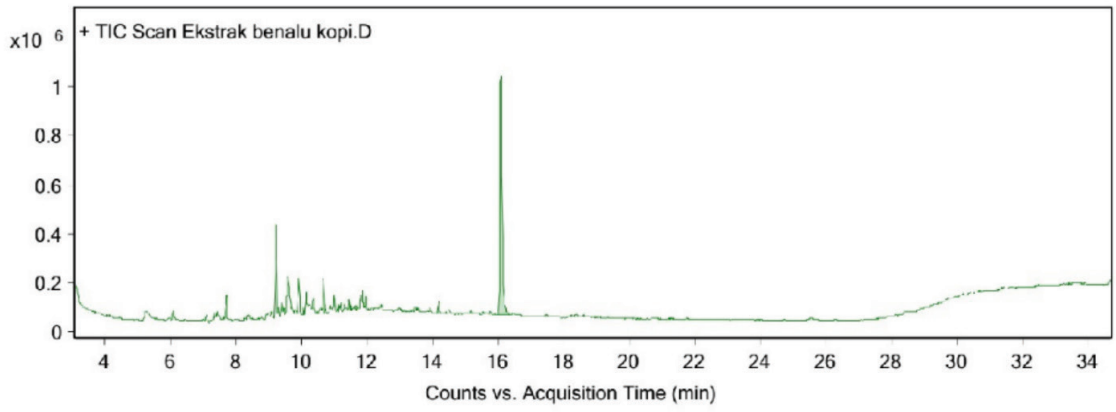

Figure 6. The spectrum of separation in GC-MS analysis shows an RT of 16.073 min, indicating 100% of bis (2- Ethylhexyl) phthalate
GC-MS: Gas chromatography-mass spectrometry, RT: Retention time

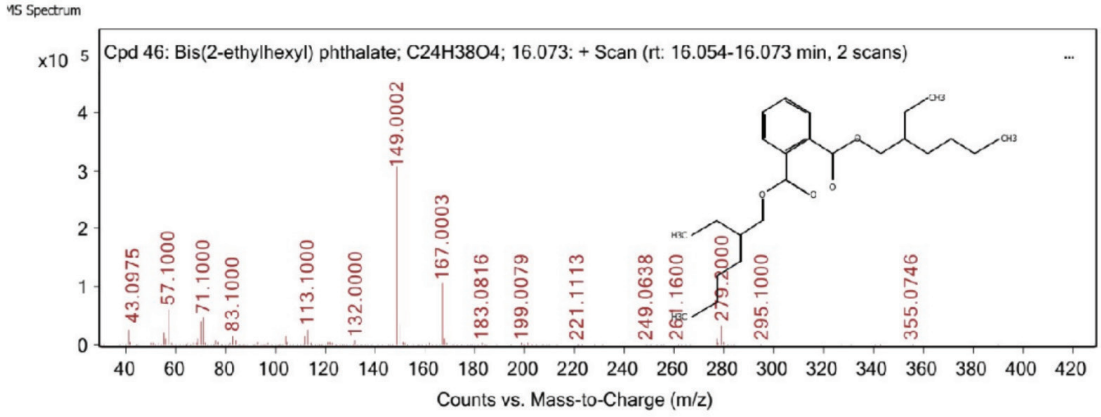

Figure 7. Peak fragmentation of compounds in GC-MS analysis showing the fragmentation of the bis (2-Ethylhexyl) phthalate
GC-MS: Gas chromatography-mass spectrometry

The log *p* value reveals a compound's hydrophobicity and lipophilicity. A negative log *p* value denotes a compound's high hydrophilicity, which prevents it from passing through the lipid bilayer. A log *p* value of more than five indicates high hydrophobicity; thus, the compound is challenging to enter the cell because it is trapped in the lipid bilayer. Drugs will be distributed more widely, thereby increasing their toxicity.[11,12] Hexadecanoic acid, methyl ester; hexanedioic acid, bis(2-Ethylhexyl) ester; oleic acid; linoleic acid; linolenic acid is indicated to be difficult to enter the cell because it is trapped in the lipid bilayer and its toxicity will increase. Rutin compounds are predicted to be unable to pass through the lipid bilayer.

The molar refractivity value indicates the distribution of the compound. Values between 40 and 130 indicate good distribution and absorption.[13] All active compounds in the coffee parasite showed good distribution and absorption. Rutin compounds violate 4 of 5 Lipinski's rules, so these compounds cannot be continued in the molecular docking process. Rutin compounds have poor bioavailability as drugs. Meanwhile, other compounds, except Rutin, only violated 1 of 5 Lipinski rules, so the ligand toxicity test was still allowed to proceed.

Tested ligands except rutin are continued to determine the drug's level of damage or adverse effects when consumed. The parameters used are human Ether-a-go-go-related gene (herG), carcinogenicity, and toxicity. HerG encodes a K+ ion channel that is involved in cardiac repolarization activity. If drug toxicity causes blocking of herG, sudden cardiac death occurs due to abnormal heart muscle repolarization.[14] Accordingly, 1,2-benzenedicarboxylic acid, 2-butoxy-2-oxoethyl butyl ester; aviculin; (-)-epicatechin-3-O-gallate; and (-)epigallocatechin-3-O-gallate were predicted to have adverse effects on herG.

Carcinogenicity tests are used to determine the potential of a compound to form tumors or cancers.[15] The carcinogenicity test results showed that 2,6-bis (1,1-dimethyl ethyl)-4-methyl phenol is carcinogenic. This compound is feared to trigger cancer and tumors when consumed.

Tested ligands except rutin are continued to determine the drug's level of damage or adverse effects when consumed. The parameters used are human Ether-a-go-go-related gene (herG), carcinogenicity, and toxicity. HerG encodes a K+ ion channel that is involved in cardiac repolarization activity. If drug toxicity causes blocking of herG, sudden cardiac death occurs

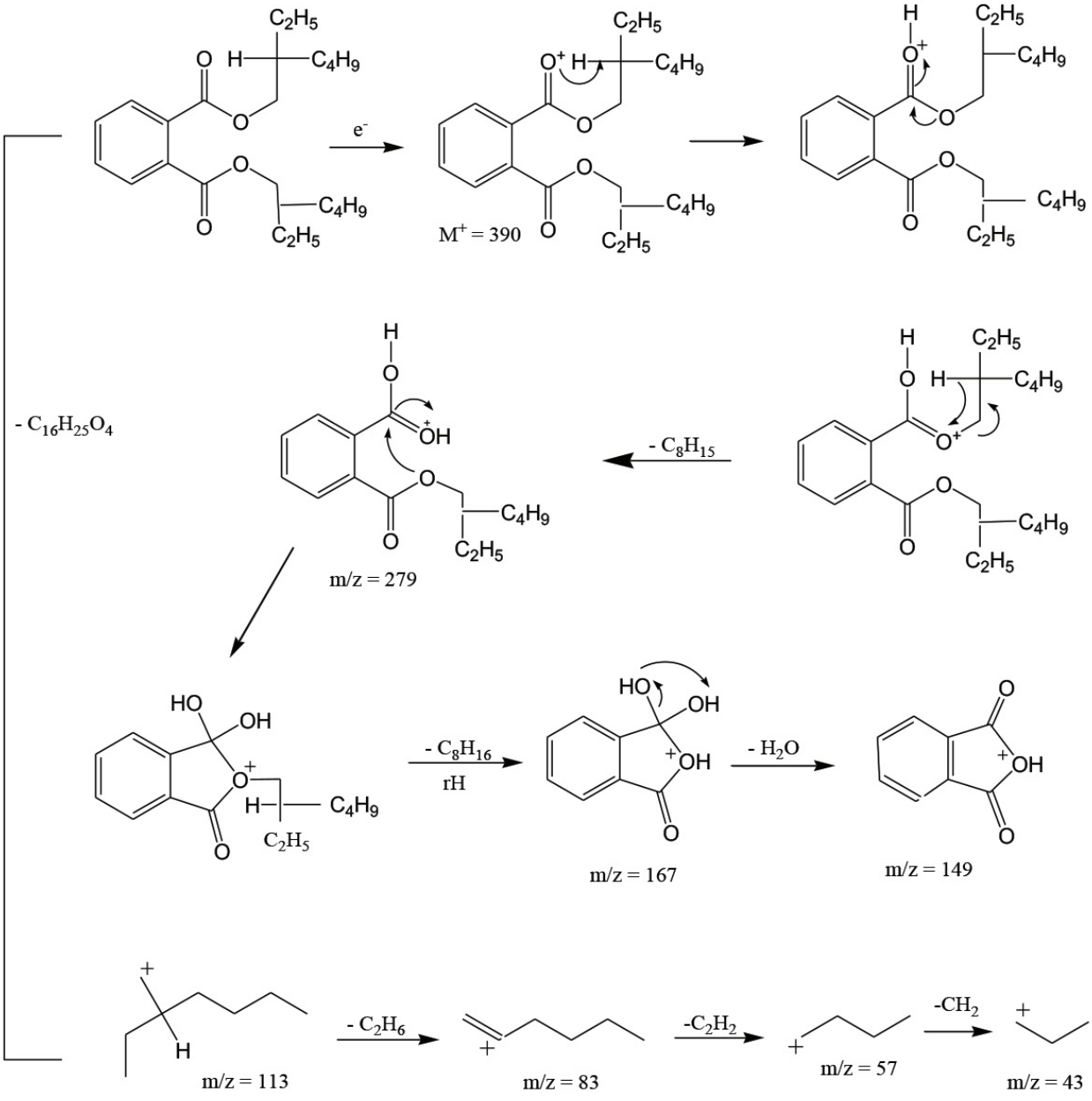

Figure 8. Fragmentation of bis (2-Ethylhexyl) phthalate compound

due to abnormal heart muscle repolarization.[14] Accordingly, 1,2-benzenedicarboxylic acid, 2-butoxy-2-oxoethyl butyl ester; aviculin; (-)-epicatechin-3-O-gallate; and (-)epigallocatechin-3-O-gallate were predicted to have adverse effects on herG.

Carcinogenicity tests are used to determine the potential of a compound to form tumors or cancers.[15] The carcinogenicity test results showed that 2,6-bis (1,1-dimethyl ethyl)-4-methyl phenol is carcinogenic. This compound is feared to trigger cancer and tumors when consumed.

There are four classifications of acute oral toxicity. Category 1 (LD_{50} 50 mg/kg), Category 2 (LD_{50} 500 mg/kg), Category 3 (LD_{50} 5000 mg/kg), and Category 4 (LD_{50} 5000 mg/kg) are the four different concentration categories. Categories 1 and 2 tended to be toxic, while Categories 3 and 4 were non-toxic.[16] Quercetin compounds are included in category 2, and they tend to be toxic and dangerous when consumed orally. In contrast, other compounds are included in the non-toxic category. Compounds that are not carcinogenic, do not block herG, and are not toxic are continued in the molecular docking process.

Negative values of affinity energy indicate the tendency of a compound to form spontaneous bonds so that the reaction does not require energy or is exothermic.[17] Catechins and epicatechin have the most negative energy, this means that these two ligands interact better with the HER2 receptor than breast cancer therapy drugs.

Several amino acids are associated with catalytic activity, including leu726; val734; lys753; thr862; phe864; leu796; met774; leu785; ser783; gly729; asp863; met801.[18] These 12 amino acids were detected in all visualized ligands. This visualization shows that natural and other ligands bind to the same side to produce the same affinity as natural ligands in inhibiting HER2 protein.[19]

The more the number of hydrophobic bonds, the more negative the affinity energy. The greater the number of hydrogen bonds, the greater the energy required to bond.[20] However, hexanedioic acid, bis(2-Ethylhexyl) ester has the most hydrophobic bonds and no hydrogen bonds; its affinity energy is not the most negative. Likewise, although catechins and epicatechin have the most hydrogen bonds, the energy required is not as large as that required for other ligands. Therefore, there is no relationship between the quantity of hydrogen bonds and the quantity of hydrophobic bonds to affinity energy. Hydrogen bonding also affects the strength of the ligand-receptor interaction. The shorter the hydrogen bond, the stronger the interaction.[21] Although natural ligands have the longest hydrogen-bond distances among other ligands, their interactions are still more potent than those of other ligands. Thus, the hydrogen bond length does not affect the binding affinity.

However, compounds such as 2-Methoxy-4-vinyl phenol; Hexadecanoic acid, methyl ester; Hexanedioic acid, bis(2-Ethylhexyl) ester; Oleic acid; Linoleic acid; Linolenic acid; Octadeca-8-10-dinoic acid; Octadeca-8-10-12-trinoate; Quercitrin; (+)-Catechins; (-)-Epicatechin has potential as anticancer agents because of their better binding affinity than commercial therapeutic drugs.

Antioxidant activity

The difference in absorbance between the absorbance of the sample and that of DPPH was measured using an ultraviolet-vis spectrophotometer. The DPPH technique (2,2-diphenyl-1-picrylhydrazyl) was used to quantitatively measure the antioxidant activity. The DPPH method is a test method to ascertain antioxidant activity to fend off free radicals. The percentage inhibition of DPPH free radicals by ethanol extract served as a measure of its antioxidant activity. A linear regression equation (Y= aX + b), where Y is 50, denoting 50%, and X is the IC_{50} value of the test sample, can be used to obtain the IC_{50} value. According to the IC_{50} value, the ethanolic extract has a strong antioxidant activity.[5]

Anticancer activity

According to The National Cancer Institute, the IC_{50} value of this coffee parasite extract is low or inactive.[22] The anticancer activity increased as the IC_{50} value decreased. Very powerful anticancer substances have an IC_{50} value of less than 50 ppm, strong anticancer substances have an IC_{50} value of 50-100 ppm, adequate anticancer substances have an IC_{50} value of 100-150 ppm, and a weak anticancer if it is between 151-200 ppm.[23] The coffee parasite extract is inactive as anticancer because it's IC_{50} value more than 150 ppm.

Isolation of secondary metabolites

The peak at m/z 279 comes from $C_{24}H_{38}O_4^+$ due to the release of $C_8H_{15}\bullet$ (1-Ethylhexyl) from the molecular ion, followed by the release of C_8H_{16} (octene) to form $C_8H_7O_4^+$, as shown at m/z 167. As a result, the ion releases H_2O and creates a base peak at m/z 149. The breakdown of two esters, which involves the rearrangement of two H atoms (McLafferty rearrangement) and the release of H_2O, results in the classic phthalate peak at m/z 149.[24] The molecular ion releases $C_{16}H_{25}O_4$ to generate $C_8H_{17}^+$, which is visible at m/z 113 and then releases C_2H_6 to form $C_6H_{11}^+$, which is visible at m/z 83. This fragmentation also occurs in carbon and oxygen bonding in ester compound. The release of C_2H_2 from C_6H_{11}, followed by the release of CH_2 to generate $C_3H_7^+$, as observed at m/z 43, causes $C_4H_9^+$ to reach its peak at m/z 57. Figure 8 provides a clearer illustration of the bis (2-Ethylhexyl) phthalate compound's fragmentation.

Bis (2-Ethylhexyl) phthalate is a secondary metabolite compound that belongs to the fatty acid group. Bis (2-Ethylhexyl) phthalate is cytotoxic, and it can damage cancer and normal cells.[24] However, it is still necessary to predict the toxicity and bioavailability of bis(2-Ethylhexyl) phthalate when used as an anticancer. The results of the bioavailability test show that the log *p* value of bis(2-Ethylhexyl) is 6.4330, which is more than five, indicating high hydrophobicity. Thus, the compound will be challenging to enter the cell because it is trapped in the lipid bilayer. Drugs will be distributed more widely, thereby increasing their toxicity. The bis(2-Ethylhexyl) toxicity was included in the strong inhibitor category with a score of 0.8276. It causes blocking of herG; there will be sudden cardiac death occurs due to abnormal heart muscle repolarization.

CONCLUSION

An *in silico* study of the coffee stem parasite [*S. ferruginea* (Roxb. ex Jack) Danser] showed that several flavonoids and fatty acid compounds have better potential as HER2 inhibitors than cyclophosphamide. The *in vitro* test results showed that the coffee stem parasite extract has potent antioxidant activity with an IC_{50} value of 59,7359 ppm. However, it is not active against HeLa and MCF-7 breast cancer cells. Isolation of secondary metabolites from the extract of coffee stem parasites revealed that they contained bis (2-Ethylhexyl) phthalate compounds, which are toxic if used as anticancer drugs. Although coffee stem parasite extract does not function as an anti-cancer agent, its antioxidant activity has potential for other applications.

Acknowledgments

The author would like to thank the funding assistance from Medan State University. The author would also like to express gratitude to the Dean and all academics of the Department of Chemistry, FMIPA University.

Ethics

Ethics Committee Approval: This article does not contain any studies with human or animal subjects.

Informed Consent: Informed consent is not applicable.

Authorship Contributions

Concept: D.R., G.F., Design: D.R., G.F., T.J., Data Collection or Processing: G.F., E.I., Y.A.W., Analysis or Interpretation: D.R., G.F., T.J., Literature Search: G.F., E.I., Y.A.W., T.J., Writing: D.R., G.F.

Conflict of Interest: The authors have no conflicts of interest to declare.

Financial Disclosure: This research was supported by the Medan State University PNBP Fund for the 2021 fiscal year.

REFERENCES

1. Pitojo S. Benalu hortikultura pengendalian dan pemanfaatan. Ungaran; Trubus Agriwidya; 1996.
2. Chen W, Weng YM, Tseng CY. Antioxidative and antimutagenic activities of healthy herbal drinks from Chinese medicinal herbs. Am J Chin Med. 2003;31:523-532.
3. Moghadamtousi SZ, Kamarudin MN, Chan CK, Goh BH, Kadir HA. Phytochemistry and biology of Loranthus parasiticus Merr, a commonly used herbal medicine. Am J Chin Med. 2014;42:23-35.
4. Manurung FDM. Uji skrining fitokimia, aktivitas antioksidan dan antibakteri ekstrak metanol dan etil asetat daun benalu kopi [*Scurulla ferruginea* (Roxb. ex Jack) Danser]. Skripsi, Kimia, Univesitas Sumatera Utara, Medan; 2016.
5. Baigi MM, Amini N, Supriyanto E, Jamil S, Khangholi S. Total phenolic content, antioxidant and antibacterial properties of *Scurrula ferruginea* extracts. J Teknol. 2014; 70.
6. Ameer OZ, Salman IM, Yam MF, Abd Allah HH, Abdulla MH, Shah AM, Asmawi MZ. Vasorelaxant properties of Loranthus ferrugineus Roxb. methanolic extract. Int J Pharmacol. 2009;5:44-50.
7. Ameer OZ, Salman IM, Quek KJ, Asmawi MZ. *Loranthus ferrugineus*: a Mistletoe from traditional uses to laboratory bench. J Pharmacopuncture. 2015;18:007-018.
8. Lohézic-Le Dévéhat F, Tomasi S, Fontanel D, Boustie J. Flavonols from *Scurrula ferruginea* Danser (Loranthaceae). Z Naturforsch C J Biosci. 2002;57:1092-1095.
9. Wong DZ, Kadir HA, Ling SK. Bioassay-guided isolation of neuroprotective compounds from Loranthus parasiticus against H_2O_2-induced oxidative damage in NG108-15 cells. J Ethnopharmacol. 2012;139:256-264.
10. Hong X, Mat Isa N, Fakurazi S, Safinar Ismail I. Phytochemical and anti-inflammatory properties of Scurrula ferruginea (Jack) Danser parasitising on three different host plants elucidated by NMR-based metabolomics. Phytochem Anal. 2020;31:15-27.
11. Syahputra G, Ambarsari L, Sumaryada T. Simulasi docking kurkumin enol, bisdemetoksikurkumin dan analognya sebagai inhibitor enzim 12-lipoksigenase. Jurnal biofisika. 2014;10:55-67.
12. Rachmania RA, Supandi, Larasati OA. Analisis in-silico senyawa diterpenoid lakton herba sambiloto (Andrographis paniculata Nees) pada reseptor alpha-glucosidase sebagai antidiabetes tipe II. Pharmacy. 2015;12:210-222.
13. Nindita LD, Sanjaya IGM. Modeling hubungan kuantitatif struktur dan aktivitas (HKSA) pinocembrin dan turunannya sebagai anti kankermodelling a quantitative structure and activity relationship (QSAR) in pinocembrin and its derivative as the anti-cancer. UNESA journal of chemistry. 2014;3:26-34.
14. Du-Cuny L, Chen L, Zhang S. A critical assessment of combined ligand- and structure-based approaches to HERG channel blocker modeling. J Chem Inf Model. 2011;51:2948-2960.
15. Aydın A, Aktay G, Yesilada E. A guidance manual for the toxicity assessment of traditional herbal medicines. Nat Prod Commun. 2016;11:1763-1773.
16. Guan L, Yang H, Cai Y, Sun L, Di P, Li W, Liu G, Tang Y. ADMET-score-a comprehensive scoring function for evaluation of chemical drug-likeness. Medchemcomm. 2018;10:148-157.
17. Du X, Li Y, Xia YL, Ai SM, Liang J, Sang P, Ji XL, Liu SQ. Insights into protein-ligand interactions: mechanisms, models, and methods. Int J Mol Sci. 2016;17:144.
18. Aertgeerts K, Skene R, Yano J, Sang BC, Zou H, Snell G, Jennings A, Iwamoto K, Habuka N, Hirokawa A, Ishikawa T, Tanaka T, Miki H, Ohta Y, Sogabe S. Structural analysis of the mechanism of inhibition and allosteric activation of the kinase domain of HER2 protein. J Biol Chem. 2011;286:18756-18765.
19. Rastini MBO, Giantari NKM, Adnyani KD, Laksmiani NPL. Molecular docking aktivitas antikanker dari kuersetin terhadap kanker payudara *in silico*. JCHEM. 2019;13:180-184.
20. Moretti A, Li J, Donini S, Sobol RW, Rizzi M, Garavaglia S. Crystal structure of human aldehyde dehydrogenase 1A3 complexed with NAD+ and retinoic acid. Sci Rep. 2016;6:35710.
21. Ernanda D. Penapisan virtual senyawa aktif tumbuhan manggis, meniran, dan klabet sebagai obat kanker ovarium [skripsi]. 2019. Bogor (ID): Institut Pertanian Bogor.
22. Suffness M, Pezzuto JM. *Methods for plant biochemical assays and bioactivity*. Methods in Plant Biochemistry. In: Hostettmann, 6th Edition, Academic Press, London. 1990;**6:**71-33.
23. Rini YC, Susilowati F, Amal ASS. Uji aktivitas antioksidan ekstrak etanol dan ekstrak air biji habbatussauda (Nigella sativa). Pharmaceutical Journal of Islamic Pharmacy. 2020;4:1-8. https://ejournal.unida.gontor.ac.id/index.php/pharmasipha/article/view/3945
24. Thenmozhi S, Rajan S. GC-MS analysis of bioactive compounds in Psidium guajava leaves. J pharmacogn phytochem. 2015;3:162-166.

Turk J Pharm Sci 2024;21(5):474-482
DOI: 10.4274/tjps.galenos.2023.56736

ORIGINAL ARTICLE

Longitudinal Evaluation of Developmental Protein Malnutrition Resembling Marasmic-Kwashiorkor Condition in Wistar Rats

Varsha AUGUSTIN[1], Murali BADANTHADKA[1]*, Madhura R.J.[1], Vinitha DSOUZA[1], B. Mohana KUMAR[2], A. Veena SHETTY[3]

[1]Nitte (Deemed to be University), Nitte Gulabi Shetty Memorial Institute of Pharmaceutical Sciences (NGSMIPS), Department of Nitte University Centre for Animal Research and Experimentation (NUCARE),Karnataka, India
[2]Nitte (Deemed to be University), K.S. Hegde Medical Academy, Nitte University Center for Stem Cell Research and Regenerative Medicine, Karnataka, India
[3]Nitte (Deemed to be University), K.S. Hegde Medical Academy, Academy, Department of Microbiology, Karnataka, India

ABSTRACT

Objectives: Protein malnutrition (PMN) is a significant public health concern that can aggravate pathological states. The impact of early malnutrition on metabolism needs extensive evaluation. Current models employ short-term diet restriction and are neither ethically correct nor clinically relevant. This study aimed to develop a PMN rat model to evaluate the effects of a low-protein diet (LPD) on physiological, hematological, biochemical, and histological changes affected by malnourishment from postweaning to the 40th week.

Materials and Methods: The PMN model was developed in Wistar rats (post-weaning) by assigning animals to patented LPD (10% protein) and a control group to a normal diet (18% protein). Developed model was confirmed by biometric, biochemcial parameters and Gomez classification of malnutrition.

Results: LPD-induced PMN showed stunted growth, altered biochemical (albumin range, 1.9 - 2.4 g/dL, total protein range, 5.1 - 6.4 g/dL), and hematological markers mean corpuscular volume (52.03 ± 1.34, 47.45 ± 0.44, p≤0.01), mean corpuscular hemoglobin (17.67 ± 0.47, 15.37 ± 0.18, p≤0.001) and mean corpuscular haemoglobin concentration (33.87 ± 0.22, 32.37 ± 0.24, p≤0.001) and significantly affected hepatic histology. A long-term study was conducted to analyze the pattern of developmental PMN and its stabilization over time.

Conclusion: The developed PMN rat model imitates clinical conditions and is confirmed as a stable, reproducible, and reliable model for short- and long-term studies. The clinical relevance of this approach opens new avenues for research in treatment, drug development, molecular interactions, and disease model development.

Keywords: Animal model, biochemical parameters, low protein diet, marasmic-kwashiorkor, protein malnutrition, rats

INTRODUCTION

Malnutrition is a condition caused by an imbalance in the intake of nutrients in terms of quantity, quality, or both at any point inlife.[1,2] A report by the Food and Agriculture Organization stated that 728 million people around the globe were malnourished in 2020.[3] World hunger statistics 2021 report a drastic increase of approximately 161 million malnourished people between 2019 and 2020. This crisis can be attributed to climate change and COVID-19 consequences.[4] Malnutrition at critical growth period results in short- or long-term metabolic impairments.[5] The metabolic activity of an individual is controlled by the nervous system, which generally develops in the early stage of life. Early undernutrition processes information to the nervous system for permanent self-programming to save energy in the form of fat and to reduce growth. This anatomical and physiological adaptation is required to secure survival under possible adverse conditions.[1,5]

*Correspondence: murali@nitte.edu.in, ORCID-ID: orcid.org/0000-0002-4313-5111
Received: 19.08.2023, Accepted: 23.12.2023

Malnutrition is not a disease; it is considered one of the primary concerns that lead to the burden of disease in developing countries. Protein malnutrition (PMN) can be categorized into three forms based on its clinical manifestations: kwashiorkor, marasmus, and an intermediate stage termed marasmic-kwashiorkor. Clinical features depend on the severity, duration, stage of life, and degree of nutritional deficiency.[6] Kwashiorkor is typically defined as edematous malnutrition, with clinical characteristics such as skin lesions, hair loss, hypoalbuminemia[7], and hepatic abnormalities (hepatomegaly and fatty infiltrations). Whereas marasmus isa form of non-edematous malnutrition characterized by significant weight loss, lack of subcutaneous fat, muscular atrophy, and a poor weight-for- height ratio.[8] Marasmic-kwashiorkor is a clinical manifestation characterized by a combination of the clinical features of two types of malnutrition. Body composition, gastrointestinal tract, liver, kidney, tissue protein, body fluids, plasma, and hormones are targets of protein-energy malnutrition-mediated physiological and functional changes.[9]

Experimental animal models serve as important sources of information for understanding the effects and consequences of various diseases and drug actions.[10] Laboratory animals are extensively used to assess the effects of variables at various degrees of malnutrition and individual pathologies related to malnutrition. The highly controlled evaluation of each nutritional parameter individually gave more consistent results in animal models than in humans. Nutritional insults like protein malnutrition during the early and developmental phases of life, induce weak hallmarks of metabolic malfunctions and can impair lifelong metabolism patterns.[11] Protein deficiency in Wistar rats induces changes in body weight and body and organ growth and leads to hepatic steatosis.[12] Malnutrition negatively affects biochemical parameters like total protein (TP) and albumin (ALB),[13,14] phosphorous[15], and triglyceride (TG).[16] Liver function markers such as alkaline phosphatase (ALP), aspartate aminotransferase (AST), and alanine aminotransferase (ALT) increase with malnutrition.[17,18]

The global prevalence of PMN requires a better understanding of the underlying pathophysiological mechanisms. The effects of undernutrition in humans are not restricted to early development but also exert lasting effects. However, studies on the consequences of long-term malnutrition and its metabolic risks are limited. It is necessary to have a stable, long-term, and clinically relevant malnutrition model to carry out this kind of research. Malnutrition models using different animals employ starvation/diet restriction, which are generally short-term models developed for context-specific experiments. This study aimed to develop a PMN rat model to evaluate the effects of a low-protein diet (LPD) on physiological, hematological, biochemical, and histological changes affected by malnourishment from postweaning to the 40th week.

MATERIALS AND METHODS

Chemicals and instruments

Semi-Auto Analyzer model: Star 21 Plus from Rapid Diagnostic Group of Companies, India; Automated hematology analyzer: Nihon Kohen, India; Biochemical reagent kits: Aspen Laboratories Pvt. Ltd., Formaldehyde (LobaChemie Pvt. Ltd., #01460). Normal diet (ND) (Amruth feeds, Pune, Maharashtra), Corn oil (Grainotch Industries Ltd., Cornlite), Sucrose (Shree Renuka Sugars Limited, Madhur sugars), Wheat bran (Liberty brand from local market), Vitamin mix (SIDDON BIOTECH, LBCE150205), Mineral mix (SIDDON BIOTECH, LBCE150203), Maize starch (SB-IMPEX, CHE150196).

Experimental animals

Healthy female Wistar rats were selected at weaning and housed in polypropylene cages with rice husk bedding at NUCARE (Nitte University Center for Animal Research and Experimentation). Standard laboratory conditions were maintained (12 hours light/dark cycle; temperature 22 ± 2 ˚C; relative humidity 60 ± 5%) were maintained with free access to food and water. All animal experiments were conducted according to the guidelines of the committee for the Purpose of Control and Supervision of Experiments on Animals (approval number: NGSMIPS/Dec-2020/2022, date: 29.12.2020).

Experimental design

The animals chosen were divided into two groups: ND and low-protein diet (LPD).[19,20] Details of the diet composition are presented in Table 1. The ND and LPD groups received anND (18% protein) and LPD (MB diet, 10% protein) *ad libitum*. Body weight and length (nose-to-anus length) were assessed weekly as biometrical parameters, and rats were classified into malnourished categories according to the Gomez classification of malnutrition.[21,3]

The body mass index (BMI) of rats was calculated using the standard formula.

Blood and tissue sampling

Blood was sampled on the first day of every alternate week by puncturing the retro-orbital plexus under isoflurane anesthesia. The collected blood samples were allowed to clot at room temperature and centrifuged at 3000 rpm for 5

Table 1. Composition of a LPD (10% protein) for the development of malnourished rat model

Serial number	Ingredients (ND)	g/kg	Ingredients (LPD)	g/kg
1	Wheat flour	56.2	ND	44.440
2	DCP (rock base)	1.8	Corn oil	2.415
3	Calcite powder	1.0	Sucrose	6.038
4	LAF premix	1.0	Wheat bran	3.019
5	Linseed	5.0	Vitamin mix	0.603
6	Maize gluten	5.0	Mineral mix	2.113
7	Roasted gram flour	25.0	Maize starch	41.360
8	Skimmed milk powder	5.0		

LPD: Low-protein diet, ND: Normal diet, DCP: Dicalcium phosphate, LAF: Laboratroy animal feed

minutes to separate the serum. At the end of the experiment, rats were euthanized using isoflurane anesthesia. Liver tissue was excised, washed, weighed, and fixed in 10% formalin for histopathological examination.

Hematological analysis

Blood samples collected in EDTA-coated tubes were analyzed immediately after collection using an automated hematology analyzer.

Serum biochemical analysis

Biochemical parameters were quantified using standard commercial kits according to the manufacturer's instructions. Stored serum samples were thawed and analyzed for ALB, TP, TG, phosphorous, AST, ALT, and ALP.

Statistical analysis

Statistical analysis was performed using the mean population and standard error of the mean. The test of significance or statistical analysis was the Student's t-test. $p \leq 0.05$ was considered statistically significant. The Graph Pad Prism (version 8.4.3) (GraphPAD, San Diego, CA, USA) software was used for statistical analysis.

RESULTS

Biometric parameters

The body weight and BMI of the LPD group were significantly decreased ($p \leq 0.001$) compared with the normal age-matched rats. Body weight increased in the ND group during the first 6 weeks, after which it stabilized. The gradual rate of weight gain in LPD patients may be attributed to lower dietary protein (Figure 1A, B).The body weight and BMI of the LPD group confirm the development of a stable malnourished rat model compared with age-matched controls. The LPD group animals were categorized into various degrees of malnutrition based on the principles of Gomez classification concerning the body weight of the ND group rats. By the end of week 1, LPD shows grade II malnutrition (moderate malnutrition), progressing to grade III malnutrition (*i.e.*, severe malnutrition) from week 2 to 12. Subsequently, a slow improvement in malnutrition was observed from weeks 13 to 27. Later, malnutrition shifted to mild or grade I malnutrition (Figure 1C), which may be by survival adaptations.[22]

Table 2. Hematological parameters of ND and LPD animal groups at 10th week (n=6)

Parameter (Unit)	ND group	LPD group
WBC (103/uL)	10.53 ± 0.97	11.80 ± 1.24
RBC (106/uL)	8.36 ± 0.25	8.41 ± 0.69
HGB (g/dL)	14.75 ± 0.53	12.87 ± 0.98
HCT (%)	43.52 ± 1.56	39.82 ± 3.02
MCV (fL)	52.03 ± 1.34	47.45 ± 0.44**
MCH (pg)	17.67 ± 0.47	15.37 ± 0.18***
MCHC (g/dL)	33.87 ± 0.22	32.37 ± 0.24***
PLT (10^3/uL)	740.33 ± 60.59	681.52 ± 60.70
RDWCV (%)	12.30 ± 0.34	13.27 ± 0.15
RDWSD (fL)	25.62 ± 0.85	25.18 ± 0.32
PCT (%)	0.42 ± 0.05	0.37 ± 0.32
MPV (fL)	5.53 ± 0.03	5.48 ± 0.07
PDW (%)	15.40 ± 0.07	15.03 ± 0.12

All values are mean ± SEM. Bars represent the standard error, $p < 0.05$*, < 0.01** and $p < 0.001$** when compared to the ND group. WBC: White blood cells, RBC: Red blood cell, ND: Normal diet, LPD: Low-protein diet, HGB: Hemoglobin, HCT: Haematocrit, MCV: Mean corpuscular haemoglobin, MCH: Mean corpuscular haemoglobin, MCHC: Mean corpuscular haemoglobin concentration, PLT: Platelet, RDWCV: Red blood cell distribution width, RDWSD: Standard deviation red blood cell distribution width, PCT: Procalcitonin, MPV: Mean plateletvolume, PDW: Platelet distribution width

Hematological parameter

The hemoglobin (Hb), hematocrit (HCT), platelets (PLTs), and PLT Crit (PCT) counts in blood were lower in the LPD group than in the ND group (Table 2). Although the red blood cell (RBC) count was normal in the LPD group, RBC indices like mean corpuscular volume (MCV) (52.03 ± 1.34, 47.45 ± 0.44, $p \leq 0.01$), mean corpuscular Hb (MCH) (17.67 ± 0.47, 15.37 ± 0.18, $p \leq 0.001$) and mean corpuscular Hb concentration (MCHC) (33.87 ± 0.22, 32.37 ± 0.24, $p \leq 0.001$) were significantly low. On the other hand, the white blood cell (WBC) count increased compared to normal.

Biochemical parameters

TP and ALB, clinically relevant markers of PMN, both decreased significantly in LPD ($p \leq 0.05, 0.01, 0.001$) owing to prolonged low protein intake. The average serum ALB ranged between 1.9 and 2.4 g/dL from week 4 to week 22, and TP ranged between 5.1 to 6.4 g/dL from week 10 to week 24 in LPD (Figure 2A, B), which corresponds to clinical data and previous reports.[13,14] ALT and AST levels increased in the LPD group (Figure 2C, D) because PMN alters liver function. The significant increase in AST ($p \leq 0.01$) and ALT ($p \leq 0.05$) was positively correlated with the degree of malnutrition; grades II and III showed the highest level of injury. Serum ALP also increased substantially in the LPD group. Phosphorous levels were significantly higher in the ND group initially but stabilized later (Figure 2E, F). PMN remarkably decreased plasma TG levels (Figure 2G), possibly due to lipid accumulation in the liver, as shown in the histopathological results (Figure 3). The present study also demonstrated that the relative liver weight was higher in patients with LPD than in healthy controls (Figure 2H). Fat accumulation and hydropic changes may increase liver weight in patients with LPD.

Histopathology

Histopathological examination of the liver at weeks 10, 18, 20, and 26 captures the histological changes in the liver during PMN development in rats. Liver sections of the LPD group showed ballooning degeneration due to hydropic changes. Both Kupffer cells and dilated sinusoids around the central vein are evident. Nuclear displacement toward the periphery from fat

deposition in hepatocytes with vacuoles. These remarkable changes in liver histology confirmed the stable malnourished rat model. We used only week 10 slides for comparison.

Model validation

The model was validated by examining the biometric parameters of malnourished rats that were refed with ND (18% protein). Our results showed that LPD can induce PMN in rats, resulting in body weight loss, which can be reversed by refeeding. The BMI and body weight (Figure 4) of these animals increased significantly compared with the ND group ($p \leq 0.001$). During the 15 weeks of diet rehabilitation, we observed that the refed rats exhibited catch-up growth of (60.4%) and recovered from grade II (65%) to grade I (89.36%) malnutrition according to the

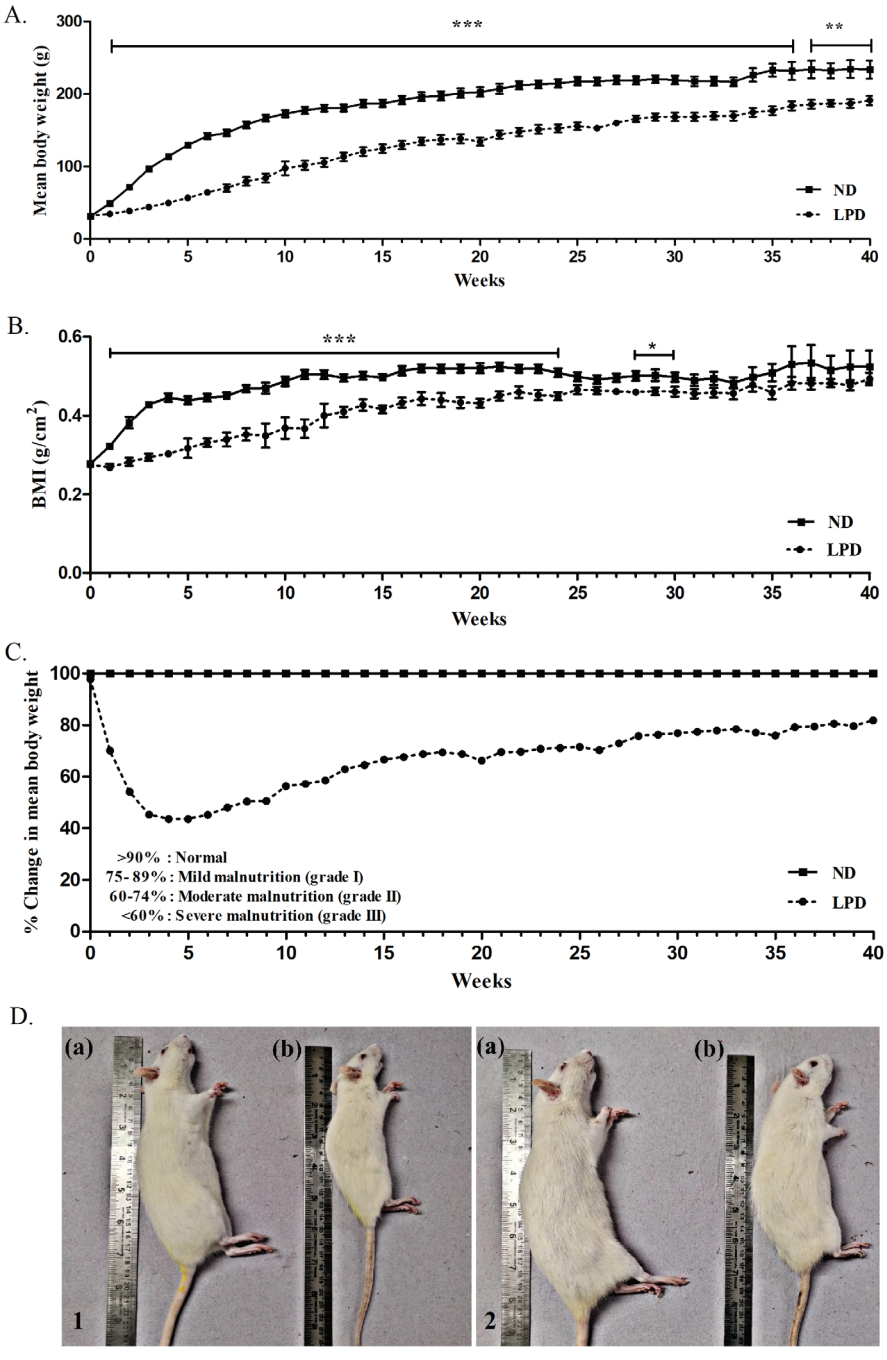

Figure 1. Graphical representation of (A) rat body weight (g) from weaning to 40 weeks in the ND and LPD groups (B) BMI of the ND and LPD groups (C). Percentage of change in body weight of LPD with respect to the ND group, and (D) photographic representation of ND (a) and LPD (b) at week 10 (1) and week 34 (2) of the study (n= 6). Significant differences are indicated by *, $p \leq 0.05$; **, $p \leq 0.01$; ***, $p \leq 0.001$

ND: Normal diet, LPD: Low-protein diet, BMI: Body mass index

Gomez classification. This finding supports the importance of protein content in the diet and demonstrates that treating protein-deficient malnutrition requires increased dietary protein intake.

DISCUSSION

As stated in the hypothesis, we developed a stable, reproducible, and clinically relevant PMN rat model that could be used in short- and long-term studies. Morphology showing stunted growth and skeletal structure in the LPD group. Skeletal muscles are the main protein reservoirs in the body and are sensitive to protein deficiency. Therefore, the depletion of differentiating muscle fibers weakens skeletal muscles,[23] leading to a decrease in weight gain. Opaque fur coating, voracious feeding, and a stooped posture were also noted.

The levels of hematology markers such as MCV, MCH, MCHC, Hb, HCT, PLT, and PCT in the PMN group were significantly reduced. Despite a normal RBC count, the altered RBC indices (MCV, MCH, and MCHC) indicate reduced Hb in the RBCs, resulting in compromised cell size, which resembles iron deficiency-induced hypochromic microcytic anemia.

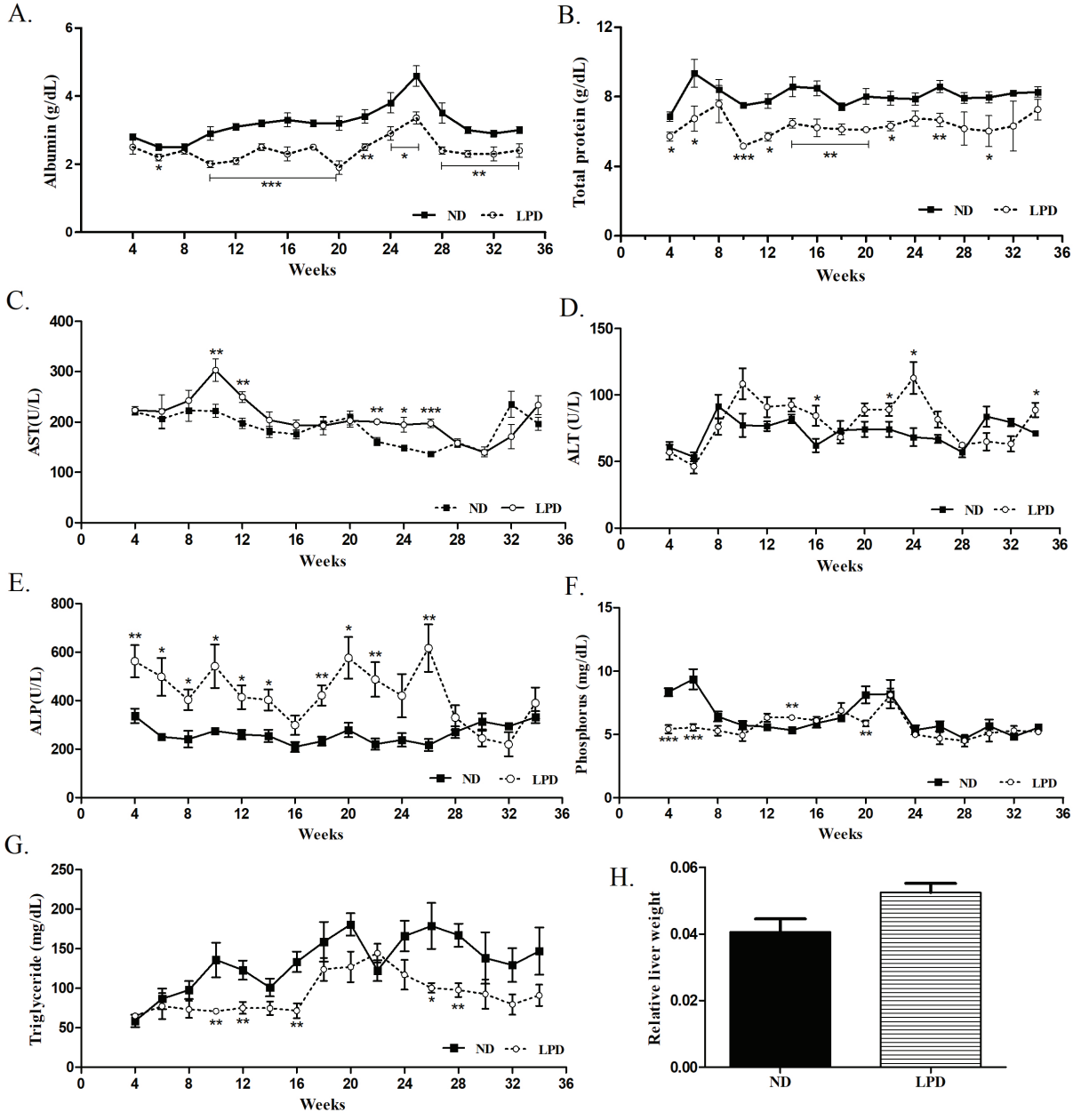

Figure 2. Serum biochemical parameters in patients with ND and LPD (n=6): (A) ALB, (B) total protein, (C) AST, (D) alanine aminotransferase, (E) ALB, (F) phosphorus, and (G) TG and (H) relative liver weight at week 10 (n= 6). Significant differences are indicated by *, $p \leq 0.05$; **, $p \leq 0.01$; ***, $p \leq 0.001$

ND: Normal diet, LPD: Low-protein diet, ALB: Albumin, AST: Aspartate aminotransferase, TG: Triglyceride

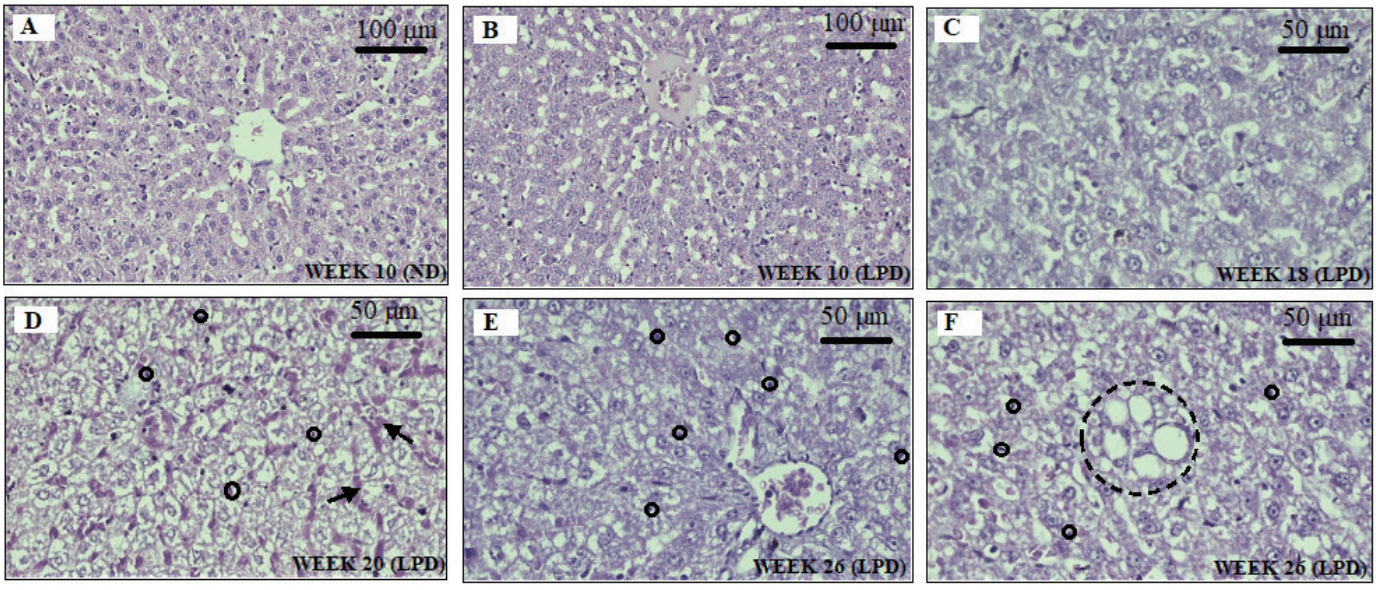

Figure 3. Photomicrographs of H&E sections of the liver (A) ND group showing normal cellular architecture with hepatocytes radiating from the central vein and sinusoidal space at week 10 of study (20X) (B) week 10 LPD group showing mild hydropic changes in the hepatocytes (20X) at week 10 (C) LPD group showing ballooning degeneration with irregular cytoplasm (40X) at week 18 (D) LPD group showing dilation of sinusoidal space (black arrows) with marked hydropic change (40X) at week 20 (E) LPD group showing central vein with marked hydropic change and presence of kupffer cells (black circles) (40X) and (F) macro-vesicular fat droplets (black discontinued circle) occupying the cytoplasm and displacing the nucleus to the periphery (40X) at week 26

LPD: Low-protein diet, ND: Normal diet

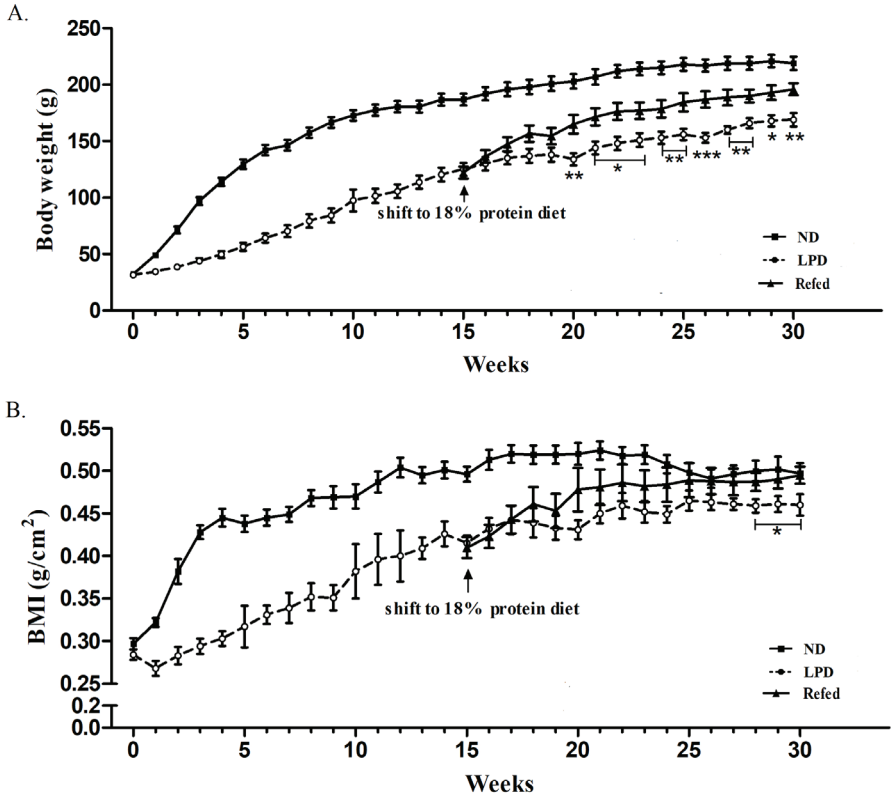

Figure 4. Graphical representations of (A) body weight (B) BMI of the ND, LPD, and refed groups during the rehabilitation period.Significant differences are indicated by *, $p \leq 0.05$; **, $p \leq 0.01$; ***, $p \leq 0.001$

ND: Normal diet, LPD: Low-protein diet, BMI: Body mass index

Red Cell Distribution Width, which increases in iron deficiency anemia[24] is possiblebecause total iron binding capacity is decreased in PMN.[25] Moderate anemia is prevalent in Kwashorkor[26] and marasmic conditions.[27] High WBC count in the LPD group, indicating susceptibility to infection. A reduction in PLT count may be attributed to compromised bone marrow activity.[28]

Depletion of amino acid precursors possibly led to a significant decrease in ALB levels in the LPD group.[29] ALB is synthesized solely in the liver on polysomes bound to the endoplasmic reticulum. After synthesis, ALB is transported from the rough endoplasmic reticulum to the Golgibodies and released directly into the systemic circulation. In PMN, loss of hepatic RNA and disaggregation of polysomes together upsets ALB synthesis.[30] Clinically, hypoalbuminemia is more severe in children with kwashiorkor than with marasmus.[31] Serum ALB levelsof less than 2.3 g/dL are considered undernourished. Lower ALB levels in LPD correlate with earlier studies and are clinically relevant.[14]

Both AST and ALT levels are elevated in PMN, possibly because of hepatic tissue damage. Malnutrition affects hepatocytes and releases these enzymes into the bloodstream under clinical conditions.[32] Our PMN model mirrors these clinical data, thereby validating the model.[33] Impaired bone development and liver function raiseALP. Elevated ALP in PMN[34] has already been reported. Early rise (initial weeks) in ALP might be the result of compromised bone development rather than liver dysfunction.[35] This observation is strengthened by low phosphorous levels during early development. PMN depletes phosphorous levels, impairing bone development, and causing defects in bone maturation. Compensatory osteoblast activity is increased as a positive feedback mechanism to overcome this impairment, thereby elevating ALP.[36] In later stages, liver dysfunction is accompanied by elevated ALP levels, which correlates with AST and ALT levels.

PMN decreases fatty acid oxidation, leading to increased lipogenesis and TG storage in the liver.[2,7] Hepatocytes recognize the amino acid profile, controlled by dietary protein intake that alters hepatocyte TG secretion,[37] resulting in decreased serum levels. Further, a reduction in TG secretion can also be attributed to a reduction in the rate of very low-density lipoprotein synthesis, resulting in hypertriglyceridemia during protein deprivation.[38] TGs in the serum are frequently low in kwashiorkor, but they are normal or increased in the marasmus condition.[10]

Severe but reversible liver changes are characterized by hepatocyte ballooning due to hydropic changes in the tissue. Edema enlarges the cell, and characterized by irregular cytoplasmic accumulation of water and fat droplets in the vacuoles. Initially, the vacuoles are small and surround the nucleus. Subsequently, the vacuoles become more prominent and displace the nucleus to the periphery, forming a signet-ring structure. The fat deposited in the vacuoles is predominantly TG. The accumulation of TG in the liver leads to fatty changes that decrease hepatic TG secretion.[39]

In the present study, LPD showed the presence of hepatomegaly, which, along with fatty liver, constitutes an essential clinical feature of kwashiorkor. Likewise, children with marasmus also present with hepatic steatosis and hepatomegaly, demonstrating clinical relevance.[40] The fatty liver is more intense in kwashiorkor than in marasmus. In marasmus, the liver increases the synthesis of plasma lipoproteins in response to an excess of fatty acids, whereas in kwashiorkor, the liver, which cannot dispose of fatty acids, accumulates lipids in the liver.[10]

In the present study, LPD showed the presence of hepatomegaly, which, along with fatty liver, constitutes an essential clinical feature of kwashiorkor. Likewise, children with marasmus also present with hepatic steatosis and hepatomegaly, demonstrating clinical relevance.[40] The fatty liver is more intense in kwashiorkor than in marasmus. In marasmus, the liver increases the synthesis of plasma lipoproteins in response to an excess of fatty acids, whereas in kwashiorkor, the liver, which cannot dispose of fatty acids, accumulates lipids in the liver.[10]

The clinical features of kwashiorkor include hepatomegaly, fatty liver, hair loss, stooped posture, hypoalbuminemia, and low serum phosphate, TP, and TG levels. However, there was no edema in PMN rats, which is a key indicator of kwashiorkor. Interestingly, PMN rats also exhibited marasmic features, such as significant weight loss, low BMI, lack of subcutaneous fat, muscular atrophy, fat deposition in the liver, and a poor weight-for-height ratio. Hence, our model clinically represents the marasmic-kwashiorkor condition.

Study limitations

The study focused on biochemical, hematological, and histological changes but did not thoroughly investigate other molecular interactions involved in malnutrition.

CONCLUSION

The PMN rat model using a 10% protein diet mimicked the clinical manifestations of the marasmic-kwashiorkor condition. This model is inexpensive to develop, easy to maintain, repeatable, predictable, ethical, and clinically relevant. The model can be used in research in the fields of drug kinetics, disease model development, drug interaction studies, and drug discovery. Being a long-term model, the LPD-induced malnutrition rat model will also be appropriate for studying maternal and intragenerational malnutrition. The PMN model can be appropriately and adaptively modeled to suit different experimental situations to evaluate multiple clinical and biological attributes.

Acknowledgments

The authors thank Nitte (Deemed to be University) for financial support and NUCARE staff for assistance. Dr. M. K. Unnikrishnan, Professor, Pharmacy Practice, NGSMIPS, for corrections and proofreading.

Ethics

Ethics Committee Approval: All animal experiments were conducted according to the guidelines of the committee for the Purpose of Control and Supervision of Experiments on Animals (approval number: NGSMIPS/Dec-2020/2022, date: 29.12.2020).

Informed Consent: Informed consent is not required.

Authorship Contributions

Surgical and Medical Practices: V.A., Concept: V.A., M.B., Design: V.A., M.B., Data Collection or Processing: V.A., M.R.J., V.D., Analysis or Interpretation: V.A., Literature Search: V.A., M.R.J., V.D., Writing: V.A., M.R.J., V.D., B.M.K., A.V.S.

Conflict of Interest: The authors have no conflicts of interest to declare.

Financial Disclosure: This work was supported by Nitte (Deemed to be University) (grant: NUFR-22-038).

REFERENCES

1. Sawaya AL. Malnutrition: Longterm consequences and nutritional recovery effects. Estudios Avançados. 2006;20:147-158.
2. Maleta K. Undernutrition. Malawi Med J. 2006;18:189-205.
3. Ferreira-Paes T, Seixas-Costa P, Almeida-Amaral EE. Validation of a feed protocol in a mouse model that mimics marasmic malnutrition. Front Vet Sci. 2021;8:757136.
4. Éliás BA, Jámbor A. Food security and COVID-19: A systematic review of the first-year experience. Sustainability. 2021;13:5294.
5. Miñana-Solis Mdel C, Escobar C. Post-weaning protein malnutrition in the rat produces short and long term metabolic impairment, in contrast to earlier and later periods. Int J Biol Sci. 2008;4:422-432.
6. Eyzaguirre-Velásquez J, Olavarría-Ramírez L, González-Arancibia C, Díaz-Merino C, Ariz R, López S, Quiroz W, Beltrán CJ, Bravo JA, Julio-Pieper M. Protein malnutrition during juvenile age increases ileal and colonic permeability in rats. J Pediatr Gastroenterol Nutr. 2017;64:707-712.
7. Madani S, Prost J, Belleville J. Dietary protein level and origin (casein and highly purified soybean protein) affect hepatic storage, plasma lipid transport, and antioxidative defense status in the rat. Nutrition. 2000;16:368-375.
8. Pham TP, Alou MT, Golden MH, Million M, Raoult D. Difference between kwashiorkor and marasmus: Comparative meta-analysis of pathogenic characteristics and implications for treatment. Microb Pathog. 2021;150:104702.
9. Oshikoya KA, Senbanjo IO. Pathophysiological changes that affect drug disposition in protein-energy malnourished children. Nutr Metab (Lond). 2009;6:50.
10. Singh VK, Seed TM. How necessary are animal models for modern drug discovery? Expert Opin Drug Discov. 2021;16:1391-1397.
11. Malta A, de Oliveira JC, Ribeiro TA, Tófolo LP, Barella LF, Prates KV, Miranda RA, Elmhiri G, Franco CC, Agostinho AR, Trombini AB, Pavanello A, Gravena C, Abdennebi-Najar L, Mathias PC. Low-protein diet in adult male rats has long-term effects on metabolism. J Endocrinol. 2014;221:285-295.
12. Weltman MD, Farrell GC, Liddle C. Increased hepatocyte CYP2E1 expression in a rat nutritional model of hepatic steatosis with inflammation. Gastroenterology. 1996;111:1645-1653.
13. Merino-Sanjuán M, Catalán-Latorre A, Nácher A, Miralles-Arnau S, Jiménez-Torres NV. Animal model of undernutrition for the evaluation of drug pharmacokinetics. Nutr Hosp. 2011;26:1296-1304.
14. Gupta SS, Gupta PS. Serum albumin and total protein level as plausible marker for diagnosis of protein energy malnutrition in children under age 5 years. 2020;7:1758.
15. Chanchal R, Gupta S, Kanta C, Singh K, Koonwar S. Hypophosphataemia in severe acute malnutrition: a prospective observational study. British Journal of Nutrition. 2019;121:306-311.
16. Verma GK, Yadav YS, Yadav RK, Sharma IK, Bharat K, Yadav KK. Study of lipid profile levels in malnourished and healthy children: a case control study. Pediatric Rev Int J Pediatric Res. 2018;5:156-161.
17. Oyagbemi AA, Odetola AA. Hepatoprotective and nephroprotective effects of Cnidoscolus aconitifolius in protein energy malnutrition induced liver and kidney damage. Pharmacognosy Res. 2013;5:260-264.
18. Karmacharya K, Islam MN. Role of serum alanine aminotransferase aspartate aminotransferase and alkaline phosphatase in early detection of protein energy malnutrition. J Nepal Paediatr Soc. 2007;27:68-72.
19. RJ Madhura, A Varsha, Chakraborthy A, Kumar M, Shetty V, Badanthadka M. Protein malnutrition in BALB/C mice: A model mimicking clinical scenario of marasmic-kwashiorkor malnutrition. J Pharmacol Toxicol Methods. 2023;119:107231.
20. Badanthadka M, Prathibha G. Diet composition to produce malnourished animal model. Patent number: 377420. Official journal of the patent office. 2021;01:215.
21. Gomez F, Galvan RR, Frenk S, Munoz JC, Chavez R, Vazquez J. Mortality in second and third degree malnutrition. J Trop Pediatr (Lond). 1956;2:77-83.
22. Hoffer LJ. Clinical nutrition: 1. Protein-energy malnutrition in the inpatient. CMAJ. 2001;165:1345-1349.
23. Alves AP, Dâmaso AR, Dal Pai V. The effects of prenatal and postnatal malnutrition on the morphology, differentiation, and metabolism of skeletal striated muscle tissue in rats. J Pediatr (Rio J). 2008;84:264-271.
24. Li N, Zhou H, Tang Q. Red blood cell distribution width: A novel predictive indicator for cardiovascular and cerebrovascular diseases. Dis Markers. 2017;2017:7089493.
25. Bainton DF, Finch CA. The diagnosis of iron deficiency anemia. Am J Med. 1964;37:62-70.
26. Pereira SM, Baker SJ. Hematologic studies in kwashiorkor. Am J ClinNutr. 1966;18:413-420.
27. Adams EB, Scragg JN. Serum vitamin B12 concentrations in megaloblastic anemia associated with kwashiorkor and marasmus. J Pediatr. 1962;60:580-585.
28. Getawa S, Getaneh Z, Melku M. Hematological Abnormalities and Associated Factors Among Undernourished Under-Five Children Attending University of Gondar Specialized Referral Hospital, Northwest Ethiopia. J Blood Med. 2020;11:465-478.
29. Goel A, Dani V, Dhawan DK. Protective effects of zinc on lipid peroxidation, antioxidant enzymes and hepatic histoarchitecture in chlorpyrifos-induced toxicity. Chem Biol Interact. 2005;156:131-140.

30. Rothschild MA, Oratz M, Schreiber SS. Effects of nutrition and alcohol on albumin synthesis. Alcohol Clin Exp Res. 1983;7:28-30.

31. Soeters PB, Wolfe RR, Shenkin A. Hypoalbuminemia: Pathogenesis and clinical significance. JPEN J Parenter Enteral Nutr. 2019;43:181-193.

32. Karajibani M, Montazerifar F, Hosseini R, Suni F, Dashipour AR, Fadaaeimokhtarkanlo M. The relationship between malnutrition and liver enzymes in hospitalized children in Zahedan: A Case-control Study. Zahedan j res med. Sci. 2021;23.

33. Chowdhury MSI, Rahman AZ, Haque M, Nahar N, Taher A. Serum aspartate aminotransferase (AST) and alanine aminotransferase (ALT) levels in different grades of protein energy malnutrition. J Bangladesh Soc Physiol. 2007;2:17-19.

34. Freiman I, Pettifor JM, Moodley GM. Serum phosphorus in protein energy malnutrition. J Pediatr Gastroenterol Nutr. 1982;1:547-550.

35. Nandivada P, Potemkin AK, Carlson SJ, Chang MI, Cowan E, O'Loughlin AA, Gura KM, Puder M. Elevated alkaline phosphatase in infants with parenteral nutrition-associated liver disease reflects bone rather than liver disease. JPEN J Parenter Enteral Nutr. 2015;39:973-976.

36. Fukumoto S, Ozono K, Michigami T, Minagawa M, Okazaki R, Sugimoto T, Takeuchi Y, Matsumoto T. Pathogenesis and diagnostic criteria for rickets and osteomalacia-proposal by an expert panel supported by Ministry of Health, Labour and Welfare, Japan, The Japanese Society for Bone and Mineral Research and The Japan Endocrine Society. Endocr J. 2015;62:665-671.

37. Nishi H, Yamanaka D, Kamei H, Goda Y, Kumano M, Toyoshima Y, Takenaka A, Masuda M, Nakabayashi Y, Shioya R, Kataoka N, Hakuno F, Takahashi SI. Importance of serum amino acid profile for induction of hepatic steatosis under protein malnutrition. Sci Rep. 2018;8:5461.

38. Treviño-Villarreal JH, Reynolds JS, Bartelt A, Langston PK, MacArthur MR, Arduini A, Tosti V, Veronese N, Bertozzi B, Brace LE, Mejia P, Trocha K, Kajitani GS, Longchamp A, Harputlugil E, Gathungu R, Bird SS, Bullock AD, Figenshau RS, Andriole GL, Thompson A, Heeren J, Ozaki CK, Kristal BS, Fontana L, Mitchell JR. Dietary protein restriction reduces circulating VLDL triglyceride levels via CREBH-APOA5-dependent and -independent mechanisms. JCI Insight. 2018;3:e99470.

39. Truswell AS, Hansen JD. Fatty liver in protein-calorie malnutrition. S Afr Med J. 1969;43:280-283.

40. Doherty JF, Adam EJ, Griffin GE, Golden MH. Ultrasonographic assessment of the extent of hepatic steatosis in severe malnutrition. Arch Dis Child. 1992;67:1348-1352.

Turk J Pharm Sci 2024;21(5):483-488
DOI: 10.4274/tjps.galenos.2023.10663

ORIGINAL ARTICLE

A Novel Controlled Release Implant of Insulin Based on Poly(3-hydroxybutyrate-co-3-hydroxyvalerate) Polymer Prepared by Extrusion

Fatemeh DADGAR PAKDEL[1]*, Javad DADGAR PAKDEL[2], Ali NAJMEDDIN[3], Afshin PEIROVI[4], Mohammad Hossein NICKNAM[5], Farid Abedin DORKOOSH[6]

[1]Tehran University of Medical Sciences Faculty of Medicine, Department of Immunology, Tehran, Iran
[2]Pasteur Institute, Department of Pharmaceutical Biotechnology, Tehran, Iran
[3]Tehran University of Medical Sciences Faculty of Pharmacy, Department of Pharmaceutics, Tehran, Iran
[4]New Technology Research Group, Pasteur Institute, Department of Nanobiotechnology, Tehran, Iran
[5]Tehran University of Medical Sciences, Molecular Immunology Research Center, Tehran, Iran
[6]Tehran University of Medical Sciences, Medical Biomaterial Research Centre, Tehran, Iran

ABSTRACT

Objectives: The aim of this study was to develop a biodegradable implant with a slow release of insulin to minimize the amount of repeated drug injections in patients.Developing and designing implants with controlled release of active protein has always been a challenge. To optimize and control the release of insulin in this project, the drug complexing mechanism was used by dextran sulfate sodium (DS) and Poly(3-hydroxybutyrate-co-3-hydroxyvalerate) (PHBV) polymer.

Materials and Methods: The efficacy of drug binding was evaluated under different molecular ratios of DS, and then a thermogravimetric analysis test was done to check the stability of the drug complex in extrusion. In the final stage, rod-shaped implants of complexed insulin were prepared by an extrusion process, and the drug release was evaluated within 32 days. The drug release kinetics were evaluated using mathematical models.

Results: The results showed an increase in insulin binding efficiency percent, up to a ratio of 2.6. The drug release from the implant containing complex insulin was completely controlled. The drug release followed a zero-order release model. Interestingly, the complex form of the drug showed a temperature resistance of 160 ˚C for ten minutes.

Conclusion: In this study, for the first time, a controlled release implant of insulin has been developed based on a PHBV polymer. In this method, the extrusion process has been used, which provides the possibility of preparing implants on an industrial scale in the future. Also, their development appears to be a promising treatment for diabetic patients and leads to the elimination of frequent drug injections and then more adherence of the patients to the continuation of the treatment process.

Keywords: Insulin, PHBV, controlled release, implant, extrusion

INTRODUCTION

Diabetes is a metabolic disease with symptoms of high blood glucose, glycosuria, hyperlipidemia, and nitrogen imbalance that leads to several kidney, eye, vascular, and heart complications. It can be diagnosed in two forms: type 1 and type 2 diabetes. There are about 415 million people with diabetes in the world, almost 1 in 11 people in the population, and the number of people with diabetes worldwide will reach 642 million by 2040.[1-3]

One of the main methods of treatment in patients is insulin injection to reduce blood sugar, but repeated insulin injections in patients are a tiring method and reduce the patient's adherence to continue treatment. Insulin has an *in vivo* short half-life.

*Correspondence: fdadgarpakdel@yahoo.com, Phone: +9802166452621, ORCID-ID: orcid.org/0000-0003-3863-1599
Received: 17.05.2023 , Accepted: 22.08.2023

Nowadays, the development of drug delivery systems has placed promising methods in front of treatment systems. One of these methods is the development of biodegradable implants for the controlled and slow release of insulin in patients. The use of polymeric sustained-release implants increases the half-life of this drug, but the lack of toxicity and biocompatibility of the polymeric compound used in the manufacturing of implants is very important.[1-5]

Biodegradable polymers are an excellent option in medical applications because they are easily destroyed in the environment and then removed from the body. These polymers have various applications in the production of implants, surgical sutures, and drug delivery systems. Many synthetic and natural biodegradable polymers have been evaluated for creating implants. Natural polymers, like collagen, albumin, and gelatin, have been assessed for drug delivery. Nonetheless with their use, their use is limited because of their higher price and purity.[6,7] Polyhydroxyalkanoates are biodegradable polyesters that can be produced through bacterial and synthetic methods.[6,7] The excellent properties of Poly(3-hydroxybutyrate-co-3-hydroxyvalerate) (PHBV), like its biological origin, adsorption capacity, and low toxicity, make it an appropriate option for biotechnological applications, like the fabrication of cardiovascular stents and drug delivery systems. It is used in medical packaging and for absorbable surgical sutures, tissue engineering, biosensors, degradable implants, and the construction of porous scaffolds.[8-10]

Implants containing biodegradable polymers can be divided into two categories: matrix systems and reservoir systems. In the matrix system used in this study, the polymer degraded slowly under physiological conditions. Thus, the drug is released via diffusion from the pores of the matrix. In reservoir systems, membrane degradation is slower compared to drug release. In spite of the fact that much research has been done in the field of designing and manufacturing biodegradable implants, only a few of them are in the phase of clinical studies. The most important problem facing biodegradable implants is the problem of designing a formulation with optimal drug release.[11,12]

MATERIALS AND METHODS

Materials

PHBV polymer with 3 *wt.* polyhydroxyvalerate % (PHV) was purchased from Tianan Biologic Materials Ltd., Ningbo (China). Polyethylene glycol (PEG) 6000 was prepared by Sigma-Aldrich (St. Louis, USA). Dextran sulfate sodium (DS) from Leuconostoc *spp*. Mr 5,000 and hydrochloric acid (HCL) were purchased from Merck (Germany). Insulin was prepared from Ronak Daroo (Iran). The Micro BCA assay kit and phosphate-buffered saline (PBS) tablets were obtained from Biobasic (Canada).

Preparation of insulin complexes (Ins.com) using insulin with DS salt at pH 3 and different molar ratios

Insulin (Ronak Daroo company) was used for hydrophobic ion pairing (HIP) complex preparation. Stocks of DS from Leuconostoc *spp.* Mr 5,000 (Merck, Germany), as ion-pairing agent, was prepared in double-distilled water. Briefly, DS in different concentrations was added to the insulin solution with pH 3. To provide more basic amino acid ionization and positive charges on the protein, the insulin solution pH was adjusted with 0.1 N of HCL (Merck, Germany) to the pH value of 3. After mixing two solutions in an optimum ratio by vigorous cortexin, the created HIP complex was centrifuged at 14000 RPM for 15 minutes to isolate the supernatant. The obtained complex was lyophilized into a powder. The micro BCA assay (Biobasic, Canada) was used to measure uncomplexed insulin in the supernatant.

The effect of different molar ratios of DS into the insulin was evaluated. For this purpose, we investigate the impact of different molar ratios -0.88, 1.75, 2.6, 3.5, 5.2, and 8.7- on the binding efficiency percentage. As mentioned above, after mixing insulin solution at pH 3 with the above six molar ratios and vigorous cortexin, centrifugation was performed at 14000 RPM for 15 minutes for supernatant separation, and then, uncomplex insulin was measured by HPLC.

The HIP complexes were washed three times with deionized water and then lyophilized. The insulin complexation efficiency [CE (%)] was calculated by measuring the supernatant levels of insulin using HPLC. Then based on the formula below, CE (%) is calculated, and the levels of insulin in the complex are calculated based on the initial amount of insulin that was added.

$$CE\ (\%) = M_i - M_f / (M_i \times 100\%)$$

Where M_i represents the primary insulin amount that was added to the reaction, while M_f denotes the free insulin amount in the supernatant.

Fourier transform infrared spectroscopy (FTIR) of insulin: DS complexes

FTIR analysis was done by an FTIR spectrophotometer (Tensor 27, Bruker) to investigate the chemical properties of the DS, insulin, and HIP complex separately. The test samples scanned between 500-4000 cm^{-1} in the mid-infrared range. This analysis was completed to determine the molecular modifications induced by the addition of DS and HIP complex production, along with investigating chemical properties on the molecule surface after the complexation reaction. Furthermore, FTIR analysis assessed drug-polymer interaction. For this purpose, the resulting complexes (0.1 mg) were mixed with 1 mL of deionized water and located in a shaker bath at room temperature. Then, 24 hours later, the solution underwent centrifugation at 14000 RPM over 10 minutes; the obtained supernatant passed through a 0.45 µm syringe filter, and the insulin concentration was measured by HPLC.[13]

Preparation of biodegradable insulin implants based on poly(phenylbenzothiazoline-6-sulfonic acid) polymers

For preparation of the rod-shaped implant, 3 *wt.* of PHBV was used. Percent of PHV (Tianan Biologic Materials Ltd., China) and PEG (molecular weight of 600 g/mol) as a pore former (Sigma, Germany) in the ratio of 1:4 (PHBV: PEG) was used.[14,15] The heating process was chosen for the preparation of rod

shaped implant by extruder. In this process, complexed insulin (Ins.com) was mixed with the polymers and extruded at 160 ˚C for 10 minutes.

Release kinetics of the rod implant

HPLC test measured drug release from prepared implant in the PBS medium (pH 7.4) after 48, 96, 192, 384, and 768 hours at 37 ˚C, and then drug release kinetic was reported based on the investigation of different release kinetics equations. Different mathematical models were assessed, including the zero-order Higuchi model, first-order model, Hixson-Crowell model, and Korsmeyer-Peppas model. The final result is reported based on the highest R2 of the regression line.

Statistical analysis

Values are expressed as mean ± standard deviation. Following the evaluation of the variance homogeneity and normal distribution of data, statistical analysis was done via one-way analysis of variance (for more than two groups). Tukey's test was used as a post-hoc test. Statistical analysis was performed using GraphPad Prism version 8.0.2. Values of $p \leq 0.05$ are regarded as significant.

RESULTS

Preparation of insulin complexes with DS salt at different molar ratios

The HIP complex of insulin with dextran sulfate (ion pairing agent) was provided, and its % binding efficiency was assessed. The pKa of the sulfate group in dextran sulfate has been reported to be < 2; thus, it possesses a negative charge above pH 2.[16,17] In this research, the effect of the molar ratio of dextran sulfate to insulin was assessed to obtain maximum binding. The most appropriate molar ratio was selected based on the maximum binding percentage. The effect of 6 molar ratios on the percentage of binding efficiency was investigated. Finally, a molar ratio of 2.6 at pH 3 was considered for drug complexation. The results show an increase in insulin binding efficiency with an increment in molar ratio, but only up to a ratio of 2.6 (Figure 1).

Investigating the characteristics of the complexes

FTIR

To assess the nature of the interaction between the sulfate group of DS, and the amino group of amino acids of insulin, an FTIR test was performed (Figure 2).

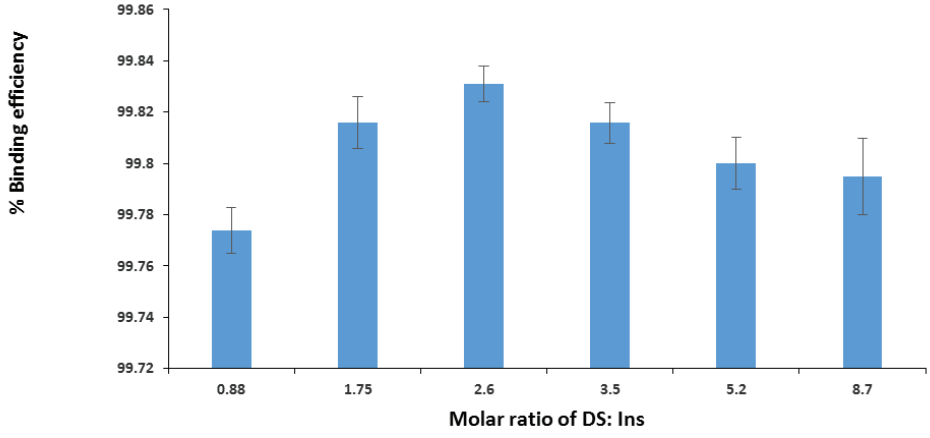

Figure 1. The % binding efficiency of ins. in different molar ratios of DS (ins). Values were represented as mean ± SD, n= 3
DS: Dextran sulfate sodium, Ins.: Insulin, SD: Standard deviation

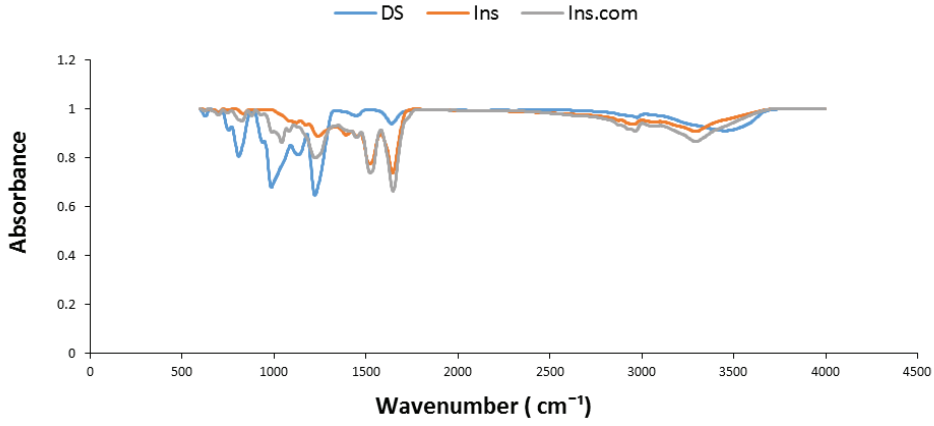

Figure 2. FTIR results of ins., DS, and Ins.com
DS: Dextran sulfate sodium, Ins.: Insulin, Ins.com: Insulin complex

Thermogravimetric analysis (TGA)

This test was performed to examine weight changes in insulin at 160 ˚C for 10 minutes. Weight changes were observed with a TGA instrument SDT Q600 V20.9 Build 20 at 30 to 160 ˚C. This test was done for evaluation of the terminal stability of insulin used in prepared implant and showed weight loss that probably is due to loss of water because this change is about 5 percent; on the other hand, the changes in weight loss have reached a relatively stable state before reaching the temperature of 160 ˚C (Figure 3).

Release kinetics of the rod implant

The drug release kinetic and dissolution behavior of implant -obtained data from *in vitro* drug release- were determined as drug cumulative percentage, drug log cumulative percentage, and remaining drug log cumulative percentage (Figure 4). The curves were then constructed according to various kinetic factors. For the interpretation of release kinetic, the R-square value was determined, and then their comparison helped us to choose the best kinetic model.[18] According to the counted R^2, the best fit kinetic model is the zero-order model (R2: 0.9942 for insulin implant), which shows the drug release at a constant rate.

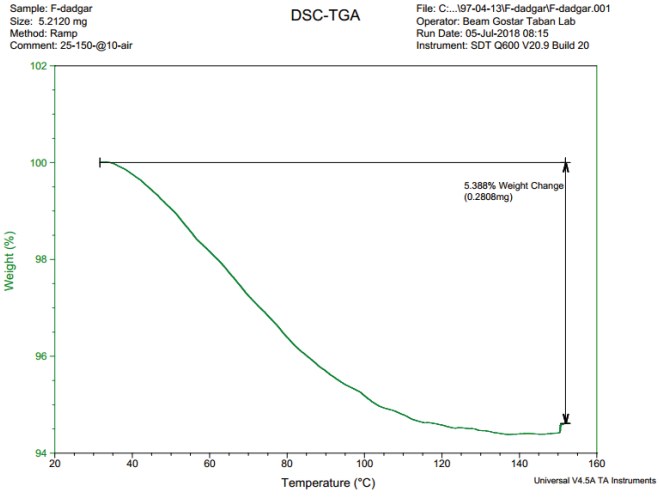

Figure 3. TGA of ins

Ins.: Insulin, TGA: Thermogravimetric analysis, DSC: Differential scanning calorimetry

DISCUSSION

The isoelectric pH (pI) of insulin is 5.3, and the protein surface charge at pH below pI will be positive and, thus, bind with the negatively charged dextran sulfate as ionic interactions. Hence, following the decrease in pH, the protein surface charge increases, and, based on Figure 1, % binding efficiency increases with a decrease in pH. The maximum % binding efficiency of insulin with DS is found when the dextran sulfate to the protein surface charge ratio is approximately 1:1.[19] In fact, at the molar ratio of 2.6, the surface charge in dextran sulfate and protein is nearly similar, and maximum binding is observed. Another point to note is that, depending on the drug's molecular weight, it is better to select the nearest molecular weight of the HIP agent to achieve the optimal molar ratio. Therefore, DS is chosen for this study.

About FTIR results, As mentioned in the literature, the characteristic peaks for sulfate groups of DS in the FTIR are 804.31 cm^{-1} (S-O-S vibration), 983.6 cm^{-1} (symmetric SOO-stretching vibration), and 1226.7 cm^{-1} (asymmetric SOO-stretching vibration). The ionic interactions that occur between amino and sulfate groups can lead to attenuation in IR peaks for the sulfate group or their shift. Due to such interactions, observed IR peaks for sulfate groups in DS showed attenuation in our investigation.In addition, this analysis was used to evaluate the stability of the secondary protein structure. The amide I and II bands are the two main bands to characterize protein secondary structure.[19] In the infrared spectroscopy (spectrum) of insulin, it can be determined that the amide I band (1698 cm^{-1}) and the amide II band (1550 cm^{-1}) of the complex insulin and its pure form are similar. Therefore, the protein's secondary structure is retained in the complex form.

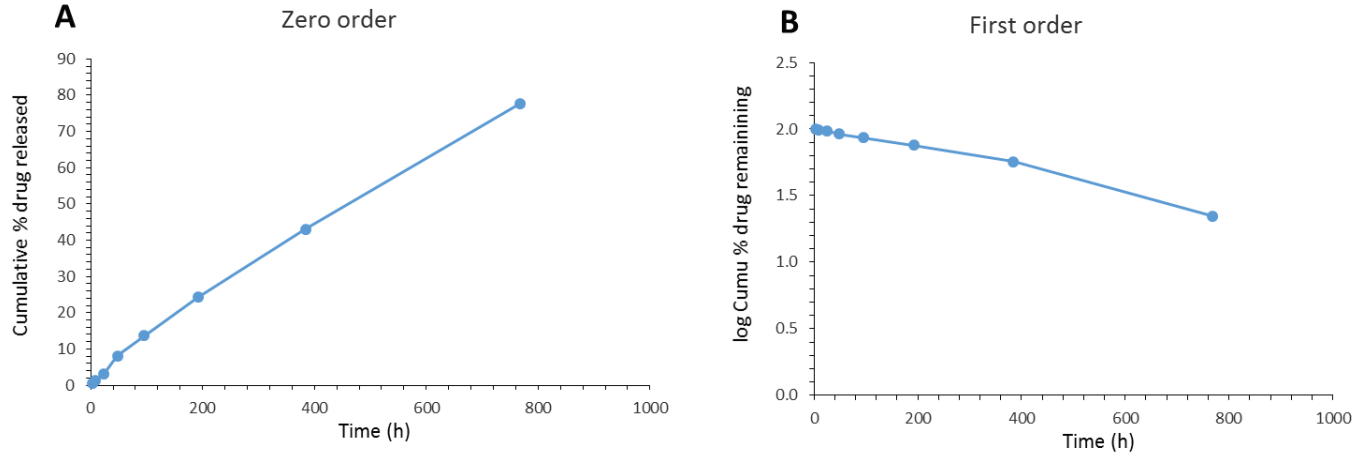

Figure 4. The release kinetics of insulin from prepared implant a protein drug: (A) zero-order model; and (B) first-order model. The error bars lie within the points (values were represented as mean ± SD, n= 3)

SD: Standard deviation

Recent research shows that protein complexing increases the heat resistance of the drug; therefore, according to these results, it is predicted that after complexing insulin with sodium dextran sulfate, the heat resistance of the drug will increase in the stages of implant preparation by the extrusion method. However, additional animal studies are required to measure the functional activity of the drug.[20,21]

The results of drug release kinetic investigation demonstrate that our formulation is sustained-release. The calculated R^2 for zero order kinetic is very close to the R^2 of the first order kinetic, indicating that the prepared implant is also a controlled release formulation that follows zero-order kinetics. Regarding the first-order model, the release profile is associated with the drug concentration in pharmaceutical formulations. It is applicable for the dissolution of water-soluble insulin in a porous matrix created from PHBV/PEG in this implant.[20-22]

CONCLUSION

Insulin implants were effectively obtained by the melting approach using PHBV and PEG-6000 as the pore former. The results of recent research projects show that by complexation, protein activity can be highly preserved under melting conditions and is applicable to developing implants containing protein drug using an extruder in research and also industry. Therefore, in this project, insulin-drug complexation was performed with the aim of the controlled release of insulin. The results show that very few weight changes occur in the insulin drug at 160 °C temperature, and probably the biological activity of the drug will be maintained to a large extent. Moreover, PHBV polymer is applicable for the preparation of sustained-released implants, including protein drugs like insulin. Due to its controlled release property, insulin implants can be a promising treatment for diabetics and lead to the elimination of frequent drug injections in patients and, as a result, more patient adherence to treatment. Optimization of formulations, and also *in vivo* studies, are needed for the production of an effective dose form of this implant for application in patients.

Acknowledgments

Research grants from the Tehran University of Medical Sciences, Deputy of Research (grant number: 35574-30-03-96), and Iran National Science Foundation (grant number: 96004866) supported this research. The authors greatly appreciate this financial support.

Ethics

Ethics Committee Approval: There is no requirement for ethical approval.

Informed Consent: There is no requirement.

Authorship Contributions

Surgical and Medical Practices: F.D.P., J.D.P., A.N., Concept: F.D.P., J.D.P., A.N., A.P., M.H.N., F.A.D., Design: F.D.P., J.D.P., A.N., A.P., M.H.N., F.A.D., Data Collection or Processing: F.D.P., J.D.P., A.N., A.P., M.H.N., F.A.D., Analysis or Interpretation: F.D.P., J.D.P., A.N., A.P., M.H.N., F.A.D., Literature Search: F.D.P., J.D.P., A.N., A.P., M.H.N., F.A.D., Writing: F.D.P., J.D.P., A.N., A.P., M.H.N., F.A.D.

Conflict of Interest: No conflict of interest was declared by the authors.

Financial Disclosure: The authors declared that this study received no financial support.

REFERENCES

1. Bayrami S, Esmaili Z, SeyedAlinaghi S, Jamali Moghadam SR, Bayrami S, Akbari Javar H, Rafiee Tehrani M, Dorkoosh FA. Fabrication of long-acting insulin formulation based on poly(3-hydroxybutyrate-co-3-hydroxyvalerate) (PHBV) nanoparticles: preparation, optimization, characterization, and *in vitro* evaluation. Pharm Dev Technol. 2019;24:176-188.
2. Zou Q, Qu K, Luo Y, Yin D, Ju Y, Tang H. Predicting diabetes mellitus with machine learning techniques. Front Genet. 2018;9:515.
3. Bodke H, Wagh V, Kakar G. Diabetes Mellitus and Prevalence of Other Comorbid Conditions: A Systematic Review. Cureus. 2023;24;15:e49374.
4. Goosen MF, Leung YF, O'Shea GM, Chou S, Sun AM. Slow release of insulin from a biodegradable matrix implanted in diabetic rats. Diabetes. 1983;32:478-481.
5. Kaniuk Ł, Stachewicz U. Development and advantages of biodegradable PHA polymers based on electrospun PHBV fibers for tissue engineering and other biomedical applications. ACS Biomater Sci Eng. 2021;7:5339-5362.
6. De Koning GJM. Prospects of bacterial poly[(R)-3-hydroxyalkanoates]. Eindhoven University of Technology. Eindhoven. 1993.
7. Madison LL, Huisman GW. Metabolic engineering of poly(3-hydroxyalkanoates): from DNA to plastic. Microbiol Mol Biol Rev. 1999;63:21-53.
8. Kotnis MA, O'Brien GS, Willett JL. Processing and mechanical properties of biodegradable poly(hydroxybutyrate-co-valerate)-starch compositions. J Environ Polym Degr. 1995;3:97-105.
9. Shogren RL. Poly(ethylene oxide)-coated granular starch-poly(hydroxybutyrate-cohydroxyvalerate) composite materials. J Environ Polym Degr. 1995;3:75-80.
10. Ramkumar DHS, Bhattacharya M. Steady shear and dynamic properties of biodegradable polyesters. Polym Eng Sci. 1998;38:1426-1435.
11. El-Hadi A, Schnabel R, Straube E, Müller G, Henning S. Correlation between degree of crystallinity, morphology, glass temperature, mechanical properties and biodegradation of poly(3-hydroxyalkanoate) PHAs and their blends. Polym Test. 2002;21:665-674.
12. Parikh M, Gross RA, McCarthy SP. The influence of injection molding conditions on biodegradable polymers. J Inject Molding Technol. 1998. pp. 21-30.
13. Dos Santos Rosa D, Calil MR, Fassina Guedes CdG, Rodrigues TC. Biodegradability of thermally aged PHB, PHB-V, and PCL in soil compostage. J Polym Environ. 2004;12:239-245.
14. Chiellini E, Solaro R. Biodegradable polymeric materials. Adv Mater. 1996;8:305-313.
15. Noda I, Green PR, Satkowski MM, Schechtman LA. Preparation and properties of a novel class of polyhydroxyalkanoate copolymers. Biomacromolecules. 2005;6:580-586.
16. Patel A, Gaudana R, Mitra AK. A novel approach for antibody nanocarriers development through hydrophobic ion-pairing complexation. J Microencapsul. 2014;31:542-550.

17. Sun S, Liang N, Kawashima Y, Xia D, Cui F. Hydrophobic ion pairing of an insulin-sodium deoxycholate complex for oral delivery of insulin. Int J Nanomedicine. 2011;6:3049-3056.

18. Fialho SL, Rego MGB, Cardillo JA, Siqueira RC, Jorge R, Silva-cunha A. Implantes biodegradáveis destinados à administração intra-ocular. Arq Bras Oftalmol. 2003;66:891-896.

19. Xie M, Liu Y. Studies on amide III infrared bands for the secondary structure determination of proteins. Chemical Journal of Chinese Universities. 2003;24.

20. Dash S, Murthy PN, Nath L, Chowdhury P. Kinetic modeling on drug release from controlled drug delivery systems. Acta Pol Pharm. 2010;67:217-223.

21. Urtti A. Challenges and obstacles of ocular pharmacokinetics and drug delivery. Adv Drug Deliv Rev. 2006;58:1131-1135.

22. Dadgar Pakdel F, Mirshahi A, Zahedi P, Mohammad K, Hemmati F, Dadgar Pakdel J, Nicknam MH, Abedin Dorkoosh F. A novel approach for development of intraocular biodegradable ranibizumab implant: a solution for stability of protein activity. adv pharm bull. 2021;11:632-642.